Axon stretch growth: Towards functional repair of the spinal cord – An early translational exercise

Malcolm Philip Brinn

B.HlthSc (Life Sc) Flinders University

B.HlthSc (Hons Anat) University of Adelaide

Discipline of Anatomy and Pathology

Adelaide Medical School

January 2017

A thesis submitted to the University of Adelaide in fulfilment of the requirements for the degree of Doctor of Philosophy

TABLE OF CONTENTS

PART 1 INTRODUCTION

PART 2 EXPERIMENTAL

LANGUAGE: OXFORD UK ENGLISH (MODIFIED)

Abstract

Axon stretch growth: Towards functional repair of the spinal cord – An early translational exercise

Background

Injury to the spinal cord often visually presents as a local injury, damaging neurons that reside in the spinal cord, their projecting axons and supporting infrastructure such as oligodendrocytes. However, damage also occurs to ascending and descending axons that communicate with the brain. Fundamentally, repair of these injuries requires two distinct restorative approaches. The local injury will require stabilisation of the local environment, the rescue of injured neurons and support infrastructure, replacement of lost cells and restoration of intra-spinal communication. The latter ascending and descending axon injury will require proximal and distal axon reunification to restore supra-spinal communication with the brain.

This thesis presents the results of an early translational exercise that takes a non-linear approach to facilitate investigation into axon stretch growth (ASG) - an intrinsic mechanism that allows axons to adapt to body height and size throughout life. Pioneering research has shown that in-vitro exploitation of ASG has the potential to bridge significant gaps associated with injuries to long supra-spinal nerve tracts within the spinal cord.

Although translational science can be applied across the research spectrum, the traditional practice is to intervene once the research has matured. Here, the intervention occurs early, in an environment of limited funding within a progressive school of basic sciences. At the time of intervention, no infrastructure or experience in ASG research was evident within the faculties.

Translational Methods

The absence of a robust in-vitro adult motor neuron culture was identified as a potential barrier in ASG translation. Collaborations in anatomy, neuroscience, and toxicology were formed. Three separate animal ethics applications were required. Publication of a protocol followed.

The infrastructure required to conduct necessary in-vitro investigations into ASG was determined. Multidisciplinary collaborations were formed with mechanical, electrical and electronics engineers. Design, engineering, and commissioning of the equipment followed.

The lack of a definitive translational animal model has been previously identified as a significant barrier to spinal cord injury research. Specifically, a suitable large animal model has yet to be clearly defined for ASG research. Collaborations with comparative anatomy, a large animal research centre, and a senior spinal surgeon progressed development of a sheep model. Separate multi-institutional animal ethics applications were also required.

Results

A robust peer reviewed method was established to hydraulically extrude the spinal cord of adult Sprague-Dawley rats in under 60 seconds, and a serum free culture protocol simplified to maximise the yield of motor neurons and reduce culture costs. Adult motor neurons harvested and cultured using this protocol are capable of in-vitro survival for periods exceeding 21 days.

A decommissioned infant humidicrib was successfully converted into a portable temperature (32 – 39^{o}C ± 0.1^{o}C), and carbon dioxide controlled imaging incubator. Additional modifications incorporating umbilical support for multiple tailored bioreactors was also developed. A tailored ASG bioreactor was prototyped, tested, and commissioned. Axon stretch growth of motor neurons has been initiated in the bioreactor.

The literature review suggested that non-human primates were the optimal model for final translational confirmation. However, there was sufficient evidence to indicate that ungulates (i.e. sheep or pig) may be an alternative for ASG research. Relevant information on the sheep was collated, and basic investigation on their anatomy progressed.

Conclusion Early applied translational science (as practised here) is strategic and cost effective, showing that the overall strategy facilitates research, while potentially identifying barriers that could delay progress or cause late translational failure. The introduction of an “off the shelf” early intervention funding model allocated to translational scientists should be considered as a mechanism to progress basic science investigations that are in conceptual stages of development.

Declaration

I certify that this work contains no material which has been accepted for the award of any other degree or diploma in my name, in any university or other tertiary institution and, to the best of my knowledge and belief, contains no material previously published or written by another person, except where due reference has been made in the text. In addition, I certify that no part of this work will, in the future, be used in a submission in my name, for any other degree or diploma in any university or other tertiary institution without the prior approval of the University of Adelaide and where applicable, any partner institution responsible for the joint award of this degree.

I give consent to this copy of my thesis when deposited in the University Library, being made available for loan and photocopying, subject to the provisions of the Copyright Act 1968.

I acknowledge that copyright of published works contained within this thesis resides with the copyright holder(s) of those works.

I also give permission for the digital version of my thesis to be made available on the web, via the University's digital research repository, the Library Search and also through web search engines, unless permission has been granted by the University to restrict access for a period of time

I acknowledge the support I have received for my research through the provision of an Australian Government Research Training Program Scholarship.

Malcolm Philip Brinn

2016

Modified Oxford UK/English Version

Research contribution

Publications

Brinn, MP, O'Neill, K, Musgrave, I, Freeman, BJC, Henneberg, M & Kumaratilake, J 2016, 'An optimized method for obtaining adult rat spinal cord motor neurons to be used for tissue culture'*, J Neurosci Methods*, vol.273, pp. 128-137

Brinn, MP, Al-Sarawi, SF, Lu, T-F, Freeman, BJC, Kumaratilake, J & Henneberg, M. 2016, 'A portable cell culture and imaging system with optional umbilical bioreactor using a modified infant incubator', Bioengineering

Brinn, MP, Kumaratilake, J, Al-Sarawi, SF, Lu, T-F, Freeman, BJC & Henneberg, M 2016, 'An optimized method for obtaining adult rat spinal cord motor neurons to be used for tissue culture'*, J Tissue Engineering (submitted 24th January 2017)*

Presentations

Brinn MP, Kumaratilake, J, Henneberg M, and Freeman BJC. Exploiting Axon Stretch Growth as a novel mechanism for the future repair of long nerve tracts within the spinal cord. XIII Adelaide Centre for Spinal Research Symposium 13-15 August 2015 Novotel Barossa Valley, South Australia

Posters

Brinn MP, O'Neill K, Zhao S, Kumaratilake J, Musgrave I, Tien-Fu Lu, Al-Sarawi S, Linke I, Slater, A, Freeman BJC & Henneberg M 2016 'Axon Stretch Growth – Overcoming distance: Towards repair of long nerve tracts within the spinal cord' Poster presented at The University of Adelaide, Faculty of Health Sciences Postgraduate research conference: National Wine Centre, Adelaide, August 2014

Brinn MP, Kumaratilake J, Tien-Fu Lu, Al-Sarawi, Freeman BJC & Henneberg M. 'Axon Stretch Growth of adult primary motor neurons", Proceedings of the 25th Biennial Meeting of the ISN jointly with the 13th Meeting of the APSN in conjunction with the 35th Meeting of the ANS, 23rd - 27th August 2015, Cairns Australia, p333

Dedication and Acknowledgements

This thesis is dedicated to Rosemary, who has been the love of my life for over 40 years. Thank you for sharing this journey and for your support even when you had good reasons not too. Thank you also for your love, your motivation and guidance during the highs and lows.

To my daughters Tanya and Sharlene and my son Michael, a personal thank you. I remain the proudest father and look forward to spending more time with you all now.

To my grandchildren, Johnathon, Joshua, Samantha, Scott, Emma, Nathan, Peter, Mark, and Ruby I love you all.

To my supervisors Professor Maciej Henneberg, Professor Brian Freeman and Doctor Jaylia Kumaratilake, I feel honoured that you allowed me to undertake this PhD under your guidance. Thank you for your patience and perseverance, for the multiple reads of my thesis and the encouragement and support during the highs and lows.

To Maciej, who is also my mentor, thank you personally for your guidance, for your tremendous input in bringing this study to life and for your encouragement in taking on this early translational adventure with me. I have learned much in our short time together, 5 minutes with you is equivalent to 2hrs with anyone else.

I extend a special mention to Doctor Jaylia Kumaratilake for providing the extensive funding for the in-vitro work. I particularly want to acknowledge that the funding was provided by private lecturing. This was an extraordinary gift of both your time and effort in preparing lectures and in delivering them out of hours for over three years. Jaylia, You make the world a better place.

I also extend a special mention to Professor Brian Freeman who I am indebted to on many levels. First, for his gifted surgical intervention and second for supporting my work, providing perspective and opening doors that would otherwise be difficult to open. Thank you for taking the time to involve yourself in this project.

I would like to thank Doctor Said Al-Sarawi and Doctor Tien-Fu-Lu for their collaboration, engineering technical advice, and support in the development of the axon stretch device. I also extend my warm wishes and thanks to my extended technical family; Mr Ian Linke, Mr Bradley Pullen, Mr Aubrey Benjamin Slater, Mr Hayden Westell and Mr Alban O'Brian. Thank you for your time, knowledge, experience, and skills. I could not have completed this PhD without you.

To the many staff within the medical school, particularly Doctor Ian Musgrave and Ms Katie O'Neill, thank you for your assistance with cell culture work and use of your cell culture laboratory.

To my anatomy associates and peers thank you for your support and good grace to put up with me. Special mention to Tavik, Chris, Teghan, Irena, Stella, Caitlin, Arjun, Arthur, Dante, Gary, Pen, Todd, Mojdeh, Ian, Vyith, Mounir, Julie, Eleanor, Bill, and Mark. To the young ones, I now know I will be in good hands in the nursing home. To the older ones – see you there.

To all the staff, students and friends of the Anatomy discipline, I cannot thank you enough for your support and guidance. It was a wonderful experience sharing my journey with you all. A special mention and thank you to Bob Vink for guidance and professional assistance in topic selection.

To Kristin Carson, my good friend, and an exceptional research talent. Thank you for your support, guidance, and presence.

To the many other people that have mentored, assisted, or supported me through to completion of this thesis I also extend my grateful appreciation and thanks.

Finally, it is with sadness that I cannot share this moment with both my late father Philip John Brinn and late mother Kathleen Brinn as they were exceptional parents, both caring, and giving. I lost them both during this journey, and I miss then terribly, particularly now.

Ethics Statement and Permits

All experimental studies presented in this thesis were conducted per the guidelines established by the National Health and Medical Research Council

Ethics Committee	Ethics Number	Description	Approval Date
UOA	M-2012-205	Harvesting of rat spinal cords for motor and sensory neuron culture under serum-free conditions	19/12/2012 24/09/2013
UOA	M2014-159	Long term culture of adult motor neurons obtained from the spinal cord of a Sprague Dawley rat	14/11/2014
UOA SAHMRI	M-2014-051 SAM100	Pilot study stimulating intrinsic growth in the injured spinal cord: Phase 1: Validation of the sheep model	16th April 2014 4th June 2014

UOA = University of Adelaide

SAHMRI – South Australian Health and Medical Research Institute - PIRL

List of Figures

List of Tables

List of Abbreviations

Abbreviation	Full Description
AMPA	α-amino-3-hydroxy-5-methyl-4-isoxazolepropionic acid
ASF	Artifical Cerebro-Spinal Fluid
ASG	Axon Stretch Growth
bFGF	Basic Fibroblast Growth Factor
BDNF	Brain-derived neurotrophic factor
C1-C7	Cervical Vertebrae (numbered)
Ca^{2+}	Calcium
cAMP	8(-4 Chlorophenylthic cyclic adenosine 3'5 monophosphate)
CNE	Computer Numeric Control
CNS	Central Nervous System
CNTF	Ciliary Neurotrophic Factor
CO_2	Carbon Dioxide
CSF	Cerebrospinal Fluid
CST	Corticospinal tract
Cx1 – Cx4	Coccyx Vertebrae (numbered)
DIV	Days in Vitro
DNA	Deoxyribose Nucleic Acid
DRG	Dorsal Root Ganglion
DSHB	Developmental Studies Hybridoma Bank
EDTA	Ethylene Diamine Tetra Acetic acid

Abbreviation	Full Description
ETS	Early Translational Scientist
GDNF	Glial-derived neurotrophic factor
HIB-PM	Hibernate processing medium
L1-L5	Lumbar Vertebrae (numbered)
Mg^{2+}	Magnesium
Neurobasal - CM	Neurobasal based conditioned medium
NMDA	N-methyl-D-aspartate
NTSC	Non-Traumatic SCI
^oC	Degrees Celsius
O_2	Oxygen
PBS	Phosphate buffered solution
PDL	Poly-D-Lysine
PEEK	PolyEtherEther Ketone
PEG	Polyethylene glycol
PET	Polyethylene terephthalate
PNS	Peripheral Nervous System
S1-S5	Sacral Vertebrae (numbered)
SCI	Spinal Cord Injury
T1-T12	Thoracic Vertebrae (numbered)
TSCI	Traumatic SCI

Glossary of Terms

Primary injury: An event that causes initial damage to the spinal cord

Secondary injury: A series of biochemical events that occur within the spinal cord consequential to primary injury or repair intervention.

Wallerian Degeneration: A specific form of degeneration that affects neurites (including axons) when separated from a neurons cell body. This can be further specified as anterograde or orthograde.

Acute injury: The immediate post-injury phase, where damage to the spinal cord is continuing consequential to vascular or CSF disruption, and/or secondary injury biochemical events (generally < 24 hours' post injury)

Sub-acute injury: The period where optimal neuroprotective interventions are in place. Importantly, no new damage is being initiated, but secondary biochemical events are potentially still active, and the fate of existing damaged cells can be influenced through cell rescue measures (24 hours > 10 days)

Stabilised injury: A point between sub-acute and chronic injury, where the injury to the spinal cord has not yet reached steady-state but has stabilised. Biochemical events may be continuing, but the clinical response is reactionary (10 days > 24 months)

Chronic injury: The stage where the patient has reached steady state, and all biochemical events have subsided to the extent that the spinal cord is no longer actively responding to the injury or post injury intervention (>24 months)

Acute Repair: An immediate repair intervention that occurs while the spinal cord is in either acute or early subacute phase of injury.

Planned Repair: A planned intervention that occurs during the mid to late sub-acute or chronic phase of injury. The aim is to restore connections but, the repair may not improve functional outcome.

Restoration of Function: A planned intervention that occurs during the mid to late sub-acute or chronic phase of injury and is aimed to deliver specific functional gain i.e. nerve/muscle transfer surgery.

Motto

The Surgical Treatise - Case 31 (Edwin Smith Papyrus)

In 1930, renowned Egyptologist James Henry Breasted completed and published (now out of print) a comprehensive translation of the “Edwin Smith Papyrus.” The papyrus has been dated to the sixteenth century B.C and is considered to be the earliest known health record of the spinal column and spinal cord trauma. Case 31 (hieroglyphs above) old English transliteration: “If thou examines a man having a dislocation in a vertebra of his neck, shouldst thou finds him unconscious of his two arms and his two legs on account of it, while his phallus is erected on account of it and urine drops from his member without his knowing it; his flesh has received the wind; his two eyes are blood-shot; it is a dislocation of a vertebra of his neck extending to his backbone which causes him to be unconscious of his two arms and his two legs”……”An ailment not to be treated”.

https://oi.uchicago.edu/research/publications/oip/edwin-smith-surgical-papyrus

volume-1-hieroglyphic-transliteration (Accessed: 29/5/2015)

Part 1 - Introduction

Chapter 1. Background

Identified translational issues are highlighted in intense italics.

Introductory remarks

Spinal cord injuries are devastating events that instantly change the lives of those affected. However, although excellent progress has been made towards injury mitigation, there has been limited success in effecting a repair. A significant contributor to the problem is the underlying complexity of both the neuroanatomy and neurophysiology of the spinal cord and its surrounding structures, which have contributed to high levels of specialisation, particularly within the basic sciences.

In specialising, both basic scientists and clinicians narrow their field of reference, in doing so, their pathways diverge with clinicians responding to clinical events involving multiple biological systems, and basic scientists using the parsimonious methodology to solve very specific underlying causations of these events (Rogers 2003; van der Laan & Boenink 2015).

Complexity drives specialisation, and this redefines research practice

As complexity drives specialisation, collaborations are formed giving rise to the team or transdisciplinary science (Falk-Krzesinski et al. 2011; Hadorn et al. 2008). However, this form of science can be problematic to coordinate in a spinal cord research setting (Tator et al. 2012). One solution to overcome barriers associated with specialisation has been the emergence of the translational scientist; a role which takes on many forms depending on the background training of the individual. This thesis is an attempt to apply an early translational research methodology to basic spinal cord research. The core objective is to adopt a non-linear approach that adds value, reduces barriers, and maximises the effective dissemination of knowledge.

Rationale

The design of this project is predicated on the notion that at a microscopic level there are two basic forms of injury to both brain and spinal cord. The first which affects neurons and local support systems, and is generally referred to as a focal injury, and the second that affects predominantly axon tracts which are usually referred to as a diffuse injury (Povlishock et al. 1994). While both focal and diffuse injuries result in loss of function, at the level of the spinal cord the former injury affects autonomic communication receipt and initiation of function, while the latter affects the supra-spinal transmission of functional intent from the brain.

Damaged neurons can only be rescued. Whereas, cessation of transmission prevents otherwise viable neurons below an injury from functioning (Schwab & Bartholdi 1996)

Current acute post-injury intervention strategies mitigate and rescue neurons placing appropriate emphasis on the focal injury and therefore rescue of lost autonomic function. Beyond this point, it should then follow, that restoration of transmission (the diffuse) injury be prioritised to restore supraspinal control to functional neurons below the injury.

In the absence of a viable repair strategy, no timelines have been established, and the bulk of current research strategy places significant emphasis on introducing stem cells to the affected region (Coutts & Keirstead 2008; Ruff, Wilcox & Fehlings 2012). The aim being to restore local function and then to encourage targeted chemotaxis regrowth of axons to re-establish circuits. Given that most neurons within the spinal cord are interneurons (Kiernan & Barr 2009), there is merit in this strategy. However, to restore function of supraspinal axons tracts, this strategy places reliance on chemotaxis regrowth of axons and therefore assumes that the rate of axonal growth will be faster than the rate of

random degeneration of the axotomized distal axon stump – a somewhat contestable point (Coleman & Freeman 2010; Goldberg 2003; Waller 1850).

The growth of axons is known to occur during embryogenesis, following peripheral nerve injury and during the process of adaptation to body height and girth.

The latter form does not require a growth cone and therefore has been appropriately called axon stretch growth (Smith, Wolf & Meaney 2001). The in-vitro mechanisms of axon stretch growth are slowly emerging, and the technology has advanced to the extent that it appears to be a good candidate for grafting interventions aimed at long nerve tract injuries. Although it seems an appropriate conservative strategy, this approach requires two connections one to connect the proximal and one to connect the distal axotomized stump.

Stimulation of axon stretch growth *in-vivo* has not yet been attempted and would be considered by many neuroscientists as a high-risk strategy. However, new technologies are emerging and this would likely be more efficacious as the number of connections would be halved compared to grafting i.e. one instead of two connections per axon. However, the risk of avulsion cannot be understated, and it would be essential to extensively evaluate in animal models.

It is known that embryonic dorsal root ganglion (sensory neurons) can be mechanically stretched at fast rates without disconnection and that they remain electrically active (Pfister et al. 2006). More recently embryonic motor neurons have also been shown to be capable of the simultaneous cell body and neurite stretch growth (Feng et al. 2016). However, as yet, no direct evidence that adult motor neurons are capable of axon stretch growth.

To progress forward with in-vivo axon stretch growth studies, it will be necessary to establish first the in-vitro infrastructure to determine if it is possible to stretch adult motor neurons and secondly to determine the maximal stretch rate before

disconnection. In addition, it will be necessary to develop an appropriate animal model suitable to conduct both graft and in-vivo axon stretch growth experiments.

This represents an ideal early stage translational intervention.

Aims and Objectives

Aim

To apply a non-linear early translational approach towards developing and researching axon stretch growth (ASG) technology as a future mechanism to restore supra-spinal function following spinal cord injury.

Objectives:

Facilitate future axon stretch growth research by:

- Developing suitable in-vitro ASG infrastructure;
- Progressing research into adult motor neurons by establishing an adult motor neuron in-vitro harvesting and culture protocol; and
- Collate pertinent literature to progress a suitable ASG large animal model.

Evaluate early translational involvement by:

- Applying a critique to the concept of early translational intervention as applied to the innovative early stage basic science investigation.

Primer

Spinal cord injury (SCI) induces motor and/or sensory deficits by disrupting local spinal or supraspinal communication. Once injured, the body's natural response seeks to mitigate damage, but the complex circuitry remains refractory to repair. At the level of the neuron, and integral to this complexity, communication occurs through cells reaching electric potentials which are constantly regenerated by transmembrane voltage sensitive ion channels (Kandel, Schwartz & Jessell 2013). As differing ion channels have different voltage sensitivities, this selectively varies intracellular ionic concentrations, allowing neurons to either grade a response through temporal summation or combine a response through spatial summation. In the context of cephalization, where neurons may not be adjacent, the neuron has evolved an axon which projects from the cell body to its intended target. Axons retain transmembrane sensitive ion channels and therefore the ability to propagate electronic potentials over distance (Figure 1).

Layperson Outline - Neurons are best envisaged in a simplified network setting

Consider comparing a neuronal network to that of a railway network. Where typically there is a central station (Brain) and multiple suburban stations (body systems). The rail network has both direct and indirect tracks (neural pathways) that allow trains (action potentials) to travel independently to and from the central station as well as within local networks.

Train speed and track condition govern transportation time. Here, myelinated axons are best viewed as express tracks that cover a long distance (i.e. the corticospinal pathway). Action potentials on express "neural pathways" are delivered at much faster speeds than those delivered on local "suburban" tracks (unmyelinated axons).

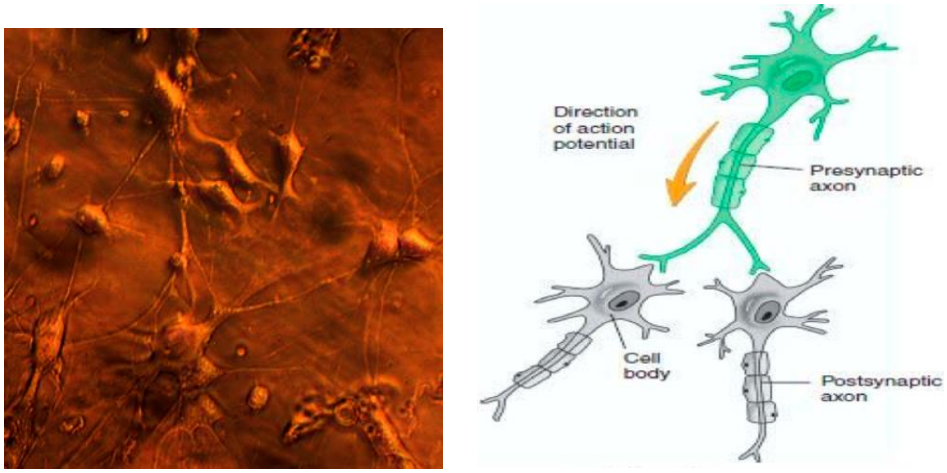

Figure 1: Picture and drawing representation of neuron connectivity

The neurons in the picture (left) were taken at 40x magnification through an inverted microscope at day 28 of culture. It shows the extensive connectivity of cells (predominantly neurons in this image). The drawing on the right at first view suggests a one-to-many connection. However, this is a many-to-many relationship where neurons are brought to threshold potential through summation which can occur from a single or series of many synapses, or via the extracellular environment. Picture: MB, Drawing Internet public domain.

Although speed is important, in neural networks, the fidelity of transmission has a higher priority. Passengers (activating enzymes) in this network are pre-delivered (in parts) by slower forms of transport (axon transport) and assembled into neurotransmitters. However, they cannot be released until a key arrives from the initiating station. To ensure the release of enzymes more than one action potential with the same key can arrive at the destination or the size of the action potential can be increased.

Disruption to neural networks – Introducing the concept of two forms of central nervous system communication disruption

The two most considered forms of acute disruption to neural networks are consequential to injuries occurring to the neuron or the axon. In these circumstances either the neuron or its local environment are damaged which threaten the survival of the neuron itself, or, either the axon has been crushed or severed preventing the neuron's capacity to influence its destination target (cell or muscle).

Cell bodies require high levels of vascularization, nutrient and waste infrastructure and therefore are more susceptible to acute and early subacute molecular events (Figure 2).

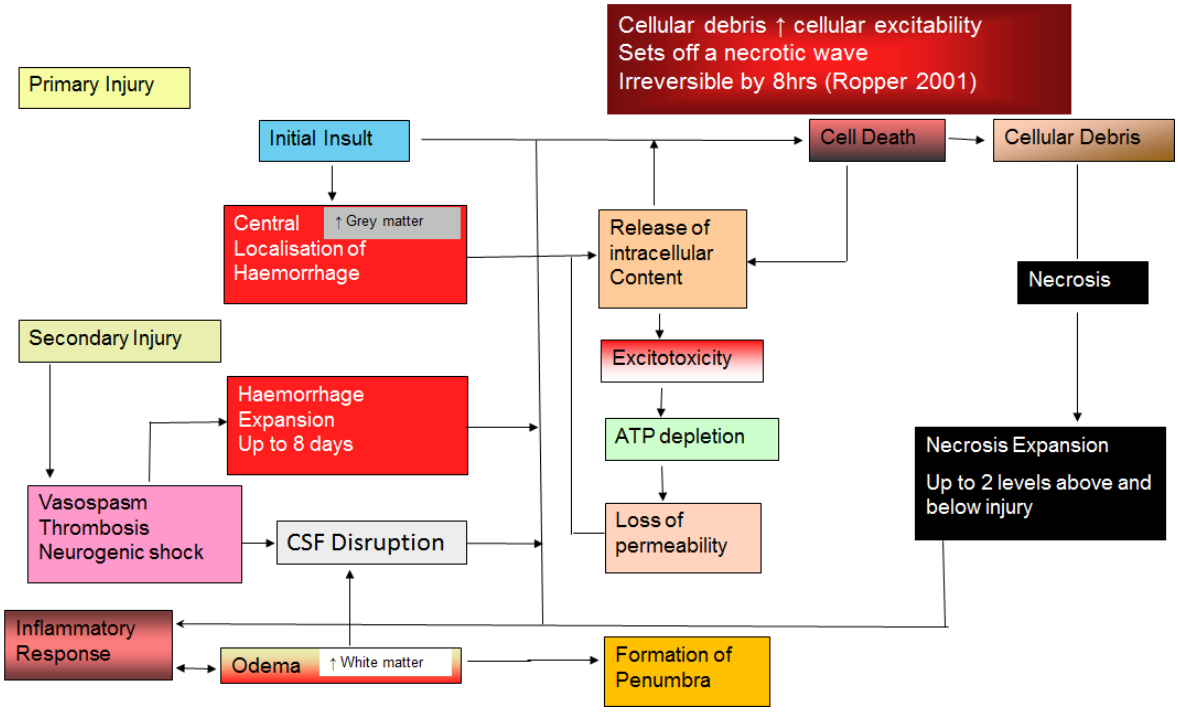

Figure 2: Schematic of acute and subacute molecular events

Following the primary injury local acute and sub-acute secondary injury events predominantly affect cell bodies that reside in the grey matter (Silva et al. 2014). This is partly due to the higher levels of vascularization in this region, but also due to the excitotoxic effects of damage done to cell bodies and disruption to CSF flow. This becomes significant when considering time since the injury.

Supraspinal axons are long i.e. those in the corticospinal tract (CST). This tract extends from the brain to progressively terminate along the longitudinal length of the spinal cord. In adult males, the human spinal cord as measured from the foramen magnum is approximately 450mm long (Standring 2008). Therefore, axons within the central nervous system can reach significant lengths. The same can be said of axons within the peripheral nervous system where axons from cell bodies that reside in the spinal cord can terminate within the furthest extremities of limbs by as much as 1500mm (estimate).

Axons deliver support material along the axon and package neurotransmitters within the terminal end (bouton). Through the action potential, the neuron initiates neurotransmitter release. Therefore, within the axon, there is less reliance on vascularization, nutrient and waste infrastructure, but a significant reliance on contiguity (Figure 3).

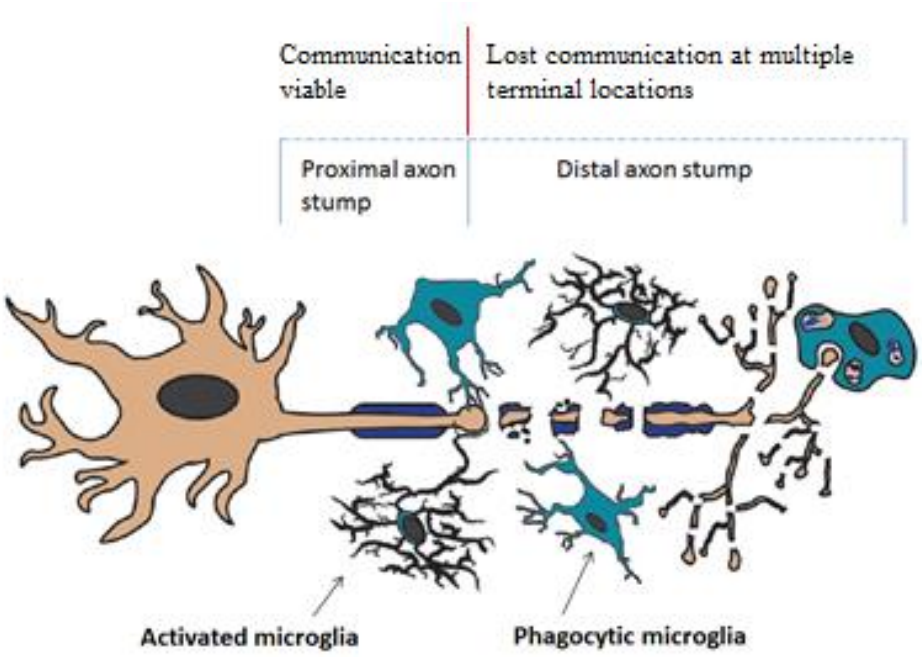

Figure 3: Wallerian degeneration occurs at random foci along the length of the distal axon stump

Picture adapted from: (Lafrenaye 2016) by Tavik Morganstern.

Following injury to a long axon within the central nervous system, degeneration at random foci along an axon can commence as early as 4hrs and continue for months/years. Thus, degeneration can quickly expand the distance between viable proximal and distal damaged axon stumps.

Following injury and at the microscopic level of injury, axons are severed or crushed, and the proximal and injured distal stumps recoil and separate. Calcium influx into the axon triggers sealing of both stumps and damage to the underlying microtubule network leads to the formation of the proximal retraction bulb

(Bradke, Fawcett & Spira 2012; Chierzi et al. 2005; Ertürk et al. 2007; Hellal et al. 2011). Although both the proximal and distal stumps of severed axons seal at the same time, their fate differs (Spira, Benbassat & Dormann 1993). As the proximal stump retains the cell body, it often remains viable, but the distal stump, which lacks the cell body degenerates at random foci along its remaining length (Spira, Benbassat & Dormann 1993; Waller 1850). Therefore, at the point of injury, the distance from the proximal stump to the viable distal stump can vary for each axon, not only due to the distal stump termination point but also as a consequence of the degeneration.

Natural communication redundancy within the spinal cord

Approximately 95% of neurons that reside in the spinal cord are interneurons that have relatively short axon projections (Kiernan & Barr 2009).

As supraspinal axons typically descend onto multiple interneuron synapses, most motor neurons that reside in the ventral horn of the spinal cord are brought to threshold through summation. In non-primates, as supraspinal axons descend onto multiple targets, there is built-in redundancy in the delivery from the supra-spinal pathway to the target pathway i.e. many to many relationships (Figure 1). However, in the case of primates, this organisation does have some variation, particularly in the corticospinal tract where in many instances there are direct corticomotoneuronal connections (Lemon 2008)

Relevant Gross Anatomy

The osseous spinal column

The adult spinal column consists of up to 33 vertebral segments divided into five regions which are anatomically described as comprising seven cervical (C1-C7), 12 thoracics (T1-T12), five lumbar (L1-L5), five sacral (S1-S5) and four coccyges (Cx1–Cx4) (Standring 2008). Bones of the sacral and coccyx regions are typically fused by adulthood. Vertebrae in cervical regions are less robust than

thoracic or lumbar regions (Figure 4). Because of this anatomy, surgical access to the ventral segments of the spinal cord can be challenging.

In large animal models, cannulation into the spinal canal can be achieved between thoracic and lumbar spinal process. More general access can occur through the widening of the intervertebral foramina, dorsal laminectomy, or vertebral corpectomy. In small animal models (with recovery) options are restricted by size and a lack of fixation capability.

The bony wall of the spinal canal is lined with ligaments, which create a smooth internal surface, in combination with the externally attached ligaments, these ligaments allow osseous structures to move during flexion and extension. Epidural fat serves to lubricate the inferior surface between the ligaments, spinal dura, and nerve roots.

Ligaments of the spinal column

- The supraspinous ligament runs a rostrocaudal path along the tips of the spinous process C7 to Sacrum. This ligament embeds fibres across several vertebrae;

- The ligament nuchae is an extension of the supraspinous ligament supporting the head and cervical vertebrae from the occipital protuberance to C7;

- Inferior to the supraspinous ligament, the interspinous ligaments attach between the root and apex of each spinal process and connect to the adjacent spinal processes;

- Inferior and abutting to the inferior aspect of the root of the interspinous ligaments the *ligamentum flavum* attaches between the laminae of each neural arch, in effect, attaching the posterolateral aspect of adjacent vertebra together;

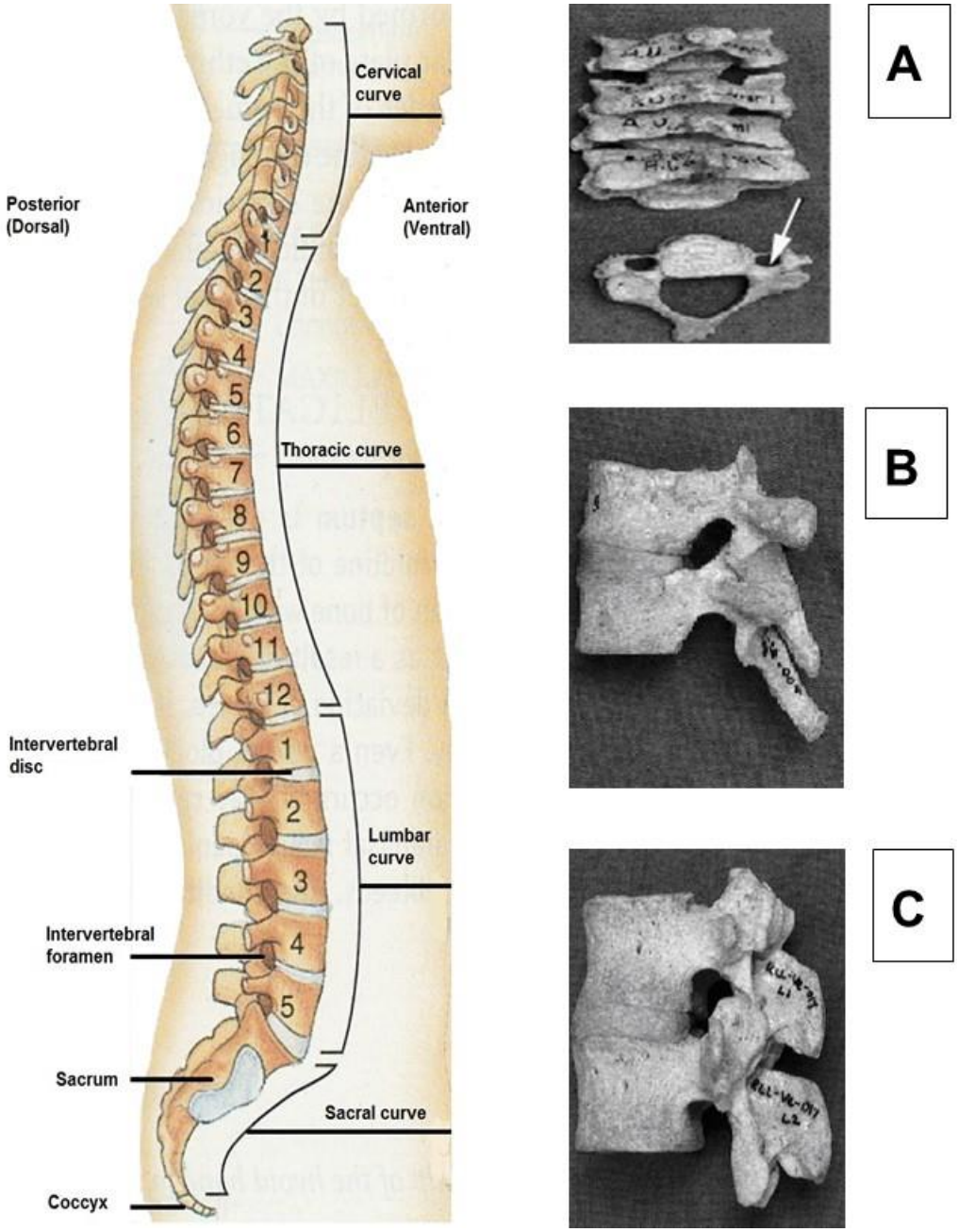

Figure 4: Right lateral drawing of the vertebral column and pictures of the osseous vertebra.

Stock image left is showing the arrangement of vertebrae (Left). Pictures A, B, and C highlight how the vertebrae become more robust caudally. Sacral and Coccyx vertebrae (not shown on the right) are fused by adulthood. Note the lordosis curvature of the cervical and lumbar regions and the kyphotic curvature of the thoracic and Sacral/Coccyx regions. Adapted image (Left) from (Tortora & Grabowski 1993) under license 3967361467187.

- Inferior to the ligamentum flavum, a thin strip of the posterior longitudinal ligament runs a rostrocaudal path inferior to the apex of the neural arch;

- The anterior longitudinal ligament is wide and extends to cover both the anterolateral aspects of the vertebral body and intervertebral foramina C1 through to Sacrum. This ligament is thicker medially and embeds into intervertebral discs, effectively attaching adjacent vertebra and intervertebral discs together; and

- The vertebral canal is lined with ligaments, creating a smooth internal surface. Adjacent to the spinal canal wall, the epidural space contains the internal vertebral venous plexus and is filled with epidural fat.

Contents of the Spinal Canal

The inner layer of the cranial dura adheres to the foramen magnum and descends within the vertebral canal as the spinal dura forming the outer layer of the meningeal tube. Adjacent to the spinal canal wall, the epidural space contains the internal vertebral venous plexus, and is filled with epidural fat. The spinal cord sits within the meningeal tube, and its broad relationships are diagrammatically depicted (Figure 5).

The Meninges

Neural tissue is fragile. The spatial gravity of cerebrospinal fluid (CSF) and neural tissue are equal, therefore in the absence of CSF, the structure is lost, and nervous tissue collapses.

The inner layer of the cranial dura adheres to the foramen magnum and descends within the vertebral canal as the spinal dura forming the outer layer of the meningeal tube.

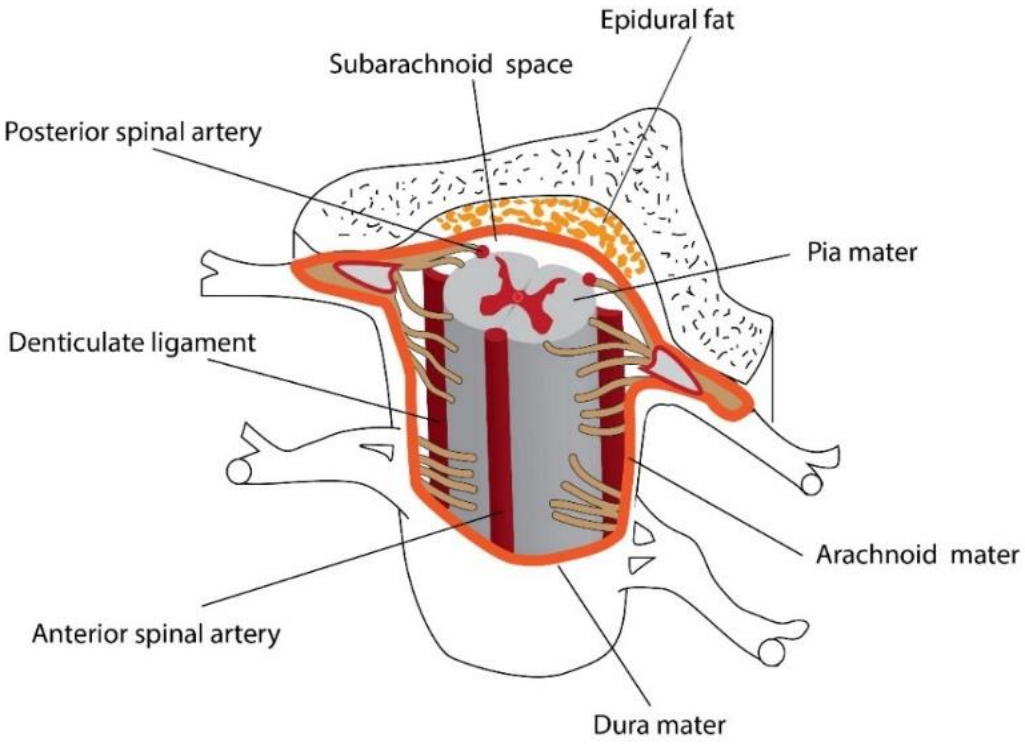

Figure 5: Diagram of structural relationships

Epidural fat distribution in the fetus circumferential whereas, in adults, distribution is proximal to the vertebral arches primarily at disc level (Beaujeux et al. 1997). This arrangement appears to be facilitatory to lubrication of the dura and nerve roots. Image. Tavik Morganstern.

The meninges are described as having three layers (Figure 6) being the spinal dura, arachnoid, and pia mater. Between the spinal dura and arachnoid mater (subdural space), a thin layer of “lymphlike” fluid acts as a fluid buffer and lubricant. The arachnoid membrane is non-vascular, retaining rhomboid shaped trabeculae often described as spider-like networks which insert into the pia mater, creating the subarachnoid space. The subarachnoid space facilitates circulation of CSF, blood, nutrient and waste exchange as well as providing a protective buffer. The pia mater is a bi-layered vascular membrane, with the superficial layer comprised of collagenous fibres investing the surface of the cord but not in direct contact with nerve cells or fibres (Leeson & Leeson 1981). The inner layer consists of fine reticular and elastic fibres adherent to nervous tissue.

Given that the brain and spinal cord are both constrained within the osseous cranial vault and spinal canal, a pressure gradient is established within the meninges by circulating CSF, blood volume, tissue expansion and the underlying capacity of cells to maintain osmotic homoeostasis (Goldsmith 2009).

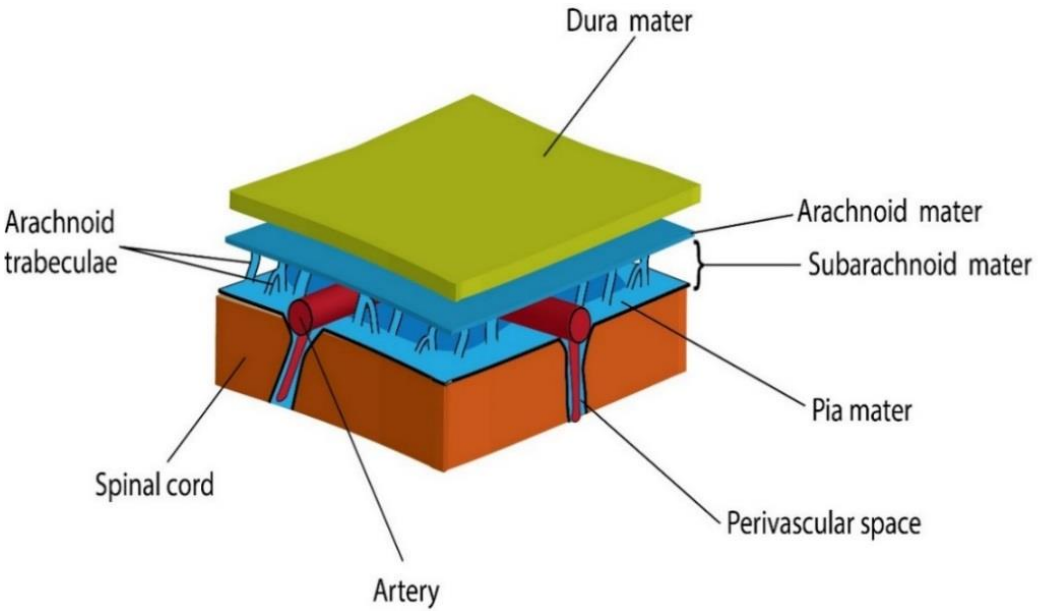

Figure 6: Diagrammatic representation of the Meninges surrounding the spinal cord (detail)

Image Tavik Morganstern

There is evident significance about aetiology and vascular access to the spinal canal (Crock 1996). Arteries that feed into the spinal cord also project to the vertebrae and therefore differ at the level of the vertebral column referenced. Inter-segmental vessels are present in thoracic and lumbar regions. In these regions, the arterial supply to the ventral aspect of the vertebral body occurs through bilateral precentral branches of the thoracic or lumbar artery respectfully, which then invests anterolaterally.

Vascular arborization of the spinal cord and surrounding structures

Arterial supply to the dorsal aspect of the vertebral body occurs from bilateral postcentral branches of the spinal artery which access through intervertebral foramina. Arterial supply to the pedicles and overall neural arch occurs from the post and pre-laminar branches of the spinal artery. The pre-lamina branch also passes through the intervertebral foramina. Veins of the spinal column are devoid of valves and retain similar pathways to the arterial supply anastomosing with Intervertebral and Segmental veins. An important difference is that the veins are contiguous by forming two specific venous plexuses, one that surrounds the vertebral body and the other that surrounds the anterior of the vertebral canal. This plexus arrangement supports alternate routeing of venous drainage.

The blood supply to the spinal cord, roots, and nerves originate from the vertebral, posterior intercostal, lumbar, sacral, segmental medullary feeder and radicular arteries. Supply contribution of these arteries varies along the longitudinal length of the cord. As the vertebral arteries branch from the subclavian arteries, blood supply to the upper third of the spinal cord (delivered through spinal and segmental medullary arteries) originates primarily from the vertebral arteries and deep cervical arteries. The vertebral arteries travel rostral through the transverse processes via the foramen of the cervical vertebrae towards the cranial cavity where they anastomose to form the basilar artery. Before the formation of the basilar artery, the two vertebral arteries branch off anteriorly to anastomose with the anterior spinal artery and posteriorly to either the ipsilateral left of the right posterior spinal artery.

In addition to the direct supply to the longitudinal arteries, supplemental segmental medullary arteries supplied by the vertebral artery or deep cervical arteries enter through the intervertebral foramina anastomosing with anterior and posterior radicular arteries that go on to anastomose with the appropriate spinal artery. By themselves, the vertebral and deep cervical arteries are insufficient to supply the remaining two-thirds of the cord. The arteria radicularis magna (artery

of Adamkiewicz) heavily supplies the remaining lower two-thirds of the spinal cord. Although normally it is located on the left side, of surgical importance, the segmental position of the artery varies within individuals (range T9 –L2) (Standring 2008).

Three longitudinal arteries distribute blood to the spinal cord (Figure 7). The anterior spinal artery invests into the anterior median fissure forming the sulcal arteries, which in turn supply the grey matter and deeper parts of the lateral and posterior funiculus. The paired posterior spinal arteries descend in the posterolateral sulcus, supplying the tips of the spinal horns and most the white matter excluding the more centralised deeper regions. At the conus, both the anterior and posterior spinal arteries loop forming an anastomosing plexus (Crock 1996; Standring 2008). Overall, the anterior spinal artery distributes blood to about $^{2}/_{3}$ of the cross-sectional area of the spinal cord.

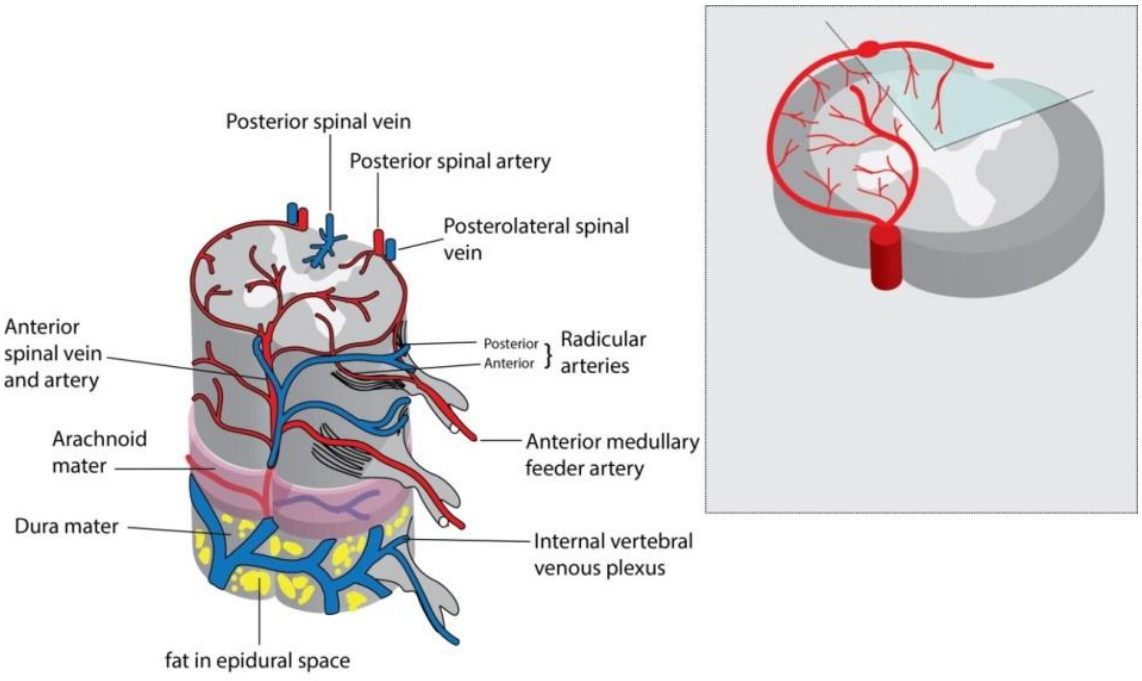

Figure 7: Vascular supply to the spinal cord

Overall, the anterior spinal artery distributes blood to about $^{2}/_{3}$ of the cross-sectional area of the spinal cord. Disruption of blood supply to the longitudinal arteries, in particular, the anterior spinal artery can be catastrophic, resulting in ischemia and significant loss of function. Image. Tavik Morganstern.

References

Beaujeux, R, Wolfram-Gabel, R, Kehrli, P, Fabre, M, Dietemann, JL, Maitrot, D & Bourjat, P 1997, 'Posterior lumbar epidural fat as a functional structure? Histologic specificities', *Spine (Phila Pa 1976)*, vol. 22, no. 11, Jun 1, pp. 1264-1268; discussion 1269.

Bradke, F, Fawcett, JW & Spira, ME 2012, 'Assembly of a new growth cone after axotomy: the precursor to axon regeneration', *Nat Rev Neurosci*, vol. 13, no. 3, pp. 183-193.

Chierzi, S, Ratto, GM, Verma, P & Fawcett, JW 2005, 'The ability of axons to regenerate their growth cones depends on axonal type and age, and is regulated by calcium, cAMP and ERK', *European Journal of Neuroscience*, vol. 21, no. 8, pp. 2051-2062.

Coleman, MP & Freeman, MR 2010, 'Wallerian Degeneration, WldS, and Nmnat', *Annual Review of Neuroscience*, vol. 33, no. 1, pp. 245-267.

Coutts, M & Keirstead, HS 2008, 'Stem cells for the treatment of spinal cord injury', *Exp Neurol*, vol. 209, no. 2, Feb, pp. 368-377.

Crock, HV 1996, *An atlas of the vascular anatomy of the skeleton and spinal cord*, Martin Dunitz.

Ertürk, A, Hellal, F, Enes, J & Bradke, F 2007, 'Disorganized Microtubules Underlie the Formation of Retraction Bulbs and the Failure of Axonal Regeneration', *The Journal of Neuroscience*, vol. 27, no. 34, August 22, 2007, pp. 9169-9180.

Falk-Krzesinski, HJ, Contractor, N, Fiore, SM, Hall, KL, Kane, C, Keyton, J, Klein, JT, Spring, B, Stokols, D & Trochim, W 2011, 'Mapping a research agenda for the science of team science', *Research Evaluation*, vol. 20, no. 2, June 1, 2011, pp. 145-158.

Feng, ZQ, Franz, EW, Leach, MK, Winterroth, F, White, CM, Rastogi, A, Gu, ZZ & Corey, JM 2016, 'Mechanical tension applied to substrate films specifies location of neuritogenesis and promotes major neurite growth at the expense of minor neurite development', *J Biomed Mater Res A*, vol. 104, no. 4, Apr, pp. 966-974.

Goldberg, JL 2003, 'How does an axon grow?', *Genes Dev*, vol. 17, no. 8, Apr 15, pp. 941-958.

Goldsmith, HS 2009, 'Treatment of Acute Spinal Cord Injury by Omental Transposition: A New Approach', *Journal of the American College of Surgeons*, vol. 208, no. 2, 2//, pp. 289-292.

Hadorn, GH, Biber-Klemm, S, Grossenbacher-Mansuy, W, Hoffmann-Riem, H, Joye, D, Pohl, C, Wiesmann, U & Zemp, E 2008, *Handbook of transdisciplinary research*, Springer.

Hellal, F, Hurtado, A, Ruschel, J, Flynn, KC, Laskowski, CJ, Umlauf, M, Kapitein, LC, Strikis, D, Lemmon, V, Bixby, J, Hoogenraad, CC & Bradke, F 2011, 'Microtubule stabilization reduces scarring and causes axon regeneration after spinal cord injury', *Science*, vol. 331, no. 6019, Feb 18, pp. 928-931.

Kandel, E, Schwartz, JH & Jessell, TM 2013, *Principles of neural science*, 5th edn, eds ER Kandel & AES Mack, McGraw-Hill Medical.

Kiernan, JA & Barr, ML 2009, *Barr's the Human Nervous System: An Anatomical Viewpoint*, 9th edn, Wolters Kluwer Health/Lippincott Williams & Wilkins.

Lafrenaye, AD 2016, 'Physical interactions between activated microglia and injured axons: do all contacts lead to phagocytosis?', *Neural regeneration research*, vol. 11, no. 4, p. 538.

Leeson, TS & Leeson, CR 1981, *Histology*, W.B. Saunders Company, Philadelphia/London/Toronto.

Lemon, RN 2008, 'Descending pathways in motor control', *Annu Rev Neurosci*, vol. 31, pp. 195-218.

Pfister, BJ, Iwata, A, Taylor, AG, Wolf, JA, Meaney, DF & Smith, DH 2006, 'Development of transplantable nervous tissue constructs comprised of stretch-grown axons', *J Neurosci Methods*, vol. 153, no. 1, May 15, pp. 95-103.

Povlishock, JT, Hayes, R, L, Michel, ME & McIntosh, TK 1994, 'Workshop on animal models of traumatic brain injury', *Journal of Neurotrauma*, vol. 11, no. 6, pp. 723-732.

Rogers, E 2003, 'Diffusion of Innovations', Free Press, New York.

Ruff, CA, Wilcox, JT & Fehlings, MG 2012, 'Cell-based transplantation strategies to promote plasticity following spinal cord injury', *Exp Neurol*, vol. 235, no. 1, 5//, pp. 78-90.

Schwab, ME & Bartholdi, D 1996, 'Degeneration and regeneration of axons in the lesioned spinal cord', *Physiological Reviews*, vol. 76, no. 2, 1996/04//, p. 319+.

Silva, NA, Sousa, N, Reis, RL & Salgado, AJ 2014, 'From basics to clinical: a comprehensive review on spinal cord injury', *Prog Neurobiol*, vol. 114, Mar, pp. 25-57.

Smith, DH, Wolf, JA & Meaney, DF 2001, 'A new strategy to produce sustained growth of central nervous system axons: Continuous Mechanical Tension', *Tissue Engineering*, vol. 7, no. 2, pp. 131-139.

Spira, ME, Benbassat, D & Dormann, A 1993, 'Resealing of the proximal and distal cut ends of transected axons: Electrophysiological and ultrastructural analysis', *Journal of Neurobiology*, vol. 24, no. 3, pp. 300-316.

Standring, S 2008, *Gray's Anatomy The Anatomical Basis of Clinical Practice*, 40th edn, ed. S Standring, Elsevier Health Sciences UK, London.

Tator, CH, Hashimoto, R, Raich, A, Norvell, D, Fehlings, MG, Harrop, JS, Guest, J, Aarabi, B & Grossman, RG 2012, 'Translational potential of preclinical trials of neuroprotection through pharmacotherapy for spinal cord injury', *J Neurosurg Spine*, vol. 17, no. 1, Sep, pp. 157-229.

Tortora, GJ & Grabowski, SR 1993, *Principles of anatomy and physiology*, Ninth edn, HarperCollinsCollege.

van der Laan, AL & Boenink, M 2015, 'Beyond bench and bedside: disentangling the concept of translational research', *Health Care Anal*, vol. 23, no. 1, Mar, pp. 32-49.

Waller, A 1850, 'Experiments on the section of the Glossopharyngeal and Hypoglossal nerves of the frog, and observations of the alterations produced thereby in the structure of there primitive fibres ', *Philosophical Transactions of the Royal Society of London.*, vol. 140, pp. 423-429.

Chapter 2. Morbidity, Epidemiology, and Aetiology of spinal cord injury

Morbidity Cost

Information collected relating to the Lifetime costs of SCI are variable and often understated in countries with a limited resource (Bickenbach et al. 2012).

In the United States of America, the estimated 2009 lifetime direct cost of spinal cord injury was between US$ 2.1 – US$5.4 million for persons injured at age 25 (Cao, Chen & DeVivo 2011; DeVivo et al. 2011). In Australia, lifetime costs have been estimated dependent on injury severity at between AU$ 4.8 million and AU$ 7.6 million (Access Economics Pty Ltd. 2009) and in Canada dependent on injury severity at between CAD$1.4 and CAD$3 million (CDIC 2013)

Epidemiology

The World Health Organisation in conjunction with the International Spinal Cord Society estimates that the current global incidence of spinal cord injury (SCI) exceeds 40 new cases per million of population per annum, with an average, estimated prevalence of 600 persons per million of the worldwide population[1] (Bickenbach et al. 2012). Over half (50-70%) of traumatic SCI's occur in cervical regions (Ackery, Tator & Krassioukov 2004; Chiu et al. 2010; Devivo 2012; Knutsdottir et al. 2012; Lenehan et al. 2012; Ning et al. 2011), with an increasing number being in the higher cervical range (Knutsdottir et al. 2012; Norton 2010; O'Connor & Brown 2006; Wyndaele & Wyndaele 2006). Injury to the cervical cord region results in incomplete or complete tetraplegia. Those with high cervical injuries may also lose vital autonomic functions, including those leading to respiratory failure or cardiac events. Injuries below the cervical region, although generally with less extensive consequence, will often cause paraplegia with the possible loss of autonomic

[1] Based on data obtained from 6 countries using varying methodological techniques

control of trunk, temperature regulation, bowel, bladder and or sexual function.

Incidence levels are lower in developed countries while prevalence rates are higher (Lee et al. 2014). This association highlights improvements in prevention, emergency response and long-term management in developed countries (Sekhon & Fehlings 2001; Whiteneck et al. 1992). In less developed countries a reduced level of preventative measures increases the risk of SCI (Chiu et al. 2010; Ezzati et al. 2002). Risk taking practices in less developed countries are a significant cause of SCI and result in a higher mortality and morbidity rate due to lack of health care and/or follow-up resource (Draulans et al. 2011; Lee et al. 2014). These latter issues influence direct costs associated with injuries such as the provision of emergency care, hospitalisation, imaging and surgical intervention. No matter how thorough preventative measures can be, some injuries will still occur and need intervention to improve patient outcomes.

Aetiology of spinal cord injury

Worldwide, between 80% and 90% of all spinal cord injuries are a result of trauma (Bickenbach et al. 2012; Draulans et al. 2011; Norton 2010; US National Spinal Cord Injury Statistical Center 2014). In the vast majority of these incidents, impact energy from collisions arising from motor vehicle accidents, falls, violence or unsafe work practice are the initiating mechanisms (Table 1). There is also both epidemiologic evidence and aetiology correlation based on gender and age (Figure 8) evidenced in detailed US statistics and more broadly in global mapping of epidemiology (Ackery, Tator & Krassioukov 2004; Lee et al. 2014).

Table 1: Aetiology of traumatic spinal cord injury by proportion of males and females

In the United States, higher rates of injury occur in males (4:1 ratio) than females.

Description	Proportion Males	Proportion Male %	Proportion Females	Proportion Female %
Road Accidents	10,052	75.73%	3,222	24.27%
Violence Gunshot	4,373	87.46%	627	12.54%
Falls	5,406	81.07%	1,262	18.93%
Sport/Leisure activity	2,780	89.88%	313	10.12%
Other	2,006	81.38%	459	18.62%
Total	24,617	80.71%	5,883	19.29%

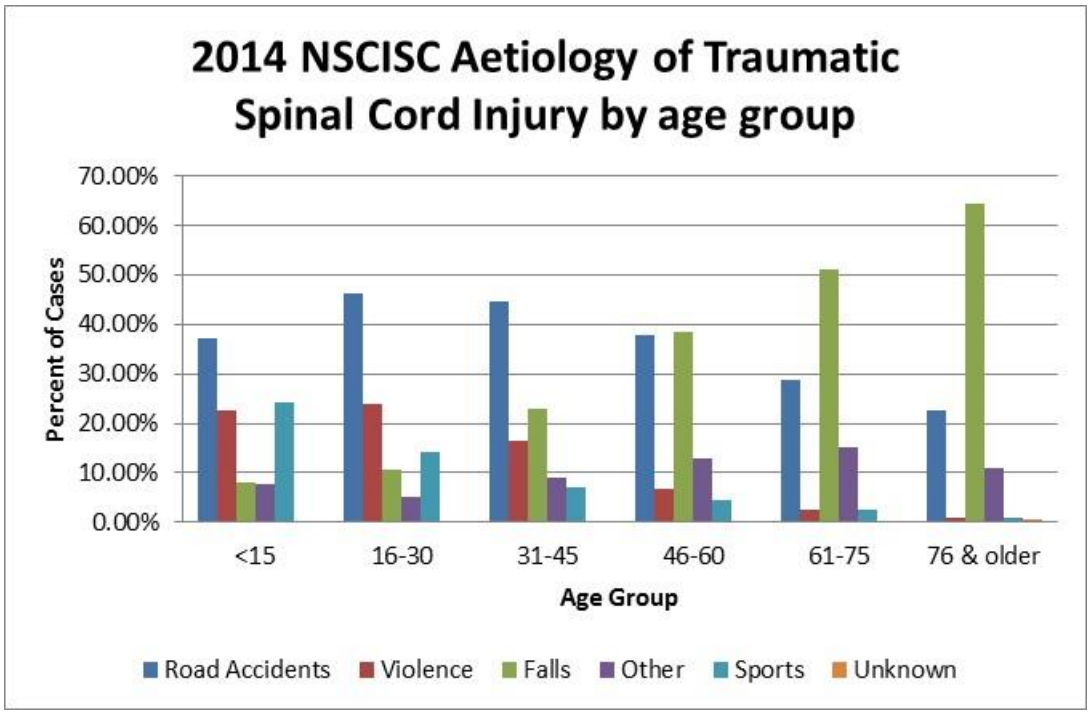

Figure 8: Aetiology of traumatic spinal cord injury by age (2012)

Higher rates of a motor vehicle and violence-related injury occur between the ages of 15 - 45 years and higher rates of fall-related injuries occur aged > 45years. Source data: (US National Spinal Cord Injury Statistical Center 2014)

Injury Classification (Clinical)

Spinal cord anatomy is a determinant factor in the severity of an injury, with prognosis being heavily influenced by the level at which the spinal cord injury is sustained, associated with the extent of damage caused to underlying osseous, vascular and neural structures (Sekhon & Fehlings 2001).

To determine the extent and severity of a spinal cord injury, a prominent instrument used to classify patients is the International Standards for Neurological Classification of Spinal Cord Injury (ISNCSCI). This instrument, was formerly ASIA impairment scale (AIS) (American Spinal Injury Association 2015), which first deconstructs to five grades (A-E) denoting the level of motor and sensory function, then further provides more detailed information on muscle strength (motor index score) and sensory response (sensory index score). Incomplete injuries can be further deconstructed into syndromes that are typically descriptive of the injury and the level affected (Table 2) (Kirshblum et al. 2011).

Mechanism of Primary Injury

Primary injuries to the spinal cord broadly occur as a result of adverse mechanical tension. The mechanism of injury can be grouped into laceration or lesion (Breig 1978), contusion, crush or displacement of surrounding structures such as vertebrae, ligaments, intervertebral discs or spinal dura (Devivo 2012; Fehlings, Michael G. et al. 2012; Leucht et al. 2009; Schwab & Bartholdi 1996; Sekhon & Fehlings 2001; Tator 1995)

Description	Location	Clinical Presentation
Central Cord Syndrome	Cervical Hyperextension Injury could also result in compression of the cord	Disproportionate impairment of upper extremity function than in lower extremity
Anterior Cord Syndrome	Disrupted or loss of blood supply to the anterior two-thirds of the spinal column Damaged or compromised corticospinal and spinothalamic tracts (Dorsal columns are spared)	Complete motor paralysis below the level of injury. Loss of pain and temperature perception at and below the injury. Intact proprioception and vibratory senses
Brown-Sequard Syndrome	Hemisection of the spinal cord	Ipsilateral loss of proprioception, vibration and motor control at or below the level of lesion Sensory loss of all modalities at the level of the lesion Contralateral loss of pain and temperature sensation
Conus Medullaris Syndrome	Conus Medullaris (may be difficult to distinguish from Cauda Equina Syndrome)	Mixed upper and lower motor neuron loss of function. Dependent on the area of conus injured, sacral segments may show preservation.
Cauda Equina Syndrome	Lumbosacral nerve roots of cauda equina Cord may be spared	Flaccid paralysis of lower limb muscles, areflexic bowel, and bladder. All sensory reflexes similarly impaired Variable loss of sensation

Table 2: Defined spinal cord syndromes (revised)

Kirshblum, SC, Burns, SP, Biering-Sorensen, F, Donovan, W, Graves, DE, Jha, A, Johansen, M, Jones, L, Krassioukov, A, Mulcahey, MJ, Schmidt-Read, M & Waring, W 2011, 'International standards for neurological classification of spinal cord injury (Revised 2011)', *J Spinal Cord Med*, vol. 34, no. 6, pp. 535-546.

a) Adverse mechanical tension (colloquially referred to as severe whiplash)

Clinical Presentation: Central Cord Syndrome. Hyperextension injury (Aarabi, Koltz & Ibrahimi 2008) that causes both local vascular and parenchymal damage, as well as damage to supra-spinal nerve tracts (Figure 9).

Adverse mechanical tension is the condition where the tension applied to the spinal cord is greater than the intrinsic threshold allowed, thus causing injury (Breig 1978). The typical initiating aetiologies are motor vehicle accidents, falls or sports injury. In many of these injuries, the body is positioned in a partially flexed or extended position at the time of the incident. Rapid motion, followed by abrupt stopping, overrides the supporting structures of the head. In extreme cases, the brain rapidly moves forward within the cranial vault, while the cervical vertebrae rapidly transition. The weight of the head in combination with force pulls both stabilising structures and the spinal cord beyond their tensile boundaries (Aarabi, Koltz & Ibrahimi 2008; Maak 2006; Meaney et al. 1995; Panjabi et al. 1998; Smith, Meaney & Shull 2003). Rupture of supraspinal axons ensues causing a diffuse rostrocaudal injury, often later evidenced by consistent haemorrhage sites in the brain hemispheres, brainstem and spinal cord (Gosch, Gooding & Schneider 1970). Force can also cause a cavitation effect as the brain “wobbles” (like jelly) affecting local neurons residing in the brain (Gosch, Gooding & Schneider 1970). Rupture of local brain and spinal cord vascular structures (Sandler & Tator 1976; Tator 1990) and likely disruption of cerebrospinal fluid flow follows contributing to secondary injury mediated damage (Jones et al. 2013).

The effects of adverse mechanical tension can also be prolonged through entrapment of the spinal cord typically by posteriorly displaced vertebral body (Figure 9). The ensuing pincer effect can maintain lateral axon tracts under adverse tension. If not surgically decompressed this can contribute to

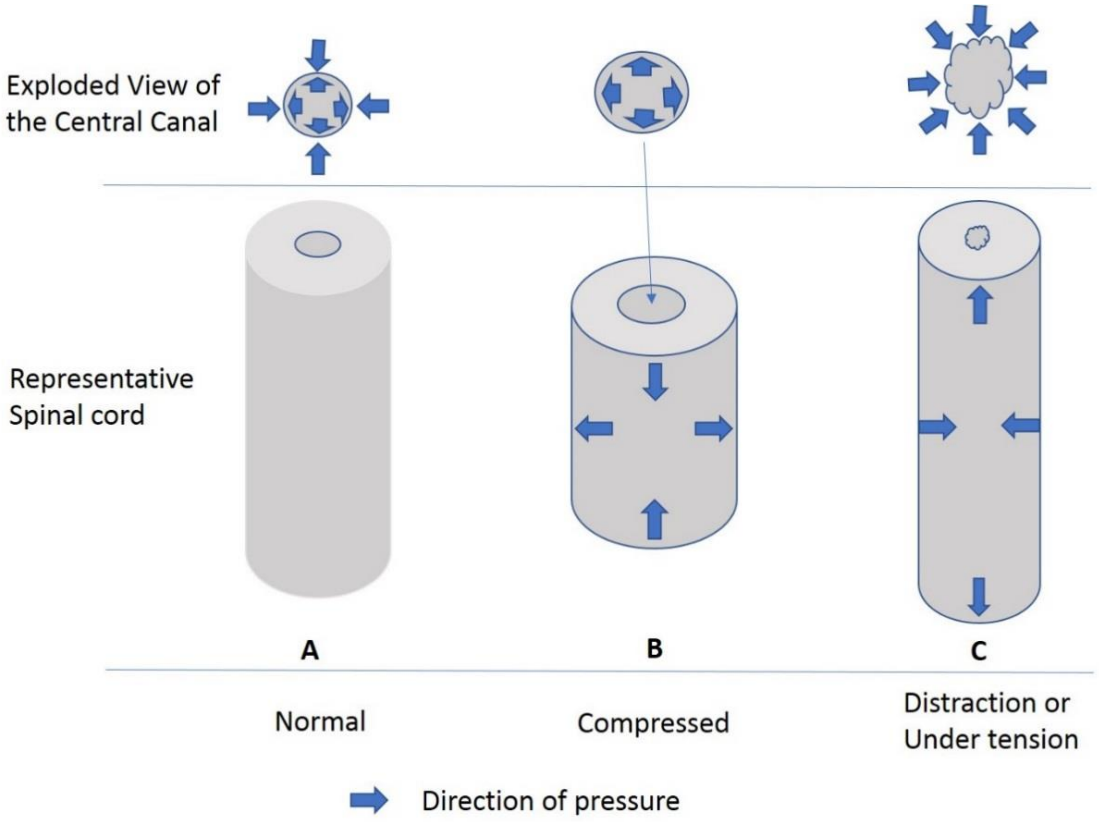

T2 weighted post-injury cervical spine

Figure 9: Adverse Mechanical Tension

Diagram left: A: Normal, patency of the central canal, vascular structures, and subarachnoid space are maintained. B: Compression of the spinal cord places lateral pressure on the central canal wall (increasing diameter) C: Distraction injury thins the spinal cord, placing medial pressure onto the wall of the central canal (reducing diameter). Sagittal MRI: an extreme example of the "pincer effect." Not only does this action disrupt vascular and CSF supply this action also can maintain lateral longitudinal axons under tension causing diffuse damage. MRI: Stock B.Freeman

prolonged diffuse axonal damage above and below the lesion (Aarabi, Koltz & Ibrahimi 2008; Breig 1978; Choo et al. 2008).

b) Laceration or lesion to the spinal cord causes both an immediate local injury as well as disruption to communication to otherwise viable neurons below the injury.

Clinical presentation: No damage to the brain, Local damage to the vascular and parenchymal structures of the spinal cord and initially only local damage to supra-spinal tracts (can present as Anterior cord syndrome or Brown-Sequard syndrome).

These injuries are rare in a clinical setting, and unlike gunshot, contusion or crush injuries they do not cause significant collateral damage (Norenberg, Smith & Marcillo 2004). However, damage to the vascular supply can have significant repercussion, especially when affecting the anterior spinal artery leading to anterior cord syndrome. This restricted form of injury is inflicted by a sharp instrument which generally penetrates and either incompletely or completely severs the spinal cord (Choo et al. 2008; Yeung & Karim 2012). Injury to the spinal cord is localised to the immediate injury zone (Figure 10). The severing of supraspinal axons causes ipsilateral loss of motor and proprioception followed immediately by vascular damage leading to local cord ischemia. Contralateral loss of pain and temperature sensation. Dependent on depth, angle, and location, penetration will interrupt autonomous function and feedback mechanisms between dorsal and ventral horn, also leading to loss of sense of deep touch, pressure, vibration. These injuries, although devastating, cause limited collateral damage (Figure 10 red circle). The severing of the spinal cord itself is, of course, a severe injury with significant clinical repercussions. However, at the histological level, this is the simplest form of spinal cord injury, with limited damage to local neurons and unified separation of longitudinal axons.

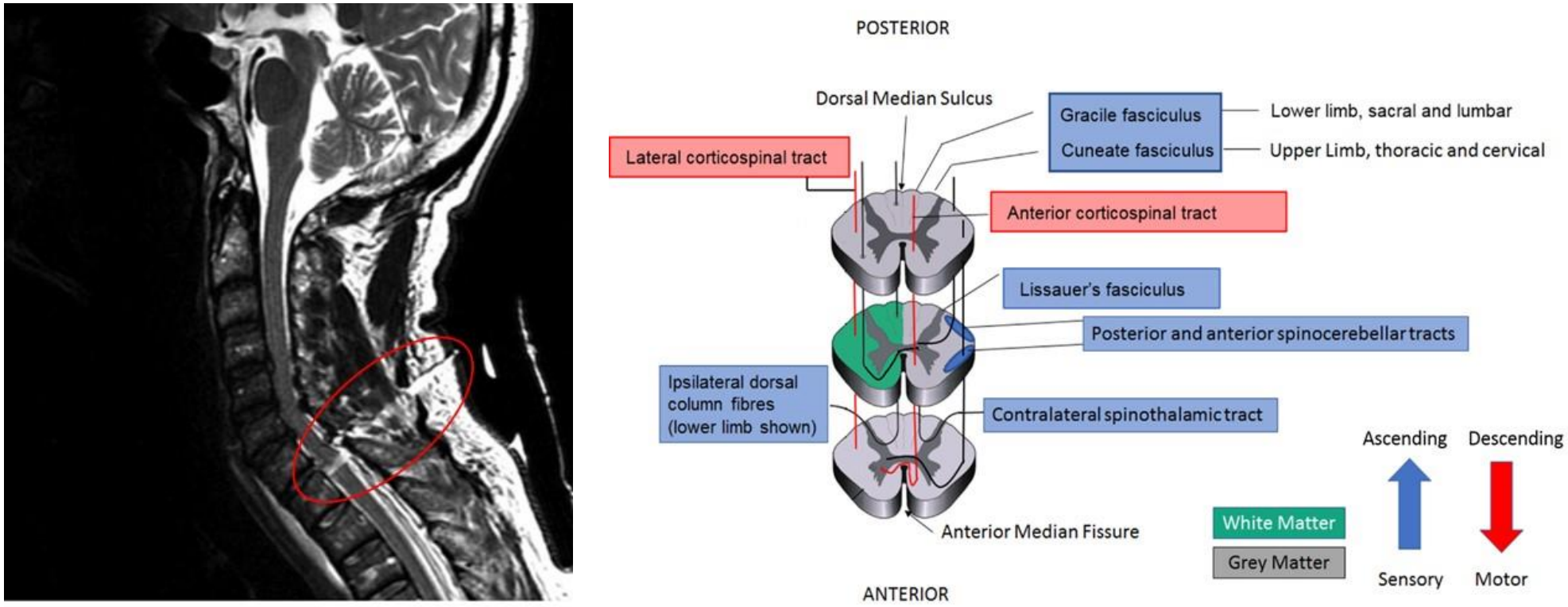

Figure 10: Nerve tracts - communication pathways

Sagittal MRI (Left): Example of a knife penetration wound severing the spinal cord with limited collateral damage. Drawing (Right): Not all nerve tracts shown. The image highlights that within the spinal cord (below the medulla) white and grey matter ascending and descending tracts travel longitudinally through the spinal cord. Decussation occurs either in the medulla (not shown) or locally dependent on tract. Following an injury to the spinal cord (below the medulla), Surrounding lateral white matter is damaged prior to grey matter. A lateral injury will first affect either anterior or posterior spinocerebellar tracts (proprioception). Next affected the lateral corticospinal tract (and rubrospinal tract not shown) (limb voluntary movement) and spinothalamic tracts (pain/temperature). Deep wounds will affect anterior and posterior feedback mechanisms. Posterior injuries will affect Dorsal columns (Gracile and Cuneate fasciculus) responsible for sensation (touch, vibration). Anterior injuries will affect anterior corticospinal tract trunk movement - shared with other brainstem pathways. Sagittal MRI: (Yeung & Karim 2012)

c) Contusion, Crush, Compression injuries with varying complexity cause indiscriminate local and distributed damage

These injuries are the most common spinal cord injury.

Clinical Presentation: Multifactorial damage to the surrounding osseous structures with collateral damage to the spinal cord and surrounding tissues.

Although primary aetiologies can broadly differ, at the cellular level, these injuries cause similar underlying physical damage (Figure 11), with the same consequential secondary injury events (Sekhon & Fehlings 2001). In many of these injuries, the damage to the spinal cord will spread across more than one vertebral segment (Watson & Harvey 2009; Watson & Kayalioglu 2009). The underlying cellular damage can be difficult to determine using standard non-invasive technologies, but this same technology will often reveal substantive damage to the osseous structures, related ligaments and structures surrounding the spinal cord. The presence of neurogenic shock and vasospasm complicates clinical assessment. However, rapid assessment followed by appropriate mitigation and rescue has been shown to optimise long-term outcomes (Schouten, Albert & Kwon 2012)

As these injuries contuse, crush or compress the spinal cord, the injury will not be as narrowly focal as the simplistic laceration injury (Choo et al. 2008). At the histological level, these injuries are broad which can cause widespread autonomic dysfunction and significant supra-spinal disruption. Descending axons are often immediately damaged over a distance of several millimetres.

Axon damage in combination with axon recoil further quickly increases the distance between severed proximal and distal injured stumps.

In the event of reunification, homologous reconnection would be improbable placing emphasis on neural plasticity for functional restoration.

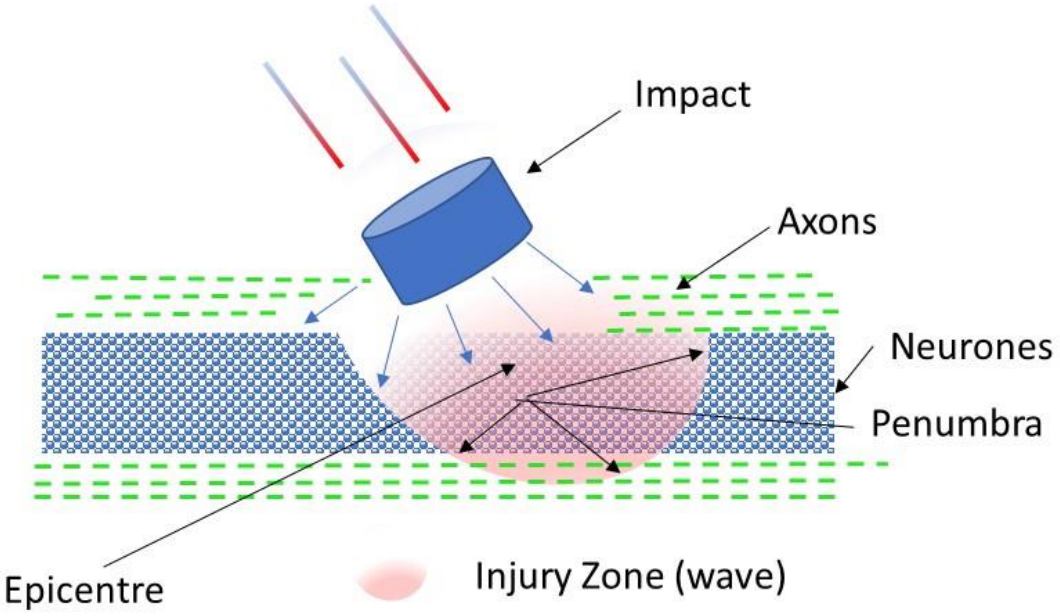

Figure 11: Contusion, crush, and compression injuries with varying complexity

At the impact zone, axons are severed or crushed, and surrounding cells are damaged. Damage to cells is highest at the epicentre. As the impact passes into the spinal cord proximal and distal damaged axon stump seal, but their fate differs. As axons seal, they are less susceptible to the local extracellular environment. However, surviving local neurons will be subjected to extracellular changes within the injury zone. The timeline for neuronal injury will, therefore, vary from the epicentre out to the penumbra.

Secondary Injury Events – Revisited

Beyond the primary injury, and at the molecular level, the mechanisms driving secondary injury events are (as previously stated) directly related to vascular/CSF disruption, the release of intracellular content, cell death and degeneration (Figure 12). However, for the most part, these issues directly affect neurons and supporting glia not injured axons (Figure 12). Therefore, there is good evidence, that early attenuation to the underlying mechanisms contributing to cell injury improves mitigation and improves prospects for cell rescue (Beattie et al. 2002; Kwon et al. 2004; Mortazavi et al. 2015; Profyris et al. 2004; Ropper 2001; Szabo 2005; Tator 1995; Tator & Fehlings 1991). This also extends out to the clinical management of spinal cord compression

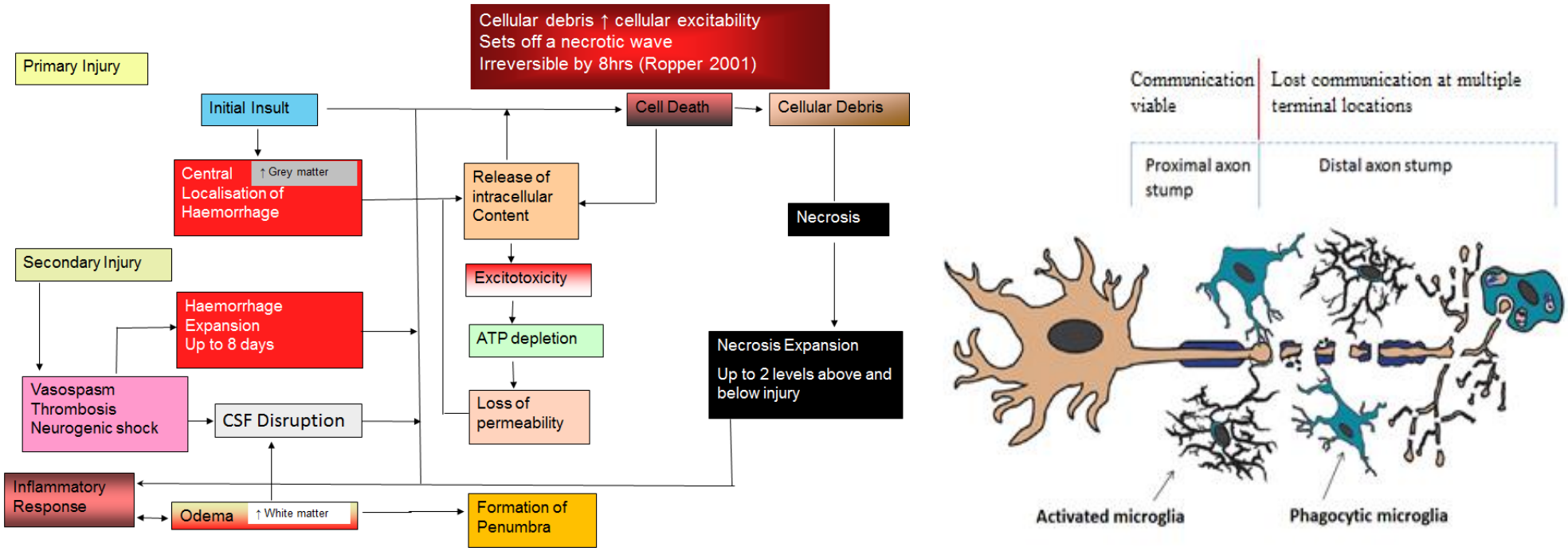

Figure 12: Secondary injury mechanisms (Figures 2 & 3) revisited

Following the primary injury, secondary injury events driven primarily by vascular disruption, the release of intracellular content and cell death continue until homoeostasis can be intrinsically reached (Beattie et al. 2002; Doble 1999). Picture Right: $Ca+^{2}$ influx triggers proximal and distal stumps of axons to seal stabilising intracellular content (Bradke, Fawcett & Spira 2012; Chierzi et al. 2005; Ertürk et al. 2007; Hellal et al. 2011; Wolf et al. 2001). Degeneration of the distal injured stump of the axon can commence as early as 4h post injury.

injuries (Raslan & Nemecek 2012), where there is good correlation between early decompression intervention and improvements in neurological AIS grade (Battistuzzo et al. 2015) (Figure 13).

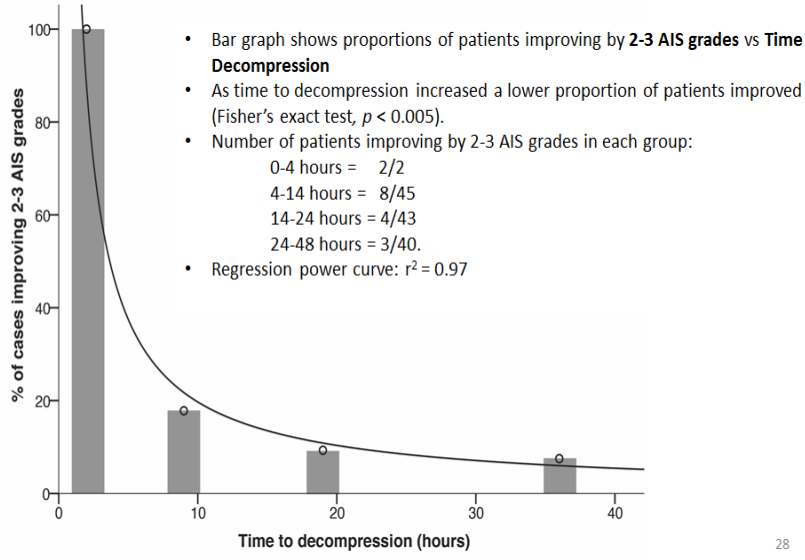

Figure 13: AIS grade vs. Time to Decompression

Bar graph highlights how early decompression of an injury zone can translate to significant improvements in AIS grade. Image (Battistuzzo et al. 2015) Under Licence 4017431413610.

In relation to supraspinal axons, there is some limited evidence suggesting axon tract re-attachment can reinstitute some supraspinal function (spinal cord myelorrhaphy [2]) (Canavero et al. 2016; Goodkin, Budzilovich & Campbell 1976; Jelliffe & Na 1903; Puchala & Windle 1977; Stauffer, Goodman & Nickel 1976; Stewart & Harte 1902). This is somewhat interesting because in the myelorrhaphy papers cited, no additional post-surgical functional loss was observed. It may, therefore, be appropriate to reconsider researching this approach at least as an acute measure following open reduction. Further, as the proximal injured axons continue to discharge electronic potentials post-injury, this may also suggest that new grafting technology may be a viable option (Pfister et al. 2006; Smith, Wolf & Meaney 2001) or as we suspect potentially in-vivo axon stretch growth.

[2] Reunification of the spinal cord through suture

Intervention Timing - Receptor sensitivity and secondary injury

As the wave of injury moves from the epicentre out to the penumbra (refer Figure 11 for detail), neurons and supporting cells affected by the primary injury will either die and contribute to excitotoxic events, or alternatively survive and be progressively subjected to the extracellular excitotoxic environment. Excitotoxicity interferes with homeostatic receptors α-amino-3-hydroxy-5-methyl-4-isoxazolepropionic acid (AMPA), Kainate and N-methyl-D-aspartate (NMDA), increasing membrane permeability for sodium and potassium and in the case of the NMDA receptor calcium (Doble 1999; Wolf et al. 2001). Thus pharmacological interventions such as Riluzole (Chow et al. 2012; Fehlings, Michael G et al. 2012; Wilson, Jefferson R & Fehlings 2014) and Magnesium Sulphate/ Polyethylene glycol (Kwon et al. 2009) delivered early in the intervention either block / antagonise receptor channels or are anti-glutamate agents that reduce effect of secondary injury in neurons (Figure 14).

In contrast, Calcium (Ca^{+}) influx into damaged supra-spinal axons triggers rapid sealing of the injured stumps. As Magnesium serves as a NMDA receptor antagonist through competitive inhibition of the receptors ion channel, this suggests that immediate targeting of the NMDA receptor to prevent damage to the neuron cell body may be contra-indicated as an immediate intervention for axons earlier than 2h post-injury (Figure 15).

Transportation – a factor in timing for treatment

Retrieval or transfer of patients following acute spinal cord injury is always a problematic undertaking, and it is well known to carry significant risk. Therefore, it can be anticipated that there will be a delay in transportation from the accident scene to a suitable definitive care centre. However, there is good evidence to suggest that interventions conducted within a 24h fare better than those treated after 24h (Ahn et al. 2011; Battistuzzo et al. 2015; Hadley et al. 2013; Walters et al. 2013; Wilson, J. R. et al. 2016)

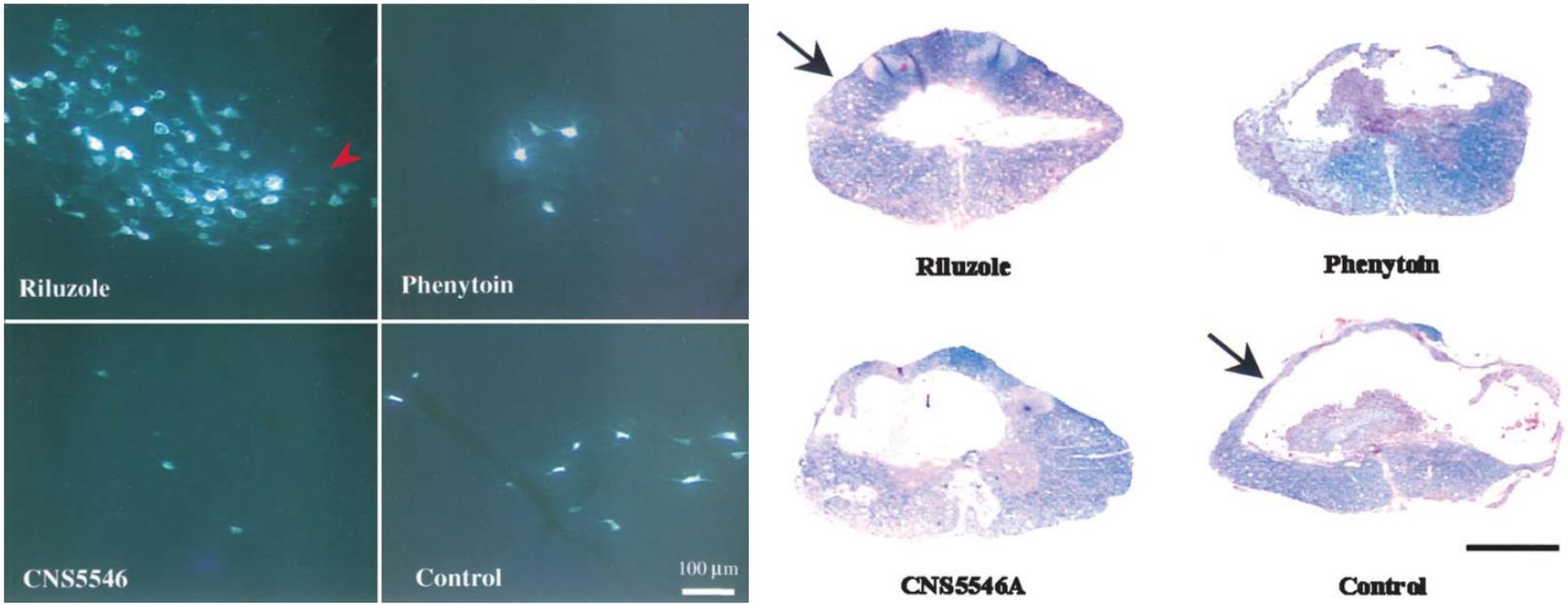

Figure 14: Riluzole compared with other treatments at 7weeks post-SCI (Rat)

A: Fluorescence micrographs showing retrogradely fluorogold labelled neurons in the red nucleus 7 weeks after a severe spinal cord compression injury. Red arrowhead indicates the large diameter cells, typifying magnocellular neurons, preferentially spared in the Riluzole group compared with other treatments. B: Representative cross sections of luxol fast blue–and H & E–stained SCI epicentre from riluzole-, phenytoin-,CNS5546A-, and control-treated cords. Note the preferential sparing of dorsolateral white matter columns, including the rubrospinal tract, in the riluzole, treated animals compared with controls (arrows). Bar = 1 mm. Comments and Image (Schwartz & Fehlings 2001) with permission

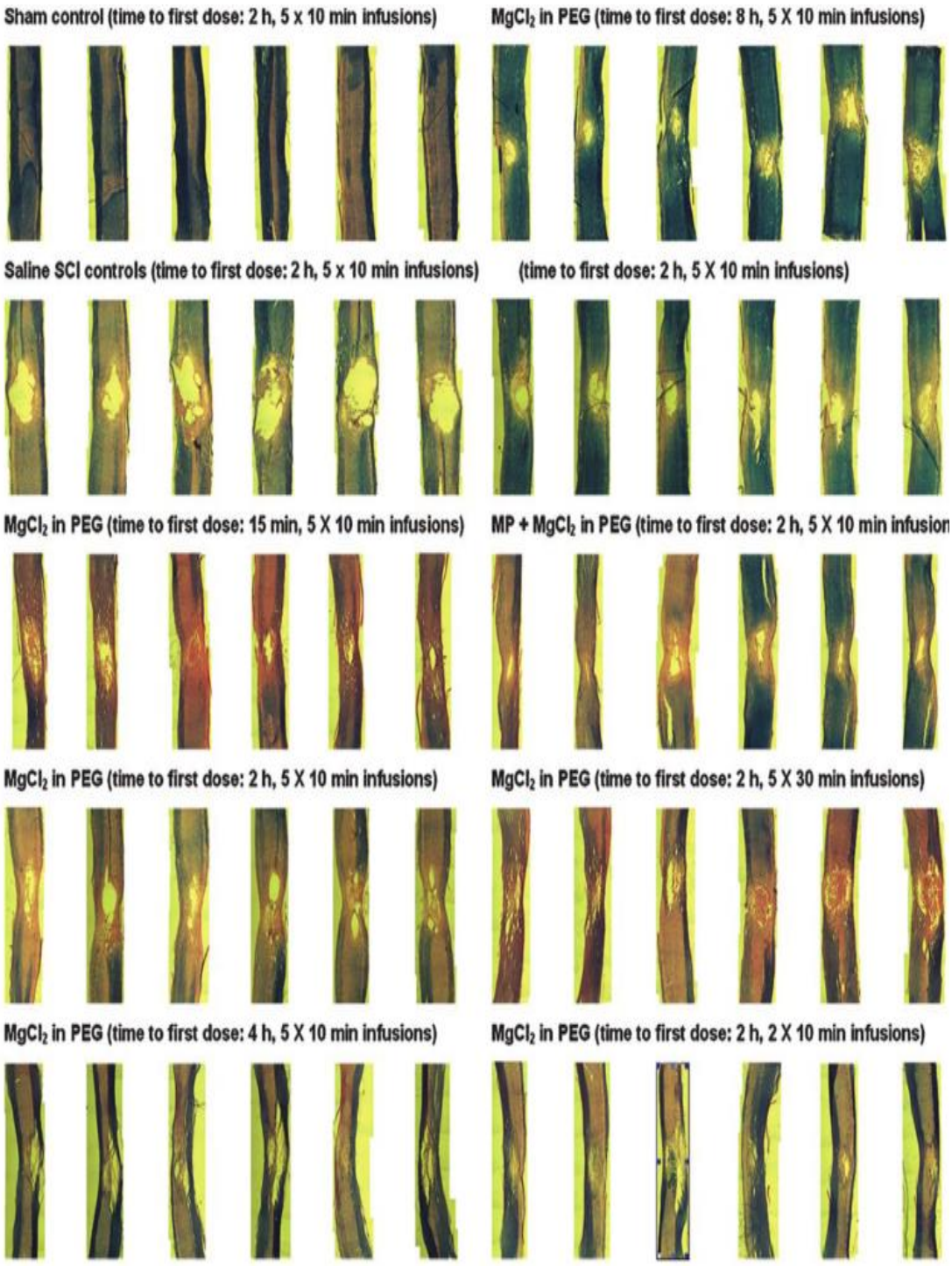

Figure 15: Time-dependent treatment targeting NMDA receptors

Image highlights the effects of $MgCl_2$ in PEG at different time-points. It shows significant cavitation in the saline controls as compared to the MgCl2 in PEG formulation at early administration time points. Image (Kwon et al. 2009) with permission 4035320799821

Consolidated – Timelines for intervention

The terms Acute, Sub-Acute, and Chronic have become embedded in the treatment of patients. Along with this terminology comes the expectation that there is linear injury progression. However, at the molecular level of injury we have shown that progression is staggered and has much shorter timeframes than at a clinical level. Therefore, there is some importance in consolidating the timeframes to determine more accurately "windows of opportunity**" (**Figure 16**)**

In this figure we introduce "Stabilised Injury" and suggest that this be included into the Secondary Injury terminology for spinal cord injured patients.

Windows of Opportunity - Summary

- **There is good evidence that the intervention time frame for supraspinal axons is optimal within 4h.** If reunification of proximal and distal injured stumps (although unlikely to be homologous) are successful, it theoretically will provide the potential for functional return through neuroplasticity. Beyond this period, the distal axon stump can degenerate causing diffuse or distributed damage. Grafting, implants, or In-vivo axon stretch growth should be considered as additional options to restore these connections beyond this timeframe.

- **There is good evidence to support delivery of cell death mitigation treatments from 2h post-injury, optimally before 24h has elapsed.** These interventions should continue to be delivered out to 10 days post injury. Although more research is required, current evidence suggests that beyond 10 days of an injury, no further cell rescue will occur.

- **Beyond 10 days, there is good evidence to support that the injury is stabilised and interventions are reactionary.** Improvements in functionality can be achieved during this time through neuroplasticity.

- **There is emerging evidence to suggest that stem cell interventions should be delivered beyond the Acute injury phase.** Although more research is required, optimal delivery would be in the Stabilised injury phase of intervention.
- **Although all patients differ, Chronic injury can be considered to occur from 24 months.** This is an administrative point at which the new "normality" for the patient is determined.

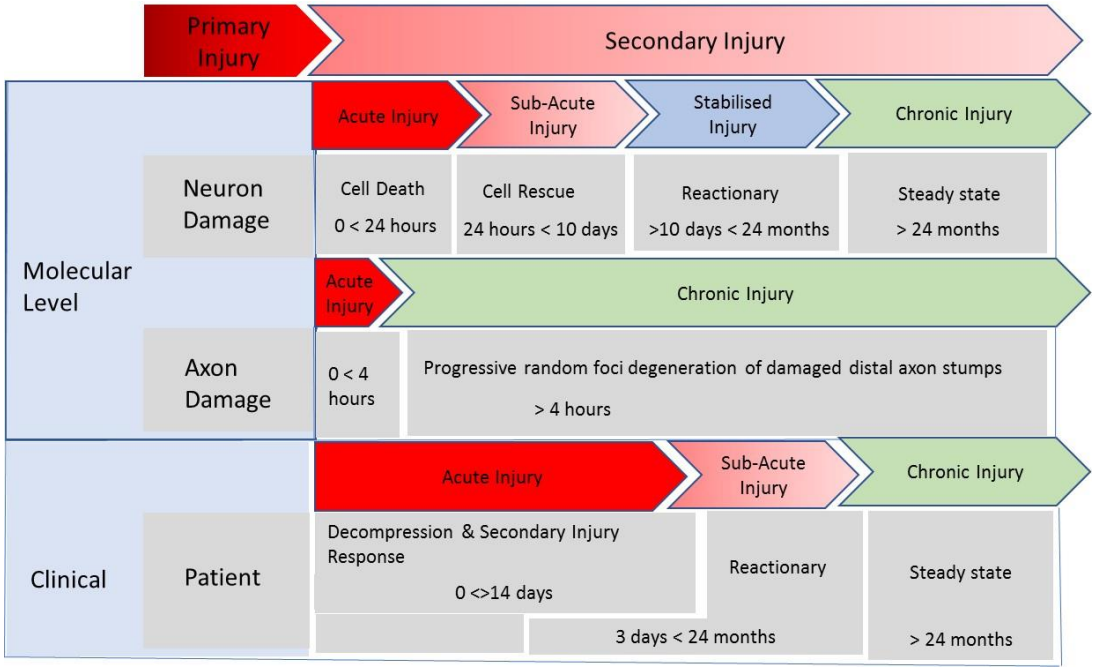

Figure 16: Time-course (collated) Clinical vs. Molecular level injury

Molecular level: At this level, the injury time-course is simplified to local damage caused to neurons, surrounding support cells, intracellular and extracellular mechanisms. Injury to the spinal cord initiates graded vascular and CSF disruption and inflammatory responses which in combination with glutamate excitotoxicity or calcium, sodium/potassium imbalance contribute to cell death (Profyris et al. 2004; Silva et al. 2014; Tarlov 1957). Thus, attenuation of local damage in response to the SCI is time critical and measured in hours. Wallerian degeneration of axotomized distal axon stumps commences as early as 4h post injury but may continue for many months, even years.

Clinical: Clinicians typically view the first 14 days as being within the acute period, where, intervention can yield clinical improvements not necessarily specific to the spinal cord. Beyond this period, it then follows that the sub-acute phase will extend out until injury stabilisation occurs. Therefore, the sub-acute phase of intervention is reactionary based on existing problems that continue beyond the acute phase of injury. Chronic injury represents steady state, and this is considered normalisation suitable for compensation payouts

References

Aarabi, B, Koltz, M & Ibrahimi, D 2008, 'Hyperextension cervical spine injuries and traumatic central cord syndrome', *Neurosurg Focus*, vol. 25, no. 5, p. E9.

Access Economics Pty Ltd. 2009, *The economic cost of spinal cord injury and traumatic brain injury in Australia*, Access Economics

Ackery, A, Tator, CH & Krassioukov, A 2004, 'A Global Perspective on Spinal Cord Injury Epidemiology', *Journal of Neurotrauma*, vol. 21, no. 10, pp. 1355-1370.

Ahn, H, Singh, J, Nathens, A, MacDonald, RD, Travers, A, Tallon, J, Fehlings, MG & Yee, A 2011, 'Pre-hospital care management of a potential spinal cord injured patient: a systematic review of the literature and evidence-based guidelines', *J Neurotrauma*, vol. 28, no. 8, Aug, pp. 1341-1361.

American Spinal Injury Association 2015, 'ASIA Impairment Scale (AIS)', International Standards for Neurological Classification of Spinal Cord Injury, in AI Scale (ed.)American Spinal Injury Association

Battistuzzo, CR, Armstrong, A, Clark, J, Worley, L, Sharwood, L, Lin, P, Rooke, G, Skeers, P, Nolan, S, Geragthy, T, Nunn, A, Brown, DJ, Hill, S, Alexander, J, Millard, M, Cox, SF, Rao, S, Watts, A, Goods, L, Allison, GT, Laurenson, J, Cameron, P, Mosley, I, Liew, SM, Geddes, T, Middleton, J, Buchanan, J, Rosenfeld, JV, Bernard, S, Atresh, S, Patel, A, Schouten, R, Freeman, BJ, Dunlop, SA & Batchelor, PE 2015, 'Early decompression following cervical spinal injury: Examining the process of care from accident scene to surgery', *J Neurotrauma*, vol. XX, no. 00, 10/12/2010.

Beattie, MS, Hermann, GE, Rogers, RC & Beshnahan, JC 2002, 'Cell death in models of spinal cord injury', in L McKerracher, G Doucet & S Rossignol (eds), *Progress in Brain Research*, vol. 137, Elsevier Science B.V, p. 37.

Bickenbach, J, Boldt, I, Brinkhof, M, Chamberlain, J, Cripps, R, Fitzharris, M, Lee, B, Marshall, R, Meier, S, Neukamp, M, New, P, Nicol, R, Officer, A, Perez, B, von Groote, P & Wing, P 2012, 'A global picture of spinal cord injury', in JE Bickenbach, C Bodine, D Brown, A Burns, R Campbell, D Cardenas, S Charlifue, Y Chen, D Gray, L Li, A Officer, M Post, T Shakespeare, A Sinnot, P von Groote & X Xiong (eds), *International Perspective on Spinal Cord Injury*, World Health Organization, The International Spinal Cord Society, Malta, pp. 11-28.

Bradke, F, Fawcett, JW & Spira, ME 2012, 'Assembly of a new growth cone after axotomy: the precursor to axon regeneration', *Nat Rev Neurosci*, vol. 13, no. 3, pp. 183-193.

Breig, A 1978, *Adverse Mechanical Tension in the Central Nervous System - An analysis of cause and effect- relief by functional neurosurgery*, Almqvist and Wiksell International: Stockholm, Sweden and John Wiley and Sons: New York.

Canavero, S, Ren, X, Kim, CY & Rosati, E 2016, 'Neurologic foundations of spinal cord fusion (GEMINI)', *Surgery*, vol. 160, no. 1, 7//, pp. 11-19.

Cao, Y, Chen, Y & DeVivo, M 2011, 'Lifetime direct costs after spinal cord injury', *Topics in Spinal Cord Injury Rehabilitation*, vol. 16, no. 4, pp. 10-16.

CDIC 2013, *Chronic Diseases and Injuries in Canada*, 3, vol. 33, University of British Columbia, Vancouver and Rick Hansen Institute, Vancouver, British Columbia, Canada, Canada.

Chierzi, S, Ratto, GM, Verma, P & Fawcett, JW 2005, 'The ability of axons to regenerate their growth cones depends on axonal type and age, and is regulated by calcium, cAMP and ERK', *European Journal of Neuroscience*, vol. 21, no. 8, pp. 2051-2062.

Chiu, WT, Lin, HC, Lam, C, Chu, SF, Chiang, YH & Tsai, SH 2010, 'Review paper: Epidemiology of traumatic spinal cord injury: comparisons between developed and developing countries', *Asia Pac J Public Health*, vol. 22, no. 1, Jan, pp. 9-18.

Choo, AM, Liu, J, Dvorak, M, Tetzlaff, W & Oxland, TR 2008, 'Secondary pathology following contusion, dislocation, and distraction spinal cord injuries', *Exp Neurol*, vol. 212, no. 2, pp. 490-506.

Chow, DS, Teng, Y, Toups, EG, Aarabi, B, Harrop, JS, Shaffrey, CI, Johnson, MM, Boakye, M, Frankowski, RF & Fehlings, MG 2012, 'Pharmacology of riluzole in acute spinal cord injury', *Journal of Neurosurgery: Spine*, vol. 17, no. Suppl1, pp. 129-140.

Devivo, MJ 2012, 'Epidemiology of traumatic spinal cord injury: trends and future implications', *Spinal Cord*, Jan 2012, pp. 1-8.

DeVivo, MJ, Chen, Y, Mennemeyer, S & Deutsch, A 2011, 'Costs of Care Following Spinal Cord Injury', *Topics in Spinal Cord Injury Rehabilitation*, vol. 16, no. 4, pp. 1-9.

Doble, A 1999, 'The role of excitotoxicity in neurodegenerative disease: implications for therapy', *Pharmacology & therapeutics*, vol. 81, no. 3, pp. 163-221.

Draulans, N, Kiekens, C, Roels, E & Peers, K 2011, 'Etiology of spinal cord injuries in Sub-Saharan Africa', *Spinal Cord*, vol. 49, no. 12, Dec, pp. 1148-1154.

Ertürk, A, Hellal, F, Enes, J & Bradke, F 2007, 'Disorganized Microtubules Underlie the Formation of Retraction Bulbs and the Failure of Axonal Regeneration', *The Journal of Neuroscience*, vol. 27, no. 34, August 22, 2007, pp. 9169-9180.

Ezzati, M, Lopez, AD, Rodgers, A, Vander Hoorn, S & Murray, CJL 2002, 'Selected major risk factors and global and regional burden of disease', *The Lancet*, vol. 360, no. 9343, Feb 11, pp. 1347-1360.

Fehlings, MG, Vaccaro, A, Wilson, JR, Singh, A, W. Cadotte, D, Harrop, JS, Aarabi, B, Shaffrey, C, Dvorak, M, Fisher, C, Arnold, P, Massicotte, EM, Lewis, S & Rampersaud, R 2012, 'Early versus Delayed Decompression for Traumatic Cervical Spinal Cord Injury: Results of the Surgical Timing in Acute Spinal Cord Injury Study (STASCIS)', *PLoS One*, vol. 7, no. 2, p. e32037.

Fehlings, MG, Wilson, JR, Frankowski, RF, Toups, EG, Aarabi, B, Harrop, JS, Shaffrey, CI, Harkema, SJ, Guest, JD & Tator, CH 2012, 'Riluzole for the treatment of acute traumatic spinal cord injury: rationale for and design of the NACTN Phase I clinical trial', *Journal of Neurosurgery: Spine*, vol. 17, no. Suppl1, pp. 151-156.

Goodkin, R, Budzilovich, GN & Campbell, JB 1976, 'Myelorrhaphy: Part II', *Spine (Phila Pa 1976)*, vol. 1, no. 4, pp. 193-196.

Gosch, HH, Gooding, E & Schneider, RC 1970, 'Cervical spinal cord hemorrhages in experimental head injuries', *Journal of Neurosurgery*, vol. 33, no. 6, pp. 640-645.

Hadley, MN, Walters, BC, Grabb, P, Oyesiku, NM, Przbylski, GJ, Resnick, DK & Ryken, TC 2013, *Guidelines for the Management of Acute Cervical Spine and Spinal Cord Injuries*, American Association of Neurological Surgeons., America.

Hellal, F, Hurtado, A, Ruschel, J, Flynn, KC, Laskowski, CJ, Umlauf, M, Kapitein, LC, Strikis, D, Lemmon, V, Bixby, J, Hoogenraad, CC & Bradke, F 2011, 'Microtubule stabilization reduces scarring and causes axon regeneration after spinal cord injury', *Science*, vol. 331, no. 6019, Feb 18, pp. 928-931.

Jelliffe & Na 1903, 'Myelorrhaphy Followed by Return of Function', *The Journal of Nervous and Mental Disease*, vol. 30, no. 2, p. 124.

Jones, CF, Lee, JH, Burstyn, U, Okon, EB, Kwon, BK & Cripton, PA 2013, 'Cerebrospinal fluid pressures resulting from experimental traumatic spinal cord injuries in a pig model', *J Biomech Eng*, vol. 135, no. 10, Oct, p. 101005.

Kirshblum, SC, Burns, SP, Biering-Sorensen, F, Donovan, W, Graves, DE, Jha, A, Johansen, M, Jones, L, Krassioukov, A, Mulcahey, MJ, Schmidt-Read, M & Waring, W 2011, 'International standards for neurological classification of spinal cord injury (Revised 2011)', *J Spinal Cord Med*, vol. 34, no. 6, pp. 535-546.

Knutsdottir, S, Thorisdottir, H, Sigvaldason, K, Jonsson, H, Jr., Bjornsson, A & Ingvarsson, P 2012, 'Epidemiology of traumatic spinal cord injuries in Iceland from 1975 to 2009', *Spinal Cord*, vol. 50, no. 2, Feb, pp. 123-126.

Kwon, BK, Roy, J, Lee, JH, Okon, E, Zhang, H, Marx, JC & Kindy, MS 2009, 'Magnesium chloride in a polyethylene glycol formulation as a neuroprotective therapy for acute spinal cord injury: preclinical refinement and optimization', *Journal of Neurotrauma*, vol. 26, no. 8, pp. 1379-1393.

Kwon, BK, Tetzlaff, W, Grauer, JN, Beiner, J & Vaccaro, AR 2004, 'Pathophysiology and pharmacologic treatment of acute spinal cord injury', *The Spine Journal*, vol. 4, no. 4, pp. 451-464.

Lee, BB, Cripps, RA, Fitzharris, M & Wing, PC 2014, 'The global map for traumatic spinal cord injury epidemiology: update 2011, global incidence rate', *Spinal Cord*, vol. 52, no. 2, 02//print, pp. 110-116.

Lenehan, B, Street, J, Kwon, BK, Noonan, V, Zhang, H, Fisher, CG & Dvorak, MF 2012, 'The epidemiology of traumatic spinal cord injury in British Columbia, Canada', *Spine (Phila Pa 1976)*, vol. 37, no. 4, Feb 15, pp. 321-329.

Leucht, P, Fischer, K, Muhr, G & Mueller, EJ 2009, 'Epidemiology of traumatic spine fractures', *Injury*, vol. 40, no. 2, Feb, pp. 166-172.

Maak, T 2006, 'Dynamic intervertebral foramen narrowing during whiplash', Yale University School of Medicine, Degree of Doctor of Medicine thesis, Yale University, New Haven Connecticut.

Meaney, DF, Smith, DH, Shreiber, DI, Bain, AC, Miller, RT, Ross, DT & Gennarelli, TA 1995, 'Biomechanical analysis of experimental diffuse axonal injury', *Journal of Neurotrauma*, vol. 12, no. 4, pp. 689-694.

Mortazavi, MM, Verma, K, Harmon, OA, Griessenauer, CJ, Adeeb, N, Theodore, N & Tubbs, RS 2015, 'The microanatomy of spinal cord injury: A review', *Clinical Anatomy*, vol. 28, no. 1, pp. 27-36.

Ning, GZ, Yu, TQ, Feng, SQ, Zhou, XH, Ban, DX, Liu, Y & Jiao, XX 2011, 'Epidemiology of traumatic spinal cord injury in Tianjin, China', *Spinal Cord*, vol. 49, no. 3, Mar, pp. 386-390.

Norenberg, MD, Smith, J & Marcillo, A 2004, 'The pathology of human spinal cord injury: defining the problems', *J Neurotrauma*, vol. 21, no. 4, Apr, pp. 429-440.

Norton, L 2010, *Spinal cord injury, Australia 2007-08*, Australian Government, Canberra.

O'Connor, PJ & Brown, D 2006, 'Relative risk of spinal cord injury in road crashes involving seriously injured occupants of light passenger vehicles', *Accident Analysis & Prevention*, vol. 38, no. 6, 11//, pp. 1081-1086.

Panjabi, MM, Cholewicki, J, Nibu, K, Grauer, JN, Babat, LB & Dvorak, J 1998, 'Mechanism of whiplash injury', *Clinical biomechanics*, vol. 13, no. 4–5, 6//, pp. 239-249.

Pfister, BJ, Iwata, A, Taylor, AG, Wolf, JA, Meaney, DF & Smith, DH 2006, 'Development of transplantable nervous tissue constructs comprised of stretch-grown axons', *J Neurosci Methods*, vol. 153, no. 1, May 15, pp. 95-103.

Profyris, C, Cheema, SS, Zang, D, Azari, MF, Boyle, K & Petratos, S 2004, 'Degenerative and regenerative mechanisms governing spinal cord injury', *Neurobiol Dis*, vol. 15, no. 3, Apr, pp. 415-436.

Puchala, E & Windle, WF 1977, 'The possibility of structural and functional restituion after spinal cord injury. A review', *Exp Neurol*, vol. 55, no. 1, pp. 1-42.

Raslan, AM & Nemecek, AN 2012, 'Controversies in the surgical management of spinal cord injuries', *Neurol Res Int*, vol. 2012, p. 417834.

Ropper, AH 2001, 'Traumatic injuries of the head and spine', *HARRISONS PRINCIPLES OF INTERNAL MEDICINE*, vol. 2, pp. 2434-2441.

Sandler, AN & Tator, CH 1976, 'Review of the effect of spinal cord trauma on the vessels and blood flow in the spinal cord', *Journal of Neurosurgery*, vol. 45, no. 6, pp. 638-646.

Schouten, R, Albert, T & Kwon, BK 2012, 'The spine-injured patient: initial assessment and emergency treatment', *J Am Acad Orthop Surg*, vol. 20, no. 6, Jun, pp. 336-346.

Schwab, ME & Bartholdi, D 1996, 'Degeneration and regeneration of axons in the lesioned spinal cord', *Physiological Reviews*, vol. 76, no. 2, 1996/04//, p. 319+.

Schwartz, G & Fehlings, MG 2001, 'Evaluation of the neuroprotective effects of sodium channel blockers after spinal cord injury: improved behavioral and neuroanatomical recovery with riluzole', *Journal of Neurosurgery: Spine*, vol. 94, no. 2, pp. 245-256.

Sekhon, LHS & Fehlings, MG 2001, 'Epidemiology, Demographics, and Pathophysiology of Acute Spinal Cord Injury', *Spine (Phila Pa 1976)*, vol. 26, no. 245, pp. S2-S12.

Silva, NA, Sousa, N, Reis, RL & Salgado, AJ 2014, 'From basics to clinical: a comprehensive review on spinal cord injury', *Prog Neurobiol*, vol. 114, Mar, pp. 25-57.

Smith, DH, Meaney, DF & Shull, WH 2003, 'Diffuse axonal injury in head trauma', *J Head Trauma Rehabil*, vol. 18, no. 4, Jul-Aug, pp. 307-316.

Smith, DH, Wolf, JA & Meaney, DF 2001, 'A new strategy to produce sustained growth of central nervous system axons: Continuous Mechanical Tension', *Tissue Engineering*, vol. 7, no. 2, pp. 131-139.

Stauffer, ES, Goodman, FG & Nickel, VL 1976, 'Myelorrhaphy: Part I', *Spine (Phila Pa 1976)*, vol. 1, no. 4, pp. 189-192.

Stewart, FT & Harte, RH 1902, 'Myelorrhaphy', *Journal of the American Medical Association*, vol. XXXVIII, no. 25, pp. 1626-1626.

Szabo, C 2005, 'Mechanisms of cell necrosis', *Critical Care Medicine*, vol. 33, no. Suppl, pp. S530-S534.

Tarlov, IM 1957, *Spinal cord compression: mechanism of paralysis and treatment*, Thomas.

Tator, CH 1990, 'Review of experimental spinal cord injury with emphasis on the local and systemic circulatory effects', *Neuro-Chirurgie*, vol. 37, no. 5, pp. 291-302.

Tator, CH 1995, 'Update on the Pathophysiology and Pathology of Acute Spinal Cord Injury', *Brain Pathology*, vol. 5, pp. 407-413.

Tator, CH & Fehlings, MG 1991, 'Review of the secondary injury theory of acute spinal cord trauma with emphasis on vascular mechanisms', *Journal of Neurosurgery*, vol. 75, no. 1, pp. 15-26.

US National Spinal Cord Injury Statistical Center 2014, *Complete Public Version of The 2012 Annual Statistical Report for the Spinal Cord Injury Model Systems*, National Spinal Cord Injury Statistical Center, Birmingham, Alabama.

Walters, BC, Hadley, MN, Hurlbert, RJ, Aarabi, B, Dhall, SS, Gelb, DE, Harrigan, MR, Rozelle, CJ, Ryken, TC & Theodore, N 2013, 'Guidelines for the Management of Acute Cervical Spine and Spinal Cord Injuries: 2013 Update', *Neurosurgery*, vol. 60, pp. 82-91.

Watson, C & Harvey, AR 2009, 'Chapter 11 - Projections from the Brain to the Spinal Cord', in CWP Kayalioglu (ed.), *The Spinal Cord*, Academic Press, San Diego, pp. 168-179.

Watson, C & Kayalioglu, G 2009, 'Chapter 1 - The Organization of the Spinal Cord', in CWP Kayalioglu (ed.), *The Spinal Cord*, Academic Press, San Diego, pp. 1-7.

Whiteneck, GG, Charlifue, SW, Frankel, HL, Fraser, MH, Gardner, BP, Gerhart, KA, Krishnan, KR, Menter, RR, Nuseibeh, I, Short, DJ & Silver, JR 1992, 'Mortality, morbidity, and psychosocial outcomes of persons spinal cord injured more than 20 years ago', *Paraplegia*, vol. 30, no. 9, 09//print, pp. 617-630.

Wilson, JR & Fehlings, MG 2014, 'Riluzole for acute traumatic spinal cord injury: a promising neuroprotective treatment strategy', *World neurosurgery*, vol. 81, no. 5, pp. 825-829.

Wilson, JR, Voth, J, Singh, A, Middleton, J, Jaglal, SB, Singh, JM, Mainprize, TG, Yee, A & Fehlings, MG 2016, 'Defining the Pathway to Definitive Care and Surgical Decompression after Traumatic Spinal Cord Injury: Results of a Canadian Population-Based Cohort Study', *J Neurotrauma*, Feb 11.

Wolf, JA, Stys, PK, Lusardi, T, Meaney, DF & Smith, DH 2001, 'Traumatic Axonal Injury Induces Calcium Influx Modulated by Tetrodotoxin-Sensitive Sodium Channels', *The Journal of Neuroscience*, vol. 21, no. 6, pp. 1923-1930.

Wyndaele, M & Wyndaele, JJ 2006, 'Incidence, prevalence and epidemiology of spinal cord injury: what learns a worldwide literature survey?', *Spinal Cord*, vol. 44, no. 9, Sep, pp. 523-529.

Yeung, J & Karim, A 2012, 'Complete spinal cord transection from a stab wound with surgical precision', *Journal of emergencies, trauma, and shock*, vol. 5, no. 2, p. 204.

Part 2 - Experimental

Chapter 3. Axon stretch growth - An early translational perspective

Background

There is a paucity of literature relating to the natural biological events associated with axon stretch growth. Much of what is known has been concluded from observations on the behaviour of the spinal cord during flexion and extension and the cord's underlying microscopic histology.

When performing neck flexion and extension, the measured human cervical spinal canal increases in length - Anterior wall ~15mm to Posterior surface ~50mm (O'Connell 1955) (Figure 17). During this time, the termination of the spinal cord (*conus medullaris*) does not appreciably move longitudinally within the spinal canal (Breig 1960, 1970; Fettes et al. 2006). The spinal cord must therefore adapt.

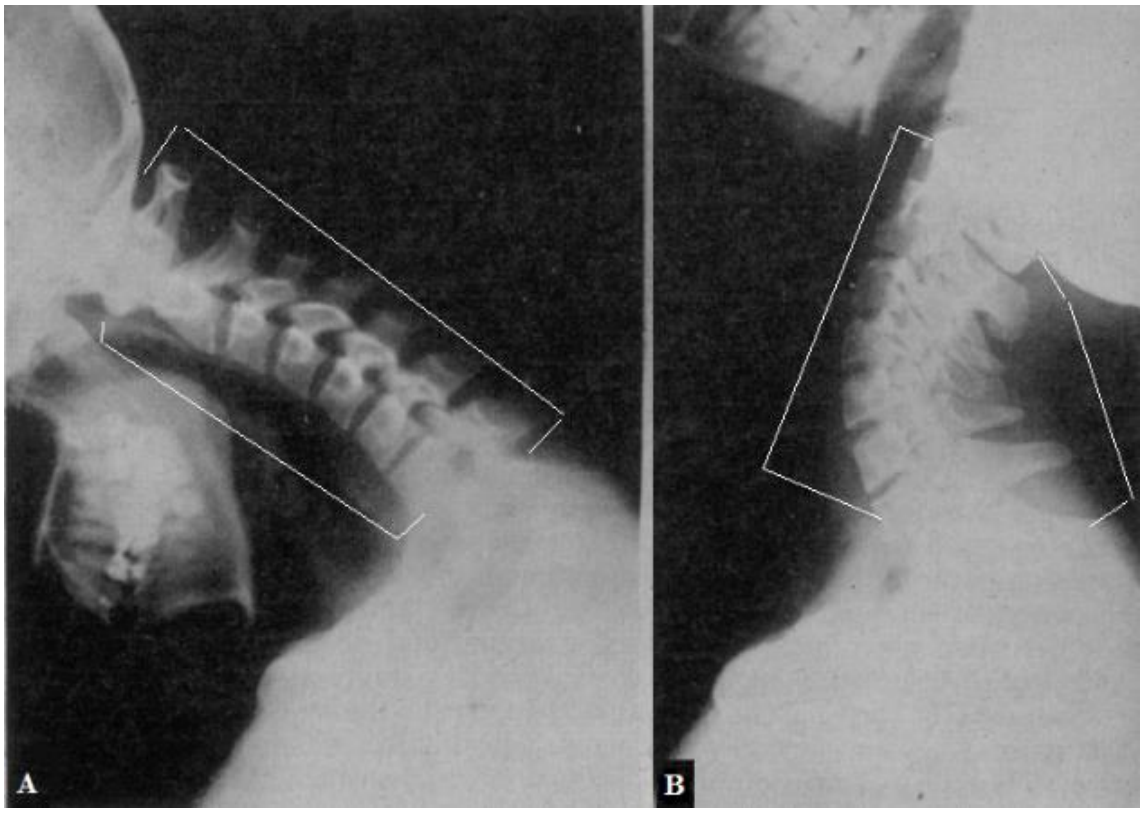

Figure 17: Original radiograph cervical spine in flexion (A) and extension (B)

adapted from (O'Connell 1955) under license 3967350299754

Investigations in the early 1960's by Breig suggested that the spinal cord does not move longitudinally but elongates like a concertina (Breig 1960). However, other research suggested the spinal cord moved up and down and stretched to adapt (Adams & Logue 1971; Reid 1960).

Breig's histological sagittal silver stained sections of the spinal cord (Breig 1978), show that when not under tension, the lateral longitudinal axons of the long nerve tracts retain a wavy appearance (Figure 18B) but, when tension is applied to the rostral or caudal spinal cord, these axons straighten (Figure 18A). This behaviour is in contrast to the most medial structures (predominantly interneurons and cell bodies) which maintain the classical spaghetti appearance (Figure 18 Inset).

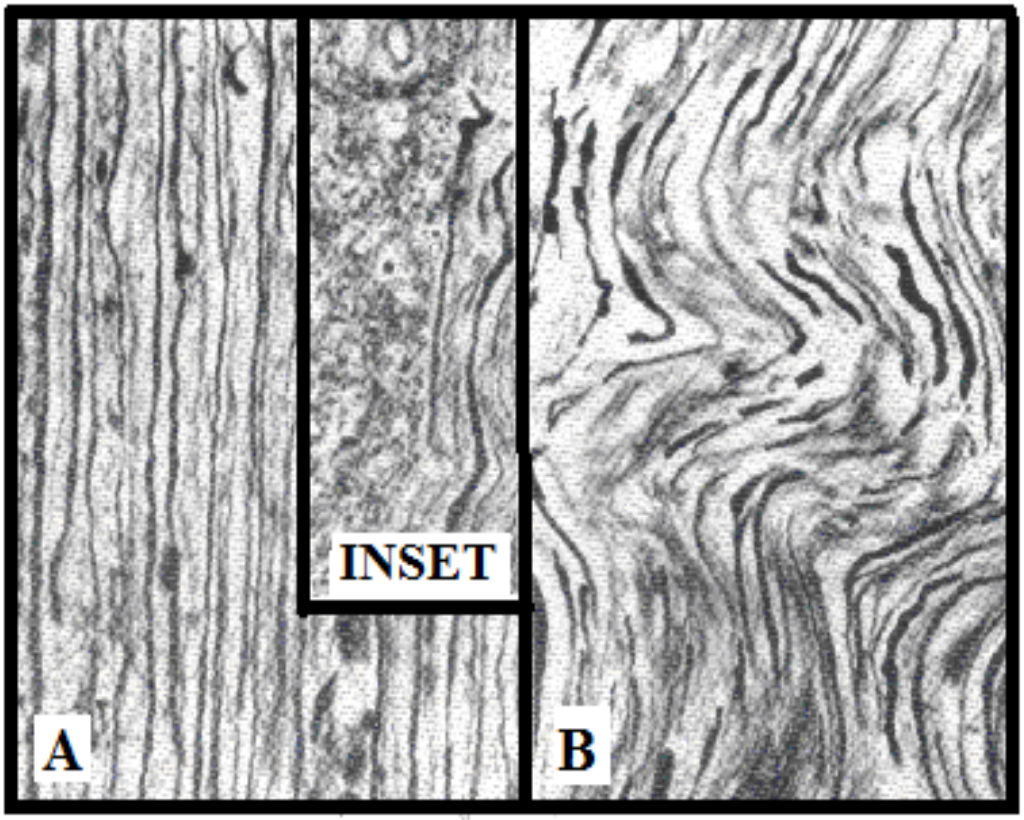

Figure 18: Longitudinal sagittal sections of the spinal cord (silver stained)

The inset shows the boundary between the spinal cords grey (Left) and white matter (right) during quiescence. If during flexion or extension longitudinal tension is applied to the cord, the wavy appearance of white matter (Magnified panel B) can straighten thus aligning the axons (Magnified panel A). Adapted image from (Breig 1978) under license 3967350299754.

Modelling[3] suggests, if at the peak of vertebral transition the measured length of the spinal canal and spinal cord (including the *filum terminale*) were the same, then the movement of the spinal cord towards the shortest axis within the spinal canal would be sufficient to prevent appreciable longitudinal movement of the spinal cord. However, in cadaver and therefore in the absence of a pressurised spinal canal, a necroscopy spinal cord (i.e. not fixed) has been shown to separate during flexion and return during extension (Figure 19) demonstrating the presence of some tension.

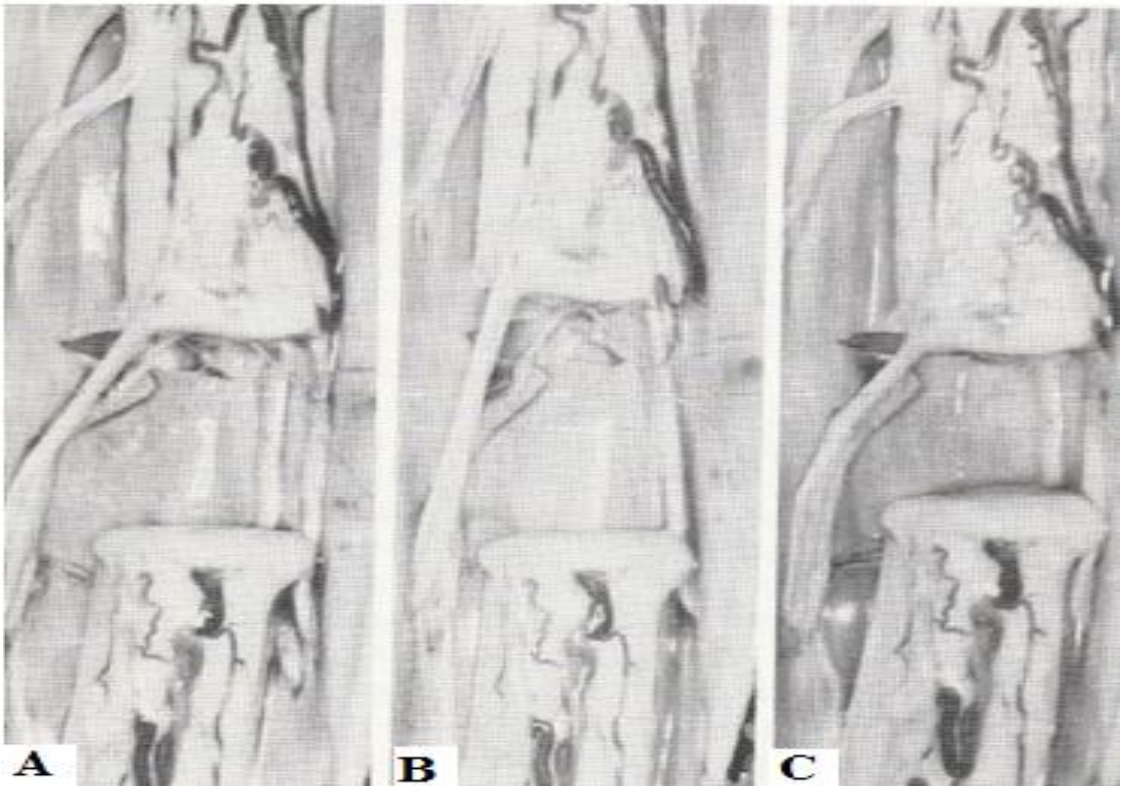

Figure 19: Cadaver spinal cord response to axial load on the pons-cord tract

The figure shows a transverse section of the spinal cord at the (thoracic region) at various postures of the thoracolumbar spine: A: Neutral Posture, B: following Flexion, C: following Extension. Adapted Image from (Breig 1978) under license 3967350299754

[3] If both a 500mm long 10mm diameter string and 15mm diameter clear hollow tube are marked 2/3rds along the longitudinal length and the string then inserted into the tube and fixed at both ends, it is possible to bend the tube from a straight position to simulate spinal curvature without displacing the marked point on the string.

These observations support the view that during flexion and extension, the spinal cord adapts to osseous movement by initially moving towards the shortest longitudinal axis within the spinal canal. As the spinal cord is anchored both rostrally and caudally, tension in combination with the diameter of the spinal cord is sufficient for axons on the outer lateral surface to straighten. At the point of maximum straightening of these axons, there is a reliance on viscoelastic or intercalated growth properties.

Viscoelastic and Intercalated growth properties

The viscoelastic properties of the spinal cord allow longitudinally aligned axons to initially stretch (thin) to accommodate transient changes in length. However, when tension is removed, the axon returns to original length and girth (Campenot 1985; Dennerll et al. 1989). Long-term there are opposing responses - intercalated growth (Dennerll et al. 1989; Mitchison & Kirschner 1988) and sinusoidal retraction (Dennerll et al. 1989; George et al. 1988). When axons or dendrites are exposed to continuously applied forces of ~1^{-6} N and tension is not above membrane disruption threshold, during periods of dormancy, growth occurs through intercalated mass addition i.e. it is reliant on microtubule assembly.

There are three phases of neurite response to tensile force: (1) Viscoelastic (passive), (2) Mass Addition reliant on microtubule assembly (Active) and (3) Sinusoidal Retraction (Active) (Campenot 1985; Dennerll et al. 1989).

Boundaries of axon stretch growth

Spinal nerve roots that attach to the spinal cord have similar properties to peripheral nerves (about 15% of original length stretch capability). However, under extreme tension, spinal nerve roots commonly avulse within the spinal cord funiculus before this limit is reached (Sunderland & Bradley 1960), thus indicating

a potential upper stretch threshold of below 15% of their length for spinal cord white matter tract fibres.

Within definable boundaries, intercalated loss or addition of the axon membrane can routinely occur during dormancy (Campenot 1985; Lamoureux et al. 2010) outside of these boundaries; membrane disruption causes localised metabolic collapse (Profyris et al. 2004).

Given that these boundaries exist, is there evidence to support the presence of natural axon stretch growth beyond birth?

Natural Axon Stretch Growth: Comparing the Human and Giraffe

In humans it is evident through the growth of limbs that axon stretch growth occurs within the peripheral nervous system, and although the *conus medularis* ascends from sacral position to lumbar L2 by birth (Zalel et al. 2006), the human spinal cord still at least doubles in length from birth to adulthood[4] (Lassek & Rasmussen 1938),.

In comparison, the tallest land-based mammal is the giraffe which is an ungulate (as are sheep and pigs). The giraffe spinal cord extends to sacral regions and does not ascend in ontogeny. Therefore, while no giraffe spinal cord length measurements have been currently published, height can be used as a guide to determine the growth ratio from birth to maturity. At birth, the average height of a giraffe calf is 1.85m (range 1.7 – 2.0m) (Nowak 1999) The adult male giraffe height approximates 5m (range 4.3 – 5.7m) also representing **2.7 times** calculated increase in a giraffes' overall height at maturity.

[4] the length of the human spinal cord approximates 150mm and in the adult 410mm which represents **2.7 times** calculated increase in the length at maturity

,

Segmental growth rates of the giraffe's spinal cord have not yet been quantified. By calculation using adult neck length in proportion to body height, the new-born giraffe neck growth rate approximates **2.8 times**[5] which is within ranges comparative to humans, where cervical growth rate is 2.4 times and the highest growth rate observed is in the thorax which is 3.0 times (Lassek & Rasmussen 1938).

In-Vitro Axon Stretch Growth

In-vitro mechanical stimulation of axon stretch growth has been achieved extending the length of axons, potentially making them suitable for implantation (Huang et al. 2008; Pfister et al. 2004; Pfister et al. 2006) (Figure 20).

The use of axon stretch growth technology took a technological leap forward following the development of a robust axon elongation device (Smith, D. H. , Pfister & Meaney 2001). Over several years, the device has been refined and has since demonstrated quite remarkable achievements (predominantly with embryonic dorsal root ganglion (DRG) axons) exceeding stretch rates of 8mm per day and up to 100mm without disconnection (Pfister et al. 2004). What highlights these achievements are that the girth of these axons over long distances can increase, clearly demonstrating a conflict with our current understanding of axon transport mechanisms which suggest this rate of growth cannot be achieved over the length of an axon via fast axonal transport mechanisms (Pfister et al. 2006; Smith, D. H. 2009).

[5] Calculation: Giraffe, adult neck length approximates 2.0 – 2.4m =42% of adult giraffe height. If 42% of height was the representative figure of neck length in new born giraffes, this would place the neck length at birth at approximately 840mm. On this basis, the growth rate from newborn to adult giraffe is 2.8 times.

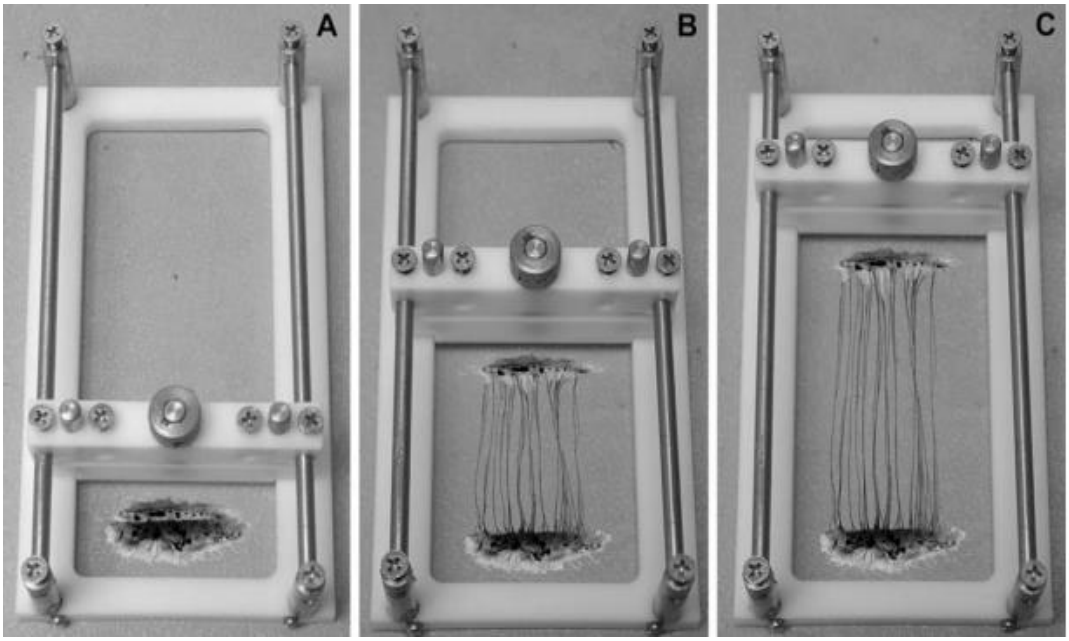

Figure 20: Classical schematic of mechanical axon stretch growth

Neurons are plated across two adjacent substrates (A) After a short period; axons bridge the two substrates. One section of the stretching frame then moves, and axons are elongated through applied mechanical tension. Growth achieved using this technique has exceeded 150mm. Image (Pfister et al. 2006) reproduced with permission under license 11603044.

Smith and colleagues in early studies used PC12 cells as well as cells from the N-Tera-2 and N-Tera-2N [6] cell lines (Smith, D. H. et al. 1999; Smith, D. H., Wolf & Meaney 2001), However, we were unable to locate in the literature any information relating to ASG experiments using adult primary motor neurons.

[6] The N-Tera-2 cell line is a human teratocarcinoma cell line which can be differentiated into mature neurons (Pleasure & Lee 1993). In the presence of retinoic acid these cells undergo terminal differentiation and are immuno-positive for a broad range of markers including choline acetyl-transferase (ChAT (Podrygajlo et al. 2009)). Interestingly, in their study only 34.0 ± 6.7% of cells were ChAT positive and 37.6%± 1.26% are SM132 – positive (Podrygajlo et al. 2009). Earlier literature has also shown although electrically active, the majority of cells are also GABAergic 66.5% and many are immune-responsive to both markers (Coyle, Li & Baccei 2011; Guillemain et al. 2000).

Development of a transplantable dorsal root ganglion (DRG), nervous tissue construct for research use, was achieved by Bryan Pfister and associates in 2006 (Pfister et al. 2006). Two methods were employed; The first encased cultured cells in a collagen hydrogel and then subsequently transferred the stretched neurons and axons into a synthetic conduit. The second method involved seeding cells direct onto a stretchable surgical membrane. A more moderate stretch rate was used in this study but nonetheless, the rates of longitudinal growth of axons still well exceeded unaided maximal possible embryonic growth rates.

Human DRG's also survive in culture following post-mortem ganglionectomy indicating suitability for culture and implant following axon stretch growth (Kim, Warren & Kalia 1979). Moreover, in later studies, Huang and associates harvested, dissociated and cultured DRG's from live patients and subjected them to in-vitro axon stretch growth with good effect (Huang et al. 2008).

Experiments in these laboratories are ongoing, and improvements to the in-vitro technology are certainly progressing. Loverde and associates more recent contributions, improving the imaging and graft access technology and on preliminary defining disconnection boundaries of axon stretch growth are an important contribution to the overall picture (Loverde et al. 2011a, 2011b; Loverde, Tolentino & Pfister 2011).

Nerve Constructs

DRG's are exceptionally robust (particularly embryonic). Therefore, these cultures potentially make excellent candidates. However, as the purpose for these nerve constructs will be to build a communication bridge across damaged nerve stumps, once they are stretched, they will be grafted within the CNS, posing a new set of challenges.

Perhaps the most significant challenge will be to infiltrate the existing network which consists of a variety of neurons and related glia and restore some form of

functional activity. Earlier studies have shown that DRG neurons survive following transplantation in both the rat CNS and PNS (Bauchet et al. 2001; Davies et al. 1999; Kuhlengel et al. 1990; Rosario et al. 1993). Iwata and associates have also since shown infiltration and survival of transplanted DRG neurons until animals were humanely killed at four weeks (Iwata et al. 2006). However, importantly, intraspinal activity between host and graft has not yet been evidenced. This work is obviously advancing to a late translational stage, with a view towards using autogulous grafts.

At this stage, there is no evidence to suggest that these relays will not be established. However, there are important differences between sensory and motor neurons and between adult and embryonic neurons. Thus, as dorsal root ganglion are sensory not motor neurons, and the vast majority of research has been conducted on embryonic neurons, for adequate translation, it is essential that comparative axon stretch growth experiments be conducted on adult motor neurons.

Neuroplasticity of the spinal cord

The clear majority of reunited connections will not be homologous.

Following disconnection, long axons recoil and the prospects of homologous reunion are diminished. It is known that in incomplete injuries there is some measure of neuroplasticity which can be leveraged. However, following complete injury, the question remains unanswered as to whether re-wiring of the circuits following repair in humans will translate to functional connections (Iwata et al. 2006). The need for an appropriate animal model is, therefore, necessary both for in-vitro and possibly later *in-vivo* use.

Axon stretch growth – animal model

Choice of appropriate animal model for late translational research is yet to be determined. *Ethics compliance will also be understandably complex as most institutions (In Australia) will require more than one ethics committee approval as the long-term intention is for extended survival and paralysis post injury. The current experiments on stretch growth must obviously keep this animal model in mind.*

Animal models are selected for a variety of reasons, but translational capability, tractability, costs and social acceptability are important considerations (Davidson, Lindsey & Davis 1987). The use of rodents and other small animal models continue to address many questions but, it is emerging that in animals with a less developed motoneuronal cortex, translation can be problematic (Lemon 2008; Lemon & Griffiths 2005).

An area yet to be addressed in translation is the considerable variation in direct vs. indirect corticomotoneuronal connectivity between primates and non-primates (Lemon 2008).

In addition, within the field of spinal cord injury, secondary injury cascades invariably lead to an expansion of the original lesion which can occur in both antegrade and retrograde directions (Profyris et al. 2004). Therefore, to study the chronic injury (>21 days) where an injury zone could project over several centimetres, the length of the spinal cord, and thus the level of incapacity to the injured animal can be problematic for survival studies.

In combination, these issues suggest that an intermediate larger animal model of a size comparable to that of humans will be required (Kwon, Hillyer & Tetzlaff 2010)

As the giraffe (an ungulate) has demonstrated physiological ASG, both the pig and sheep may be good intermediate translational candidates for axon stretch growth research.

Ungulates such as the sheep and pig have a less well developed corticospinal tract than primates, and sensorimotor control of the limbs is less complex (Badlangana et al. 2007). King (1911) induced experimental lesions in the lower medulla oblongata and spinal cord of sheep and found that there were two well-developed descending paths to the sacrum, one located in the dorsal part of the ventrolateral column and the other following a ventrolateral path directly connected with the ventral horn cells. Disruption to these paths results in partial or full paralysis.

In Australia, the sheep animal model is popular for orthopaedic research (Potes et al. 2008) as sheep spinal morphology in the lower thoracic and lumbar regions is comparable to that of the human (Sheng et al. 2010; Wilke et al. 1997). The domestic pigs' gross anatomy is also likely to be suitable for intermediate axon stretch growth research but is problematic due to growth rates and significant weight gain in this species. In Spain, the adult Yukon mini pigs have been recently established as a viable chronic SCI model (Zurita et al. 2012). However, the cost of the animal and its international availability are significant barriers.

Dynamically observing the injury zone - Access

In the chronic SCI, in vivo model, the aim is to maintain the animal with the injury for long periods ≥ 6 months. However, this becomes of little value if the injured axon cannot be adequately and repeatedly monitored, accessed, or treated.

In the small animal model, there have been several different external implants designed that facilitate *in vivo* visualisation and treatment of the dorsal spinal cord (Farrar et al. 2012). However, in a sheep or pig animal model, these devices represent significant engineering and surgical challenges. To date, no external large animal implant or chamber has been developed for axon stretch growth research that will be suitable for universal application.

To gain access to the lateral corticospinal tract in the sheep or pig model, the location of the chamber would need to be carefully considered. As sheep are quadrupeds, the cervical vertebral bodies are larger and stronger. Anterior vertebral body height in the sheep has been measured at 56.3 ± 3.1mm (SD) at C2 to 26.6 ± 1.4mm (SD) at C7 (Sheng et al. 2010; Wilke et al. 1997), which suggests adequate room for a patent tailored anterolateral viewing cage.

Surgical access to the thoracic and lumbar regions can be achieved through laminectomy, but any potential viewing chamber would then be mounted dorsally which may be problematic for gaining repeated access to the ventral or lateral regions of the spinal cord.

An alternative to in-vitro ASG is in-vivo ASG.

While it may be impossible now to foresee how *in-vivo* ASG could be implemented, new advances such as injectable nanotechnology may open this area of research up as an option. Therefore, it should be kept in mind that for proof of concept a viewing chamber may require embedded equipment that is significantly larger than otherwise required in the late translation phase of implementation.

In-vivo Axon Stretch Growth strategy

In-vitro grafting to a long nerve tract requires at least two reconnections[7], whereas stretching the in-situ spinal cord would require one connection.

In vivo stretching of axons, in-situ carries the significant risk of avulsion, and there remain many unresolved questions regarding the applicability of this technique *in-vivo*, yet the in-vitro experience suggests that safe in-situ ASG thresholds in a living organism can be determined (Loverde et al. 2011a).

It is unlikely that an anterior approach to the spinal cord will be feasible save in the neck region, where access although challenging may be achievable for proof of concept. A posterior approach via bilateral laminectomy is less problematic, but access to the lateral nerve tracts is more difficult. A wide laminectomy can resolve this issue, but this approach would still be a more complex ASG undertaking than the cervical approach.

In the future, nanotechnology is emerging as a potential option which may see an injectable and implantable fasciculation ASG device. Of course, this technology may only stretch axons; connectivity is yet to be resolved – possibly through stem cells.

Proof of ASG concept in-vivo capacity within the CNS particularly the lateral spinal tracts is necessary.

[7] One connection to unite the proximal stump to the graft and one to unite the graft to the distal stump

Can the tail be used as an indicator of paralysis?

It is a reality that the large animal model will require both short and long-term paralysis experiments. A novel approach maybe to paralyse the tail muscles or target less intrusive muscles.

Paralysis of the tail muscles by example would not render the animal immobile, so the animal would normally be moving while experiments on how to either apply a graft of stretch axons in-situ continued. There are many advantages to this strategy (if feasible) as it would facilitate long-term survival and reduce the significant burden of care as well as limiting disruption to the animals' routine.

Sheep like dogs have voluntary and involuntary control of their tail. Thus, as sheep have a traceable but rudimentary corticospinal tract in the cervical region (King 1911) and the axons fall onto multiple synapses, it may be possible to initiate a strategic injury to the cervical cord that affects the tail only. This initially will be a complex undertaking as it is likely that the axons controlling the tail will be medial rather than lateral in line with relaxed patterning (Rexed 1954). This of course then presents potential issues of collateral damage to nerves supplying the bladder and anus etc.

In sheep, three muscles control tail movement; the *coccygeus* depresses, the *sacrococcygeal dorsalis* lifts and the *sacrococcygeus lateralis* wags the tail. These muscles are accessible for direct injection of a retrograde tracer such as Fluorogold (Naumann, Härtig & Frotscher 2000; Schmued & Fallon 1986) which would provide information as to the supraspinal termination of the controlling axons.

Pertinent Literature for Sheep Model

PubMed searches were conducted using the terms “sheep animal model spinal cord,” and “Ovine spinal cord” and to locate specific literature pertinent for use for axon stretch growth research using a sheep model. In addition, already collated reference material was then added and grouped (Table 3 – 12)

Table 3: Sheep - Reference Anatomy (Book)

Title	**Author(s)**	**Year**	***Publisher***
The Anatomy of a Sheep: A Dissection Manual	May, N.D.S.	1970	The University of Queensland Press Multiple Editions

Table 4: Sheep - General

Title	**Author(s)**	**Year**	***Journal***
A technique for in vivo vascular perfusion fixation of the sheep central nervous system	Santoreneos, S., Stoodley, M., Jones, N. R. & Brown, C. J	1998	*J Neurosci Meth* 79, 195-199

Table 5: Sheep - Vascular anatomy

Title	**Author(s)**	**Year**	***Journal***
Effects of Contusion Injury on Spinal Cord Blood Flow in the Sheep	Yeo, J.D Hales, R.S. Stabback, S. Bradley, S. Fawcett, A.A. & Kearns, R.	1984	*Spine* *9 (7)* *676-680*
Bony and vascular anatomy of the normal cervical spine in the sheep	Cain, C. C. & Fraser, R. D.	1995	*Spine (Phila Pa* 20, 759-765.

Table 6: Sheep - Orthopaedic Spine and Comparative Anatomy

Title	Author(s)	Year	Journal
Anatomy of the sheep spine and its comparison to the human spine	Wilke, H. J., Kettler, H., Wenger, K. H. & Claes, L.	1997	*Anat Record* 247, 542-555.
Comparison between sheep and human cervical spines: an anatomic, radiographic, bone mineral density, and biomechanical study	Kandziora, F. Pflugmacher, R. Scholz, M. Schnake, K. Lucke, M. Schroder, R. Mittlmeier, T.	2001	*Spine (Phila Pa* 26, 1028-1037
Anatomy of large animal spines and its comparison to the human spine: a systematic review	Sheng, S.-R., Wang, X.-Y., Xu, H.-Z., Zhu, G.-Q. & Zhou, Y.-F.	2010	*Eur Spine J* 19, 46-56.
Morphometry Research of Deer, Sheep, and Human Lumbar Spine: Feasibility of Using Deer and Sheep in Spinal Animal Models	Bai, X. *et al.*	2012	*Int J Morphol* 30, 510-520

Table 7: Sheep - Surgical General

Title	Author(s)	Year	Journal
Effects of a Novel Chitosan Gel on Mucosal Wound Healing Following Endoscopic Sinus Surgery in the Sheep Model of Chronic Rhinosinusitis	Athanasiadis, T Beule, A.G. Robinson, B.H. Robinson, S.R. Shi, Z, Wormald, P-J	2008	*Laryngoscope 118, 6 1088-1094*
Reduction in post laminectomy epidural adhesions in sheep using a fibrin sealant-based medicated adhesion barrier	Richards, P. J. *Turner, A.S. Gisler, S.M. Kraft, S. Nuss, K. Mark, S. Seim, H.B. Schense, J*	2010	*J Biomed Materials Res. Part B, Applied biomaterials* 92, 439-446,
Does PEEK/HA Enhance Bone Formation Compared with PEEK in a Sheep Cervical Fusion Model	Walsh, W.R. Pelletier, MH. Bertollo, N. Christou, C. Tan, C.	2016	*Clin Orthop Relat R 474(11) 2364-2372*

Table 8: Sheep Model of SCI

Title	Author(s)	Year	*Journal*
An Ovine model of spinal cord injury	Wilson, S Abode-lyamah, K.O. Miller, J.W. Reddy CG. Safayi, S. Fredericks, D.C. Jeffery N.D DeVries-Watson N.A. Shivapour, S.K. Viljoen, S. Dalm, B.D. Gibson-Corley, K.N. Johnson, M.D. Gillies, G.T. Howard, M.A.	2016	*J. Spinal Cord Med* *2016* *19:1-15*

Table 9: Sheep - Locomotion/Gait

Title	Author(s)	Year	*Journal*
Mechanics of locomotion of dogs (Canis familiaris) and sheep (Ovis aries)	Jayes, A. S. & Alexander, R. M.	1978	*J Zool* 185, 289-308
The inter and intraobserver reliability of a locomotion scoring scale for sheep	Kaler, J Wassink, G.J Green L.E.	2009	*Vet J* *180 (2)* *189-194*
Gait analysis of clinically healthy sheep from three different age groups using a pressure-sensitive walkway	Agostinho, F Rahal, S Araujo, F.A. Conceicao, R. Monteiro, F.O.	2012	*BMC Vet Res*
Kinematic analysis of the gait of adult sheep during treadmill locomotion: Parameter values allowable total error, and potential for use in evaluating spinal cord injury	Safayi, S. Jeffery, N.D. Shivapour, SK Zamanighomi, M. Zylstra, T.J. Bratsch-Prince, J. Wison, S. Reddy, C.G. Fredericks D.C. Gillies, G.T. Howard.M.A,	2015	*J Neurol Sci* *358(1-2)* *107-12*
Gait and posture discrimination in sheep using a tri-axial accelerometer	Radeski, M. ILieski, V.	2016	*Animal 2016* *Dec 1:1-9ec D2*

Table 10: Sheep - Animal Model Literature

Title	Author(s)	Year	Journal
Application of a stand-alone interbody fusion cage based on a novel porous TiO2/glass ceramic--2: Biomechanical evaluation after implantation in the sheep cervical spine	Korinth, M. C., Hero, T., Pandora, T. & Zell, D.	2005	*Biomedizinische Technik. Biomed Tech* 50, 111-118,
The Sheep as an Animal Model in Orthopaedic Research.	Potes, J. C. *Da Costa Reis Capela e Silva, F Relvas, C Cabrita, A.S & Antonio Simoes, J.*	2008	*Experimental Pathology and Health Sciences* 2, 29-32
Validation of the sheep as a large animal model for the study of vertebral osteoporosis.	Zarrinkalam, M. R., Beard, H., Schultz, C. G. & Moore, R. J.	2009	*Eur Spine J* 18, 244-253

Table 11: Sheep - Nerve Regeneration

Title	Author(s)	Year	*Journal*
A systematic review of animal models used to study nerve regeneration in tissue-engineered scaffolds	Angius, D. *et al.*	2012	*Biomaterials* 33 8034-8039

Table 12: Sheep - Spinal Cord Neural

Title	Author(s)	Year	Journal
The Pyramid tract and other descending paths in the spinal cord of the sheep	King, L.J.	1911	*Exp Physiol*, 133-149
The Dermatomes of the Sheep	Kirk, E.J.	1968	*J. Comp Neurol 134 353-370*
Anatomical Studies on the Ovine Spinal Cord.	RAO, G.S.	1990	*Anat Anz* 171, 261-264
Allometric growth of the spinal cord in relation to the vertebral column during prenatal and postnatal life in the sheep (Ovis aries)	Ghazi, S. R. & Gholami, S.	1994	*J. Anat* 185, 427-431
The feasibility of detecting motor and sensory potentials in a sheep model	Vialle, R. Loureiro, M-C Ilhareborde, B Liu, S Lozeron, P Tadi, M.	2006	*Lab Anim* 40, 469-473
Fluid outflow in a large-animal model of posttraumatic syringomyelia	Wong, J. et.al.	2012	*Neurosurgery* 71, 474-480 discussion 480
Motor and sensitive axonal regrowth after multiple intercosto-lumbar negotiations in a sheep model	Vialle, R. Lacroix, C. Harding, I. Loureiro, M.C. Tadie M.	2010	*Spinal Cord 48(5) 367-74*
Ovine tests of a novel spinal cord neuromodulator and dentate ligament fixation method	Gibson-Corley, K.N. Oya H. Flouty, O. Fredericks, D.C. Jeffery, N.D. Gillies, G.T. Howard M.A.	2012	*J. Invest Surg 25(6) 366-74*
Intracranial Somatosensory Responses with Direct Spinal Cord Stimulation in Anesthetized Sheep.	Flouty, O. E. Oya, H. Kawasaki, H, Reddy, C.G. Fredericks, D.C Gillies, G.T. Howard, M.A.	2013	*PloS one* 8, 1-11,

References

Adams, CB & Logue, V 1971, 'Studies in cervical spondylotic myelopathy. I. Movement of the cervical roots, dura and cord, and their relation to the course of the extrathecal roots', *Brain*, vol. 94, no. 3, pp. 557-568.

Badlangana, NL, Bhagwandin, A, Fuxe, K & Manger, PR 2007, 'Observations on the giraffe central nervous system related to the corticospinal tract, motor cortex, and spinal cord: What difference does a long neck make?', *Neuroscience*, vol. 148, no. 2, pp. 522-534.

Bauchet, L, Mille-Hamard, L, Baillet-Derbin, C & Horvat, J-C 2001, 'Transplantation of autologous dorsal root ganglia into the peroneal nerve of adult rats: uni-and bidirectional axonal regrowth from the grafted DRG neurons', *Exp Neurol*, vol. 167, no. 2, pp. 312-320.

Breig, A 1960, *Biomechanics of the central nervous system; some basic normal and pathologic phenomena concerning spine, discs and cord*, Almqvist & Wiksell, Stockholm.

Breig, A 1970, 'Overstretching of and circumscribed pathological tension in the spinal cord- A basic cause of symptoms in cord disorders', *J.Biomechanics*, vol. 3, pp. 7-9.

Breig, A 1978, *Adverse Mechanical Tension in the Central Nervous System - An analysis of cause and effect- relief by functional neurosurgery*, Almqvist and Wiksell International: Stockholm, Sweden and John Wiley and Sons: New York.

Campenot, RB 1985, 'The regulation of nerve fiber length by intercalated elongation and retraction', *Developmental Brain Research*, vol. 20, no. 1, pp. 149-154.

Coyle, DE, Li, J & Baccei, M 2011, 'Regional Differentiation of Retinoic Acid-Induced Human Pluripotent Embryonic Carcinoma Stem Cell Neurons', *PLoS One*, vol. 6, no. 1, p. e16174.

Davidson, MK, Lindsey, JR & Davis, JK 1987, 'Requirements and selection of an animal model', *Israel journal of medical sciences*, vol. 23, no. 6, pp. 551-555.

Davies, SJ, Goucher, DR, Doller, C & Silver, J 1999, 'Robust regeneration of adult sensory axons in degenerating white matter of the adult rat spinal cord', *The Journal of Neuroscience*, vol. 19, no. 14, pp. 5810-5822.

Dennerll, TJ, Lamoureux, P, Buxbaum, RE & Heidemann, SR 1989, 'The cytomechanics of axonal elongation and retraction', *The Journal of Cell Biology*, vol. 109, no. 6, December 1, 1989, pp. 3073-3083.

Farrar, MJ, Bernstein, IM, Schlafer, DH, Cleland, TA, Fetcho, JR & Schaffer, CB 2012, 'Chronic in vivo imaging in the mouse spinal cord using an implanted chamber', *Nat Methods*, vol. 9, no. 3, Mar, pp. 297-302.

Fettes, PD, Leslie, K, McNabb, S & Smith, PJ 2006, 'Effect of spinal flexion on the conus medullaris: a case series using magnetic resonance imaging', *Anaesthesia*, vol. 61, no. 6, Jun, pp. 521-523.

George, EB, Schneider, BF, Lasek, RJ & Katz, MJ 1988, 'Axonal shortening and the mechanisms of axonal motility', *Cell Motility and the Cytoskeleton*, vol. 9, no. 1, pp. 48-59.

Guillemain, I, Alonso, G, Patey, G, Privat, A & Chaudieu, I 2000, 'Human NT2 neurons express a large variety of neurotransmission phenotypes in vitro', *Journal of Comparative Neurology*, vol. 422, no. 3, pp. 380-395.

Huang, JH, Zager, EL, Zhang, J, Groff, RF, Pfister, BJ, Cohen, AS, Grady, MS, Maloney-Wilensky, E & Smith, DH 2008, 'Harvested human neurons engineered as live nervous tissue constructs: implications for transplantation. Laboratory investigation', *J Neurosurg*, vol. 108, no. 2, Feb, pp. 343-347.

Iwata, A, Browne, KD, Pfister, BJ, Gruner, JA & Smith, DH 2006, 'Long-Term Survival and Outgrowth of Mechanically Engineered Nervous Tissue Constructs Implanted Into Spinal Cord Lesions', *Tissue Eng Part A*, vol. 12, no. 1, pp. 101-110.

Kim, SU, Warren, KG & Kalia, M 1979, 'Tissue culture of adult human neurons', *Neurosci Lett*, vol. 11, no. 2, pp. 137-141.

King, L, J. 1911, 'The Pyramid tract and other descending paths in the spinal cord of the sheep', *Exp Physiol*, pp. 133-149.

Kuhlengel, KR, Bunge, MB, Bunge, RP & Burton, H 1990, 'Implantation of cultured sensory neurons and Schwann cells into lesioned neonatal rat spinal cord. II. Implant characteristics and examination of corticospinal tract growth', *Journal of Comparative Neurology*, vol. 293, no. 1, pp. 74-91.

Kwon, BK, Hillyer, J & Tetzlaff, W 2010, 'Translational research in spinal cord injury: a survey of opinion from the SCI community', *J Neurotrauma*, vol. 27, no. 1, Jan, pp. 21-33.

Lamoureux, P, Heidemann, SR, Martzke, NR & Miller, KE 2010, 'Growth and elongation within and along the axon', *Developmental Neurobiology*, vol. 70, no. 3, pp. 135-149.

Lassek, AM & Rasmussen, GL 1938, 'A quantitative study of the newborn and adult spinal cords of man', *Journal of Comparative Neurology*, vol. 69, no. 3, pp. 371-379.

Lemon, RN 2008, 'Descending pathways in motor control', *Annu Rev Neurosci*, vol. 31, pp. 195-218.

Lemon, RN & Griffiths, J 2005, 'Comparing the function of the corticospinal system in different species: organizational differences for motor specialization?', *Muscle Nerve*, vol. 32, no. 3, Sep, pp. 261-279.

Loverde, JR, Ozoka, VC, Aquino, R, Lin, LS & Pfister, BJ 2011a, 'Live imaging of axon stretch growth in embryonic and adult neurons', *J Neurotrauma*, vol. 28, no. 11, Nov, pp. 2389-2403.

Loverde, JR, Ozoka, VC, Aquino, R, Lin, LS & Pfister, BJ 2011b, 'Live imaging of axon stretch growth in embryonic and adult neurons Supplementary Data, J Neurotrauma, vol. 28, no. 11, Nov, pp. 2389-2403.', *J Neurotrauma*, vol. Vol 28, No 11, Nov, Supp Data.

Loverde, JR, Tolentino, RE & Pfister, BJ 2011, 'Axon Stretch Growth: The Mechanotransduction of Neuronal Growth', *J Vis Exp*, no. 54, p. e2753.

Mitchison, T & Kirschner, M 1988, 'Cytoskeletal dynamics and nerve growth', *Neuron*, vol. 1, no. 9, 11//, pp. 761-772.

Naumann, T, Härtig, W & Frotscher, M 2000, 'Retrograde tracing with Fluoro-Gold: different methods of tracer detection at the ultrastructural level and neurodegenerative changes of back-filled neurons in long-term studies', *J Neurosci Methods*, vol. 103, no. 1, 11/15/, pp. 11-21.

Nowak, RM 1999, *Walker's Mammals of the World*, Johns Hopkins University Press.

O'Connell, J 1955, 'Discussion on Cervical Spondylosis', in *Proceedings of the Royal Society of Medicine*, pp. Vol 49;197-206.

Pfister, BJ, Iwata, A, Meaney, DF & Smith, DH 2004, 'Extreme Stretch Growth of Integrated Axons', *J. Neurosci.*, vol. 24, no. 36, September 8, 2004, pp. 7978-7983.

Pfister, BJ, Iwata, A, Taylor, AG, Wolf, JA, Meaney, DF & Smith, DH 2006, 'Development of transplantable nervous tissue constructs comprised of stretch-grown axons', *J Neurosci Methods*, vol. 153, no. 1, May 15, pp. 95-103.

Pleasure, S & Lee, VY 1993, 'NTera 2 cells: a human cell line which displays characteristics expected of a human committed neuronal progenitor cell', *J Neurosci Res*, vol. 35, no. 6, pp. 585-602.

Podrygajlo, G, Tegenge, MA, Gierse, A, Paquet-Durand, F, Tan, S, Bicker, G & Stern, M 2009, 'Cellular phenotypes of human model neurons (NT2) after differentiation in aggregate culture', *Cell Tissue Res*, vol. 336, no. 3, Jun, pp. 439-452.

Potes, JC, da Costa Reis, J, Capela e Silva, F, Relvas, C, Cabrita, AS & Antonio Simoes, J 2008, 'The Sheep as an Animal Model in Orthopaedic Research', *Experimental Pathology and Health Sciences*, vol. 2, no. 1, pp. 29-32.

Profyris, C, Cheema, SS, Zang, D, Azari, MF, Boyle, K & Petratos, S 2004, 'Degenerative and regenerative mechanisms governing spinal cord injury', *Neurobiol Dis*, vol. 15, no. 3, Apr, pp. 415-436.

Reid, JD 1960, 'Effects of flexion-extension movements of the head and spine upon the spinal cord and nerve roots', *J Neurol Neurosurg Psychiatry*, vol. 23, Aug, pp. 214-221.

Rexed, B 1954, 'A cytoarchitectonic atlas of the spinal cord in the cat', *The Journal of Comparative Neurology*, vol. 100, no. 2, pp. 297-379.

Rosario, C, Aldskogius, H, Carlstedt, T & Sidman, R 1993, 'Differentiation and axonal outgrowth pattern of fetal dorsal root ganglion cells orthotopically allografted into adult rats', *Exp Neurol*, vol. 120, no. 1, pp. 16-31.

Schmued, LC & Fallon, JH 1986, 'Fluoro-Gold: a new fluorescent retrograde axonal tracer with numerous unique properties', *Brain Res*, vol. 377, no. 1, Jul 2, pp. 147-154.

Sheng, S-R, Wang, X-Y, Xu, H-Z, Zhu, G-Q & Zhou, Y-F 2010, 'Anatomy of large animal spines and its comparison to the human spine: a systematic review', *Eur Spine J*, vol. 19, no. 1, Jan, pp. 46-56. Epub 2009 Oct 2030.

Smith, DH 2009, 'Stretch growth of integrated axon tracts: Extremes and exploitations', *Prog Neurobiol*, vol. 89, no. 3, 11//, pp. 231-239.

Smith, DH, Pfister, BJ & Meaney, DF 2001, *Device and method using integrated neuronal cells and an electronic device*, Smith Douglas Hamilton, Bryan Pfister, Meaney David F., US 7429267 B2, United States.

Smith, DH, Wolf, JA, Lusardi, TA, Lee, VM-Y & Meaney, DF 1999, 'High Tolerance and Delayed Elastic Response of Cultured Axons to Dynamic Stretch Injury', *The Journal of Neuroscience*, vol. 19, no. 11, June 1, 1999, pp. 4263-4269.

Smith, DH, Wolf, JA & Meaney, DF 2001, 'A new strategy to produce sustained growth of central nervous system axons: Continuous Mechanical Tension', *Tissue Engineering*, vol. 7, no. 2, pp. 131-139.

Sunderland, S & Bradley, KC 1960, 'Stress-Strain Phenomena in Human Spinal Nerve Roots', *Brain*, vol. 84, no. 1, pp. 120-124.

Wilke, HJ, Kettler, H, Wenger, KH & Claes, L 1997, 'Anatomy of the sheep spine and its comparison to the human spine', *Anat Rec*, vol. 247, no. 4, Apr, pp. 542-555.

Zalel, Y, Lehavi, O, Aizenstein, O & Achiron, R 2006, 'Development of the fetal spinal cord: time of ascendance of the normal conus medullaris as detected by sonography.', *Journal Ultrasound Medicine*, vol. 25, pp. 1397-1401.

Zurita, M, Aguayo, C, Bonilla, C, Otero, L, Rico, M, Rodriguez, A & Vaquero, J 2012, 'The pig model of chronic paraplegia: a challenge for experimental studies in spinal cord injury', *Prog Neurobiol*, vol. 97, no. 3, Jun, pp. 288-303.

Chapter 4. An Optimised method for obtaining adult rat spinal cord motor neurons to be used for tissue culture

Introduction to Published Article

Injuries to the spinal cord typically involve mature neurons. These neurons have undergone terminal differentiation and have thus exited from mitosis. While there is mounting evidence that adult neurons, their associated neurites, and neuroglia can adapt to body shape and size *in vivo*, there is currently no definitive *in-vitro* models consistently demonstrating axon stretch growth of adult motor neurons.

The complex homeostatic cellular requirements, in relation to growth factors, temperature, osmolality, and pH make motor neurons particularly difficult to culture for periods more than seven days. Therefore, in this publication, we sought to develop a suitable adult motor neuron harvesting and culture protocol that could be used for comparative research into axon stretch growth.

An optimised method for obtaining adult rat spinal cord motor neurons to be used for tissue culture

Publication Status	☑ Published ☐ Accepted for Publication ☐ Submitted for Publication ☐ Publication Style
Journal Name	Journal of Neuroscience Methods

Authors:

Malcolm Brinn[1], Katie O'Neill[2], Ian Musgrave[2], Brian J C Freeman [3&4], Maciej Henneberg[1] and Jaliya Kumaratilake[1].

[1] Discipline of Anatomy and Pathology, University of Adelaide, Adelaide, South Australia

[2] Discipline of Pharmacology, University of Adelaide, Adelaide, South Australia

[3] Department of Spinal Surgery Royal Adelaide Hospital, South Australia

[4] Discipline of Orthopaedics and Trauma, School of Medicine, University of Adelaide, Adelaide, South Australia

Corresponding Author: malcolm.brinn@adelaide.edu.au

011+061+ 8+83135480: 011+061+8+83133788

Medical School, The University of Adelaide, South Australia, 5005, Australia

Abbreviations

^{o}C - Degrees Celcius, ACSF – Artificial Cerebro-Spinal Fluid, bFGF – Basic Fibroblast Growth Factor, BDNF - Brain-derived neurotrophic factor, Ca^{2}+ - Calcium, cAMP - 8(-4 Chlorophenylthio cyclic adenosine 3'5' monophosphate), CO_2 – Carbon Dioxide, CNTF – Ciliary Neurotrophic Factor, DIV-Days in vitro, DNA –Deoxyribose Nucleic Acid, DSHB-Developmental Studies Hybridoma Bank, EDTA Ethylene Diamine Tetra Acetic acid, GDNF – Glial-derived neurotrophic factor, HIB-PM – Hibernate processing medium, O_2-Oxygen, PBS - Phosphate buffered solution, PDL – Poly-D-Lysine, PET -polyethylene terephthalate, Neurobasal CM – Neurobasal based conditioned medium, Mg^{2}+ Magnesium

Abstract

Background: There is a paucity of detailed methods describing how to harvest and process motor neurons obtained from the adult rat spinal cord.

New Method: Removal of intra-cardiac perfusion step. The spinal cord is extruded intact from the rat in under 60 seconds' post-decapitation and without differentiation of ventral and dorsal regions. The temperature during processing was maintained at room temperature (22^{o}C) except during the Papain step where it was increased to 30^{o}C.

Results: Cell debris interfered with the counting of cells at the time of plating. In addition, cell types could not be identified since they appear rounded structures with no projections. Cell viability counts reduced to 91% and 63% from day 7 to day 14 and days 7 to 28 respectively. Red blood cell counts in stepped density gradient layers 2 and 3 were low.

Comparison with Existing Method(s): No requirement for intra-cardiac perfusion. No requirement to cool to 4^{o}C post harvesting, No requirement for specialized substrates. Reduces processing time by at least 2hrs and reduces the potential for processing errors through a reduction in complexity. Procedures are also explained suitable for those new to the culture of primary adult motor neurons.

Conclusions: Cell viability counts indicate that removal of the perfusion step has a minimal effect on the viability of the cultured nerve cells. This may be due to the reduction in the spinal cord harvesting time and the inclusion of Hibernate based media during extrusion and processing.

Keywords: Serum Free Medium, Adult Rat Motor Neurons, Primary Cell Culture, Spinal Cord, Tissue Culture, Neuroscience protocol

Introduction

In the absence of cell division, adult primary neurons are difficult to maintain in culture for extended periods. Therefore, it is common for neuroscientists to use either embryonic neurons, immortalised neural cell lines or in more recent time's stem cells for in vitro experiments. However, these cells can differ in important aspects from the adult primary neuron (Bar 2000; Cameron & Núñez-Abades 2000; Carrascal et al. 2005; Gingras et al. 2007; Jacobson 1985; Viana, Bayliss & Berger 1994). Therefore, the use of these cells or cell lines for the investigation of spinal cord injury or degenerative diseases such as Amyotrophic Lateral Sclerosis, Parkinson's disease, and Multiple Sclerosis can be problematic in clinical translation. Neuroscientists are thus, always interested in a well-defined adult primary neuronal cell culture for comparative purposes.

Brewer, G, J. (1997) succinctly described the sequence of steps required in which to bring adult primary neurons into in-vitro culture successfully, that of; (1) Harvesting, (2) Separation of cells from the extracellular matrix, (3) Removal of growth inhibitory factors, (4) Targeted specificity of cell type, and (5) Provision of an adequate substrate and nutrients to ensure viability. When considered in their entirety, these steps can come together to build a robust protocol. However, in isolation, each step has benefits and consequences that must be carefully balanced. One such example is between media selection, temperature, and time.

Here we describe a protocol to harvest adult rat spinal cords and isolate and process neurons to in-vitro culture. The choice of hydraulic extraction of the spinal cord (de Sousa & Horrocks 1979; Meikle & Martin 1981) demonstrates how the risk of ischemia can be balanced to negate the requirement for intracardiac perfusion. We also reiterate the benefits of using Hibernate during processing in ambient air (Brewer, D, J & Price 1996; Brewer, G, J. & Cotman 1989). To demonstrate that these processing methods are robust, the neurons were cultured in excess of 21 days using the combination C2C12 conditioned media first described by (Montoya-Gacharna, J et al. 2009). Montoya-Gacharna and

associates also used cyclic adenosine-3′,5′-monophosphate (cAMP), which has been previously shown to substantially reduce the need for high quantities of growth factors (Hanson et al. 1998; Meyer-Franke et al. 1998).

Materials and Methods

A detailed description of all steps in this protocol follows in a format that can be directly applied in the laboratory for the extraction of rat spinal cord motor neurons and their long-term culture.

Pre-surgical preparation

Prepare the C2C12 muscle conditioned medium in advance (> 14 days) from the C2C12 myoblast cell line as previously described by (Montoya-Gacharna, J et al. 2009; Montoya-Gacharna, JV et al. 2012). Briefly, myoblasts are cultured in Dulbecco's modified Eagle medium (DMEM) containing L-Glutamine 20mM (Sigma), Gentamicin 10µg/mL and 10% fetal bovine serum (Sigma) reaching 30% confluence. Differentiate the cells into myocytes by replacing the current culture medium with new culture medium containing 10% horse serum (Sigma). After differentiation (i.e. in 3 days), wash the cells in warm phosphate buffered saline (PBS). Then, culture in a serum-free medium containing Neurobasal-A™ (Gibco), 2% B27™ supplement 50x (Gibco), Glutamax 0.5mM (Invitrogen) and Gentamicin (Invitrogen) 10µg/mL for 2 days. The supernatant (the conditioned medium) is then collected, filtered through a 0.22 syringe filter, and stored at -20^{o}C until required.

At least 24h before spinal cord harvesting, sterilise glass 12mm coverslips. Then, within a laminar flow hood insert them into 24-well culture plates (Corning). Apply to the surface of individual coverslips 100µL sterile poly-d-lysine (PDL) (50µg/mL) (Sigma). Note: There is variation in methods of this procedure http://protocolsonline.com/recipes/stock-solutions/polylysine-coated-tissue-culture-surfaces/ (Accessed 4/10/2015). In this protocol apply PDL, and then

transfer the culture plates to a culture oven at 37°C for 1h. Excess PDL solution is aspirated, and the surface of the coverslip rinsed twice with sterile water. Leave these culture plates within the laminar flow hood under Ultraviolet light overnight to dry off.

Prepare 24h prior to use, 150mL of Hibernate™ based processing medium (Hib-PM) containing Hibernate-A (Gibco), 2% B27 supplement 50x (Gibco), Glutamax .05mM (Sigma) and Gentamicin 10µg/mL (Invitrogen) (Brewer, GJ & Torricelli 2007)

- Transfer 50mL of Hib-PM into a 50mL conical tube mark, "Hib-PM" processing
- Transfer 7mL of Hib-PM to each of 3x 15mL conical tubes, mark as "Hib-PM" processing
- Leave in the laminar flow hood 15mL of Hib-PM in a 15mL conical tube, mark as "G1."

Store the remaining Hib-PM with the four conical tubes marked Hib-PM processing (1x 50mL, 3x 15mL) at 4°C wrapped in foil. Mark x4 15mL conical tubes D1 through to D4. Then, prepare stage 1 of the Brewer and Torricelli Optiprep™ 1:32 (Sigma) density gradient using the Hib-PM from the tube marked G1 (Brewer, GJ & Torricelli 2007) (Table 13). On completion of preparation of the stage 1 density gradients, vortex each tube, wrap in foil and store at 4°C.

Table 13: Preparation of Optiprep density gradients

Prepare in 4 separate 15 mL conical tubes Marked D1-D4				
Conical Tubes	Optiprep 1.32g/mL v/v%	Optiprep 1.32 (µL)	Hib-PM (µL)	Total (µL)
Conical 1	17.50%	525	2475	3000
Conical 2	12.50%	375	2625	3000
Conical 3	10%	300	2700	3000
Conical 4	7.50%	225	2775	3000

Prepare 24hr before use with modifications indicated by asterisks (Table 14) Neurobasal™ based conditioned medium (Neurobasal-CM) as described by (Montoya-Gacharna, J et al. 2009; Montoya-Gacharna, JV et al. 2012). Transfer 5mL of Neurobasal-CM to a 15mL conical tube and mark "Plating Neurobasal-CM." Transfer 150mL of Neurobasal-CM to 3x 50ml conical tubes marked "Neurobasal-CM feed."

Store the remaining Neurobasal-CM, and the plating and feed marked Neurobasal-CM at 4^{o}C wrapped in foil. The conical tubes are working solutions reducing the risk of contamination of the main feed supply.

Table 14: Neurobasal conditioned medium (Neurobasal-CM)

Maintain at 4^{o}C			
Product	**Concentration Required**	**Qty per 100mLs**	**From**
Neurobasal A	65%	65mL	Gibco
C2C12 conditioned media	33%	33mL	Sigma
B27(50x supplement)	2%	2mL	Gibco
Glutamax 100mL stock 200mM	0.5mM	250µL	Sigma
BDNF Stock 100ng/200µL	1ng/mL	200µL	Sigma
GDNF Stock 100ng/200µL	1ng/mL	200µL	Sigma
*CNTF Stock 1000ng/200µL	10ng/mL	200µL	Sigma
*bFGF Stock 200ng/200µL	2ng/mL	200µL	Sigma
Gentamicin 10mg/mL	10µg/mL	100µL	Invitrogen
8(-4 Chlorophenylthio cyclic adenosine 3'5' monophosphate) cAMP 100mg = MW 493.7	125µM	618µL	Sigma

*** CNTF and bFGF added to the medium to support the survival of nerve cells post-axotomy (Grothe et al. 1991; Sendtner et al. 1991). Note: bFGF at a higher dosage > 20ng/mL has**

the potential to isolate progenitors found in the adult mammalian spinal cord (Shihabuddin, Ray & Gage 1997).

Sterile instruments required for surgical extraction of the rat spinal cord

- Bone cutters
- Large scissors
- Locating probe
- Curved thumb serrated forceps
- Tooth thumb forceps
- Scalpel with size ten blade
- 16 gauge trocar cannula shortened to 20mm in length
- 30mL syringe
- Petri-dish (catchment tray)

On the day of surgery, set up the surgical field containing all instruments suitably arranged for use. Place on ice to the side of the established surgical field, the pre-prepared 50mL conical tube containing 50mL Hib-PM, the three 15mL conical tubes containing 7mL of Hib-PM each and the cord catchment tray. Attach the 16-gauge trocar to the 30mL syringe and draw up 25mL of Hib-PM from the pre-prepared 50mL conical tube, then lay the syringe adjacent to the instruments.

Animal ethics and harvesting of the spinal cord

This study was approved by The University of Adelaide Animal Ethics Committee in accordance with the Australian Code of Practice for the care and use of animals for scientific purposes (7th edition 2004) Permit M-2012-205. Adult Sprague-Dawley rats, male or female, aged between 8 and12 weeks and weighing between 230 and 560g were anaesthetised by a single intraperitoneal injection of Ketamine (80mg/kg) and Xylazine (12mg/kg) (The University of Sydney PGC 1988). A state of deep anaesthesia is confirmed by toe pinch method using thumb toothed forceps.

Following confirmation of deep anaesthesia, using the bone cutter and large scissors, the vertebral column was severed at the lumbosacral junction; thus dissociating the hind limbs from the body. The field of interest is bloody, as

several main arteries are severed, and the heart remains rhythmically beating. However, it is relatively easy when using a thumb probe to locate the caudal end of the spinal canal and insert the trocar. Decapitate the rat and place the rostral end of the spinal canal over the catchment tray. Extrude the spinal cord by pressurised hydraulic ejection (de Sousa & Horrocks 1979; Meikle & Martin 1981). Top up the catchment tray containing the spinal cord, using the remaining 25mL of cold (4^{o}C) Hib-PM from the 50mL conical tube. Transfer the catchment tray back onto the ice bed for further processing. For those new to the technique, we suggest practice on previously culled animals (Figure 21).

Isolation of cells and proteolytic separation from the extracellular matrix

On a suitably lighted surface and while the spinal cord remains immersed in the cold (on ice) Hib-PM solution, use the scalpel and curved thumb forceps to remove the meninges and cauda equina. Then, without differentiation of ventral and dorsal regions, rapidly cut the cord into 1mm segments, increasing the overall surface area and penetration of the Hib-PM into the tissue. Transfer the cut segments to one of the three pre-prepared 15mL conical tubes containing 7mL of fresh Hib-PM, and keep the cord segments suspended. Allow the two remaining 15mL conical tubes containing 7mL Hib-PM and the 15mL conical tube now containing the cord segments to transition normally to room temperature (i.e., 18-22^{o}C). Activities are now transitioning to the sterile laminar flow hood.
At this point when working within the laminar flow hood, appropriate Level 2 techniques are employed. Transfer all x3 15mL conical tubes and the remaining supply of stored Hib-PM to the laminar flow hood and allow all tubes to reach room temperature. On reaching near room temperature, centrifuge the 15mL conical tube containing the cord segments and one of the two 15mL conical tubes containing Hib-PM (acting as a centrifuge balance) at 200g for 2 minutes. Centrifugation forms a loose pellet of the cord segments.

During centrifugation, weigh out 18mg of Papain (Sigma) and under the laminar flow hood, add this to the remaining 15mL conical tube containing 7ml of room

temperature Hib-PM. Vortex and filter the Papain/Hib-PM solution through a 0.22µm syringe filter (achieving approximately 36 Units/mL) (Brewer, GJ & Torricelli 2007). Note Trypsin has been shown to be inferior to Papain for this purpose (Kaiser et al. 2013).

On completion of centrifugation transfer the two 15mL conical tubes to the laminar flow hood. Discard the supernatant from the conical tube containing the cut spinal cord segments as a loose pellet, and resuspend the cord segments at room temperature with fresh Papain/Hib-PM solution. Place into a rotating incubator the last remaining 15mL conical tube containing 7mLs of Hib-PM (previously used as a balance during centrifugation) together with the 15mL conical tube containing both the Papain/Hib-PM solution and the cut cord segments. Rotate the suspensions for 40 minutes at 30^{o}C. Note: At this temperature, Papain is activated, thus breaking the links between the cells and extracellular matrix. The rotating incubator keeps the tissue suspended (Brewer, G, J. 1997).

While the rotating incubator processing is in progress, retrieve and place in the laminar flow hood the four labelled (D1 through to D4) pre-prepared stage 1 density gradients from 4^{o}C storage and gently rotate the tubes ensuring the Optiprep/Hib-PM solution is mixed. Mark two empty tubes “DG1” and “DG2” and prepare “Stage 2” of the Brewer and Torricelli (Brewer, GJ & Torricelli 2007) stepped density gradients (Table 15) Allow these two gradients to reach room temperature. Note: Although only two stepped gradients are prepared, there is sufficient solution in the tubes labelled D1 through to D4 to prepare three stepped density gradients.

Removal of inhibitory myelin and cell isolation

On completion of the Papain/Hib-PM rotation incubation cycle, centrifuge at 400g for 2 minutes the 15mL conical tube containing the Papain/Hib-PM suspension and the 15mL conical tube containing fresh 7mL Hib-PM. Centrifugation achieves a firm pellet in the Papain/Hib-PM tube. After centrifugation and within the laminar flow hood, discard the supernatant from the tube containing the pellet

and resuspend the pellet in 2mLs of the fresh Hib-PM obtained from the conical tube that acted as the centrifuge balance. Both solutions are then allowed to return to room temperature. Upon the solutions returning to room temperature, cell isolation and separation of the extracellular matrix occurs through gentle trituration, using a series of “fire polished,” pre-prepared silicone coated (Sigma) Pasteur pipettes with a reduced nozzle size (1.0mm to 0.5mm) (Brewer, G, J. 1997). After each trituration, the suspension is allowed to settle, and the supernatant (cell suspension) is collected and filtered through a 70µm cell strainer (Corning).

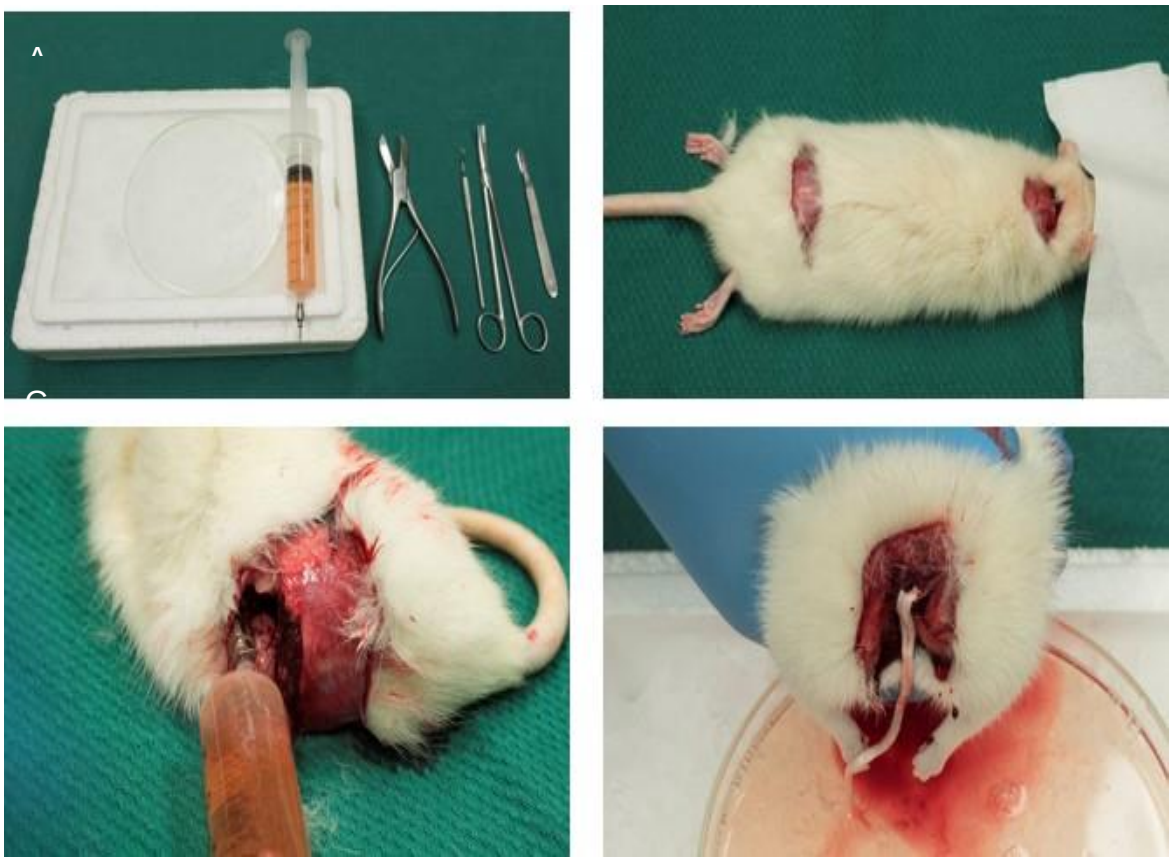

Figure 21: Spinal Cord Harvesting Technique

Standard equipment used to extract the spinal cord. (A) The modified trocar attached to the syringe. (B) Under anaesthesia, horizontal skin incisions were made at the atlantooccipital joint and at the lumbosacral junction. (C) The spinal column was severed at the lumbosacral junction using bone cutters; the spinal canal was located using a probe then the trocar attached to the syringe was introduced into the canal. (D) The rat is decapitated using the bone cutters and scissors, and the spinal cord was hydrostatically forced into the petri-dish using pressure from the syringe. This procedure took approximately 40 to 45 seconds.

Table 15: Preparing the stepped density gradient

Using Stage 1 density gradient tubes marked **D1 through to D4 (Containing Optiprep 1:32 in Hib-PM)** In tubes marked "DG 1" and "DG2" slowly add to the side of the tube 1000µL of each prepared solution from the tubes marked D1 through to D4 in the following order.	Total (µL)
D1 Conical-Bottom	1000
D2 Conical 2	1000
D3 Conical 3	1000
D4 Conical 4 Top	1000
Step D1 into tube marked DG(x) D2 onto D1, D3 onto D2 and D4 onto D3	

The process is repeated until all the remaining fresh Hib-PM from the conical tube previously used as the centrifuge balance is used. Of the 7mL of Hib-PM used for this processing step, approximately 6mL of cell suspension is recovered for further processing.

Application of the Four Step Density gradient - Cell selection

From the approximate 6mL of cell suspension recovered, equal amounts are slowly added to the side of the two stepped density gradient tubes marked DG1 and DG2 (Brewer, GJ & Torricelli 2007). These stepped gradients are then centrifuged at room temperature at 800g for 15 minutes (Brewer, GJ & Torricelli 2007). During centrifugation retrieve the stored 15mL conical tube marked plating Neurobasal-CM (5mL) and warm to 30^{o}C. Also, retrieve x1 50mL conical tube marked Neurobasal-CM feed (50mL) and warm this to 37^{o}C.

On completion of centrifugation, collect Fractions A and B (Brewer, GJ & Torricelli 2007) (Figure 22), and dilute from stock with 5mL of room temperature Hib-PM. Re-centrifuge at 200g for 2 minutes forming a loose pellet thus removing the Optiprep. Discard the supernatant and resuspend again with 2mL of fresh room temperature stock Hib-PM. Either conduct a cell count and plate at a high density

up to 300mm^2 (Brewer, GJ & Torricelli 2007) or add 600µL of Neurobasal-CM and plate using 20µL per coverslip.

On completion of the cell count calculation, re -centrifuge the 15mL conical tube containing the 2mL of Hib-PM and cell suspension at 200g for 2 minutes forming the last loose pellet (removing Hibernate). Discard the supernatant and add to the cell pellet the calculated dilution of previously warmed (30^{o}C) Neurobasal-CM using the 5mL of plating Neurobasal-CM. Note: Neurobasal-CM does not provide buffering against ambient C0$_2$. Therefore, the lid must remain on the conical tube when not in use.

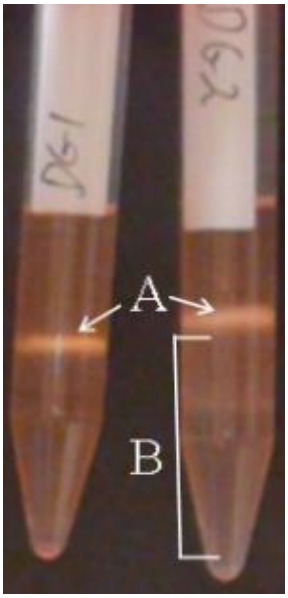

Figure 22: Post centrifugation image of 4 layered Optiprep density gradient

Note the white band fraction (A) contains debris (myelin) and neurons of high density. Below the white band, but not including the pellet fraction, (B) contains predominantly motor neurons but at a lower density

Plating of the neurons after completion of the cell count

Apply 20µL of the Neurobasal-CM cell suspension onto each previously coated sterile poly-d-lysine (50µg/mL) 12mm glass coverslip, and within 3 minutes transfer the culture well to a standard culture oven set at 37^{o}C and 5% CO_2. Note: between 45 minutes and 1 hour, cells attach to the substrates. During this period, it is important to monitor the culture plates to ensure they do not dry out. Once cells are attached, additional Neurobasal -CM delivered at 37^{o}C is slowly added against the side wall of each culture well. Care must be taken not to dislodge the attached cells.

Optional debris removal

At 24h post plating, separate debris from attached cells by angling the wells, and gently aspirating off excess fluid. Then, rinse the coverslips twice with small amounts of fresh (37^{o}C) Hib-PM, gently aspirating off the excess. On completion replace the Hib-PM again with fresh Neurobasal-CM and maintain in the culture oven at 37^{o}C with 5% CO_2. Care must be taken not to dislodge the attached cells.

Ongoing medium replacement

Replace approximately 2/3 of the Neurobasal–CM culture medium every 3-4 days per medium colour change. In our laboratory, these cell cultures are routinely maintained for 28 days. However, longer periods are achievable.

Immunohistochemistry

Immunohistochemistry was performed to identify motor neurons amongst other cells growing in the cell culture. All primary and secondary antibodies are listed in (Table 16), all solutions used in (Table 17). Standard procedures as per Damon and associates protocol were used (Damon et al. 2008). Briefly, coverslips containing cells were soaked three times in washing buffer for 5 minutes, and then cells fixed for 10 minutes at room temperature. The fixative was removed by soaking the cells three times in washing buffer for 10 minutes. Following removal of the washing buffer, cells were soaked in Glycine solution for 20 minutes at room temperature then the Glycine was removed and replaced with 150µL blocking solution for 30 minutes.

The blocking solution was removed, and 150µL of primary antibodies were then applied to specifically determined coverslips or 150µL of blocking solution to specific controls. Cells were then incubated at room temperature for 1hr and refrigerated at 4^{o}C for 24hrs. After 24hrs, solutions were carefully aspirated, and the cells washed three times in blocking solution for 5 minutes. In the dark, blocking solution was then aspirated, and the secondary antibody applied and

cells incubated for 1hr at room temperature. Following the aspiration of the secondary antibody, cells were soaked three times in 150µL of blocking solution for 5 minutes. At the conclusion, the blocking solution was removed, and the Glycerol solution used during reverse mounting of coverslips onto slides. Slides were placed in the fridge for microscopic evaluation.

Table 16: List of antibodies for primary cell culture

Primary Antibody	**Dilution**	**Company**
2H3 monoclonal antibody isotype IgG1 raised against rat brain membranes, 165 kDa molecule and localises on neurofilaments of nerve cells (Dodd et al., 1988).	Supernatant 1:200 (Concentration not stated)	Developmental Studies Hybridoma Bank
Anti-Choline Acetyltransferase antibody IgG1 ab35948 50µL, specific for cholinergic neurons in the central nervous system	1:250 (0.004mg/mL)	Abcam
Secondary Antibody		
Alexa Fluor 488 goat anti-mouse IgG(H+L) 2mg/mL, highly cross-absorbed	1:500 (0.004mg/mL)	Molecular Probes

Post Plating Cell Count (Day 7,14,28)

Following Immunohistochemistry using the primary antibody Anti-Choline Acetyltransferase (ab35948) and the secondary antibody Alexa Fluor 488 (Table 16), five random fields of view were selected and imaged from 5 coverslips using Nikon (NIS) Element software version 3.22.4, calibrated to a digital sight DS-5Mc camera attached to an Olympus BHB phase contrast and inverted fluorescent microscope using 20x objectives. Fluorescent cells were counted, and the mean per mm^2 was determined.

Table 17: Immunohistochemistry solutions

Description	Amount	Store
0.1M Phosphate Buffer Solution (PBS)		
Na_2HPO_4 (anhydrous) KH_2P0_4 NaCl DD H_20	1.290g 0.272g 8.70g 1Ltr	4^oC
Glycine Solution (Made on day of use)		
0.02M Glycine 0.1M PBS	0.150g 100mLs	4^oC
Washing Buffer (Made day prior to use) per 24 wells		
0.1M PBS 8% Sucrose	150mLs 12g	4^oC
Fixing Solution (Made day prior to use)		
Para-formaldehyde* 4% Sucrose 0.1M PBS *Paraformaldehyde does not dissolve readily in water or buffer. Dissolve Sucrose into 60mLs 0.1M PBS (at room temperature) Dissolve Paraformaldehyde initially into this PBS/Sucrose solution at 60^oC, with frequent mixing. To minimise polymerization, add 1 to 2 drops of 1N NaOH then allow to cool. Monitor pH and add as required more 1N NaOH or 1N HCL to achieve a pH 7.4. Bring final volume to 100mL with 0.1M PBS.	4g 8g 100mLs	4^oC
Blocking Solution (As required) 20mls req for 12 of 24 wells		
0.01M PBS* (7.4) *Dilute 1mL of 0.1M PBS into 9mLs of DD H_20 1.1% Bovine Serum Albumin (BSA) 2% Goat or Horse Serum 0.1% Triton X-100 0.05% Tween 20 Notes: Vortex BSA Following vortex and after adding proteins don't shake as it causes frothing & loss of proteins in solution.	10 mLs 0.11g 200µL 10µL 5µL	

Results and Discussion

Media, temperature, ischemia, pH fluctuation, and debris are the main factors that influence primary neuron viability during harvesting or processing to culture. In this study, we refine the protocol to harvest spinal cords from rats in less than 60 seconds without the need to perform intracardiac perfusion or to deviate significantly from using ambient solution temperatures. The overall protocol has been previously shown to be robust (Montoya-Gacharna, J et al. 2009; Montoya-Gacharna, JV et al. 2012). These modifications reduce complexity and save approximately 2 hours of processing time.

Intracardiac perfusion with artificial cerebrospinal fluid can be omitted when hydraulic extrusion of the spinal cord is used

To minimise the effects of hypoxia and to reduce the presence of red blood cells (RBC's), during harvesting of the spinal cord, cold (4^{o}C) artificial cerebrospinal fluid (ACSF) saturated with 95% Oxygen (O_2) and 5% Carbon dioxide (CO_2) has been previously intracardially perfused (Montoya-Gacharna, J et al. 2009; Montoya-Gacharna, JV et al. 2012). The rapid cooling is considered to reduce the metabolic rate (Bektas & Ozturk 2013) and the perfusion will saturate the nerve cells with O_2 during extraction, as well as remove RBC's from the tissue. In this study, the spinal cord was extruded/harvested in less than 45 seconds minimising the risk of hypoxia. Similarly, the spinal cord has been extruded using a similar technique in 60 seconds without the perfusion step (de Sousa & Horrocks 1979). The omission of the perfusion step has the disadvantage of retention of whole blood in the spinal cord. Red blood cells and other debris in tissue culture may affect the attachment of nerve cells to the substrate during plating.

The effects of omission of perfusion on the retention of RBC's was assessed by staining smears prepared from the four layers of the centrifuged stepped density gradient. The RBC counts of each layer of the gradient are presented in (Table 18) Fractions 2, and 3 were the density gradient layers used for cell culture plating, and these fractions had the minimum number of RBC's. The amount of debris in the culture will remain the same with or without perfusion extraction of the spinal cord. The cell debris (including any RBC's) could be removed from the culture after nerve cell attachment by introducing the optional debris removal step as described in Methods section. Therefore, perfusion with the cold ACSF was omitted from this protocol.

Table 18: Smear test to detect the presence of red blood cells in the Brewer and Torricelli (2007) density gradient without a perfusion step

Result: Fraction 4 contained the bulk of RBC's, therefore as the cell suspension was layered on the top of fraction 1 and during centrifugation; the bulk of the RBC's passed through to Fraction 4. Fraction 2 of the gradient had the next highest number of RBC's. This fraction had a high content of debris, suggesting that RBC's were trapped in this fraction, thus could not pass through to fraction 3. Fraction 3 contained a lower number of RBC's than fraction 2.

		n= Count per mm^2	St.Dev	Debris
Top	Fraction 1	0	0	Minimal
	Fraction 2	25	2	High
	Fraction 3	10	2	Low
Bottom	Fraction 4	67	4	Minimal

Stains used: Leishman followed by a Hematoxylin and Eosin (H&E), RBC's stained bright red and were counted in 4 random fields of view at 200x magnification using Image J program.

Spinal cords that were extruded using cold 4^{o}C Hib-PM have remained viable up to 2 days at room temperature in normal atmosphere (Brewer, D, J & Price 1996). Therefore, cold Hib-PM was used to extrude the spinal cord, which will lower the metabolic rate of the nerve cells allowing adequate time for the diffusion of HIB-PM into the tissue the following extraction.

Papain proteolytic separation is superior for primary neurons

Papain and Trypsin proteolytic enzymes are widely used for tissue digestion. Kaiser and Associates evaluated Papain (20U/mL) and Trypsin (0.125%) dissociation kits (in supplemented MACS® Neuro Medium) using inferior colliculi samples with or without a DNase 1 trituration phase (Kaiser et al. 2013). They found that although seeding confluences were comparable, using a 30-minute incubation period, the yield of neurons in combination with cellular arborization was superior in the Papain-only method of digestion without the use of DNase 1 for trituration. Moreover, a marked reduction in cell debris was observed. Fitzgerald and Associates (Fitzgerald et al. 1992) also compared Papain (20U/mL) in a modified Huett and Baughman solution (Huettner & Baughman 1986) and Trypsin (0.125%) to digest tissue obtained from the upper medulla. Their results were similar to Kaiser and Associates (Kaiser et al. 2013). However, Fitzgerald and Associates used DNase 1 in the Papain solution and noted that dissociation time with Papain was almost twice as long as that of Trypsin.

Brewer and Torricelli (Brewer, GJ & Torricelli 2007) commented that there might be differences in quality of Papain obtained from different suppliers. They preferred to use Papain obtained from Worthington rather than Sigma. In this study, we used Sigma Papain at the same higher concentration (36U/mL) in the Hib-PM medium for 30 minutes as described by (Brewer, GJ & Torricelli 2007; Milligan & Gifondorwa 2011) and (Montoya-Gacharna, J et al. 2009; Montoya-Gacharna, JV et al. 2012). This was followed by trituration using Hib-PM only (no DNase 1). We also found adequate proteolytic digestion, but initially a higher level of debris than expected. The Sigma papain worked well in our experiments.

In this study, the tissue suspension prepared from the spinal cord was transitioned from 4^{o}C to room temperature 22^{o}C before transferring into Papain/Hib-PM solution which initially is at room temperature. Papain enzyme activity was initiated by increasing the temperature to 30^{o}C and incubated at that temperature for 40 minutes (Shuaib et al. 1993). As cell survival at 22^{o}C has

been demonstrated in Hibernate/B27 for at least two days, beyond enzymatic digestion, processing was continued at 22^{o}C (Brewer, D, J & Price 1996)

Use of a 70µM cell strainer before use of the stepped density gradient reduces debris

In humans, the neuronal cell bodies vary in size from 5µM to 135µM (Kiernan & Barr 2009). In adult rats, the cell bodies of large motor neurons have been 40 to 55µM (Barber et al. 1984). The Montoya-Gacharna group used a 70µm filter to remove myelin and larger cell debris between the use of two separate stepped gradients. Here we did not use the first 6% Optiprep gradient used by Montoya-Garcharna and associates but strained the cell suspension using a 70µm filter before the Brewer and Torricelli 4 step density gradient. The straining of the cell suspension after trituration of the tissue reduced the presence of myelin within the density gradient.

Optiprep step density gradient processing

In this current protocol, layers 2 and 3 (i.e. top to bottom) of the 4 step density gradient were collected for cell culturing. The same layers were used by (Brewer, GJ & Torricelli 2007; Montoya-Gacharna, JV et al. 2012) for culturing of nerve cells. However, in the Montoya-Gacharna, JV et al. (2012) protocol, the use of a 6% Optiprep step, prior to the 4 step Optiprep gradient may have reduced the amount of debris including RBC and myelin more than in the current method. However, the composition of the layer 3 in the current protocol and that of Montoya-Garcharna and associated protocol may not have been much different.

Post-plating cell counts – Viability

Cells were stained per protocol using the primary antibody Anti-Choline Acetyltransferase (ab35948) and the secondary antibody Alexa Fluor 488. Cells obtained from the complete spinal cord which settled in the stepped density gradients 2 and 3 were seeded into 600µL of NFM. At day 1, to reduce the debris

field, the cell substrates were gently rinsed using Hibernate-A per protocol and Neurobasal A- Feed medium (NFM) replenished. Higher content of myelin and RBC in layer 2 (top to bottom) compared to that of Montoya-Garcharna and associates protocol, did not appear to affect the cell attachment to the substrate (Table 19)

Cell morphology of spinal cord neurons can be observed well by Day 7 of culture

It is problematic to determine cell morphology until after day three in-vitro (DIV3) at which time neurites are evident, but axons are difficult to determine (Figure 23A). By DIV7 networks and axons are present, and cell body shape is more discernible (Figure 23B). At DIV28, the projections have matured, axons are clearly evident, and networks are extensive (Figure 23C). Dendritic arborization and axon projections differ between neurons suggestive of a functional difference (Kiernan & Barr 2009). Therefore, the broad classification of spinal cord neuronal populations, in particular, differentiation between a motor neuron and sensory neuron, can be achieved through a microscope and later confirmed by immunohistochemistry (Figure 24, Figure 25 and Figure 26).

Conclusions

The method described here produces desired results to the same extent as methods used by other authors while it is more parsimonious than previously described methods. It shortens the time of processing and is less expensive.

Table 19: Post-plating motoneurones identified with anti-choline acetyltransferase (cHat) antibody

In this study, the culture medium used is as described by (Montoya-Gacharna, J et al. 2009; Montoya-Gacharna, JV et al. 2012). Thus the viability of the nerve cells should be similar to those of the above authors. However, investigation of cell viability according to the current protocol was maintained at 91% and 63% on day 14 and day 28 respectively

	Counted Sites	Neurons per mm2	StDev	% Survival From day 7
Day 7	n=25	32	3	
Day 14	n=25	29	3	91%
Day 28	n=25	20	3	63%

Acknowledgments

We would like to thank Mr Tavik Morgenstern for his assistance with photography and Mr Chris Leigh for overall technical support. We also thank Adelaide Microscopy for the use of the Olympus BX51 Fluorescence imaging microscope, the use of facilities and support of Dr Agatha Labrinidis. We would also like to thank Dr J.V. Montoya-Gacharna for his encouraging and assisting email correspondence and Dr J. Kumaratilake for providing funding for this study out of private lecturing funds. Finally, we thank the reviewers for their constructive comments and suggestions.

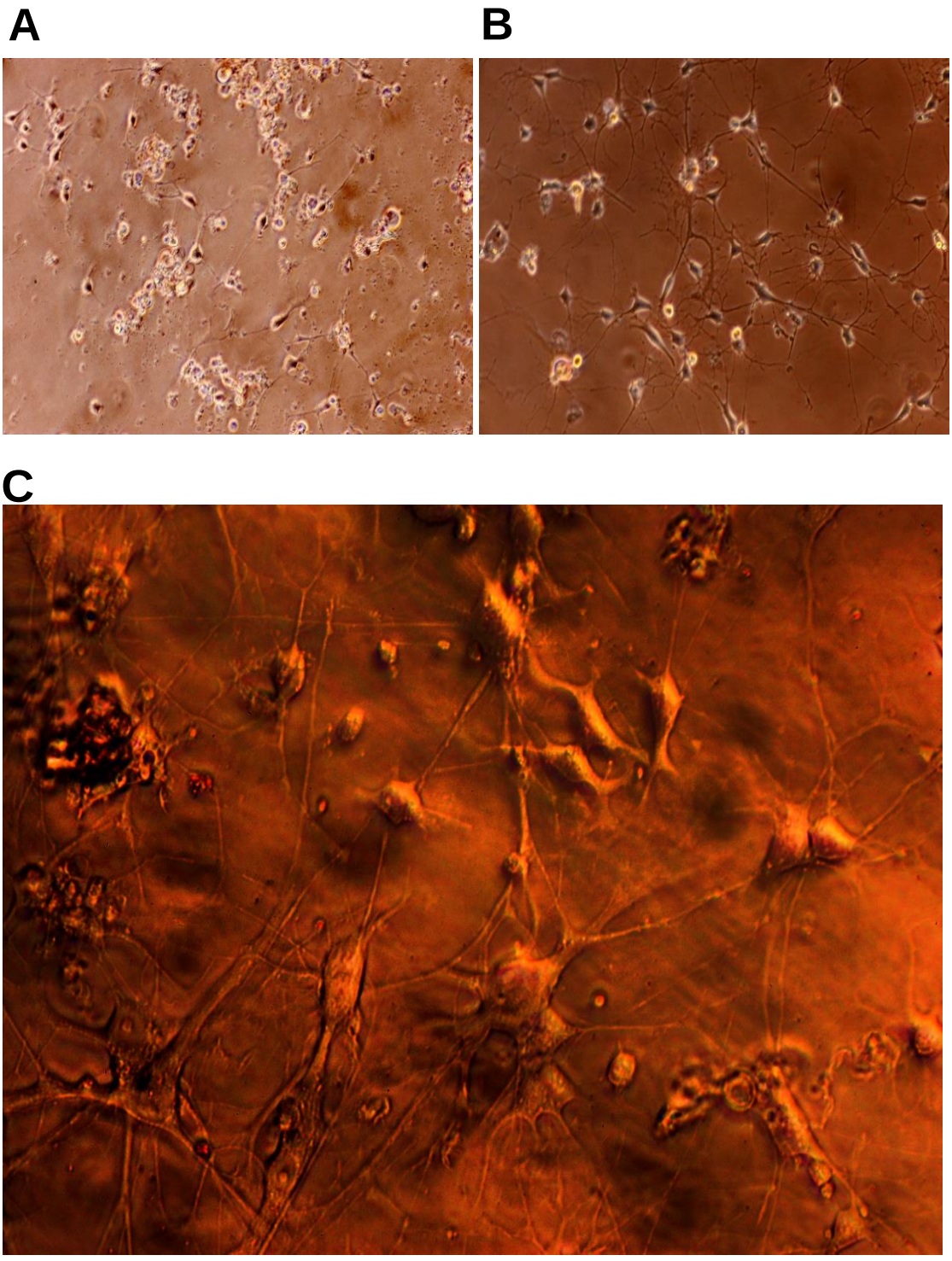

Figure 23: Images of live nerve cells in NFM culture (Day 7-28)

Live cell images A and B (x200mag) Image C (x400mag). Images were taken using a Nikon camera attached to a Nikon inverted microscope through the front camera port of the microscope (Scales not shown)

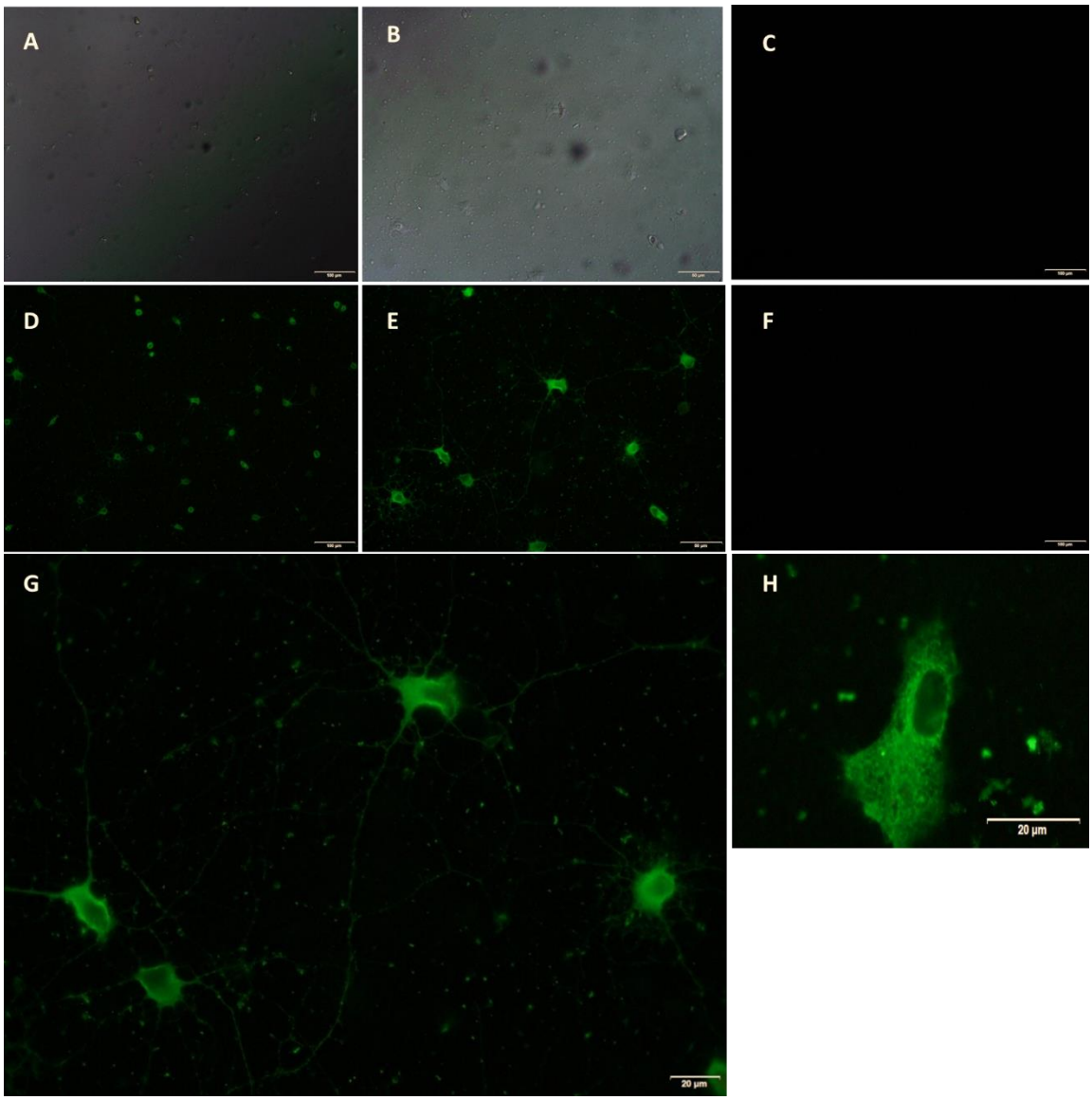

Figure 24: Simultaneous post-fixation (day 7) diffusion contrast and fluorescence images

Fluorescence: Anti-Choline Acetyltransferase antibody IgG1 (Abcam ab35948)

A & D: 200x Magnification, B & E: 400x Magnification, C: Primary no Secondary, F: Secondary no Primary, G: 1000x Magnification (oil), H: Enlarged single cell.

Note: Choline Acetyltransferase (ChAT) is expressed in motor neurons and preganglionic autonomic neurons of the spinal cord. At Day 7, although the complete spinal cord is processed, Image B and E highlight that when using C2C12 culture medium it preferences survival of motor neurons over sensory neurons.

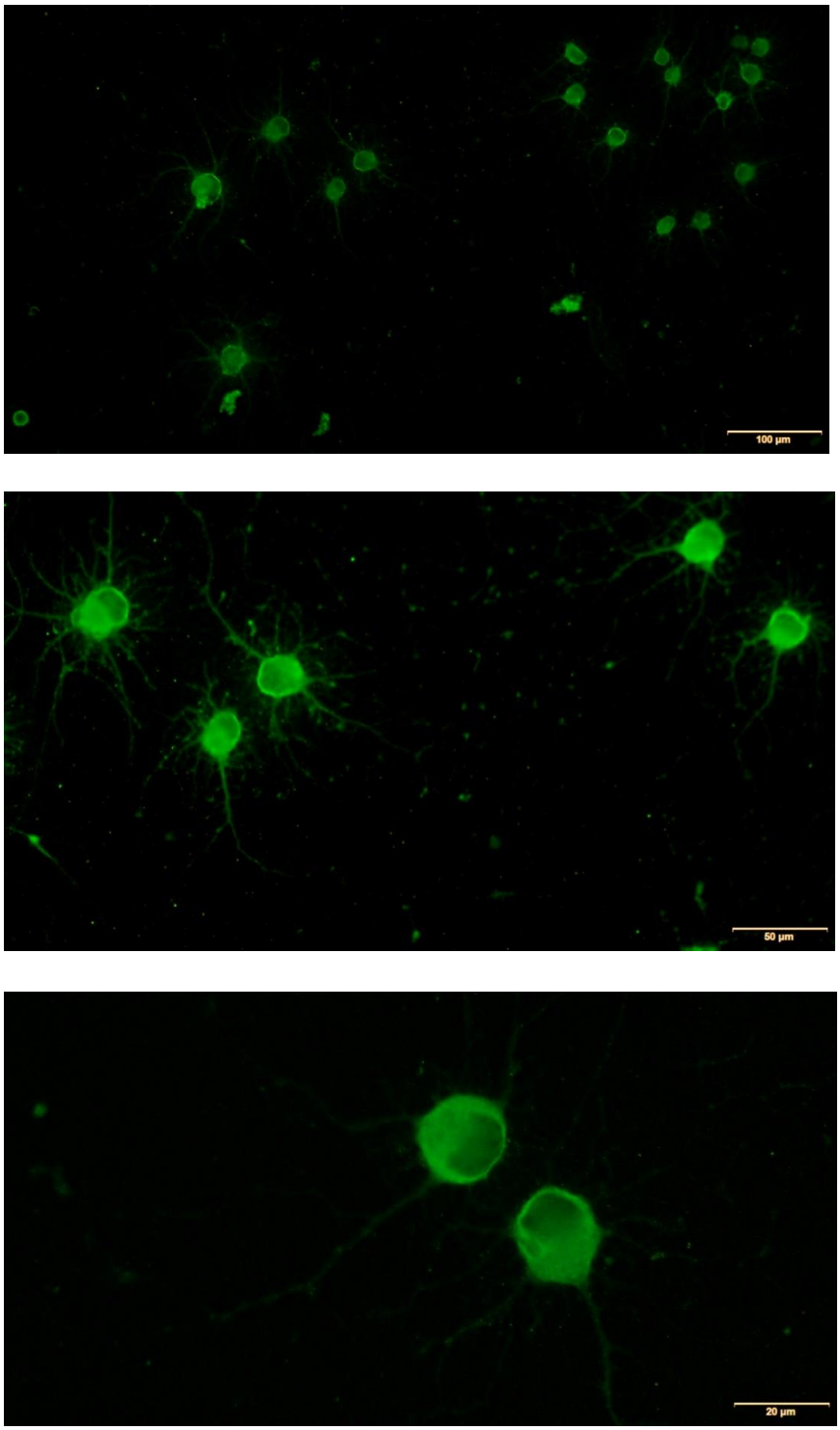

Figure 25: Immunofluorescence (day 21) anti-choline acetyltransferase antibody (ab35948)

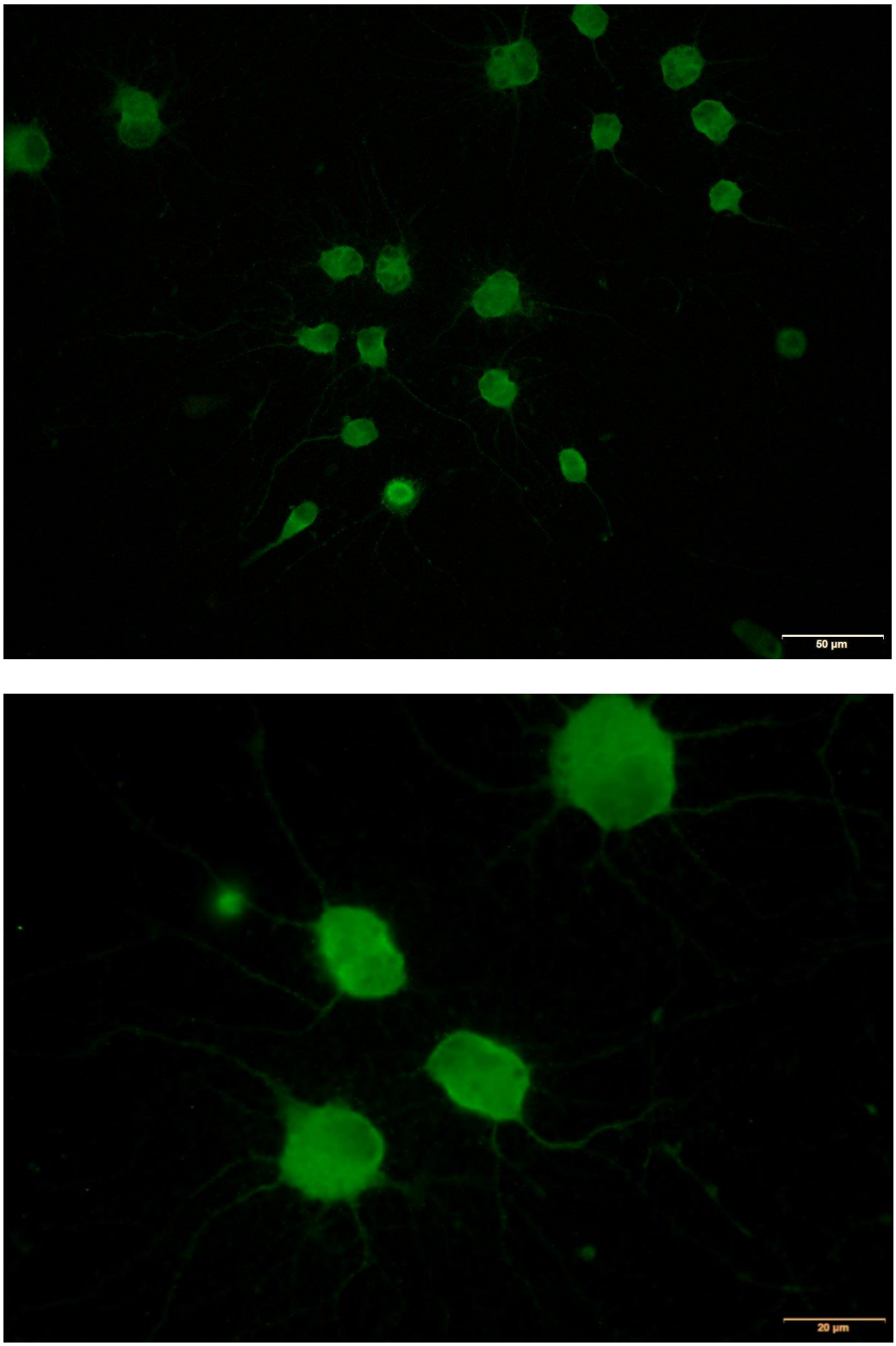

Figure 26: Immunofluorescence (day21) neurofilament 165kda antibody (DSHB: 2h3)

Contributions

Mr Malcolm Brinn contributed to defining the concept of this paper, completed the literature review, all experiments, imaging, immunohistochemistry and contributed to the manuscript content as the primary author.

Ms Katie O'Neill provided level 2 training in the use of laminar flow and culture techniques. Carried out and assisted in calculating various solution concentrations and contributed to manuscript content as the second author.

Dr Ian Musgrave supervised level 2 training, edited the procedural content of the manuscript, provided consultation during culture issues.

Prof. Brian Freeman contributed to defining the concept of this paper, provided consultative advice as well as editing of the final manuscript.

Prof. Maciej Henneberg provided mentoring, assistance with protocol design, primary editing of the manuscript and provided consultative advice on manuscript layout

Dr Jaylia Kumaratilake participated in the design of the protocol provided technical assistance with immunohistochemistry, supervision of Laboratory work, editing and layout of the manuscript and consultative advice on general laboratory techniques.

Disclosures

Funding for consumables for this investigation was provided from private lecturing funds obtained by Dr Jaliya Kumaratilake.

References

Bar, PR 2000, 'Motor neuron disease in vitro: the use of cultured motor neurons to study amyotrophic lateral sclerosis', *European Journal of Pharmacology*, no. 405, pp. 285-295.

Barber, RP, Phelps, PE, Houser, CR, Crawford, GD, Salvaterra, PM & Vaughn, JE 1984, 'The morphology and distribution of neurons containing choline acetyltransferase in the adult rat spinal cord: An immunocytochemical study', *The Journal of Comparative Neurology*, vol. 229, no. 3, pp. 329-346.

Bektas, S & Ozturk, G 2013, 'Enhancement of cultured adult motor neuron survival with cold pre-incubation', *Neurosci Lett*, vol. 533, Jan 15, pp. 23-27.

Brewer, D, J & Price, P, J. 1996, 'Viable cultured neurons in ambient carbon dioxide and hibernation storage for a month', *Neuroreport*, vol. 7, pp. 1509-1512.

Brewer, G, J. 1997, 'Isolation and culture of adult rat hippocampal neurons', *J Neurosci Methods*, vol. 71, pp. 143-155.

Brewer, G, J. & Cotman, C, W 1989, 'Survival and growth of hippocampal neurons at low density in defined medium: advantages of a sandwich culture technique or low oxygen', *Brain Res*, vol. 494, pp. 65-74.

Brewer, GJ & Torricelli, JR 2007, 'Isolation and culture of adult neurons and neurospheres', *Nat Protoc*, vol. 2, no. 6, pp. 1490-1498.

Cameron, WE & Núñez-Abades, PA 2000, 'Physiological changes accompanying anatomical remodeling of mammalian motoneurons during postnatal development', *Brain Research Bulletin*, vol. 53, no. 5, 11/15/, pp. 523-527.

Carrascal, L, Nieto-Gonzalez, JL, Cameron, WE, Torres, B & Nunez-Abades, PA 2005, 'Changes during the postnatal development in physiological and anatomical characteristics of rat motoneurons studied in vitro', *Brain Res Brain Res Rev*, vol. 49, no. 2, Sep, pp. 377-387.

Damon, BJ, Mezentseva, NV, Kumaratilake, JS, Forgacs, G & Newman, SA 2008, 'Limb bud and flank mesoderm have distinct "physical phenotypes" that may contribute to limb budding', *Dev Biol*, vol. 321, no. 2, Sep 15, pp. 319-330.

de Sousa, BN & Horrocks, LA 1979, 'Development of Rat Spinal Cord', *Developmental Neuroscience*, vol. 2, no. 3, pp. 115-121.

Fitzgerald, SC, Willis, MA, Yu, C & Rigatto, H 1992, 'In search of the central respiratory neurons: I. Dissociated cell cultures of respiratory areas from the upper medulla', *J Neurosci Res*, vol. 33, no. 4, pp. 579-589.

Gingras, M, Gagnon, V, Minotti, S, Durham, HD & Berthod, F 2007, 'Optimized protocols for isolation of primary motor neurons, astrocytes and microglia from embryonic mouse spinal cord', *J Neurosci Methods*, vol. 163, no. 1, 6/15/, pp. 111-118.

Grothe, C, Wewetzer, K, Lagrange, A & Unsicker, K 1991, 'Effects of basic fibroblast growth factor on survival and choline acetyltransferase development of spinal cord neurons', *Developmental Brain Research*, vol. 62, no. 2, 10/21/, pp. 257-261.

Hanson, MG, Shen, S, Wiemelt, AP, McMorris, FA & Barres, BA 1998, 'Cyclic AMP Elevation Is Sufficient to Promote the Survival of Spinal Motor Neurons In Vitro', *The Journal of Neuroscience*, vol. 18, no. 18, September 15, 1998, pp. 7361-7371.

Huettner, J & Baughman, R 1986, 'Primary culture of identified neurons from the visual cortex of postnatal rats', *The Journal of Neuroscience*, vol. 6, no. 10, October 1, 1986, pp. 3044-3060.

Jacobson, M 1985, 'Clonal Analysis and Cell Lineages of the Vertebrate Central Nervous System', *Annual Review of Neuroscience*, vol. 8, no. 1, pp. 71-102.

Kaiser, O, Aliuos, P, Wissel, K, Lenarz, T, Werner, D, Reuter, G, Kral, A & Warnecke, A 2013, 'Dissociated Neurons and Glial Cells Derived from Rat Inferior Colliculi after Digestion with Papain', *PLoS One*, vol. 8, no. 12, 12/12, p. e80490.

Kiernan, JA & Barr, ML 2009, *Barr's the Human Nervous System: An Anatomical Viewpoint*, 9th edn, Wolters Kluwer Health/Lippincott Williams & Wilkins.

Meikle, AD & Martin, AH 1981, 'A Rapid Method for Removal of the Spinal Cord', *Biotechnic & Histochemistry*, vol. 56, no. 4, pp. 235-237.

Meyer-Franke, A, Wilkinson, GA, Kruttgen, A, Hu, M, Munro, E, Hanson Jr, MG, Reichardt, LF & Barres, BA 1998, 'Depolarization and cAMP Elevation Rapidly Recruit TrkB to the Plasma Membrane of CNS Neurons', *Neuron*, vol. 21, no. 4, 10//, pp. 681-693.

Milligan, C & Gifondorwa, D 2011, 'Isolation and Culture of Postnatal Spinal Motoneurons', in G Manfredi & H Kawamata (eds), *Neurodegeneration*, vol. 793, Humana Press, pp. 77-85.

Montoya-Gacharna, J, Sutachan, JJ, Chan, WS, Sideris, A, Blanck, TJ & Recio-Pinto, E 2009, 'Muscle-conditioned media and cAMP promote survival and neurite outgrowth of adult spinal cord motor neurons', *Exp Neurol*, vol. 220, no. 2, Dec, pp. 303-315.

Montoya-Gacharna, JV, Sutachan, JJ, Chan, WS, Sideris, A, Blanck, TJ & Recio-Pinto, E 2012, 'Preparation of adult spinal cord motor neuron cultures under serum-free conditions', *Methods Mol Biol*, vol. 846, pp. 103-116.

Sendtner, M, Arakawa, Y, Stöckli, KA, Kreutzberg, GW & Thoenen, H 1991, 'Effect of ciliary neurotrophic factor (CNTF) on motoneuron survival', *J Cell Sci*, vol. 1991, no. Supplement 15, pp. 103-109.

Shihabuddin, LS, Ray, J & Gage, FH 1997, 'FGF-2 Is Sufficient to Isolate Progenitors Found in the Adult Mammalian Spinal Cord', *Exp Neurol*, vol. 148, no. 2, 12//, pp. 577-586.

Shuaib, A, Sochocka, E, Ishaqzay, R, Hertz, L & Code, WE 1993, 'Protective effect of hypothermia during ischemia in neural cell cultures', *Neurochemical Research*, vol. 18, no. 6, 1993/06/01, pp. 663-665.

The University of Sydney PGC 1988, *Australian Wildlife: The John Keep Refresher Course for Veterinarians: 15-19 February 1988*, The Committee.

Viana, F, Bayliss, DA & Berger, AJ 1994, 'Postnatal changes in rat hypoglossal motoneuron membrane properties', *Neuroscience*, vol. 59, no. 1, 3//, pp. 131-148.

Bar, PR 2000, 'Motor neuron disease in vitro: the use of cultured motor neurons to study amyotrophic lateral sclerosis', *European Journal of Pharmacology*, no. 405, pp. 285-295.

Barber, RP, Phelps, PE, Houser, CR, Crawford, GD, Salvaterra, PM & Vaughn, JE 1984, 'The morphology and distribution of neurons containing choline acetyltransferase in the adult rat spinal cord: An immunocytochemical study', *The Journal of Comparative Neurology*, vol. 229, no. 3, pp. 329-346.

Bektas, S & Ozturk, G 2013, 'Enhancement of cultured adult motor neuron survival with cold pre-incubation', *Neurosci Lett*, vol. 533, Jan 15, pp. 23-27.

Brewer, D, J & Price, P, J. 1996, 'Viable cultured neurons in ambient carbon dioxide and hibernation storage for a month', *Neuroreport*, vol. 7, pp. 1509-1512.

Brewer, G, J. 1997, 'Isolation and culture of adult rat hippocampal neurons', *J Neurosci Methods*, vol. 71, pp. 143-155.

Brewer, G, J. & Cotman, C, W 1989, 'Survival and growth of hippocampal neurons at low density in defined medium: advantages of a sandwich culture technique or low oxygen', *Brain Res*, vol. 494, pp. 65-74.

Brewer, GJ & Torricelli, JR 2007, 'Isolation and culture of adult neurons and neurospheres', *Nat Protoc*, vol. 2, no. 6, pp. 1490-1498.

Cameron, WE & Núñez-Abades, PA 2000, 'Physiological changes accompanying anatomical remodeling of mammalian motoneurones during postnatal development', *Brain Research Bulletin*, vol. 53, no. 5, 11/15/, pp. 523-527.

Carrascal, L, Nieto-Gonzalez, JL, Cameron, WE, Torres, B & Nunez-Abades, PA 2005, 'Changes during the postnatal development in physiological and anatomical characteristics of rat motoneurones studied in vitro', *Brain Res Brain Res Rev*, vol. 49, no. 2, Sep, pp. 377-387.

Damon, BJ, Mezentseva, NV, Kumaratilake, JS, Forgacs, G & Newman, SA 2008, 'Limb bud and flank mesoderm have distinct "physical phenotypes" that may contribute to limb budding', *Dev Biol*, vol. 321, no. 2, Sep 15, pp. 319-330.

de Sousa, BN & Horrocks, LA 1979, 'Development of Rat Spinal Cord', *Developmental Neuroscience*, vol. 2, no. 3, pp. 115-121.

Fitzgerald, SC, Willis, MA, Yu, C & Rigatto, H 1992, 'In search of the central respiratory neurons: I. Dissociated cell cultures of respiratory areas from the upper medulla', *J Neurosci Res*, vol. 33, no. 4, pp. 579-589.

Gingras, M, Gagnon, V, Minotti, S, Durham, HD & Berthod, F 2007, 'Optimized protocols for isolation of primary motor neurons, astrocytes and microglia from embryonic mouse spinal cord', *J Neurosci Methods*, vol. 163, no. 1, 6/15/, pp. 111-118.

Grothe, C, Wewetzer, K, Lagrange, A & Unsicker, K 1991, 'Effects of basic fibroblast growth factor on survival and choline acetyltransferase development of spinal cord neurons', *Developmental Brain Research*, vol. 62, no. 2, 10/21/, pp. 257-261.

Hanson, MG, Shen, S, Wiemelt, AP, McMorris, FA & Barres, BA 1998, 'Cyclic AMP Elevation Is Sufficient to Promote the Survival of Spinal Motor Neurons In Vitro', *The Journal of Neuroscience*, vol. 18, no. 18, September 15, 1998, pp. 7361-7371.

Huettner, J & Baughman, R 1986, 'Primary culture of identified neurons from the visual cortex of postnatal rats', *The Journal of Neuroscience*, vol. 6, no. 10, October 1, 1986, pp. 3044-3060.

Jacobson, M 1985, 'Clonal Analysis and Cell Lineages of the Vertebrate Central Nervous System', *Annual Review of Neuroscience*, vol. 8, no. 1, pp. 71-102.

Kaiser, O, Aliuos, P, Wissel, K, Lenarz, T, Werner, D, Reuter, G, Kral, A & Warnecke, A 2013, 'Dissociated Neurons and Glial Cells Derived from Rat Inferior Colliculi after Digestion with Papain', *PLoS One*, vol. 8, no. 12, 12/12, p. e80490.

Kiernan, JA & Barr, ML 2009, *Barr's the Human Nervous System: An Anatomical Viewpoint*, 9th edn, Wolters Kluwer Health/Lippincott Williams & Wilkins.

Meikle, AD & Martin, AH 1981, 'A Rapid Method for Removal of the Spinal Cord', *Biotechnic & Histochemistry*, vol. 56, no. 4, pp. 235-237.

Meyer-Franke, A, Wilkinson, GA, Kruttgen, A, Hu, M, Munro, E, Hanson Jr, MG, Reichardt, LF & Barres, BA 1998, 'Depolarization and cAMP Elevation Rapidly Recruit TrkB to the Plasma Membrane of CNS Neurons', *Neuron*, vol. 21, no. 4, 10//, pp. 681-693.

Milligan, C & Gifondorwa, D 2011, 'Isolation and Culture of Postnatal Spinal Motoneurones', in G Manfredi & H Kawamata (eds), *Neurodegeneration*, vol. 793, Humana Press, pp. 77-85.

Montoya-Gacharna, J, Sutachan, JJ, Chan, WS, Sideris, A, Blanck, TJ & Recio-Pinto, E 2009, 'Muscle-conditioned media and cAMP promote survival and neurite outgrowth of adult spinal cord motor neurons', *Exp Neurol*, vol. 220, no. 2, Dec, pp. 303-315.

Montoya-Gacharna, JV, Sutachan, JJ, Chan, WS, Sideris, A, Blanck, TJ & Recio-Pinto, E 2012, 'Preparation of adult spinal cord motor neuron cultures under serum-free conditions', *Methods Mol Biol*, vol. 846, pp. 103-116.

Sendtner, M, Arakawa, Y, Stöckli, KA, Kreutzberg, GW & Thoenen, H 1991, 'Effect of ciliary neurotrophic factor (CNTF) on motoneurone survival', *J Cell Sci*, vol. 1991, no. Supplement 15, pp. 103-109.

Shihabuddin, LS, Ray, J & Gage, FH 1997, 'FGF-2 Is Sufficient to Isolate Progenitors Found in the Adult Mammalian Spinal Cord', *Exp Neurol*, vol. 148, no. 2, 12//, pp. 577-586.

Shuaib, A, Sochocka, E, Ishaqzay, R, Hertz, L & Code, WE 1993, 'Protective effect of hypothermia during ischemia in neural cell cultures', *Neurochemical Research*, vol. 18, no. 6, 1993/06/01, pp. 663-665.

The University of Sydney PGC 1988, *Australian Wildlife: The John Keep Refresher Course for Veterinarians: 15-19 February 1988*, The Committee.

Viana, F, Bayliss, DA & Berger, AJ 1994, 'Postnatal changes in rat hypoglossal motoneurone membrane properties', *Neuroscience*, vol. 59, no. 1, 3//, pp. 131-148.

Chapter 5. A portable live cell culture and imaging system with optional umbilical bioreactor using a modified infant incubator

Development preamble

Developing a suitable in-vitro ASG infrastructure

As a suitable axon stretch growth bioreactor has been described in detail elsewhere; it was logical therefore to explore avenues to enhance the existing technology during development. The primary objective being, to incorporate improvements in operational functionality and research translation (Figure 27). Much of the work contained in this section did not make it into publication but was necessary to establish the in-vitro infrastructure.

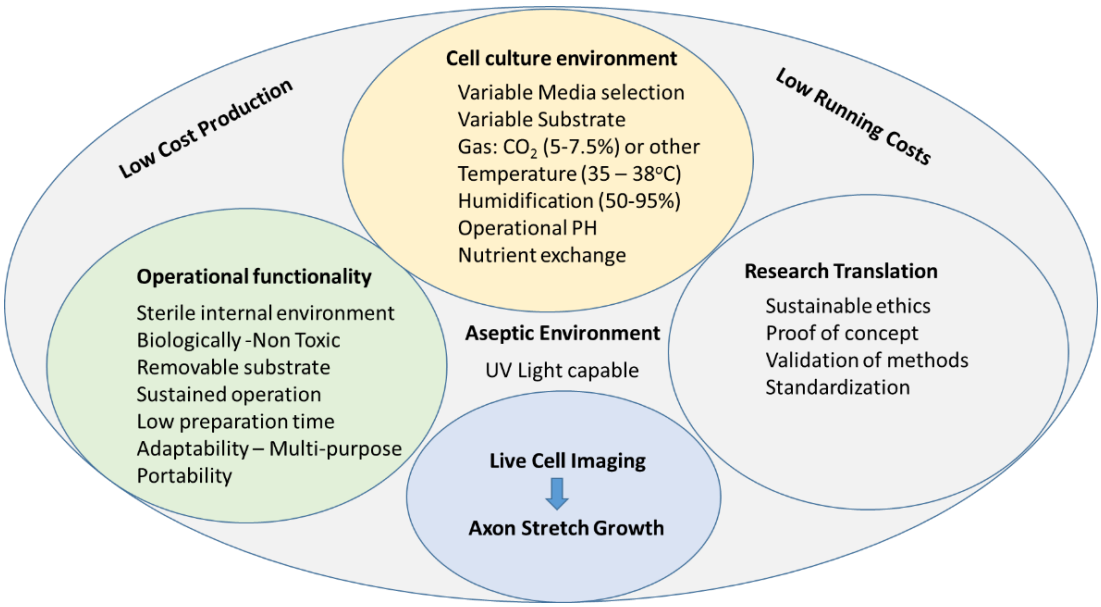

Figure 27: In-vitro requirements

Bioreactor Design Principles

A three channel device was first developed by Smith, Pfister and Meaney (2001) and has since been progressively enhanced, first by making the device robust and suitable for potential use with nerve grafts (Pfister et al. 2004; Pfister et al. 2006) and further for experimental live cell imaging (Loverde 2009; Loverde et al.

2011a, 2011b; Loverde, Tolentino & Pfister 2011). Together, these enhancements to basic design have proved suitable for use and eventually have led to several publications on axon stretch growth of dorsal root ganglion axons (DRG) predominantly obtained from embryonic rats.

From the perspective of translational use, integration and 3D printing options are the next logical steps in the evolution of the in-vitro device.

Joseph Loverde describes the existing bioreactor in detail in his PhD thesis (Loverde 2009) and later by video (Loverde, Tolentino & Pfister 2011). Briefly, the device is constructed using PolyEtherEtherKetone (PEEK) frame (PEEK although expensive tolerates steam sterilisation). In this model, cells are harvested and inserted into the bioreactor under a laminar flow hood. The device is then stored in a culture oven to allow cell growth and later transferred to an imaging microscope where it was attached to heating and CO_2.

In this project, the specification expands this device further to incorporate portability and 24h access to imaging using a variety of microscopes and variation in culture chambers (bioreactors). In the final development, the bioreactor was standardised to the same size as a standard culture plate, and the top sections were variable per requirements e.g. electrophysiology, axon stretch growth, etc.

Overall 15 iterations of the bioreactor were produced, ranging from a simple modification of pre-purchased culture flasks through to detailed engineering of Teflon and Aluminium blocks and as they became available incorporation of 3D printing and computer numeric control (CNC) systems.

Bioreactors

The first dominant design is featured in *Figure 28*. This version was stable but suffered leaking issues. The heating system was made from Nichrome wire wound within a ceramic sheath (12V). The sheath was then passed through the lower section and the middle section securing the glass in place. This unit was eventually simplified into first a two section and then a single section device once the ASG drive mechanism was resolved. The sagittal view of the device (*Figure 29*) highlights how the Aclar was inserted into the moving bar and how the auto-feed mechanism worked. Loss of fluid through evaporation was initially a problem. This was resolved through using the feed pipes to top up the fluid level. We eventually automated this with an inexpensive peristaltic pump. Fluid entering the inlet (f) was set at a slower rate than the outlet (g). By using a peristaltic pump to extract the fluid at an appropriate level, the system could be left unattended for days without drying out. Fluid leakage from the glass substrates continued to be a problem throughout the development. The cause was the lower chambers material being Teflon. On balance, we should have produced the device in PEEK, but funds were not available. The Teflon was used as it was steam sterilisable. However, even with silicone gaskets and glue the occasional leak still eventuated. Glass breakage of the lower substrate occasionally occurred when changing to high magnification objectives.

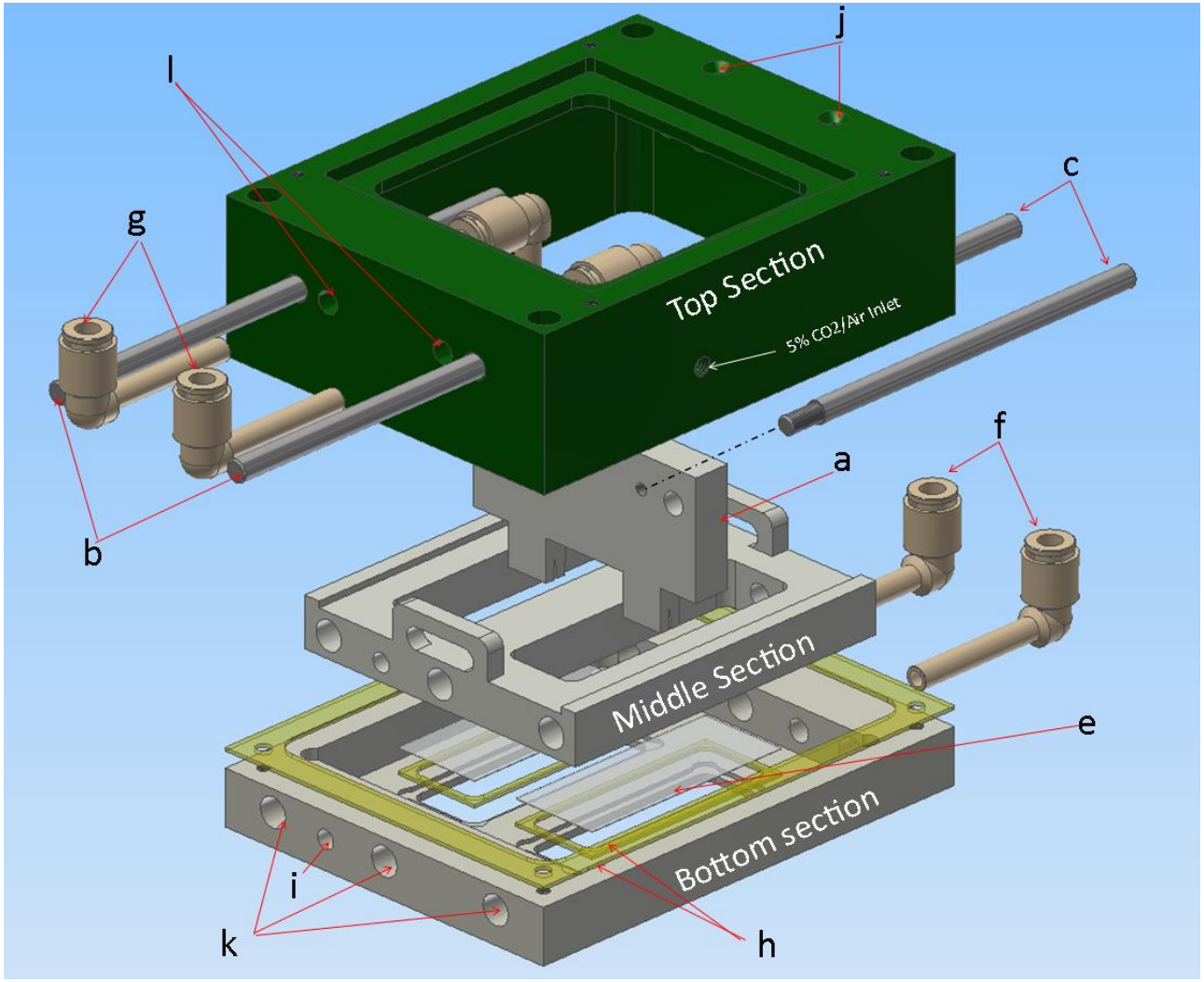

Figure 28: Stable 3 section version of axon stretch bioreactor:

To facilitate assembly and disassembly, the bioreactor was split into three demountable sections; the top section containing the internal axon stretching components, $C0_2$ gas and media inlet and outlet ports. The middle section providing two separate bottomless culture wells with parallel tunnels housing heating elements and a temperature sensor, and the bottom section retaining the removable glass substrates.

a Substrate holder
b Stainless steel support rails 6mm
c Stainless steel pull rails

e Substrate glass (24mm x 50mm)
f Feed in connecting tubes (PEEK)
g Feed out connecting tubes (PEEK)
h Silicone gasket for substrate & bottom section
i PT100 temperature probe insertion hole
j Lockdown stainless steel pull rails
k 6.01 mm holes for 6mm silicone tube (closed circuit water heating)
l holes for feed in connecting tubes

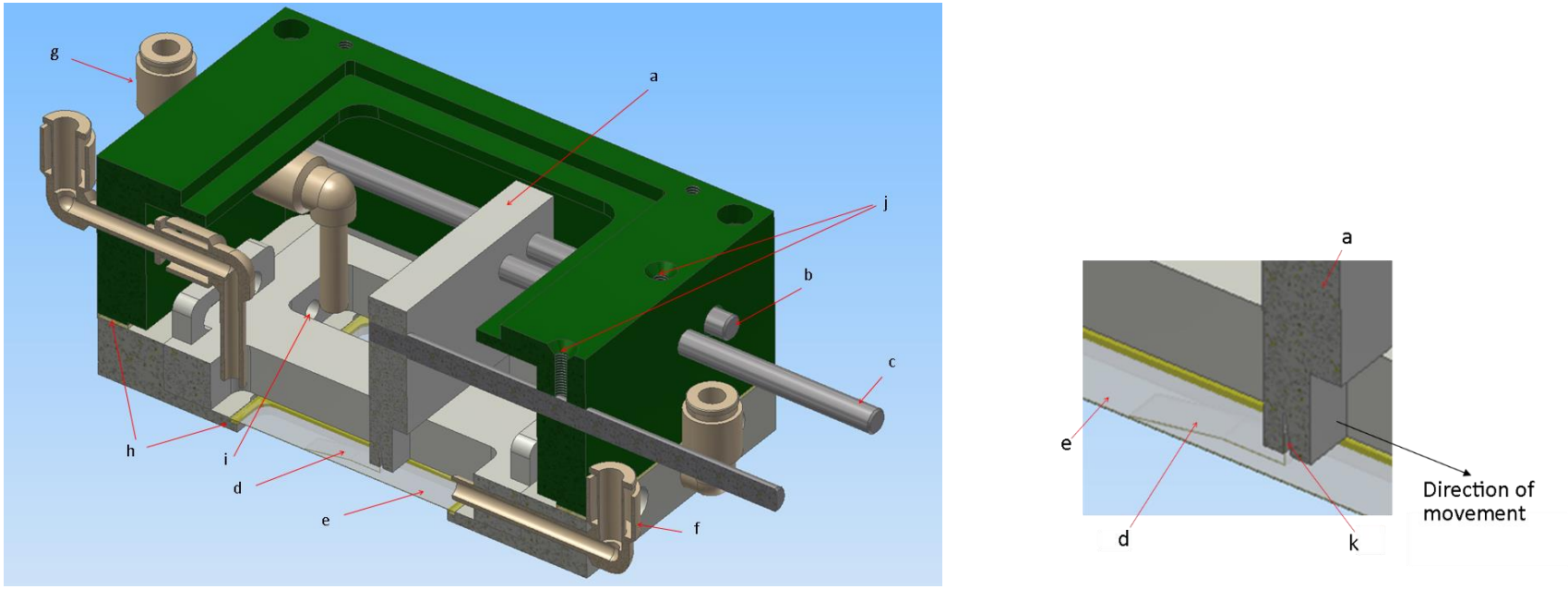

Figure 29: Sagittal view of 3 sectioned bioreactor (assembled)

(a) The axon stretching block projects across the top section and into both culture wells of the middle section, and is mounted through corrosion resistant overhead stainless steel "316" 5mm rods (b). Controlled motion of the axon stretching block (a) was achieved using two corrosion resistant stainless steel "316" 5 mm pulling rods (c), which connected the block to the external drive assembly. On the inferior surface of the axon, stretch blocks a slot facilitated insertion of a removable Aclar 05mm substrate (d), which was angled to push against the removable glass substrate (e) (enlarged view figure 2a). The media feed Inlet port (f) sits low in the media well to prevent drip waves. The media outlet port (g) sits below the top of the media well, so that it prevents disruption to the cells and maintains a constant level of culture medium. Hollow tube for a closed loop immersion PT100 temperature sensor probe (i) Threaded holes for axon stretch block locking screws (j). Note: Not shown- 5% CO_2 in the air inlet and outlets ports, or glass access top. Silicone Gaskets are used to prevent leakage or air entry (h). An enlarged view of glass and Aclar substrates to demonstrate the arrangement of glass and Aclar substrates: Shown here, the axon stretch block (a) with the Aclar substrate inserted into the holding slot on the inferior surface (k). The Aclar (d) is also angled towards the glass substrate (e) to maintain contact between both substrates during motion.

Future Direction – Bioreactor Development

The development of the bioreactor is an ongoing "experienced based" process. Since the publication of the bioreactor, two new versions have been produced. The first, a one-piece version which has been initially printed in Acrylonitrile Butadiene Styrene (ABS) for testing. This will eventually be printed using a 3D PolyEtherEtherKetone (PEEK) printer when available (Figure 30). This unit in PEEK should have limited assembly all screws are made of PEEK, and therefore the complete unit is sterilisable. (PEEK 3D printers are now available as are the separate print heads https://3dprint.com/52713/indmatec-peek-fdm-printing-filament/ accessed 1st July 2016.

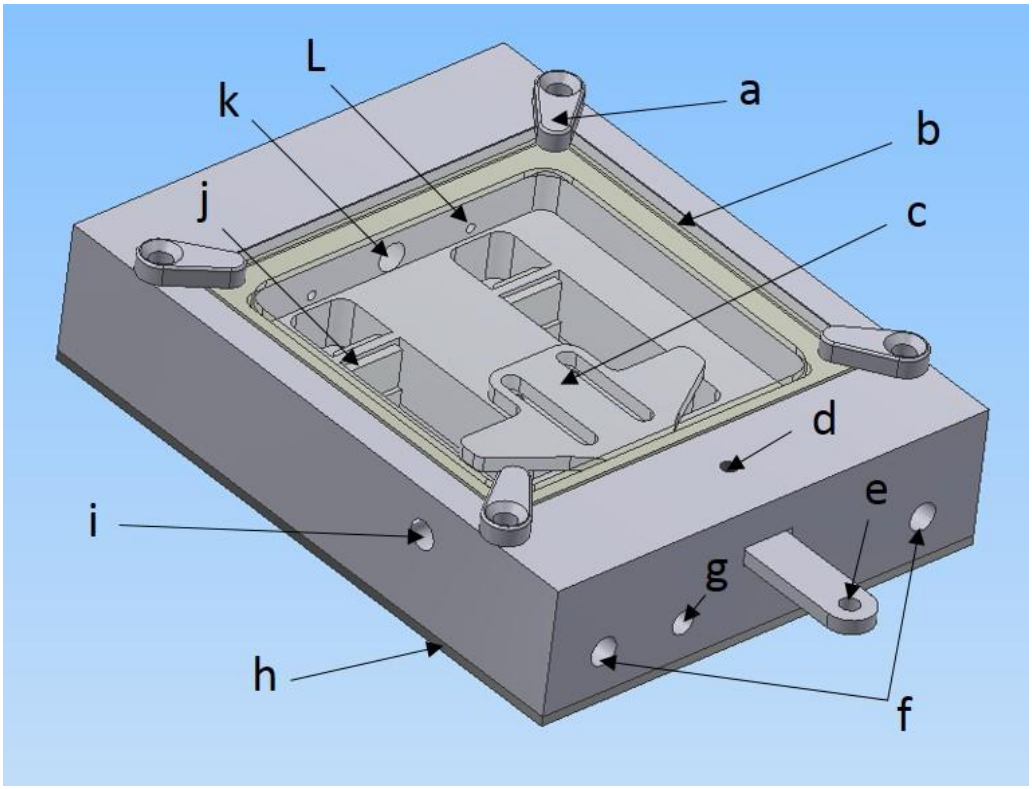

Figure 30: Single Piece 3D printed chamber

Figure shows Lockdown glass tabs (a), Glass cover and silicone gasket (b), Lockdown post stretch for Immunohistochemistry -note pull bar "e" disconnects inside chamber (c), Lockdown for pull bar (d), Pull bar (e), Provision for 6mm heating tubing (f), PT100 temperature probe (g), 3mm stainless steel screw on base (h), Inlet tubes for feed and air escape via tube into bottle with escape valve (i), Barrier insert – prevents solution disturbance feed in (j), Pre-mixed 5% CO_2 Inlet (k), Feed Inlet tubes (L)

The second unit was produced for researchers on a low budget. This integral bioreactor component cost is under AU$150. The bioreactor could alternatively be printed using a 3D printer and installed onto a flat platform. This ASG device uses a standard glass slide with an adapter as the stretch bar and slide cover on the top for viewing. The top section is touch fixed with silicone allowing for easy removal. Adapters can be placed on the internal section of the glass slide to either pull Aclar or use a stretchable membrane (Figure 31).

Supplementary Source Code attached as Appendix 1

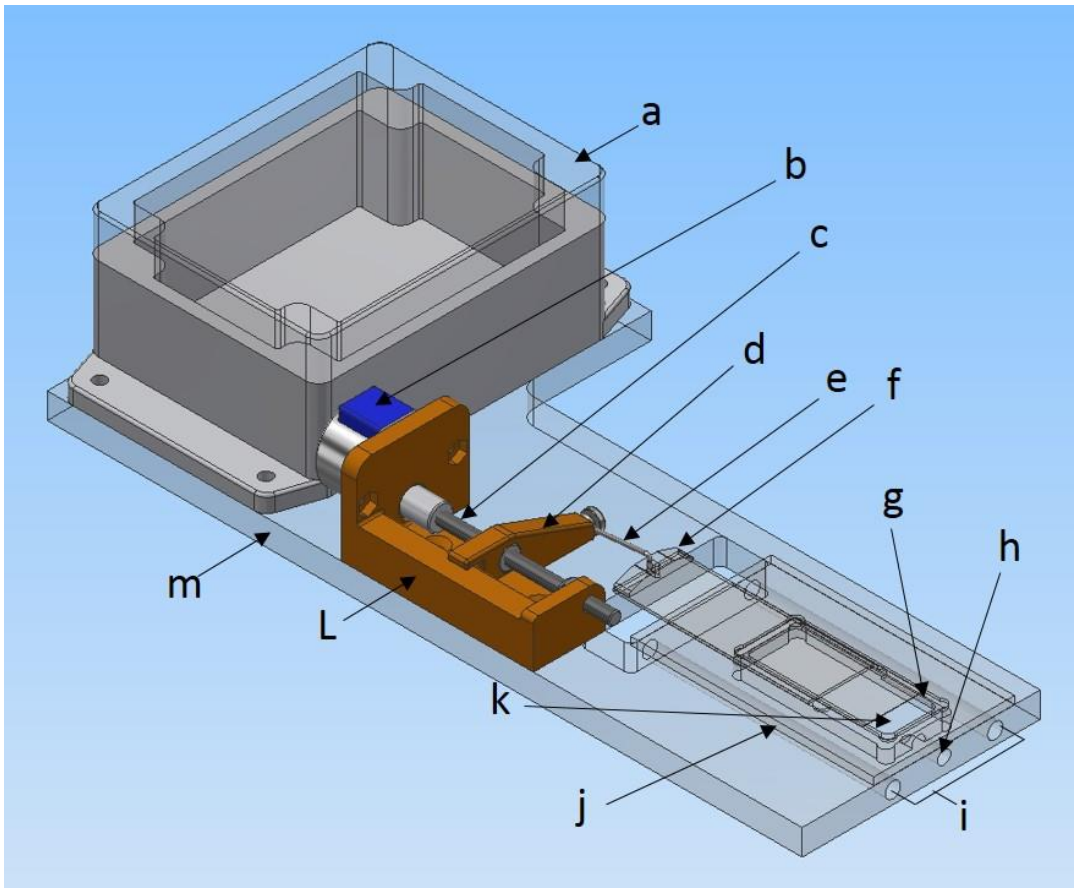

Figure 31: Low-Cost ASG integrated system

This bioreactor was designed for use in a standard culture oven and is easy to operate. Not shown is the standard Arduino board (stepper motor controller)

Housing for Arduino basic board (a), 28BYJ -48 standard stepper motor (b), 5M threaded bar 8mm distance between each thread (c), Drive arm (d), Attachment bar (e), Adapter on glass slide (f), Sliding slot for glass slide (g), PT100 temperature probe (h), provision for heating tubes (i), Removable top section (j), Solution well (note this is machined so does not penetrate the bottom of the base) (k), 3D printed drive housing (L), One piece base (m)

Decommissioned Humidicrib

As the project unfolded, a decommissioned infant humidicrib was obtained *ex gratia*, which was modified for use making the system portable. The engineering in this aspect of the work was very much trial and error. During the process, many issues were encountered that warranted incorporation into this thesis, but which as they formed part of the inherent learning curve associated with prototyping such a device and did not make it into the final publication.

The use of a decommissioned humidicrib (a practical insight)

During the development of a functional bioreactor for axon stretch growth experiments, and following a networking visit inspired by Lynne Opperman (Opperman 2015), the opportunity arose to walk through a decommissioned equipment storage area of a local large metropolitan public hospital (Flinders Medical Centre Adelaide South Australia), where several decommissioned humidicribs were being stored. Following negotiation, one of these humidicribs was acquired *ex gratia* along with some useful spare parts (Drager Air-Shields Isolette C100). The humidicrib was in excellent order having been recently replaced in service by a newer model. In the Australian context, these items once decommissioned are stored for spares and then when no longer required are disposed of generally through public auction.

In developed countries, pragmatic decommissioning of electro-medical equipment can create a storage problem. One solution is to divest the equipment to a low resource country (Loomba 2014). However, in these situations, technology transfer may be limited by utilisation capability (i.e. presence of electricity or technical resource) or, as in many cases the cost of delivery may be prohibitive. Thus, the use of these devices to assist in-vitro research has an alternative altruistic benefit.

Infant Humidicrib modifications

To use the infant humidicrib as a culture oven was not a difficult conversion. The device was already appropriately sealed, and basic control of temperature and humidity was immediately available. An existing filtered port for Oxygen was also present at the rear of the unit.

Extensive trawling through the literature on CO_2 culture ovens uncovered the Pelling Laboratories basic culture oven and CO_2 controller software.

https://github.com/pellinglab/DIY-Incubator-Dec2014/blob/master/DIY_CO2_Incubato

The CO_2 device as described by Andrew Pelling was useful as the basis for the humidicrib system and was, therefore, downloaded and modified for use to dynamically monitor gas concentration. Interestingly, this made the unit more functional that the existing laboratory culture oven. Modifications to the equipment such as solenoid use were because of changes to the tank supply. The Pelling laboratory used a DIY heating system which was not suitable for our purpose. We instead incorporated a closed loop peristaltic pump system which had water heated in 6mm tubes passed through channels in the lower part of the bioreactor. For this purpose, an inexpensive controller from a steam sterilising oven was used.

Introduction to article

The infrastructure to view and image live cells over extended periods is a useful adjunct to investigate cell behaviour. There are commercial imaging systems available but these devices are typically expensive and due to warranty issues cannot be modified. For those basic scientists wanting to conduct long-term experiments that require simple equipment, this can be a formidable issue preventing progression.

Here through a combination of repurposing, some modification to existing “do it yourself” DIY science projects and the purchase of inexpensive hardware a decommissioned humidicrib is converted into a functioning imaging culture oven able to be modified for multipurpose use (in our case) for imaging axon stretch growth experiments.

The article also describes the manufacture of the multipurpose umbilical bioreactor, which allowed the bioreactor to either be placed onto an internal microscope for observation and imaging or to be relocated outside of the humidicrib such as in a laminar flow hood or alternative.

When not in use for axon stretch growth experiments, portability allows the device to be used elsewhere for other projects. The design of the umbilical bioreactor allows users to inexpensively engineer the top section to suit different experiments such as electrophysiology.

A portable live cell culture and imaging system with optional umbilical bioreactor using a modified infant incubator

Publication Status	☐ Published ☑ Accepted for Publication ☐ Submitted for Publication ☐ Publication Style
Publication Details	**Biotechnology**

Authors

Malcolm Brinn[1], Said F. Al-Sarawi[2], Tien-Fu Lu[3], Brian J C Freeman[4&5], Jaliya Kumaratilake[1] and Maciej Henneberg[1]

[1]School of Medicine, Discipline of Anatomy and Pathology, University of Adelaide, SA 5000 Australia

[2]School of Electrical and Electronics Engineering, University of Adelaide, SA 5000 Australia.

[3]School of Mechanical Engineering, University of Adelaide, SA 5000 Australia

[4] Discipline of Orthopaedics and Trauma, School of Medicine University of Adelaide, SA 5000 Australia

[5]Department of Spinal Surgery, Royal Adelaide Hospital, North Terrace, Adelaide, SA 5000 Australia

Corresponding Author: Malcolm Brinn

malcolm.brinn@adelaide.edu.au

Keywords: Cell Culture, Bioreactor, Live Cell Imaging, Tissue Engineering

Abstract

Here, we present a staged approach for an innovative repurposing of a portable infant humidicrib into a live cell growth, observation, and imaging system. Furthermore, humidicrib can support different variations of "umbilical" bioreactors and can be used to conduct electrophysiology experiments and *in situ* immunohistochemistry. Modifications incorporate a closed loop carbon dioxide (CO_2) concentration control system with umbilical CO_2 and heating support for simple bioreactors. The repurposing cost is inexpensive and allows for the continued observation and imaging of cells.

This prototype unit has been used to continuously observe and image live primary neurons for up to 21 days. This demonstrates the repurposed units' suitability for use in tissue culture based research, especially when modifications to microscopes are required or where sensitive manipulation outside of a standard incubator is needed.

Introduction

Cell culture ovens and microscopes can typically be found in all cell culture laboratories. For many researchers, cells may only need observation at the time of passaging or during short term experiments and for this purpose quick transfer or stage top incubation systems may be employed. However, in some instances, it is necessary to observe and image cells over extended periods or to use the tailored equipment. Commercial live cell imaging systems can be useful but for some, the cost of the equipment may be prohibitive for occasional use, or warranty conditions may limit options. Repurposing of assets is one potential way in which this can be resolved, by reducing expenditure as well as outbalancing the accrued cost of asset decommissioning (Loomba 2014; Opperman 2015).

Infant humidicribs are essential devices used to support neonates who would otherwise have difficulty regulating and maintaining their homoeostasis (Burgess 1978). Advances in the design of many of these devices have enabled them to regulate oxygen and humidity while isolating the infant in an aseptic environment. In a hospital setting, failure of this type of equipment can lead to catastrophic outcomes. Therefore, these devices are often pragmatically decommissioned early in their working life cycle. However, being complex devices, we believe they retain significant inherent value for alternate use. Here we present the novel repurposing of a decommissioned infant humidicrib into a portable imaging culture oven that can support different variations of “umbilical” bioreactors in a non-critical setting.

Materials and Methods

A decommissioned humidicrib as manufactured by Drager (Drager Air-Shields Isolette® C100) was obtained exgratia from a local government hospital. Device dimensions (mm) were 1340 H x 560 D x 1160 W comprising a plexiglass enclosure with a raised bed. The bottom section contained a control module, heating element, a port of oxygen supply, and an internal humidification system (Figure 32). This particular model also has an optional height adjustable strut under the trolley frame allowing user variation to suit standing or sitting.

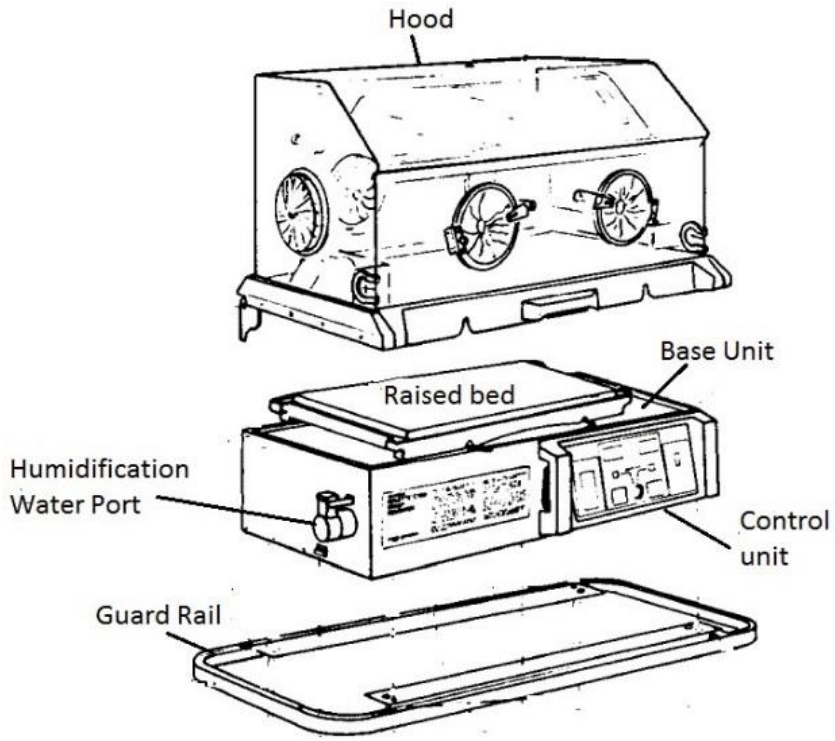

Figure 32: Adapted drawing (service manual) of the Drager Air-Shields Isolette ®. C100 Humidicrib

Air is actively circulated across a heating element within the base and over an internal humidification tank and then passes into the interior. The plexiglass interior (shroud) of the infant incubator is isolated from the surrounding air by rubber seals. The control panel, has built-in skin or air temperature control devices, with digital displays (range 0 to 38.5^{o}C ± 0.5^{o}C) and visual and audible alarms. Access to the interior of the humidicrib is provided by air tight doors or iris entry ports. The raised infant bed can also be accessed by lowering the whole front panel. Gas can be introduced into the humidicrib through an external port (rear of unit – not shown) to which a gas bottle can be connected.

Modifications to humidicrib

An Olympus IMT2 inverted research microscope was mounted centrally between the front access ports of the humidicrib shroud, so that coaxial stage controls, revolving objective turret, field brightness, coarse and fine image adjustment controls, as well as a power switch could be accessed either by the right or left hand. Detachable access panels were cut into the centre rear and at the top/front of the humidicribs plexiglass shroud to allow the binocular shaft of the microscope to project neatly through the angled top of the plexiglass. A 3-Dimensional (3D) printer was used to construct tailored trim for the binocular shaft, and silicone rubber matting was used to maintain internal seals.

Although the humidicrib had independent heating and humidity systems, it did not have an independent CO_2 monitoring and control system. This was developed using a suitable regulator; gas approved 2W025-08 electric solenoid and an in-house established Arduino controller. When stationary, the gas supply could be either co-located onto the infant incubator making it portable or kept as a larger supply next to the unit (Figure 33). CO_2 sensing was achieved through a fast acting (20 Hz) real time CO_2 sensor (SprintIR GC-0017 0-20%).

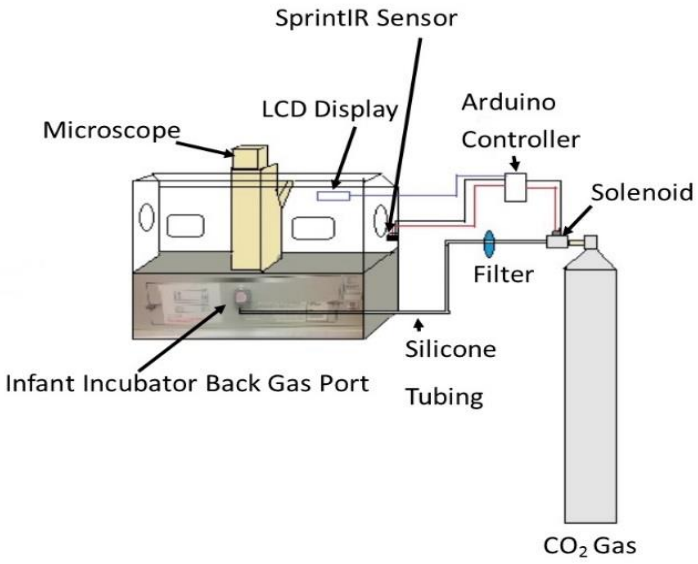

Figure 33: Diagram representing the CO2 gas connection direct to the incubator

CO_2 gas enters the port and passes over an internal humidification and heating system. A fan circulates the gas up into the shroud where the SprintIR picks up the internal concentration. The closed Arduino circuit displays the CO_2 concentration and activates the solenoid (default off).

Heating: the humidicribs existing infrastructure maintains the inner shroud temperature and humidity.

The CO_2 controller comprised a closed loop relay circuit that was routed through a standard Arduino UNO circuit board controlling both the CO_2 display powered via a standard printer USB cable and solenoid powered through a 12-volt adaptor (Figure 34). Arduino technology is an open source electronics platform intended for developing inexpensive interactive systems. Therefore, access to basic forms of Arduino circuit diagrams and source code was freely available from the internet under open access arrangements (Appendix 2: CO_2 PID Controller – Arduino Source Code)

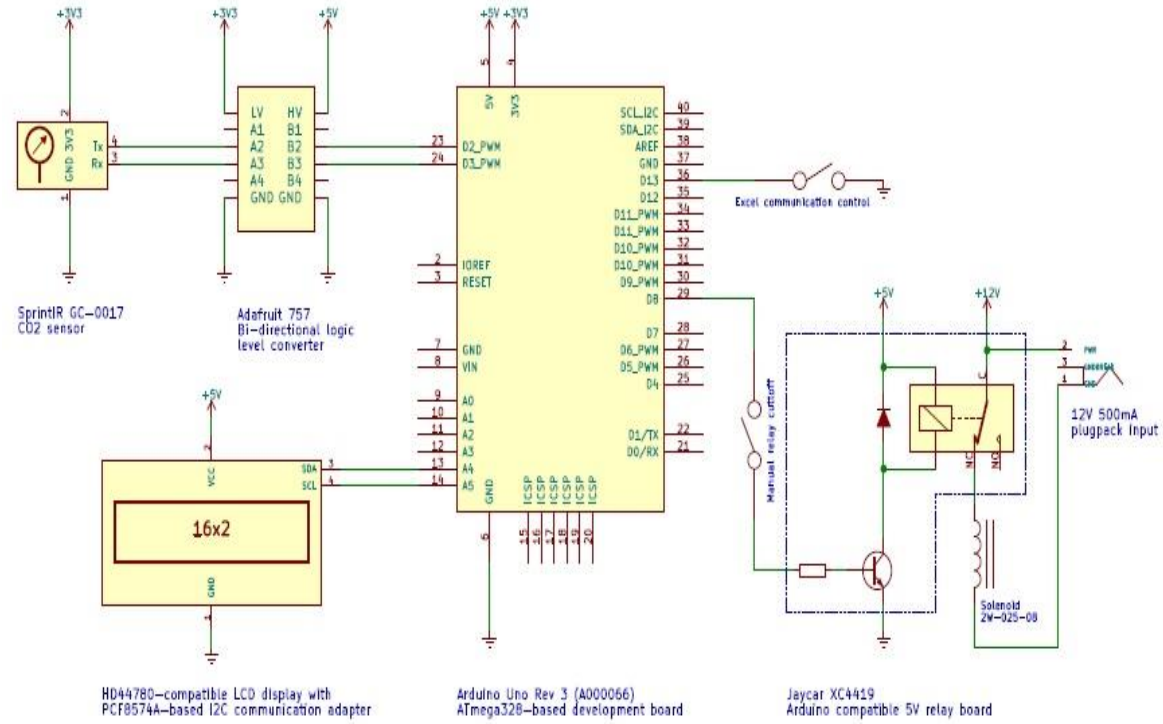

Figure 34: Arduino based circuit diagram for CO2 control

CO_2 concentration is determined and monitored via a closed loop system. Air concentration is determined using a SprintIR 0-20% CO_2 sensor routed through a bi-directional logic level converter. Gas output is controlled through a 2W-025-08 gas solenoid (Default closed). The Arduino board controls the 5V relay, switching the solenoid on and off. A Liquid Crystal Display (LCD) shows % CO_2 levels. Data logging in CVS format is facilitated through an Excel spreadsheet which can be used to monitor flow over extended periods.

Adapted from www.pellinglab.com. Schematic modifications (incorporating the logic converter, independent 5V relay board, LCD) and final fabrication.

Bioreactor development – Umbilical support (heating and gas)

Pilot investigations highlighted that removal of cultures from the humidicrib for periods more than a few minutes caused a rapid loss of temperature and in the absence of CO_2, pH variation. This was problematic for the use of equipment that could not be incorporated into the shroud and where cell/tissue homoeostasis was necessary. Provisioning the infant incubator to provide umbilical support to bioreactors rather than acting primarily as a portable culture oven, thus extends versatility and operational flexibility. The length of the umbilicus can be varied to suit requirements (Figure 35).

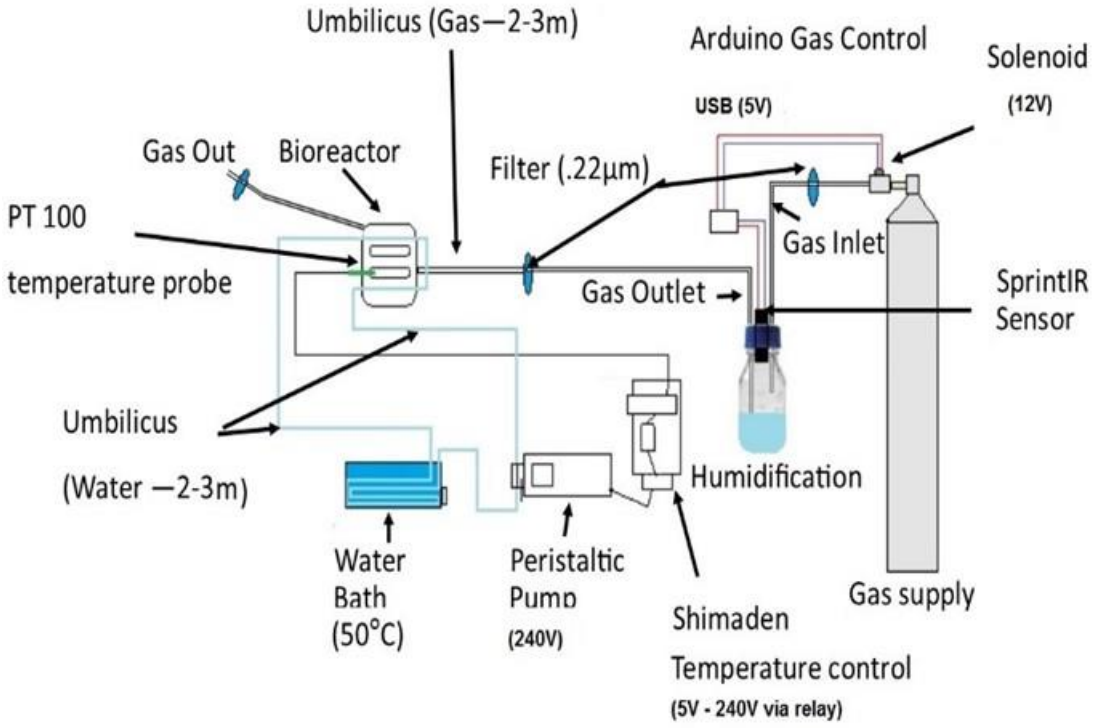

Figure 35: Diagram of heating and gas

Heating: The PT100 temperature probe picks up the temperature and passes it to the Shimaden controller. At set points, the controller triggers a relay to open power to the peristaltic pump which circulates pre-heated water through the bioreactor.

Gas: The same Arduino control is used. However, gas from the solenoid is passed through a filter into a humidification container. Then the gas is filtered before entering the bioreactor. The operation of the controller remains the same.

Umbilical heating was provided through a water filled silicone tube (6mm) which was weaved longitudinally through channels provided in each bioreactor and passed through a small sealed bath (50^{o}C). A PT100 temperature control probe in contact with the media provided feedback on temperature to a Shimaden Controller (±0.1^{0}C), Schematic details are given (Figure 36).

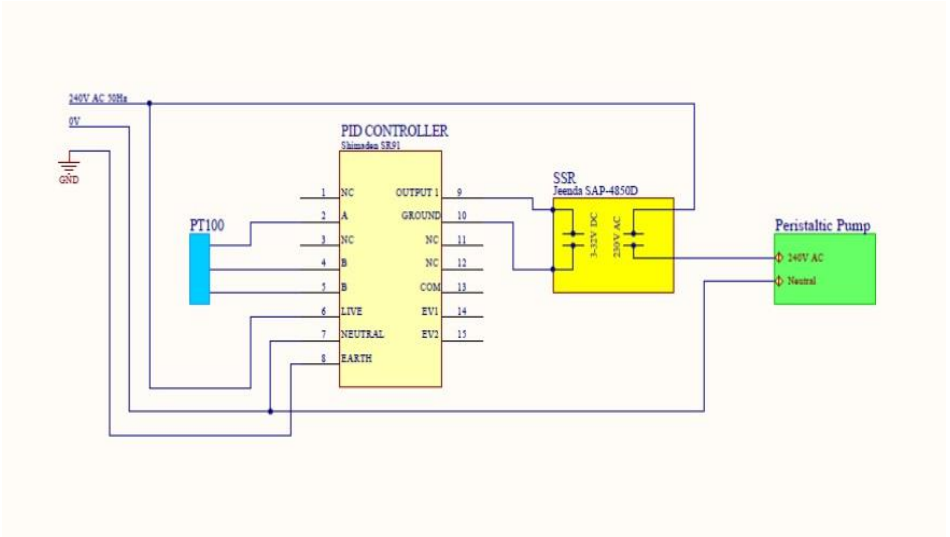

Figure 36: Schematic wiring diagram of the closed loop heating system

Culture medium temperature is determined using a PT100 temperature sensor that is wired to a Shimaden SR91 proportional integral derivative (PID) controller. The PID triggers the solid state relay (SSR) to provide on/off power to a peristaltic pump that circulates the heated water. The Shimaden controller can be programmed with user-defined minimum and maximum set points and has built-in fuzzy logic. Therefore, over time the controller determines the optimum turn on/off ranges to mitigate overshoot of temperature.

Carbon dioxide was provision to the bioreactor was achieved by fitting 6mm inlet and silicone outlet tubes and the existing CO_2 SprintIR sensor into the lid of a standard glass 500mL laboratory bottle. Before use, the assembly (excluding the sensor) was steam sterilised and then partially filled with sterile water under a laminar flow hood. Filtered (0.22 µm) CO_2 gas was then routed from the gas supply solenoid into the inlet tube. The outlet tube was tailored to appropriate length into the bioreactor CO_2 port. A filter was used on the outlet tube, but care was taken to place this close to the bioreactor as humidity over time could cause the filter to block.

Bioreactor Design, Manufacture, and Assembly

Here three bioreactors are presented (Figure 37 and Figure 38), which were developed in series for the following experiments. The first example, a basic 3D printed version with the baseplate was designed for culturing, monitoring and imaging of motor neurons. The second example, a modification separated the bioreactor component into two parts, with the lower section being machined and used with multiple different top sections. This modification achieved standardisation of the umbilical heating system, improved *in situ* immunostaining capability and facilitated material choice flexibility of the top section for various experiments such as stretching of axons.

All bioreactors were designed using Autodesk® Inventor® Professional software 2017 and were for use with the inverted microscope. All devices were manufactured internally at the University Engineering Prototyping Laboratory. Each bioreactor differed in material selection and method of manufacture. However, all bioreactors used the same supporting infrastructure for both gas and heating. Length and width (mm) were standardised to 130 (L) x 100 (W). Height varied per requirements. All designs of the bioreactor shared the key basic requirements of being non-toxic, sterilizable, and leak proof. Each featured two tissue culture medium/cell containment wells that accommodated removable standard 60 x 24 mm cover glasses as viewing bases, external culture medium heating channels and provision to use a temperature probe in direct contact with the medium (Figure 37B). A standardised base plate for all versions of the bioreactor was machined from a 3-mm thick stainless steel sheet (Figure 37C).

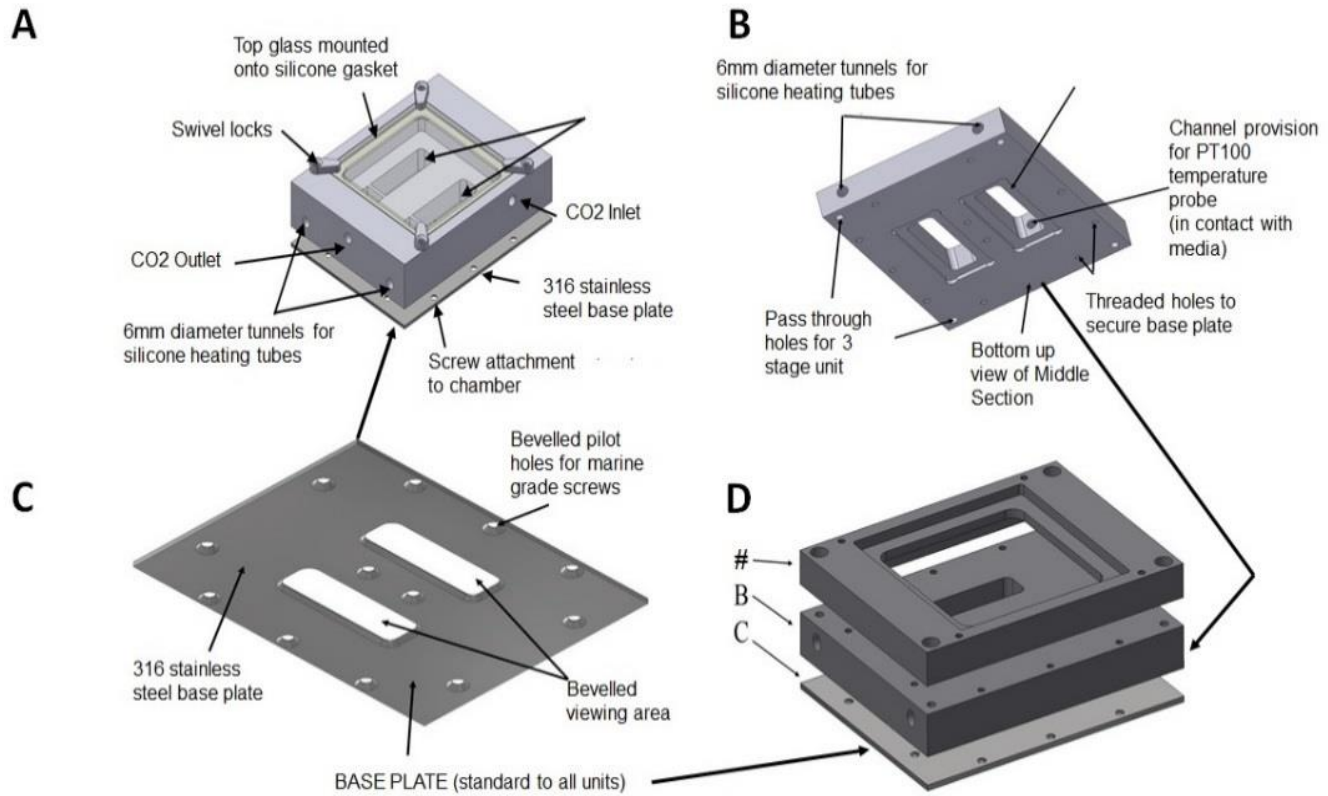

Figure 37: Basic design of bioreactors

A Top: Standard 1- piece 3D filament (Acrylonitrile Butadiene Styrene ABS) printed bioreactor with 316 stainless steel base plate **B:** Middle section of a three-piece bioreactor (including the 316 stainless steel base plate) machined from Polytetrafluoroethylene (PTFE). The top section on these units could be varied. **C**: The standard base plate common to all units **D:** Highlighting the 3-piece bioreactor assembly. **#:** The Top and Middle sections of the 3-piece bioreactor are similar to the one-piece design when assembled. However, the middle section was machined from PTFE and the top section 3D filament printed with ABS.

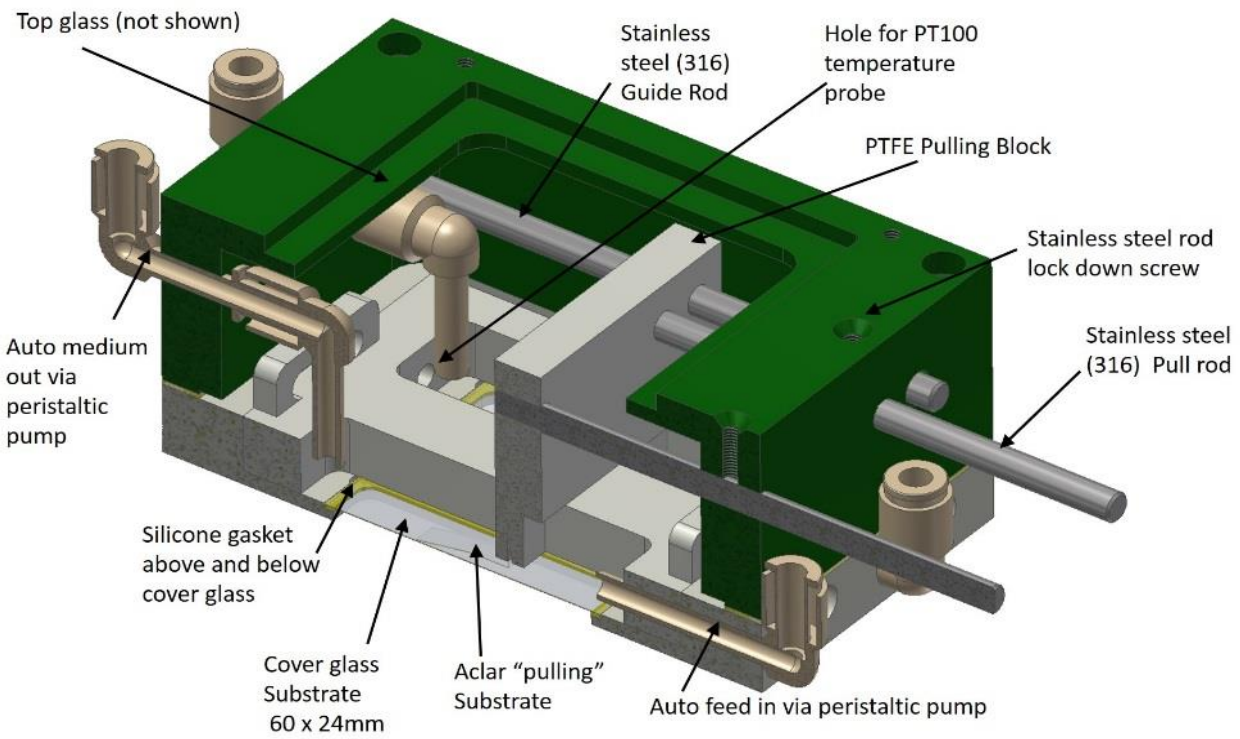

Figure 38: Sagittal view example of a more advanced bioreactor (top aluminium machined (PTFE coated) bottom section machined from solid PTFE. Standard base plate not shown

This bioreactor incorporates many specialised features. The top section could be removed to conduct electrophysiology experiments and *in situ* immunohistochemistry. It also incorporates axon stretch technology adapted from (Loverde et al. 2011a). The lower (also shown Figure 37B) incorporates a pilot version of an autofeeding system designed to prevent drying of the culture wells. The heating channels are running through the lower chamber on either side and between the medium containing wells (not visible in this view). Cover glasses can be removed for immunohistochemistry processing.

Basic Live Cell Imaging

Images obtained from this system are dependent both on the quality of the microscope and objectives, as well as on the imaging method. The Olympus IMT2 microscope used for our experiments was ideally suited for this task. We had both the option to use a commercial camera attached to the front port of the microscope or to use an ocular camera (Dino eyepiece camera AnMo Electronics Corporation). Attaching a camera to the front port of the microscope required the correct Olympus fitting for the camera, but no calibration was readily achievable. However, the Dino eyepiece could be inserted directly into one of the two ocular viewing ports and taped into orientation. The image could then be projected to screen and captured via the DinoCapture software. Captured images can be calibrated and enhanced through the software (Figure 39B).

Results

Humidicrib conversion results

The humidicrib's internal heating system was sufficient to maintain cells in standard culture flasks. The inner shroud temperature of the infant incubator remained stable within specification. However, as with fixed culture incubators, it was essential to ensure the temperature of solutions was pre-set to operational requirements before placing cells into the hood. The large space within the humidicrib, together with the mounting of an inverted research microscope and a digital camera enhanced functionality. The cutting of the front of the plexiglass shroud and fixing of custom made trim made it possible for the operation of the microscope via the front ports of the shroud without disruption to the cells.

Modifications to incorporate CO_2 control direct into the shroud provided the stand-alone capability. A reasonably large gas cylinder could be mounted onto

the trolley making the unit fully portable. Alternatively, the unit could be plugged into a gas source or to a larger cylinder at the location when in use. The SprintIR sensor operated within specifications, and the Arduino controller triggered the solenoid to open (default closed) as required to maintain CO_2 levels at the programmed concentration (in our case 5%). The gas supply entered the bottom section of the incubator through a built-in filter and humidification system; there was a slight delay in sensor receipt of the gas concentration. Following door opening, this does cause the unit to briefly overshoot gas concentration by as much as 2% for a 10-30 second period.

The above modifications converted the decommissioned humidicrib into a portable culture oven capable of conducting continuous observation and imaging for research, particularly those that require continuous monitoring and sensitive manipulations.

Bioreactor development- results

Direct supply of CO_2 to the bioreactor (via a humidification tank) reduced the consumption of CO_2. Some problems occurred with the humidification system blocking filters, which were resolved through extending the CO_2 line length and by placement of the post humidification filter closer to the bioreactor.

The internal heating system of the humidicrib was sufficient to maintain internal plexiglass shroud temperature but it a longer time to bring the inner temperature of the bioreactor to 37^{o}C. Supplemental heating of the bioreactor worked exceptionally well and maintained the temperature of the culture medium at 37^{o}C ± 0.1^{o}C. When both heating systems were in operation, the temperature of the culture medium remained very stable.

Repurposing Costs

The total cost of repurposing the humidicrib is hard to estimate beyond the cost of supplies and materials (Table 20). The cost of labour will depend on

specific skills of the staff involved and their commitment to the project. The cost of bioreactors will vary considerably based on production methods. 3D printing bioreactors once designed can be typically produced for under AU$50.00. Costs for imaging will vary per the method used. A Dino eyepiece camera can be purchased for AU$390.00.

Table 20: Equipment requirements for CO2/Air sensor and control automation

Description	Qty	Estimated Cost AU$
Plastic Reinforced Shelf Humidicrib	1	40.00
Closed loop gas supply		
COZIR CO2 sensor (SprintIR 0-20%) (Internet)	1	140.00
Clear Box (Electronics)	1	15.00
Arduino Uno Controller (Internet)	1	25.00
AdaFruit 757 Bi-Directional logic converter (Internet)	1	6.00
HD44780 Compatible LCD (Jaycar)	1	15.00
XC4419 5V Relay (Jaycar)	1	5.00
Gas Solenoid 2W-025-08	1	16.00
Cables various	1	15.00
Closed loop heating controller		
Shimaden SR1 PID Temperature Controller	1	127.00
PT100 stainless steel probe	1	50.00
Solid State Relay SSR SAP4850D	1	20.00
Electronics Box	1	15.00
Power Socket	1	7.00
Silicone Tubing 6mm	1	50.00
Hot water bath	1	In use
Total cost all		546.00

Culture Use/Experience

To date, fifty-four neuron cell cultures have been incubated in these bioreactors with experiment duration varying from 3 days to 21 days. The overall picture of the working unit is provided (Figure 39). The Recent publication of some images obtained from live cells have been published elsewhere (Brinn et al. 2016).

Discussion

Live cell observation and imaging systems suitable for continuous use over several weeks are commercially available but expensive, and due to warranty issues modification can be problematic. Here, we have resolved this problem by repurposing an infant humidicrib and by developing an independent multipurpose bioreactor.

The humidicrib only required minor modifications to allow a variation of microscopes to be used. Once a suitable binocular port and removable top panels were cut into the plexiglass shroud it was a relatively simple exercise to lift off the shroud and install a variety of different microscopes. The advantage of this approach was that it allowed us to use our specifically tailored microscope with a variety of onboard instruments. A situation that would not have been possible using a commercial system.

There were also several advantages in using our own internal microscopes. Perhaps the most important were the enhanced functionality, but familiarity was also beneficial when working with instruments. Microscopes, of course, are delicate instruments, and the risk of damage to the optics is heightened during movement. However, this must be balanced against the alternative options available. In our case, removing the shroud and electrically adjusting the height of the stand made this a simple process and limited the risk. Another key benefit was the humidicribs portability. Once the microscope was removed, it could be easily transferred to storage or another laboratory allowing its reuse with another microscope.

The incorporation of an independent 3D printable bioreactor has been another useful feature. In our case, we now have several different versions for variation in experiments. However, we continue to experiment with designs and materials. Currently, we are printing in standard plastics overnight. However, PEEK is now available for use, and it would be our intention to use this in future bioreactor development as it is autoclavable.

The independent heating system presented in this paper works well with the water filled silicone tubing passing through a standard heated water bath via a basic peristaltic pump. The controller uses a standard relay, and these can be assembled into a black box and wired by an electrician in less than an hour. The gas controller is built using Arduino technology and a standard gas solenoid, both of which are robust. Although assembly of the Arduino controller is not difficult, most electronics stores can provide this assembly service for a small fee. Source code to run the gas controller was originally written by Andrew Pelling and is available for download (www.pellinglab.net.au). We have subsequently added to the functionality and enclosed the full source code to allow operation of the device.

Equipment failure is of course always an issue. However, the dependency on the humidicrib is limited, and heating elements within the unit can always be replaced with alternatives by a qualified electrician.

Although the unit can work as a standard incubator using standard cultureware, it does not have the insulation or advanced decontamination features available in purpose built units. However, the repurposing cost is inexpensive, and these units are frequently decommissioned.

Lastly, prior to use, it is recommended that appropriate electrical safety checks are made to the humidicrib. A CO_2 warning sensor should also be present where culture ovens or this device is in use.

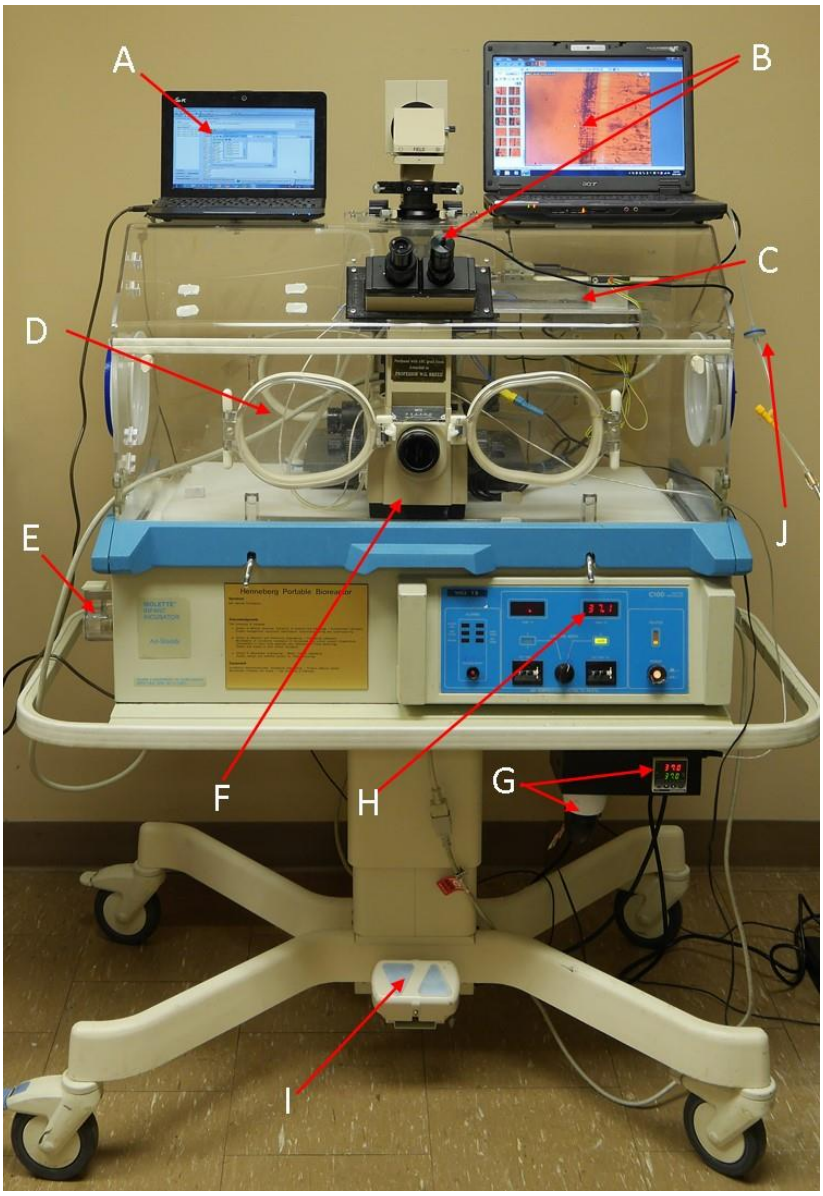

Figure 39: The complete system with assembled and functioning bioreactor in it is controlled and protected housing (humidicrib)

The paediatric humidicrib provides a secondary barrier to minimise contamination, vibrations, and external movements during operation. The bioreactor was mounted onto the sample stage (C) of an Olympus IMT2 inverted microscope (F) with 4x, 10x, 20x and 40x objectives. Pre-warmed humidified 5% CO_2 filtered air (0.22µm) was delivered through the small humidification system and piped through sterile tubing directly to the bioreactor gas inlet port (J). Temperature control was maintained using a combination of the humidicrib temperature control system (to prevent fogging) (H), and an internal PT100 sensor attached to an external proportional-integral-derivative (PID) controller (I) activating power to the peristaltic pump to circulate heated water (not shown). Time lapsed imaging was captured using a Microscope Dino-Eye (USB) camera AM7023 connected to Dino-Lite v2 software (B). Laptop system monitoring software (A). A total of 6 intervention ports could be accessed to make adjustments (D).

Conclusion

Infant incubators have inbuilt features that can be adapted for the growth of tissue cultures. Therefore, they could be modified into live cell imaging systems. Also, this apparatus can accommodate advanced technology. The cost in adopting these modifications may be inexpensive in comparison to new equipment purchase

Acknowledgements

We gratefully acknowledge the donation of the decommissioned infant incubator provided by Flinders Medical Centre, South Australia, the technical assistance of Mr Chris Leigh, School of Medicine, University of Adelaide and Mr Ian Linke, Mr Brandon Pullen, Mr Aubrey Slater, Mr Alban O'Brien, Mr Hayden Westell and Mr Danny Di Giacomo School of Electrical and Electronic Engineering, University of Adelaide.

Supplementary Source Code attached as Appendix 2

References

Brinn, MP, O'Neill, K, Musgrave, I, Freeman, BJC, Henneberg, M & Kumaratilake, J 2016, 'An optimized method for obtaining adult rat spinal cord motor neurons to be used for tissue culture', *J Neurosci Methods*, vol. 273, pp. 128-137.

Burgess, M, (President), 1978, 'Abstracts of Papers Presented at The 11th Annual Meeting', *Journal of Paediatrics and Child Health*, vol. 14, no. 2, pp. 109-127.

Loomba, APS 2014, 'Repurposing medical devices for LRCs; Sustainability considerations', *Engineering, Technology and Innovation (ICE), 2014 International ICE Conference on*, 23-25 June 2014, pp. 1-6.

Loverde, JR 2009, 'Deciphering The Biology of Axon Stretch-Growth', Biomedical Engineering, Partial Fulfillment of the Requirements for the Degree of Master of Science in Biomedical Engineering thesis, New Jersey Institute of Technology, The Van Houten Library.

Loverde, JR, Ozoka, VC, Aquino, R, Lin, LS & Pfister, BJ 2011a, 'Live imaging of axon stretch growth in embryonic and adult neurons', *J Neurotrauma*, vol. 28, no. 11, Nov, pp. 2389-2403.

Loverde, JR, Ozoka, VC, Aquino, R, Lin, LS & Pfister, BJ 2011b, 'Live imaging of axon stretch growth in embryonic and adult neurons Supplementary Data, J Neurotrauma, vol. 28, no. 11, Nov, pp. 2389-2403.', *J Neurotrauma*, vol. Vol 28, No 11, Nov, Supp Data.

Loverde, JR, Tolentino, RE & Pfister, BJ 2011, 'Axon Stretch Growth: The Mechanotransduction of Neuronal Growth', *J Vis Exp*, no. 54, p. e2753.

Opperman, LA 2015, 'Anatomist executive talks device development', *Biomedical Instrumentation and Technology*, vol. 49, no. 2, pp. 125-127.

Pfister, BJ, Iwata, A, Meaney, DF & Smith, DH 2004, 'Extreme Stretch Growth of Integrated Axons', *J. Neurosci.*, vol. 24, no. 36, September 8, 2004, pp. 7978-7983.

Pfister, BJ, Iwata, A, Taylor, AG, Wolf, JA, Meaney, DF & Smith, DH 2006, 'Development of transplantable nervous tissue constructs comprised of stretch-grown axons', *J Neurosci Methods*, vol. 153, no. 1, May 15, pp. 95-103.

Smith, DH, Pfister, BJ & Meaney, DF 2001, *Device and method using integrated neuronal cells and an electronic device*, Smith Douglas Hamilton, Bryan Pfister, Meaney David F., US 7429267 B2, United States.

Chapter 6. In-vitro axon stretch growth of adult rat motor neurons

Title of Paper	**Axon stretch growth of demyelinated adult motor neurons: an early translational exercise**
Publication Status	☐ Published ☐ Accepted for Publication ☑ Submitted for Publication ☐ Publication Style
Publication Details	**Journal of Tissue Engineering**

Malcolm Brinn[1], Jaliya Kumaratilake[1], Said Al-Sarawi[2], Tien-Fu Lu[3], Brian Freeman[4&5], and Maciej Henneberg[1]

[1]School of Medical Sciences, Discipline of Anatomy and Pathology, University of Adelaide, SA 5000 Australia

[2]School of Electrical and Electronics Engineering, University of Adelaide, SA 5000 Australia.

[3]School of Mechanical Engineering, University of Adelaide, SA 5000 Australia

[4]School of Medicine, Discipline of Surgery, University of Adelaide, SA 5000 Australia

[5]Department of Spinal Surgery, Royal Adelaide Hospital, North Terrace, Adelaide, SA 5000 Australia

Corresponding Author: Malcolm Brinn

malcolm.brinn@adelaide.edu.au

Keywords

Primary cell culture, Bioreactors, Spinal cord injury, intercalated incremental axon growth

Abstract

Background: Injury to grey matter within the spinal cord leads predominantly to localised nerve body damage. Whereas, injury to ascending and descending nerve tracts leads to a distributed axonal injury through post-axotomy degeneration commencing as early as 72h post injury. This degeneration creates multiple zones of disconnection along the axon and therefore the distance between viable proximal and distal stumps can quickly increase – well beyond the rate of normal fascicular growth.

The stretch growth of axons has already shown promise as a method to develop a bridging axon construct using neurons obtained from dorsal root ganglion. Although notoriously difficult to culture for periods greater than a few days, here we culture and subject adult motor neurons to axon stretch growth.

Method: Spinal cords were extruded from an adult Sprague-Dawley rats, ventral horn neurons are separated, adult motor neurons isolated and directly seeded within a purpose-built bioreactor across two substrates. The culture medium used was serum free C2C12 conditioned Neurobasal -A/B27 with growth factors. Neurons were given seven days to stabilise and project neurites. At day seven, a computer program initiated incremental separation of the two substrates. Those anchored neurites that crossed the two substrates were thus subjected to intermediate (serial) tension.

Results: Neurons were cHat and Neurofilament – H positive and had observable motoneuron morphology with a single axon and multiple identifiable dendrites. Despite high rates of run failure, there were some instances, where Neurons remained viable within the bioreactor for periods more than 21 days. As only a few axons crossed the substrates and were subjected to tension, the disconnection threshold could not be sufficiently determined. The rate is lower than rates previously reported for dorsal root ganglion Neurons as disconnects were frequent at this rate, but the stretch was achieved in some cases.

Conclusion

While only limited numbers of axons crossed the substrates and were subjected to tension, there was sufficient evidence to suggest that adult motoneurons and their axons retain axon stretch growth capability. However, the evidence is still weak. Improvements in seeding methodology are required to yield more robust results.

This is the first study to our knowledge that specifically targets adult motoneurons in deference to dorsal root ganglion, embryonic, cell lines or stem cells.

Introduction

Spinal cord injuries (SCI's) are catastrophic events that invariably give rise to permanent deficits in motor, sensory and autonomic function. At a cellular level, primary injuries cause immediate disruption to cord homoeostasis triggering propagation of secondary injury cascades that serve to expand injury zones and inhibit potential repair attempts (Mortazavi et al. 2015; Profyris et al. 2004). Regardless of the cause of the SCI, the morphology of the spinal cord determines different injury patterns. In grey matter, the effects of injury are rapid and predominantly localised; while in white matter, the consequences of injury are delayed and generally dispersed through axon degeneration beyond the injury zone (Beattie et al. 2002; Ek et al. 2010; Ek et al. 2012; Tator 1995; Tator & Fehlings 1991).

Here we focus on white matter injuries as these are known to involve long nerve tracts such as the corticospinal tract. Injury to these tracts rapidly disengages otherwise functional neuronal circuits leading to loss of function and atrophy compromising a repair attempt (Beattie et al. 2002; Maxwell 1996; Tator 1995; Tator & Fehlings 1991). To improve function beyond mitigation, multiple attempts have been made to re-establish connectivity to these disrupted nerve tracts. Recent findings demonstrate that a variety of techniques such as cell-based transplantation, applications of scaffolds and nerve grafts, as well as the use of growth factors have been employed to bridge the gap associated with these injuries (Bauchet et al. 2009; Macaya & Spector 2012; Mortazavi et al. 2011; Tator 2006). An emerging theme from this body of research is that future interventions will be tailored based on the primary insult as well as the consequences of secondary injury progression. Thus, combination interventions will become more prevalent and varied within injury groups, i.e. patients with the same spinal cord level of injury and incapacity may require different combination interventions.

Injuries that involve long nerve tracts may benefit from tailored interventions that involve mechanical stretching of axons to improve the rate of growth (Smith, D. H. 2009; Smith, D. H., Wolf & Meaney 2001). This technology could be viable for future grafting to re-establish lost nerve tract connectivity (Pfister et al. 2006).

Long-term survival and the outgrowth of axons from implants (i.e. placed to bridge spinal cord injuries) developed through stretching of axons has already been demonstrated using embryonic (E15) dorsal root ganglion cells. However, they have failed to establish intra-spinal relays between the host and grafted tissues (Iwata et al. 2006). Thus, further investigation into axon stretching and the establishment of intraspinal relays is warranted.

The effects of stretching of axons on the growth of Neurons has been investigated *in vitro* using immortalised cell lines such as PC12 (Bernal, Pullarkat & Melo 2007) and N-Tera2 (Smith, D. H., Wolf & Meaney 2001). In addition, embryonic dorsal root ganglion cells have been used in *in vitro* investigations and now it is the common practice to use these cells, because of their robust nature in tissue cultures (Bray 1984; Campenot 1985; Loverde et al. 2011a; O'Toole, Lamoureux & Miller 2008; Pfister et al. 2004; Pfister et al. 2006; Smith, D. H. 2009; Smith, D. H., Wolf & Meaney 2001; Weiss 1941; Zheng et al. 1991).

Spinal cord injuries commonly occur in adults. Therefore, use of adult motor or sensory Neurons rather than embryonic nerve cells in *in- vitro* investigations may be more beneficial in the translation of the methods into *in-vivo* situations (Berger, Bayliss & Viana 1996; Cameron & Núñez-Abades 2000; Carrascal et al. 2005; Jacobson 1985; Morrison, Cullen & LaPlaca 2011; Viana, Bayliss & Berger 1994).

The aim of this investigation is to determine if primary adult motoneurons can be cultured in an ASG bioreactor for sufficient time periods to conduct future ASG experiments and to conduct pilot axon stretch growth study.

Materials and Methods

Neuron isolation and culture protocol

All procedures were approved by The University of Adelaide animal ethics committee and conformed to the guidelines of the Australian code for the care and use of animals for scientific purposes - 8th edition (2013).

Neurons were isolated and processed per protocol from the spinal cord of mature (8-12 week old) Sprague-Dawley rats weighing between 245 and 560g (Brinn, O'Neill, et al. 2016). In brief, animals were anaesthetized by intraperitoneal injection of Ketamine (80mg/kg) and Xylazine (12mg/kg). Hibernate -A / 2%B27 was used to hydraulically extrude the spinal cord (de Sousa & Horrocks 1979; Meikle & Martin 1981) and the ventral sections isolated and cut into 1mm segments. Cells were dissociated by proteolytic separation (Papain 36 Units/mL) and trituration. A combination of 70µM filtration followed by use of an Optiprep 4 stepped density gradient (Brewer & Torricelli 2007) was used to isolate Neurons. As dorsal segments were not processed, the Neurons isolated were considered at study commencement to be predominantly either motor or interneurons.

The collected, processed supernatant was centrifuged at 400g for 2 minutes and the resultant pellet resuspended into 200µL of filtered (0.22µm) C2C12 conditioned serum-free culture medium (Montoya-Gacharna et al. 2009). This was supplemented with additional ciliary neurotrophic factor (10ng/mL) and basic fibroblast growth factor bFGF (2ng/mL) (Grothe et al. 1991; Sendtner et al. 1991). Cells were either seeded into the bioreactor or seeded onto control slides within a sterile culture container.

At 1h post seeding, the bioreactor was docked onto the microscope stage within the portable imaging system (previously described). Filtered media was added directly to the control container and via feed tubes into the sealed bioreactor wells. The media was monitored daily and topped up where necessary. Every three days 1/3rd of the media was replaced, and fresh media added.

Axon Stretch Growth - principle of operation

Neurons are seeded within a purpose-built bioreactor onto one of two adjoining substrates. Once the axons extend across the adjacent fixed and towing substrates, axon stretching was initiated (per principle Smith, D. H. , Pfister and Meaney (2001). Linear controlled movement was achieved through software control of the micro-motion stage and was designed to generate a sequence of stretch-rest-stretch at or below the rate previously used by for adult DRG Neurons (Table 21) (Loverde et al. 2011a).

Micro-motion stage and Piezo technology

A precise micro-motion stage was designed for axon stretch growth (Figure 40). A linear ultrasonic piezoelectric actuator (U264) manufactured by PI® was selected to drive the linear stage. This device integrates two Piezoceramic actuators using a friction bar held to the actuators.

Table 21: Programmed axon stretch rates for adult motoneurons

ASG Commencement	Increment distance	Distance Over 24hrs
Day 7	1µm	0.25mm
Day 8	1µm	0.25mm
Day 9	1µm	0.50mm
Day 10	1µm	0.50mm
Day 11	1µm	1.00mm
Day 12	1µm	1.25mm
Day 13	1µm	1.50mm
Day 14	1µm	2.00mm

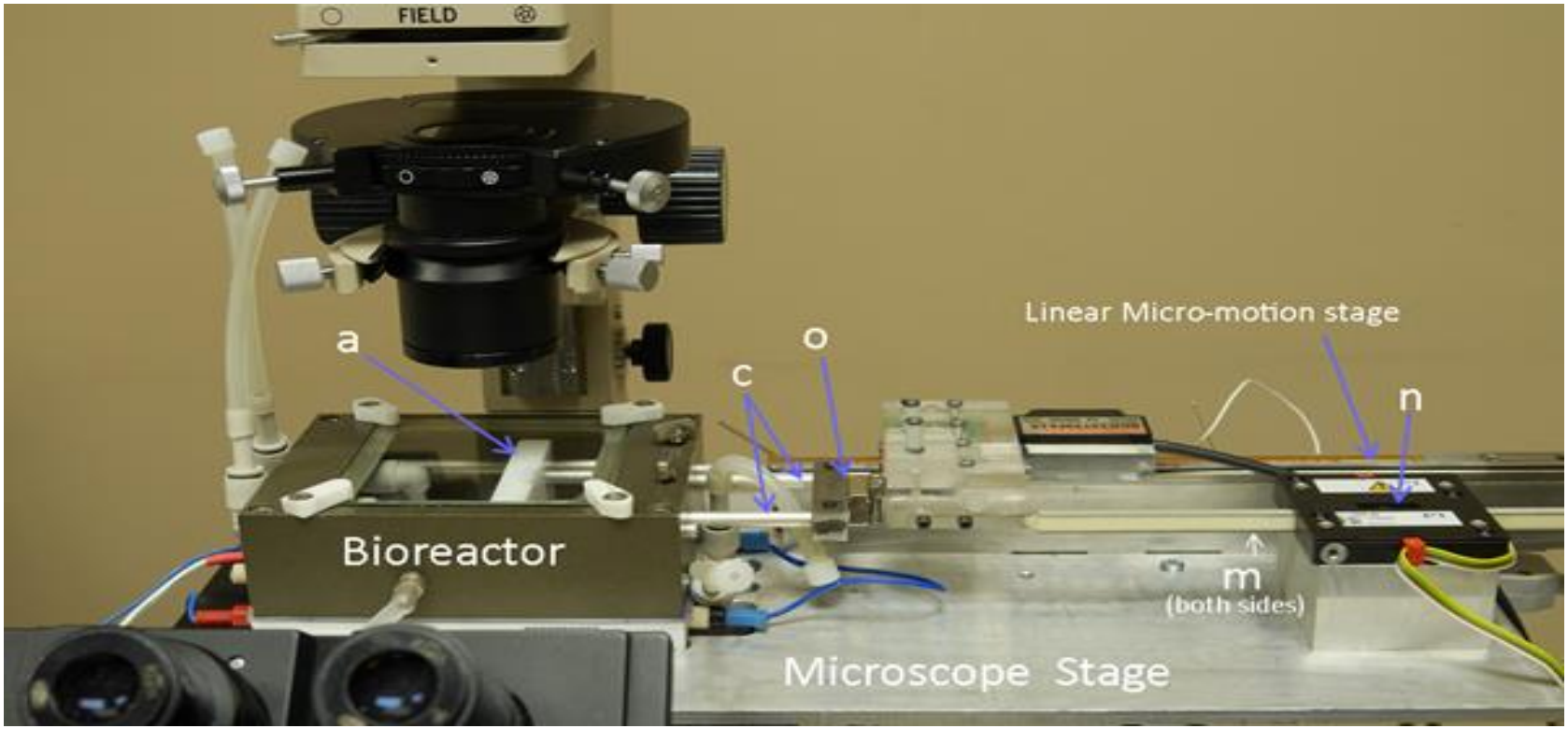

Figure 40: Image of Microscope Stage with Piezo actuators

Axons were stretched using an external precise micro-motion stage consisting of a linear ultrasonic piezoelectric motor (U264) driving a linear stage (manufactured by PI™). The device integrated two Piezoceramic actuators (m) using a friction bar held to actuators. The actuators are excited with sine waves at the resonant frequency. Osculation caused the tips of the friction bar pushers to lift and displace linearly at very high frequency. In conjunction with the pre-loading forces, this produces fast motion of the friction bar with a push force up to 12N. Together, with a corresponding controller (not shown), the performance characteristics of the actuator are adjustable. Also shown here, the bioreactor axon-stretch block (a) connection to the linear micro-motion stage by magnet (o) via the stainless steel (316) 5mm pulling rods (c)

The actuators are excited with sine waves at the resonant frequency. Osculation causes the tips of the friction bar pushers to lift and displace linearly at very high frequency. In conjunction with pre-loading forces, this produces fast motion of the friction bar with a push force up to 12N. Together with the corresponding controller, the performance characteristics of the actuator are adjustable.

The controller provides a software graphical user interface with PID servo control ability. A linear encoder made by Renishaw ® (RGH22) with a resolution from 5µm to 50nm was incorporated into the controller to achieve a close-loop control strategy. Thus, users can adjust the characteristics of the piezo-actuators and program the stretch-growing activities (i.e. the moving speed, the increment distance, and the time interval between each motion).

Bioreactor design and experimental preparation

The bioreactor used to conduct these experiments is a variation of the original device developed by Smith and associates ((Pfister et al. 2004; Pfister et al. 2006; Smith, D. H., Wolf & Meaney 2001), and which then was subsequently enhanced by Loverde and associates (Loverde 2009; Loverde et al. 2011a, 2011b; Loverde, Tolentino & Pfister 2011) to incorporate live cell imaging.

The bioreactor in use here was designed using Autodesk® Inventor® Professional software 2017 and machined and manufactured internally within the university engineering prototype laboratory. Detailed information on the overall design of the device, its operational housing (humidicrib), gas and heating systems have been previously described (Brinn, Al-Sarawi, et al. 2016). In this version of the bioreactor minor modifications were made to the bottom section and these are described (Figure 41)

Prior to use, the bioreactor and its attachments including the glass and Aclar™ substrates were assembled. The moving substrate was locked down preventing movement and the device autoclaved and transferred into a laminar flow hood. Sterile poly-d-lysine (100μg/mL) was applied at the junction of the upper and lower substrates and the unit left overnight under ultraviolet (UV) light. The substrates were then rinsed three times with sterile water and drained (not dried) under UV light. The bioreactor umbilical heating system was activated, and the internal bioreactor temperature under the laminar flow hood brought to (37^{o}C ± 0.2^{o}C). The humidicrib temperature system was also activated and the internal shroud temperature set to 37^{o}C pending use. Once cells were seeded, the bioreactor was sealed and transferred onto its operational housing, and internal bioreactor temperature and CO_2 concentrations were monitored and controlled to 37^{o}C ± 0.1 and 5% CO_2 ± 0.1 respectively.

Immunohistochemistry

At the conclusion of axon stretch growth, the culture media were discarded, and cells gently soaked (5 min) within the bioreactor wells in a prepared solution of 0.1M phosphate buffered solution (PBS) with 8% sucrose (washing buffer). Cells were then fixed in 4% paraformaldehyde solution prepared in 0.01M PBS with 8% sucrose (pH 7.4) for ten minutes. The fixative was removed by partially filling the bioreactor wells with washing buffer three times each lasting ten minutes' duration.

Cells were incubated for 20 minutes with 0.02 M glycine followed by a 30-minute incubation with a 7.4 pH blocking solution (2% normal goat serum, 1.1% bovine serum albumin, 0.1% Triton X-100, 0.05% Tween 20 in 0.01M PBS). Within the bioreactor wells, cells were then incubated overnight at 4^{o}C with the selected primary antibody at 1:500 dilutions. Controls were incubated with blocking solution in place of the primary antibody

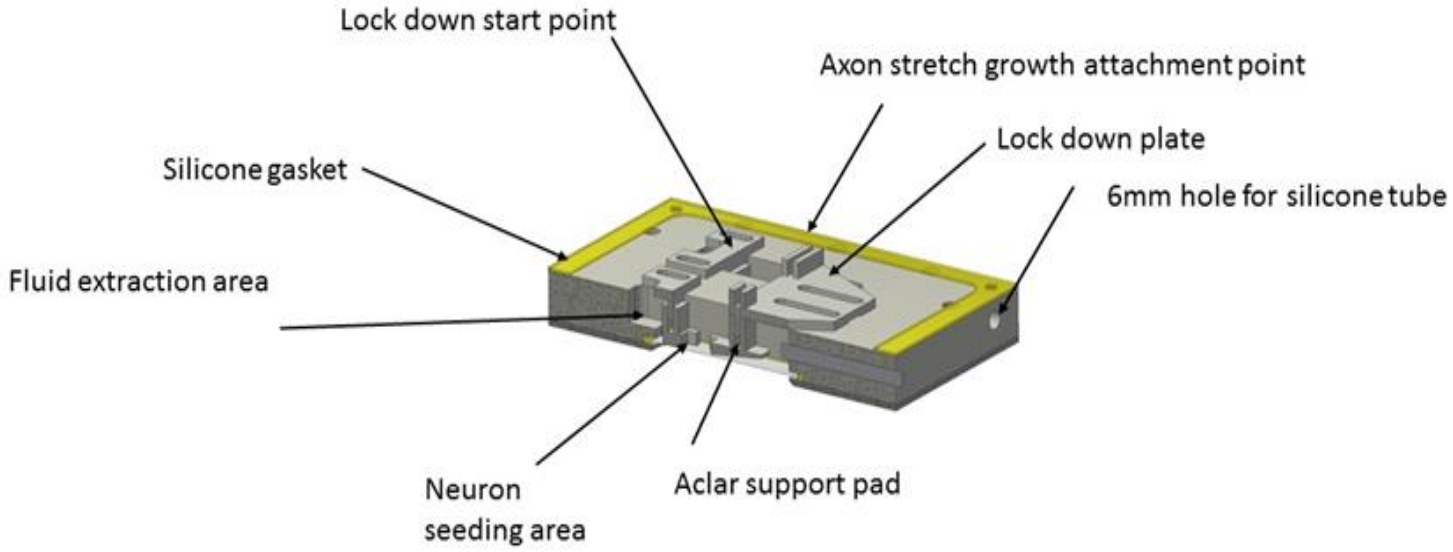

Figure 41: Cut Sagittal Image of Base Section

This sagittal cut view shows in detail the lower section of the bioreactor. This version incorporates a lock down plate which allows the top section containing the axon stretch growth slide mechanism to be removed without disturbing the axons. Note the fluid extraction area. In front of this area, a lock down start point prevents cell disturbance. The fluid extraction area is higher than the glass substrate preventing suction effect on the cells during extraction. Along the sagittal cut on the right, the fluid inlet top up tube is inserted, and this drips at a slow and constant rate and is lower than the fluid extraction port (not shown). This allows a small, inexpensive peristaltic pump to continuously run and remove fluid that reaches the top extraction point. The axon stretch growth attachment point can be lifted off the Aclar support pad. The Aclar is glued to the support pad using non-acetone based silicone. The seeding area on this unit is restricted to the "U" shape start point. Finally, a closed heating system supplies heat through two 6mm silicone tubes that run adjacent to the fluid wells. These tubes are filled with water and pass through a 60^{o}C water heating system (via a peristaltic pump). A PT100 temperature probe connected to a Shimaden temperature controller turns on the peristaltic pump that pumps the heated water through the tubes. At the correct temperature of 37^{o}C ± 0.1^{o}C the peristaltic pump that pumps the heated water switches off. Note: the Shimaden controller has fuzzy logic allowing it to adapt.

Results

Bioreactor and Axon stretch growth device commissioning

It was determined through a series of pilot studies (Brinn, O'Neill, et al. 2016) that it took up to 5 days' post seeding for neurites to appear (Figure 42). By day 21 networks had been formed and axons were clearly evident (Figure 43). As only the ventral segments of the spinal cord were processed, most Neurons were either interneurons or motor neurons (confirmed by Immunohistochemistry (Figure 44, Figure 45 and Figure 46). During commissioning of the bioreactor, a trypan blue exclusion test showed 80 - 92% cell viability at 7 days. Although initially, cell bodies were difficult to discern, they appeared round and bright against the supernatant debris. By day 5 of in vitro culture (DIV) projections were visible (Figure 42). Physical appearance identified axons, but this was a subjective observation. By day 7 and generally following the third medium change, debris had cleared, and therefore axon identification was less problematic.

Cell viability beyond 7 days in the bioreactor was consistently lower than that observed in the control group which was located in a conventional culture oven. Both the bioreactor and control groups used the same medium. However, medium evaporation was greater in the bioreactor requiring daily top-up.

Substrate separation was commenced at day 7 per protocol. There was preliminary evidence to support that primary adult motor neuron axons tolerate stretch growth (Figure 47), but disconnections were common at all ranges from 0.25mm to commencement of 1.00mm rate (Day 11). Disconnections were characterised by the axon recoiling (Figure 48). An image taken of a previously disconnected axon (estimated disconnection between day 9 and10) shows at day 14 what appears to be unexplained phase bright swellings of unknown origin (Figure 49).

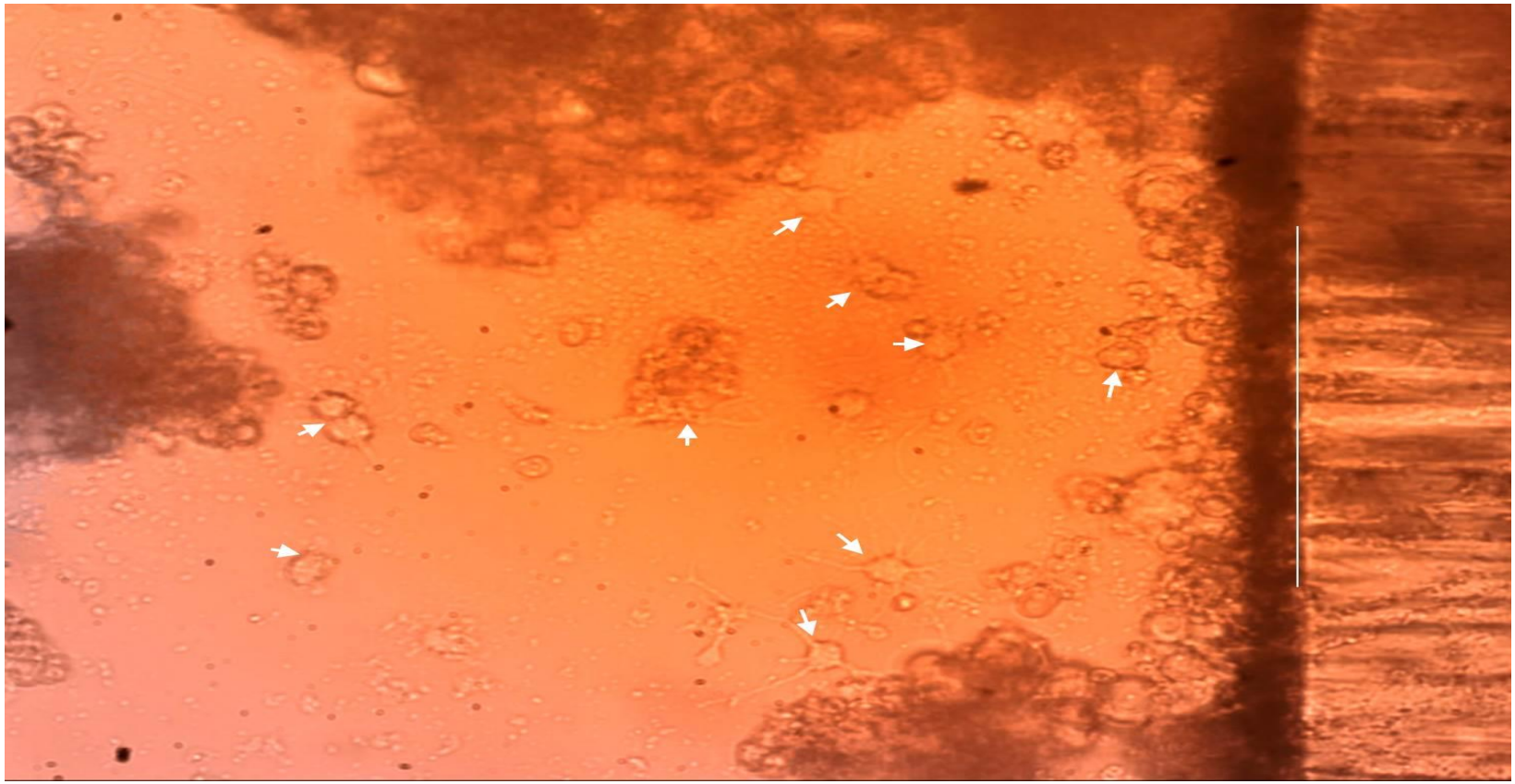

Figure 42: Image of Cells Day 5

Arrows highlight some of the cell bodies with projecting neurites. By day 5 some axons could be determined. The white line on the above image shows the substrate boundary. Careful inspection of the image shows other cell bodies (not highlighted) close to the substrate. At this stage, it cannot be determined if these projections have crossed the substrate. Note: The Aclar substrate used here (Loverde et al. 2011a) has been sanded with fine emery paper and both substrates sterilised and pre-treated with Poly-D-Lysine. Thus, it 's hard to observe if the projections have crossed the substrates.

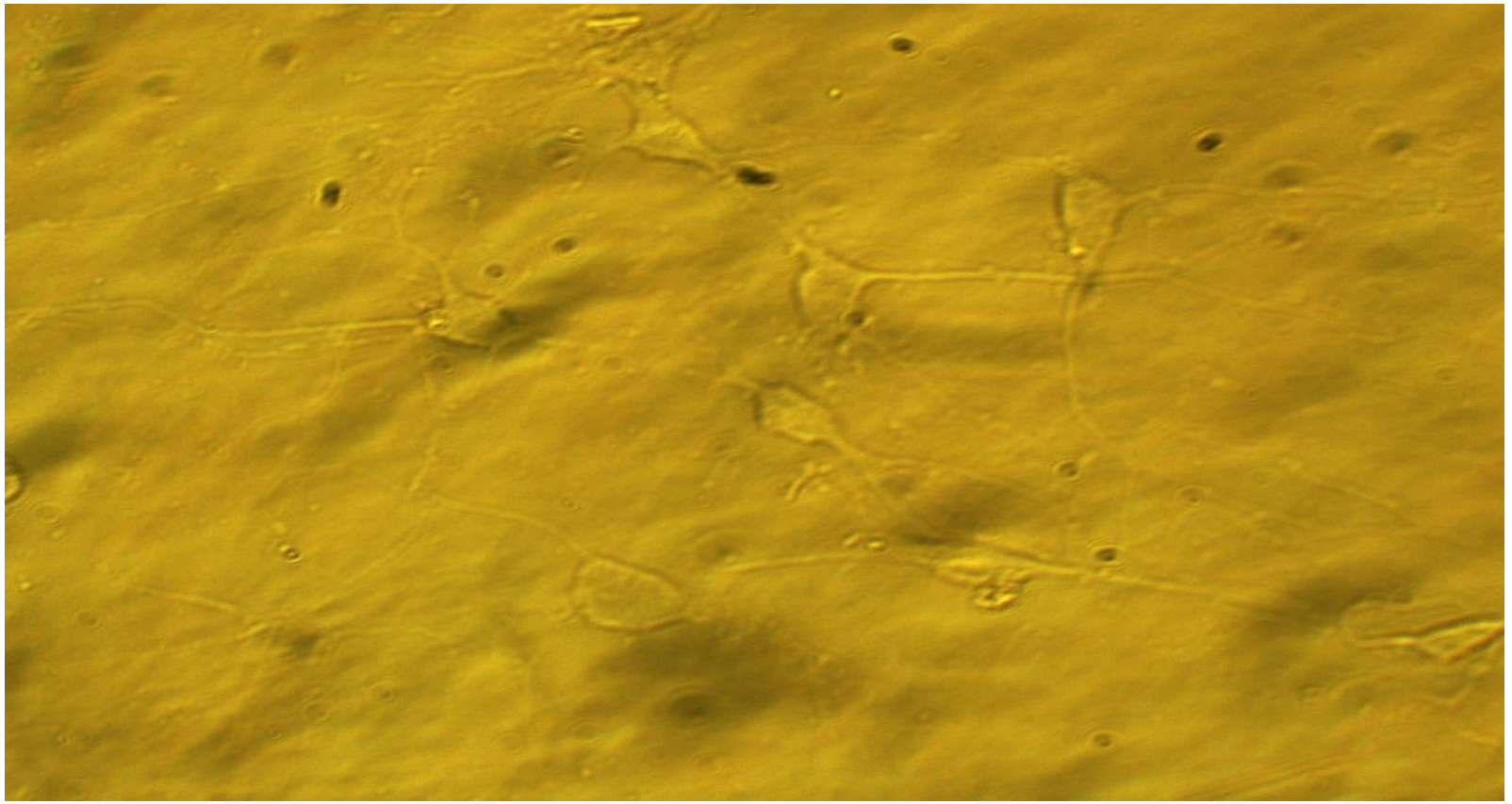

Figure 43: Image Day 21 (Under Green low light 24hr)

This image was automatically taken using a Dino eyepiece camera on day 21 (post seeding). It shows visible networking of neurites. The neurons depicted did not cross the substrates and were not therefore subjected to axon stretch growth experiments. These neurons were routinely exposed to this light source and did not appear to fade over the course of the culture. (28 days)

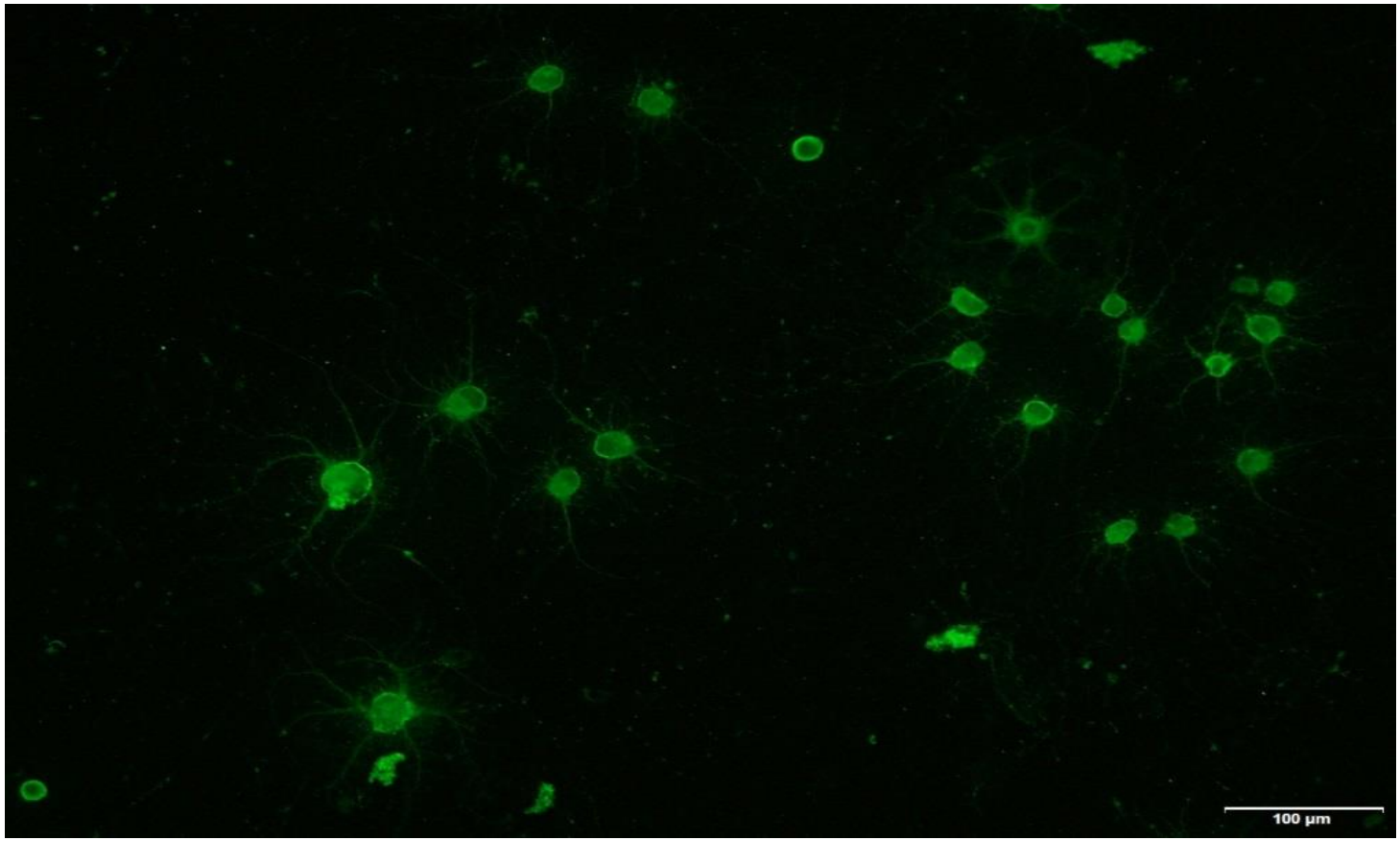

Figure 44: Image Axons Day 21 Immunohistochemistry cHat 100µm

Immunohistochemistry of neurons processed within the chamber using Anti-Choline Acetyltransferase 1:250 (0.004 mg/mL) Abcam ab35948 specific for Spinal cord motor neurons

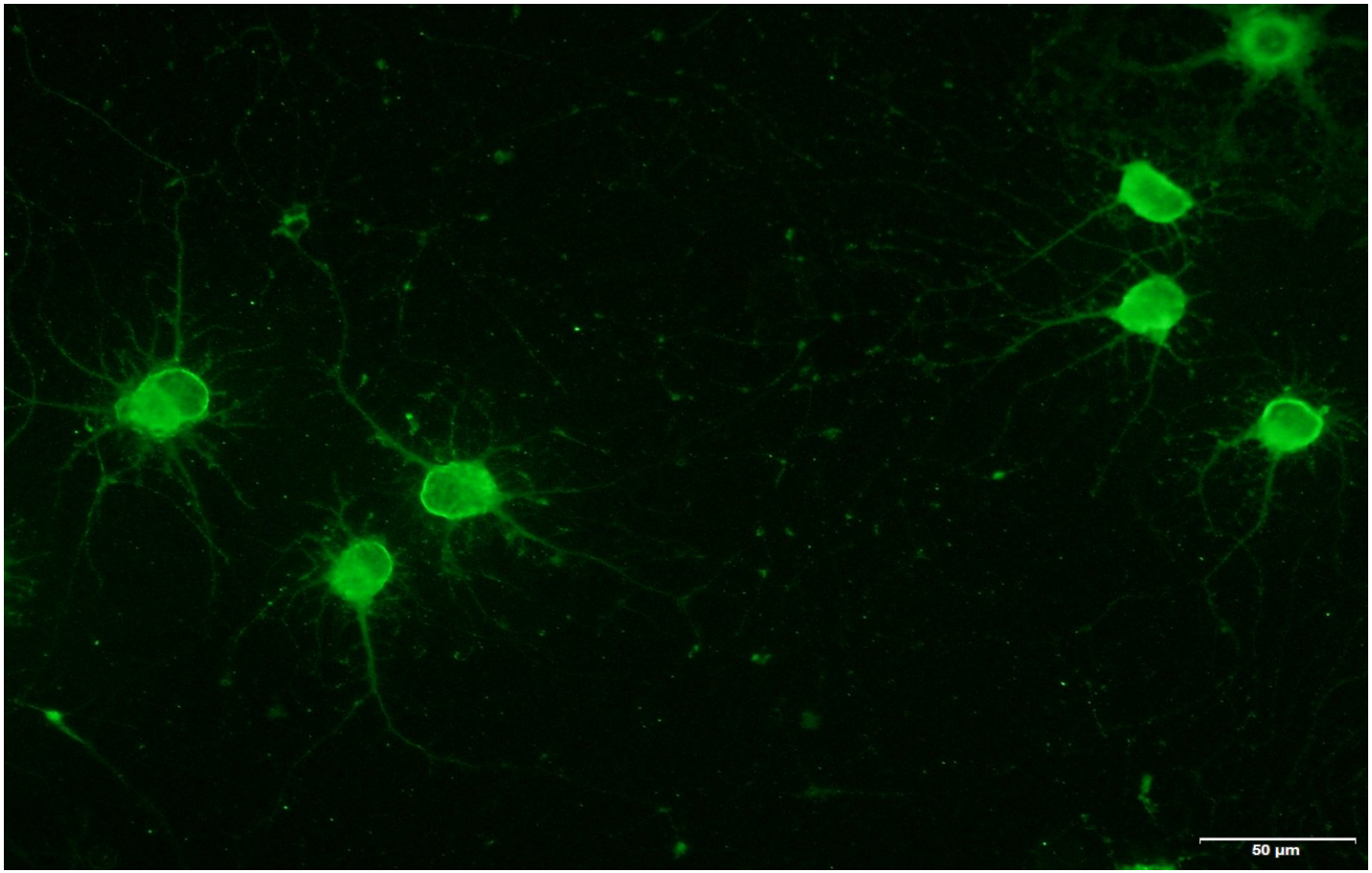

Figure 45: Image Axons Day 21 Immunohistochemistry cHat 50µm

Immunohistochemistry of neurons processed within the chamber using Anti-Choline Acetyltransferase 1:250 (0.004 mg/mL) Abcam ab35948 specific for Spinal cord motor neurons

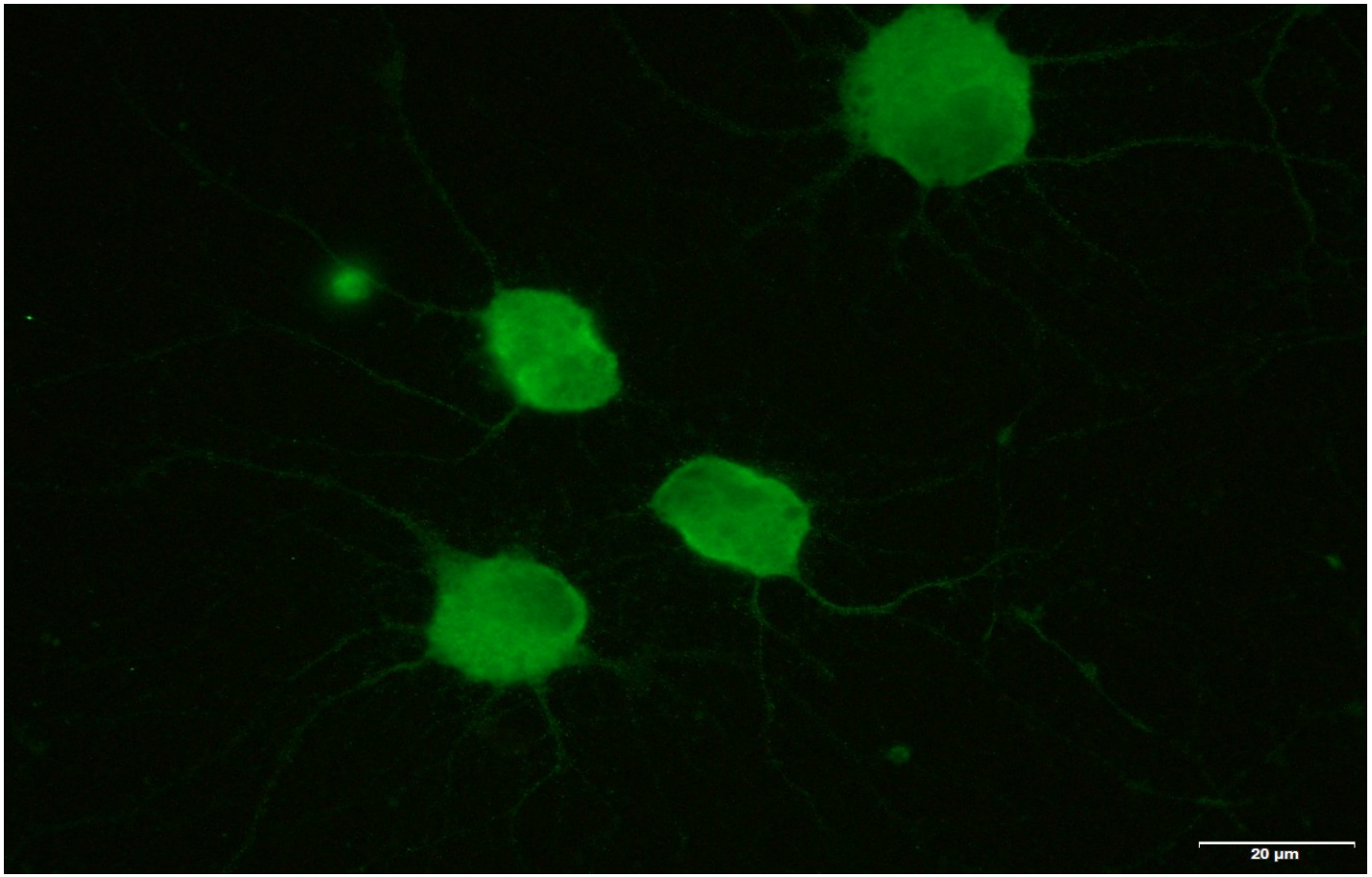

Figure 46: Image Axons Day 21 2H3 20µm

High magnification bright field using Neurofilament -H obtained from Developmental Studies Hybridoma bank 1:200. Localises on neuron neurofilaments.

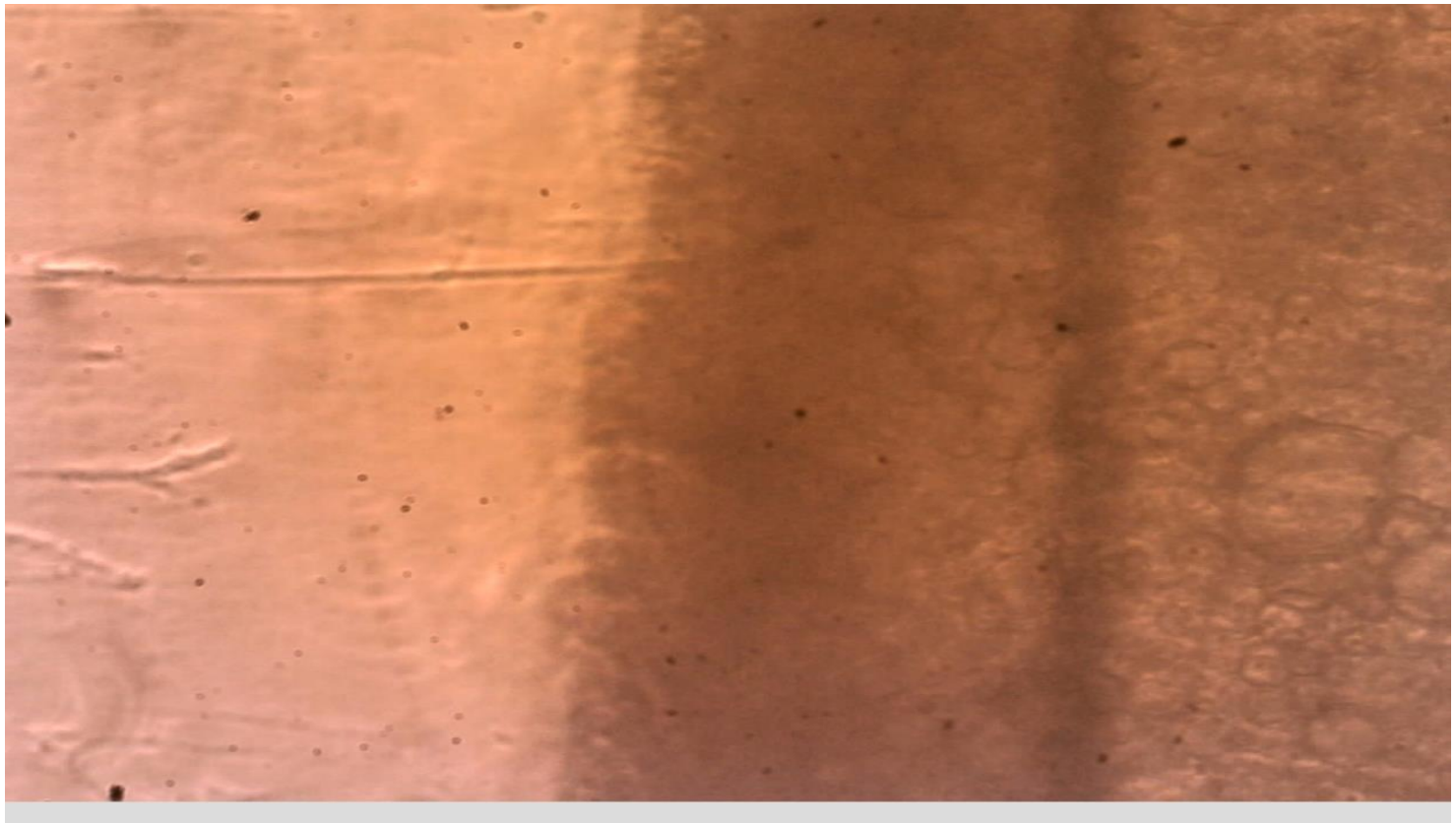

Figure 47: Image of axon stretch growth

The above field of view image was taken at day 8 and shows what appears to be a single neurite (probably axon) under stretch growth. At the time of preparation of this paper, no “stretched” neurites have been successfully processed through to immunohistochemistry to determine morphology.

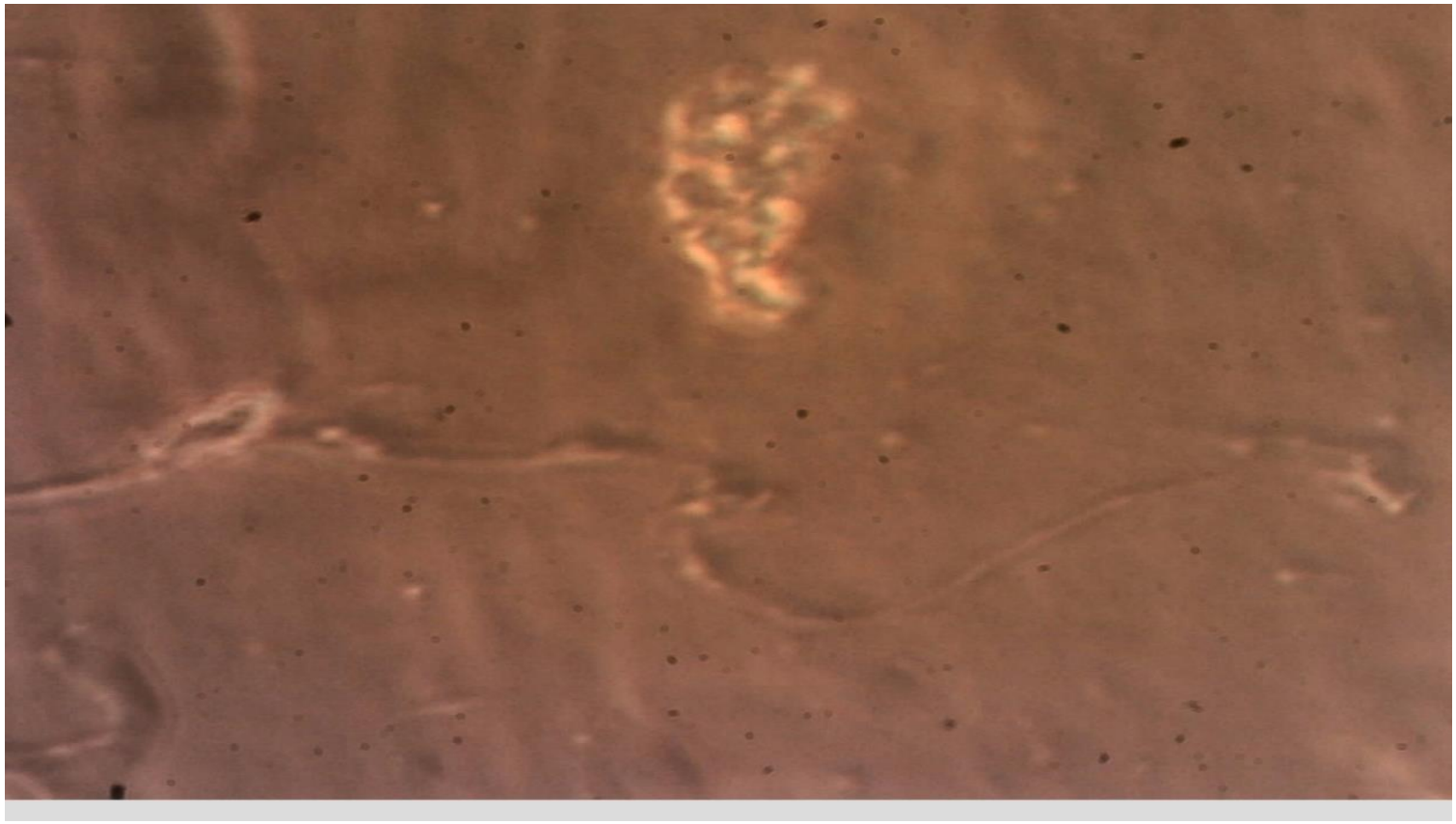

Figure 48: Image of Axon following disconnection x40 mag

This image was randomly taken using a Dino eyepiece camera during an axon stretch growth experiment. It shows, what appears to be an axon recoiling following disconnection.

Figure 49: Image x40 Magnification Axon Day 14

This interesting bright field image was taken using the Dino eyepiece at x40 magnification. The field of view shows that debris has sufficiently cleared to see morphology. It was not determined if this was an axon.

Discussion

In this early stage, translational study, we found that adult motor neurons in defined culture can tolerate periods above 21 days in a purpose-built axon stretch bioreactor. The culture used was previously reported by (Montoya-Gacharna et al. 2009) and the harvesting and isolation protocol by (Brinn, O'Neill, et al. 2016). Although more investigations are required there is emerging evidence to support that adult primary motor neurons (in the absence of myelin) are capable of in-vitro axon stretch growth.

To our knowledge this is the first study that specifically reports on adult motor neuron axon stretch growth results in deference to embryonic motor neurons (Feng et al. 2016) or adult or embryonic sensory neurons (Loverde, Tolentino & Pfister 2011; Pfister et al. 2004; Pfister et al. 2006; Smith, D. H., Wolf & Meaney 2001).

It is well known that adult motor neurons are notoriously difficult to maintain in normal culture conditions for periods more than 7 days' duration. Having exited from mitosis, these neurons are reliant on osmotic gradients, pH and temperature for nutrient and waste exchange and are very susceptible to oxidative stress. The most common cause of cell loss presents as contamination and is generally attributed to a minor procedural error that may have occurred several days prior.

The processing and culture protocol used here has previously shown a cell viability rate exceeding 60% at 28 days (Brinn, O'Neill, et al. 2016). Here, we report that viability declined in the bioreactor with contamination being the leading cause generally between day 3 and day 14.

Based on control culture survival (i.e. normal culture in culture oven), cell loss could not be attributed to harvesting or general processing techniques. For those cultures contaminating at 3 days, it is likely that the sterilisation technique could be the contributing factor. The bioreactor currently is printed using Acrylonitrile

Butadiene Styrene (ABS) rather than PolyEtherEtherKetone (PEEK) thus; it does not tolerate steam autoclave. Here, we used 70% ethanol followed by 24h in a UV hood.

Beyond 3 days it 's hard to determine the cause of increased loss of cell viability as the bioreactor is sealed and both gas and media are filtered prior to entering the unit. In many instances the colour of the media was seen to vary within the chamber, clearly indicating pH imbalance. The CO_2 controller used in these experiments had a high-performance CO_2 sensor (COZIR Sprint/R 0-20%) which was calibrated to the control oven, suggesting appropriate CO_2 concentration was being delivered to the filter. However, the flow rate is not currently being measured beyond the filter. Thus this will be rectified in future versions. The alternate explanation may be in the media change mechanism. In the control cultures, we exchange 2/3rd of the media on day 1 and then every 3 days. In the sealed bioreactor, we repeated the same procedure, but additional media was also added to compensate for condensation/humidity loss within the bioreactor.

We previously have also reported on the bioreactor infrastructure and briefly remarked on the axon stretch growth mechanism and its incorporation into an infant humidicrib (Brinn, Al-Sarawi, et al. 2016). Here, we have further enhanced the lower section of the bioreactor so it can be used without disturbing the cells for immunohistochemistry or electrophysiology experiments. The top part of the bioreactor remains unchanged save it is now printed using a 3D printer rather than being machined from aluminium and coated with Teflon. These modifications are ongoing and now inexpensive to complete.

Substrate a work in progress

As adult motor neurons have exited the differentiation cycle they no longer proliferate, therefore once seeded their position remains fixed on the substrate. The reliance on the axon to cross the two substrates is, therefore, high. The original axon stretch device as used by Pfister and associates also had a facility to use a stretchable nylon substrate, and this may be the better option for motor

neurons (Pfister et al. 2006). In a recent study, Feng and associates used substrate films for embryonic motor neurons with good effect. However, in their publication, they report evidence that tension on the soma may affect the neurite number and branching (Feng et al. 2016). On this basis, it may be preferable to culture the motor neurons for 3-4 days then trypsinized and consolidated prior to seeding within the bioreactor.

Here, we also report on the use of a Piezo drive system to manage the axon stretch growth mechanism. The piezo axon stretch growth technology is mature and has a proven record of accomplishment. Our experience was positive, and we report that the unit functioned to specifications. Movement of the substrate was tightly controlled to 1µm increments and was smooth in operation.

During commissioning, we encountered two minor issues worth raising. The first is that the Piezo unit when running is very sensitive to vibration, shutting the door of the room abruptly can cause the system to abort its routine. This does not cause disconnection of the neurons but requires the system to be manually restarted at the appropriate point. Secondly, power loss appears more detrimental than with a stepper motor system, as the Piezo controller requires to re-determine its axis position. The solution to the first issue can be as simple as using a rubber mat and appropriate signage, and the second issue can be resolved by using a backup power source to the controller and a notebook for the software. Whilst minor these are significant processing issues.

Limitations

The number of axons crossing over both substrates was also low in comparison to DRG experiments using a similar bioreactor (Loverde & Pfister 2015; Loverde, Tolentino & Pfister 2011; Pfister et al. 2004; Pfister et al. 2006; Smith, D. H., Wolf & Meaney 2001). This was to be expected given that adult neurons have exited from mitosis.

The C2C12 mouse conditioned medium used during the experiments is an interim solution to the problem of culturing adult primary motor neurons. Currently, the purchase of growth factors necessary to keep neurons alive for 28 days is expensive. By using this culture along with cAMP, there is a significant reduction in the use of growth factors and therefore in the cost. However, in the long term, more work is required to identify the growth factor requirements fully and to reduce the costs.

Summary

Injuries to the spinal cord generally occur to adult motor neurons. Therefore, it is essential that we develop a stable, well-defined in-vitro model of adult motor neuron axon stretch growth.

Adult motor neurons can be effectively used in this type of bioreactor. More work is required to improve the number of cells crossing the substrates. Experience with the culture and axon stretch growth techniques will overtime resolve this issue.

References

Bauchet, L, Lonjon, N, Perrin, FE, Gilbert, C, Privat, A & Fattal, C 2009, 'Strategies for spinal cord repair after injury: a review of the literature and information', *Ann Phys Rehabil Med*, vol. 52, no. 4, May, pp. 330-351.

Beattie, MS, Hermann, GE, Rogers, RC & Beshnahan, JC 2002, 'Cell death in models of spinal cord injury', in L McKerracher, G Doucet & S Rossignol (eds), *Progress in Brain Research*, vol. 137, Elsevier Science B.V, p. 37.

Berger, AJ, Bayliss, DA & Viana, F 1996, 'Development of hypoglossal motoneurons', *J Appl Physiol*, vol. 81, no. 3, Sep, pp. 1039-1048.

Bernal, R, Pullarkat, PA & Melo, F 2007, 'Mechanical Properties of Axons', *Physical Review Letters*, vol. 99, no. 1, p. 018301.

Bray, D 1984, 'Axonal growth in response to experimentally applied mechanical tension', *Developmental Biology*, vol. 102, pp. 379-389.

Brewer, GJ & Torricelli, JR 2007, 'Isolation and culture of adult neurons and neurospheres', *Nat Protoc*, vol. 2, no. 6, pp. 1490-1498.

Brinn, MP, Al-Sarawi, S, Yu, T-F, Freeman, BJC, Kumaratilake, J & Henneberg, M 2016, 'A portable live cell culture and imaging system with optional umbilical bioreactor using a modified infant incubator', *Bioengineering*, 19th November 2016.

Brinn, MP, O'Neill, K, Musgrave, I, Freeman, BJC, Henneberg, M & Kumaratilake, J 2016, 'An optimized method for obtaining adult rat spinal cord motor neurons to be used for tissue culture', *J Neurosci Methods*, vol. 273, pp. 128-137.

Cameron, WE & Núñez-Abades, PA 2000, 'Physiological changes accompanying anatomical remodeling of mammalian motoneurons during postnatal development', *Brain Research Bulletin*, vol. 53, no. 5, 11/15/, pp. 523-527.

Campenot, RB 1985, 'The regulation of nerve fiber length by intercalated elongation and retraction', *Developmental Brain Research*, vol. 20, no. 1, pp. 149-154.

Carrascal, L, Nieto-Gonzalez, JL, Cameron, WE, Torres, B & Nunez-Abades, PA 2005, 'Changes during the postnatal development in physiological and anatomical characteristics of rat motoneurons studied in vitro', *Brain Res Brain Res Rev*, vol. 49, no. 2, Sep, pp. 377-387.

de Sousa, BN & Horrocks, LA 1979, 'Development of Rat Spinal Cord', *Developmental Neuroscience*, vol. 2, no. 3, pp. 115-121.

Ek, CJ, Habgood, MD, Callaway, JK, Dennis, R, Dziegielewska, KM, Johansson, PA, Potter, A, Wheaton, B & Saunders, NR 2010, 'Spatio-temporal progression of grey and white matter damage following contusion injury in rat spinal cord', *PLoS One*, vol. 5, no. 8, p. e12021.

Ek, CJ, Habgood, MD, Dennis, R, Dziegielewska, KM, Mallard, C, Wheaton, B & Saunders, NR 2012, 'Pathological changes in the white matter after spinal contusion injury in the rat', *PLoS One*, vol. 7, no. 8, p. e43484.

Feng, ZQ, Franz, EW, Leach, MK, Winterroth, F, White, CM, Rastogi, A, Gu, ZZ & Corey, JM 2016, 'Mechanical tension applied to substrate films specifies location of neuritogenesis and promotes major neurite growth at the expense of minor neurite development', *J Biomed Mater Res A*, vol. 104, no. 4, Apr, pp. 966-974.

Grothe, C, Wewetzer, K, Lagrange, A & Unsicker, K 1991, 'Effects of basic fibroblast growth factor on survival and choline acetyltransferase development of spinal cord neurons', *Developmental Brain Research*, vol. 62, no. 2, 10/21/, pp. 257-261.

Iwata, A, Browne, KD, Pfister, BJ, Gruner, JA & Smith, DH 2006, 'Long-Term Survival and Outgrowth of Mechanically Engineered Nervous Tissue Constructs Implanted Into Spinal Cord Lesions', *Tissue Eng Part A*, vol. 12, no. 1, pp. 101-110.

Jacobson, M 1985, 'Clonal Analysis and Cell Lineages of the Vertebrate Central Nervous System', *Annual Review of Neuroscience*, vol. 8, no. 1, pp. 71-102.

Loverde, JR 2009, 'Deciphering The Biology of Axon Stretch-Growth', Biomedical Engineering, Partial Fulfillment of the Requirements for the Degree of Master of Science in Biomedical Engineering thesis, New Jersey Institute of Technology, The Van Houten Library.

Loverde, JR, Ozoka, VC, Aquino, R, Lin, LS & Pfister, BJ 2011a, 'Live imaging of axon stretch growth in embryonic and adult neurons', *J Neurotrauma*, vol. 28, no. 11, Nov, pp. 2389-2403.

Loverde, JR, Ozoka, VC, Aquino, R, Lin, LS & Pfister, BJ 2011b, 'Live imaging of axon stretch growth in embryonic and adult neurons Supplementary Data, J Neurotrauma, vol. 28, no. 11, Nov, pp. 2389-2403.', *J Neurotrauma*, vol. Vol 28, No 11, Nov, Supp Data.

Loverde, JR & Pfister, BJ 2015, 'Developmental axon stretch stimulates neuron growth while maintaining normal electrical activity, intracellular calcium flux, and somatic morphology', *Front Cell Neurosci*, vol. 9, p. 308.

Loverde, JR, Tolentino, RE & Pfister, BJ 2011, 'Axon Stretch Growth: The Mechanotransduction of Neuronal Growth', *J Vis Exp*, no. 54, p. e2753.

Macaya, D & Spector, M 2012, 'Injectable hydrogel materials for spinal cord regeneration: a review', *Biomed Mater*, vol. 7, no. 1, Feb, p. 012001.

Maxwell, WL 1996, 'Histopathological changes at central nodes of Ranvier after stretch-injury', *Microscopy Research and Technique*, vol. 34, no. 6, pp. 522-535.

Meikle, AD & Martin, AH 1981, 'A Rapid Method for Removal of the Spinal Cord', *Biotechnic & Histochemistry*, vol. 56, no. 4, pp. 235-237.

Montoya-Gacharna, J, Sutachan, JJ, Chan, WS, Sideris, A, Blanck, TJ & Recio-Pinto, E 2009, 'Muscle-conditioned media and cAMP promote survival and neurite outgrowth of adult spinal cord motor neurons', *Exp Neurol*, vol. 220, no. 2, Dec, pp. 303-315.

Morrison, B, Cullen, DK & LaPlaca, M 2011, 'In Vitro Models for Biomechanical Studies of Neural Tissues', vol. 3, pp. 247-285, DOI 10.1007/8415_2011_79.

Mortazavi, MM, Verma, K, Harmon, OA, Griessenauer, CJ, Adeeb, N, Theodore, N & Tubbs, RS 2015, 'The microanatomy of spinal cord injury: A review', *Clinical Anatomy*, vol. 28, no. 1, pp. 27-36.

Mortazavi, MM, Verma, K, Tubbs, RS & Theodore, N 2011, 'Cellular and paracellular transplants for spinal cord injury: a review of the literature', *Childs Nerv Syst*, vol. 27, no. 2, Feb, pp. 237-243.

O'Toole, M, Lamoureux, P & Miller, KE 2008, 'A Physical Model of Axonal Elongation: Force, Viscosity, and Adhesions Govern the Mode of Outgrowth', *Biophysical Journal*, vol. 94, no. 7, pp. 2610-2620.

Pfister, BJ, Iwata, A, Meaney, DF & Smith, DH 2004, 'Extreme Stretch Growth of Integrated Axons', *J. Neurosci.*, vol. 24, no. 36, September 8, 2004, pp. 7978-7983.

Pfister, BJ, Iwata, A, Taylor, AG, Wolf, JA, Meaney, DF & Smith, DH 2006, 'Development of transplantable nervous tissue constructs comprised of stretch-grown axons', *J Neurosci Methods*, vol. 153, no. 1, May 15, pp. 95-103.

Profyris, C, Cheema, SS, Zang, D, Azari, MF, Boyle, K & Petratos, S 2004, 'Degenerative and regenerative mechanisms governing spinal cord injury', *Neurobiol Dis*, vol. 15, no. 3, Apr, pp. 415-436.

Sendtner, M, Arakawa, Y, Stöckli, KA, Kreutzberg, GW & Thoenen, H 1991, 'Effect of ciliary neurotrophic factor (CNTF) on motoneuron survival', *J Cell Sci*, vol. 1991, no. Supplement 15, pp. 103-109.

Smith, DH 2009, 'Stretch growth of integrated axon tracts: Extremes and exploitations', *Prog Neurobiol*, vol. 89, no. 3, 11//, pp. 231-239.

Smith, DH, Pfister, BJ & Meaney, DF 2001, *Device and method using integrated neuronal cells and an electronic device*, Smith Douglas Hamilton, Bryan Pfister, Meaney David F., US 7429267 B2, United States.

Smith, DH, Wolf, JA & Meaney, DF 2001, 'A new strategy to produce sustained growth of central nervous system axons: Continuous Mechanical Tension', *Tissue Engineering*, vol. 7, no. 2, pp. 131-139.

Tator, CH 1995, 'Update on the Pathophysiology and Pathology of Acute Spinal Cord Injury', *Brain Pathology*, vol. 5, pp. 407-413.

Tator, CH 2006, 'Review of treatment trials in human spinal cord injury: issues, difficulties, and recommendations', *Neurosurgery*, vol. 59, no. 5, Nov, pp. 957-982; discussion 982-957.

Tator, CH & Fehlings, MG 1991, 'Review of the secondary injury theory of acute spinal cord trauma with emphasis on vascular mechanisms', *Journal of Neurosurgery*, vol. 75, no. 1, pp. 15-26.

Viana, F, Bayliss, DA & Berger, AJ 1994, 'Postnatal changes in rat hypoglossal motoneuron membrane properties', *Neuroscience*, vol. 59, no. 1, 3//, pp. 131-148.

Weiss, P 1941, 'Nerve patterns: The mechanics of nerve growth. Third Growth Symposium.', *Growth*, vol. 5 (Suppl.), pp. 163-203.

Zheng, J, Lamoureux, P, Santiago, V, Dennerll, T, Buxbaum, RE & Heidemann, SR 1991, 'Tensile regulation of axonal elongation and initiation', *The Journal of Neuroscience*, vol. 11, no. 4, pp. 1117-1125.

Chapter 7. Summary, Conclusions, Future Directions, and Commentary on research environment.

Summary – Early Translational Science

Spinal cord injuries are devastating, and yet we still have no cure. As complexity unfolds specialisation is unavoidable, and the approach typically becomes incremental. Once science becomes incremental it logically follows that we cease a goal orientated approach and lose sight of the end-point.

In recent times, translational science has emerged as a methodology to bridge this gap. However, at present this occurs at the late translational stage i.e. during implementation when the science is mature. The American President J.F. Kennedy in setting the goal of a moon landing built an infrastructure around a goal. In doing so, he possibly invented the concept of early intervention translational science. The complexity in the moon landing was such that the science crossed multi-disciplinary boundaries. What separates it from traditional translational science is that new discoveries were required to achieve the goal.

A core function of the early translational scientist is to remove the burdens associated with progressing basic science. This can take the form of a "gopher", - a person that fills in the gaps between disciplines, seeks grant funding, resolves all administrative tasks, and completes and follows through on all ethics applications. And/Or, it can take the form of transdisciplinary linking or active involvement.

Rapid change, specialisation and the increasing burden of compliance are emerging as significant challenges to address in scientific research this century (Hadorn et al. 2008). In pursuit of research, many barriers are present including, but not limited to, institutional structures and funding incentives (Brewer 1999; Campbell 1969).

Gary Brewer wrote, "The world has problems, but universities have departments" (Brewer 1999; Hadorn et al. 2008).

Summary – Project

The core objective of this research was to facilitate Axon Stretch Growth research at the University by:

- Developing suitable in-vitro ASG infrastructure;
- Progressing research into adult motor neurons by establishing an adult motor neuron in-vitro harvesting and culture protocol; and
- Collate pertinent literature to progress a suitable ASG large animal model.

This study is the first study to demonstrate in-vitro axon stretch growth in adult rat motor neurons (Chapter 6). The establishment of a robust harvesting protocol for adult motoneurons obtained from spinal cords of Sprague-Dawley rats is an important adjunct for future ASG experiments. Whilst yields are not suitable for grafting, the published protocol (Chapter 4) will be useful for future comparative studies between embryonic, motor, sensory and stem cells.

The repurposing and conversion of a decommissioned infant humidicrib allow the device to be broadly used as a portable imaging live cell incubator. Within the incubator, a bioreactor was developed that can be machined or printed via a standard inexpensive 3D printer (Chapter 5). By making this affordable technology, this opens the device up for those scientists unable to afford the commercial alternative. The bioreactor demonstrated flexibility and has been robust since the conversion. We also developed within this chapter an ASG detachable mechanism allowing for immunohistochemistry and where applicable electrophysiology.

Conclusions and Future Directions of this research

Axon Stretch Growth Technology – animal model

There is a need for an intermediate large animal model for chronic progressive degeneration injuries, that occur to long nerve tracts within the spinal cord. With this form of injury, the rodent small animal model is of insufficient size, and therefore the lack of this model diminishes translational capacity.

The reality is, that when developed this model will be a paralysis model, which should be suitable for dynamic evaluation of nerve grafts and potentially for an investigative study into *in-vivo* axon stretch growth options.

In this translational study, there was insufficient time or funding to progress this model beyond identifying pertinent literature for an intermediate sheep model.

Although the potential for high impact consequences occurs in the cervical region this option is recommended by the SCI community (Kwon, Hillyer & Tetzlaff 2010), access and limited biomechanical disruption also make this an attractive technical approach.

It would be useful to identify a low impact muscle group that is initiated by the supraspinal tract in this model. *Here, we suggest the tail, but other options should also be considered.*

The literature cited in chapter 3 (Table 2 – 11), identified that there is limited information on the vascular structures beyond the cervical region in sheep, and there is no current information on using viewing chambers to allow periodic review of the injury zone. Work is ongoing on CSF pressure gradients.

In-vitro progression of Axon Stretch Growth Technology

It would be useful from a translational perspective for the *in-vitro* technology to be modified to incorporate the graft transfer process. In hindsight, a modified system to resemble a syringe may be the better option (Figure 50). Clearly, from the perspective of the application, it would be beneficial to have multiple separate chambers. It may also be useful to experiment using a single twist to unite the axons creating a "rope" type of graft. The reasoning that this may be useful is primarily to provide some tension strength.

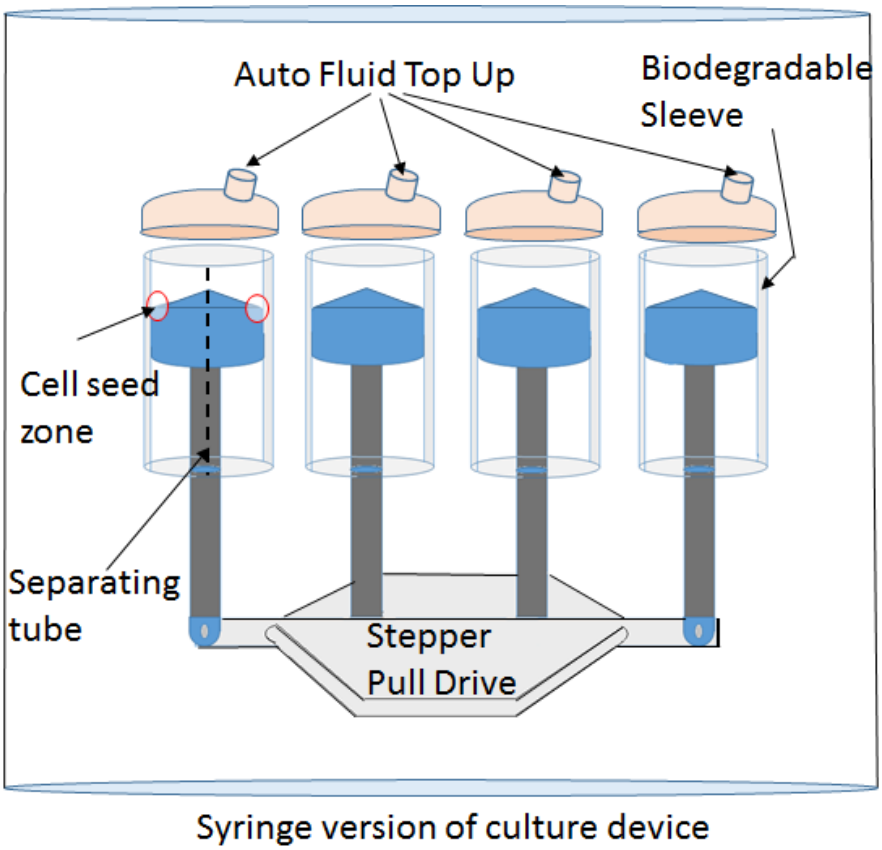

Figure 50: Concept of syringe version of ASG device

This concept version incorporates a biodegradable implant graft tube. Multiple syringes attached to the same drive would provide multiple implants and give security against contamination. These units would be sealed until used. Within the syringe type tube, a biodegradable sleeve should be developed to facilitate direct implant. The outer tube (disposable) separates for the implant.

Early *in-vitro* translational issues outstanding:

- Dynamic electrophysiology to be activated continuously and monitored during the ASG process. This will provide ongoing indication of health of the axon,
- Dynamic measurement of pH of the medium during ASG is required,
- Adult motor neuron culture medium requires ongoing refinement,
- New work on temperature variation within the culture to alter metabolism is warranted, and
- A comparative study between adult motor neuron, stem cell, and cell line are required.

The development of the adult motor neuron axon stretch culture is ongoing. There remain many questions yet to answer regarding the comparison between the adult motor and embryonic sensory axons, especially in relation to axonal transport and intercalated growth of the axon.

In-vivo progression of Axon Stretch Growth Technology

It is difficult at this early juncture to determine if *In-vivo* axon stretch growth has potential. There is good evidence to suggest that it will be possible to attach to a proximal stump of long axon tracts and mechanically stretch these across gaps. Access may be an issue initially for proof of concept but a cervical chamber option on a large animal such as Sheep or Pig will be suitable for proof of concept. It is envisaged that nanotechnology will open up more options once this in-vivo option has been demonstrated.

References

Brewer, GD 1999, 'The challenges of interdisciplinarity', *Policy sciences*, vol. 32, no. 4, pp. 327-337.

Campbell, DT 1969, 'Ethnocentrism of disciplines and the fish-scale model of omniscience', *Interdisciplinary relationships in the social sciences*, vol. 328, p. 348.

Hadorn, GH, Biber-Klemm, S, Grossenbacher-Mansuy, W, Hoffmann-Riem, H, Joye, D, Pohl, C, Wiesmann, U & Zemp, E 2008, *Handbook of transdisciplinary research*, Springer.

Kwon, BK, Hillyer, J & Tetzlaff, W 2010, 'Translational research in spinal cord injury: a survey of opinion from the SCI community', *J Neurotrauma*, vol. 27, no. 1, Jan, pp. 21-33.

Chapter 8. Appendices

Appendix 1: Stepper Motor Controller – Arduino Source code

```
#include <StepperMotor.h>

/*  Program to run 28BYJ -48 Stepper motor using an Arduino UNO
 *  Acknowledging libraries above + freeware Arduino 1.6.5
 *  Motor 28BYJ-48: 5.625 degrees per step / 360 degrees = 1:64 stepper
 *
 *  Information from original stepper motor programming author is that it takes 2048 steps to rotate 360-degree revolution despite the specs claiming 4096 steps.
 *  The stepper class of the Arduino library follows a sequence of 4 values of 4 bits but the 28BYJ-48 requires a sequence of 8 values of 4 bits.
 *  Refer to  http://www.codeproject.com/Articles/699986/An-Arduino-Library-to-Control-the-BYJ-Stepper#_comments
 *
 *  BUTTON PRESS control pin 2
 * *
 *  Figures:
 *  Total of 86,400 seconds in 24hr period, thus 86400000 milliseconds
 *  Distance between thread on 5M screw = 0.8mm
 *  4096 Steps per full rotation of stepper motor
 *  Sum= .8/4096 = 0.0001953125 per step
 * Therefore 5120 steps of the stepper motor are required to achieve 1mm
 */

#define DELAY 5000
#define _PIN1 3
#define _PIN2 4
#define _PIN3 5
#define _PIN4 6
#define ITR_PIN 2  //Start Stop button
#define ITR_NB 0

volatile bool first = true;
volatile bool moveInterrupted = false;

//Initialize the Stepper Motor
StepperMotor stepper(_PIN1, _PIN2, _PIN3, _PIN4);
void buttonPressed()//ON/OFF Button Control
```

```
{
  static volatile boolean toggle = false;
  if (!first)
  {
    if (toggle)
    {
      stepper.reset();
    }
    else
    {
      stepper.stop(true);
    }
    toggle = !toggle;
  }
  else
  {
    first = false;
  }
}
void setup() {
  long int forward = 0;

  cli();
  stepper.setPeriod(0.1);// Speed Milliseconds
  pinMode(ITR_PIN, INPUT_PULLUP);
  attachInterrupt(0, buttonPressed, FALLING);
  sei();
  /*
   *  ********************************************
   *                Day 1
   *  ********************************************
   *
  */
  do
  {
    stepper.move(1);//steps
    forward = forward + 1;
    delay (33750); //milliseconds (33.75 seconds between each step)
  }  while (forward <= 2560);  // 0.5mm distance covered
  /*
```

```
 *  ********************************************
 *              Day 2
 *  ********************************************
 * Overall distance covered at commencement 0.5mm
*/
do
{
  stepper.move(1);//steps
  forward = forward + 1;
  delay (22500); //milliseconds (25.00 seconds between each step)
}  while (forward <= 3840);  // 0.75mm distance covered
/*
 *  ********************************************
 *              Day 3
 *  ********************************************
 * Overall distance covered at commencement 1.25mm
*/
do
{
  stepper.move(1);//steps
  forward = forward + 1;
  delay (16875); //milliseconds (16.875 seconds between each step)
}  while (forward <= 5120);  // 1.00mm distance covered
/*
 *  ********************************************
 *              Day 4
 *  ********************************************
 * Overall distance covered at commencement 2.25mm
*/
do
{
  stepper.move(1);//steps
  forward = forward + 1;
  delay (13500); //milliseconds (13.500 seconds between each step)
}  while (forward <= 6400);  // 1.25mm distance covered
```

```
/*
  *  ******************************************
  *              Day 5
  *  ******************************************
  * Overall distance covered at commencement 3.50mm
 */
 do
 {
   stepper.move(1);//steps
   forward = forward + 1;
   delay (11250); //milliseconds (11.250 seconds between each step)
 }  while (forward <= 7680);  // 1.50mm distance covered
/*
  *  ******************************************
  *              Day 6
  *  ******************************************
  * Overall distance covered at commencement 5.00mm
 */
 do
 {
   stepper.move(1);//steps
   forward = forward + 1;
   delay (9642.8); //milliseconds (9.6428 seconds between each step)
 }  while (forward <= 8960);  // 1.75mm distance covered
 //Overall distance covered = 6.75mm
}
void loop()
{
} //End Source Code
```

Appendix 2: CO_2 PID Controller – Arduino Source Code

```
// Arduino IDE version used for development/compatibility reasons: 1.0.6
// https://www.arduino.cc/en/Main/OldSoftwareReleases#previous
//Acknowledgement to Andrew Pelling @ www.pellinglab.net for original version: https://github.com/pellinglab/DIY-Incubator-Dec2014/blob/master/DIY_CO2_Incubato
//Modifications: Danny Di Giacomo and Malcolm Brinn – University of Adelaide www.adelaide.edu.au
/*
 Humidifier and CO2 gas control via 12V normally closed solenoid and CO2 Sensor.
 CO2 Meter (SprintIR 0-20% GC-0017):
 http://www.co2meter.com/collections/co2-sensors/products/sprintir-100-percent-co2-sensor
 also need the latest COZIR library, download from this thread
 (Using Cozir 0-1-01.zip in this code):
 http://forum.arduino.cc/index.php?topic=91467.0
 CO2 supplied by BOC Gas
 Arduino UNO Pin Connections:
 Pin 2,3: Tx/Rx from CO2  //Pin 2 Arduino goes to Tx on Sensor Pin 4
 Pin #5:
 Pin #6:
 Pin #7:
 Pin #8: Solenoid Relay
 Pin #9:
 SCL/SDA Pins: 12C Display
 */
/* CO2 CONTROL /////////
 Control works by reading the sensor (CO2) 3 times and averaging (to flatten out noise).
 The measurement is compared to a user-defined SETPOINT. If the CO2 is below the setpoint, the solenoid opens allowing the flow of CO2 into the incubator. Once the CO2 content comes within a user-defined THRESHOLD of the setpoint, a stepping cycle begins. The solenoid opens for a user defined DURATION and then closes. The open/closed cycle repeats until the setpoint is reached. The cycles allow the system to step up to the setpoints.
 Setpoints, thresholds, and durations MUST be set according to your own system by TRIAL AND ERROR. May need to increase/decrease depending on size/shape of the Incubator, CO2 flow rate, etc.
 */
float CO2Setpoint = 1.0;   // Setpoint CO2 level in % 5
float CO2Threshold = 0.85; // Threshold to switch to stepping control in %/100
int SolenoidOnTime = 5000; // Duration time in milliseconds
```

```
// CO2 Sensors
#include "SoftwareSerial.h"
#include "cozir.h"
// Cozir library info/download: http://forum.arduino.cc/index.php?topic=91467.0
// Excel logging configuration
// http://www.robertovalgolio.com/sistemi-programmi/arduino-excel
#include <rExcel.h>
long idx = 0; // index
int outputTiming = 1000;   // packet sending timing in ms, determines the output timing
rExcel myExcel;            // class for Excel data exchanging
int save_loop_timer = 1;
/*
char worksheet[16];        // worksheet name
 char range[16];           // range set
 unsigned int row;         // row
 unsigned int column;      // column
 char value[16];           // written or read value
 */


// I2C LCD interface configuration
// http://forum.arduino.cc/index.php?topic=128635.0
// https://bitbucket.org/fmalpartida/new-liquidcrystal/downloads
// LiquidCrystal_V1.2.1.zip library used
#include <Wire.h>
#include <LCD.h>
#include <LiquidCrystal_I2C.h>
#define I2C_ADDR 0x3F
#define BACKLIGHT_PIN 3
#define En_pin 2
#define Rw_pin 1
#define Rs_pin 0
#define D4_pin 4
#define D5_pin 5
#define D6_pin 6
#define D7_pin 7
LiquidCrystal_I2C lcd(I2C_ADDR,En_pin,Rw_pin,Rs_pin,D4_pin,D5_pin,D6_pin,D7_pin);

////////* RELAY *////////
int Solenoid = 8;          // Relay for controlling 12V solenoid valve
```

```
////////* SPRINTIR COZIR CO2 SENSOR  *////////
SoftwareSerial nss(2, 3);  // Rx,Tx - Pin 3,4 on sensor
COZIR czr(nss);
float SingleCO2, CO2 = 0;
float multiplier = 0.001;  // 10/10000 (Hardware multiplier/ppm conversion).
float reading = 0;
void setup()
{
  Serial.begin(9600);               // Start serial port
  czr.SetOperatingMode(CZR_POLLING);  // Start the CO2 sensor and put into POLLING mode
  pinMode(Solenoid, OUTPUT);          // Sets pin for controlling solenoid relay
  digitalWrite(Solenoid, LOW);        // Set LOW (solenoid closed off)
  lcd.begin(16,2);
  lcd.setBacklightPin(BACKLIGHT_PIN,POSITIVE);
  lcd.clear();
  lcd.setBacklight(HIGH);
  lcd.home();
  pinMode(13, INPUT_PULLUP);
  // delay(500);                      // Wait
}
void loop()
{
  // Read CO2 sensor 3 times and determine the average.
  for (int i = 0; i < 3; i++) {
    SingleCO2 += czr.CO2() * multiplier;
  }
  CO2 = SingleCO2 / 3;
  SingleCO2 = 0;
  // Write CO2 % to LCD
  lcd.setCursor (0, 0);
  lcd.print("CO2 level: ");
  lcd.setCursor (10, 1);
  lcd.print(CO2, 2);
  lcd.print(" %");
  // If switch on GPIO 13 low, enable Excel logging
  if (digitalRead(13) == LOW) {
    static unsigned long  loopTime = 0;
    static unsigned long  time1 = 0;
  loopTime = millis();
```

```
  // Output Task
  // Arduino acts as client making requests to Excel
  // instructions performed each outputTiming ms
    if ((loopTime - time1) >= outputTiming) {
      time1 = loopTime;

   myExcel.write("Template", "A5", "%time%");             // write time to sheet "Template" cell A5
   myExcel.write("Template", "B5", CO2, 2);              // write CO2 %
   myExcel.writeIndexed("Template", idx+11, 1,"%date%");  // idx is zero initially, write date to row
idx+11, column 1
   myExcel.writeIndexed("Template", idx+11, 2,"%time%");
   myExcel.writeIndexed("Template", idx+11, 3, idx);
   myExcel.writeIndexed("Template", idx+11, 4, CO2, 2);
   idx++;
      // Save spreadsheet every 60 seconds
  save_loop_timer++;
      if (save_loop_timer == 60) {
        myExcel.save();
        myExcel.write("Template", "E1", "Autosaved: ");
        myExcel.write("Template", "F1", "%time%");
        save_loop_timer = 1;
      }
    }
  }
  // Open/close the solenoid valve based on the current CO2 reading
  // Solenoid  opens for a duration of 'SolenoidOnTime' and then closes
  if (CO2 < CO2Setpoint && CO2 < CO2Threshold * CO2Setpoint) {
    digitalWrite(Solenoid, HIGH);
  }
  else if (CO2 < CO2Setpoint && CO2 >= CO2Threshold * CO2Setpoint) {
    digitalWrite(Solenoid, HIGH);
    delay(SolenoidOnTime);
    digitalWrite(Solenoid, LOW);
  }
  else if (CO2 > CO2Setpoint) {
    digitalWrite(Solenoid, LOW);
  }
  delay(10);}  //END of  Source Code
```

Appendix 3: Paper 1: Journal of Neuroscience Methods

Journal of Neuroscience Methods 273 (2016) 128–137

Contents lists available at ScienceDirect

Journal of Neuroscience Methods

journal homepage: www.elsevier.com/locate/jneumeth

An optimized method for obtaining adult rat spinal cord motor neurons to be used for tissue culture

Malcolm Brinn[a,*], Katie O'Neill[b], Ian Musgrave[b], Brian J.C. Freeman[c,d], Maciej Henneberg[a], Jaliya Kumaratilake[a]

[a] Discipline of Anatomy and Pathology, University of Adelaide, Adelaide, Australia
[b] Discipline of Pharmacology, University of Adelaide, Adelaide, Australia
[c] Department of Spinal Surgery Royal Adelaide Hospital, Australia
[d] Discipline of Orthopaedics and Trauma, School of Medicine, University of Adelaide, Adelaide, Australia

HIGHLIGHTS

- Redefined adult rat spinal cord motor neuron extrusion and culture method.
- Method confirms primary adult motor neuron survival beyond 28 days.
- Method is robust, reduces processing time, complexity and cost.
- No requirement for Intracardiac perfusion, or to cool (4 °C) medium post extrusion.
- Results and discussion written for those new to primary culture techniques.

ARTICLE INFO

Article history:
Received 4 November 2015
Received in revised form 15 August 2016
Accepted 28 August 2016
Available online 3 September 2016

Keywords:
Serum free medium
Adult rat motor neurons
Primary cell culture
Spinal cord
Tissue culture
Neuroscience protocol

ABSTRACT

Background: There is a paucity of detailed methods describing how to harvest and process motor neurons obtained from the adult rat spinal cord.
New method: Removal of intra-cardiac perfusion step. The spinal cord is extruded intact from the rat in under 60 s post-decapitation then processed without differentiation of ventral and dorsal regions. The temperature during processing was maintained at room temperature (22 °C) except during the Papain processing step where the temperature was increased to 30 °C.
Results: Cell debris interfered with the counting of cells at the time of plating. Also, cell types could not be identified since they appear rounded structures with no projections. Cell viability counts reduced to 91% and 63% from day 7 to day 14 and days 7–28 respectively. Red blood cell counts in stepped density gradient layers 2 and 3 were low.
Comparison with existing method(s): No requirement for intra-cardiac perfusion. No requirement to cool to 4 °C post harvesting, No requirement for specialized substrates. Reduces processing time by at least 2 h and reduces the potential for processing errors through a reduction in complexity. Procedures are also explained suitable for those new to the culture of primary adult motor neurons.
Conclusions: Cell viability counts indicate that removal of the perfusion step has a minimal effect on the viability of the cultured nerve cells, which may be due to the reduction in the spinal cord harvesting time and the inclusion of Hibernate based media during extrusion and processing.

Abbreviations: °C, degrees celcius; ACSF, artificial cerebro-spinal fluid; bFGF, basic fibroblast growth factor; BDNF, brain-derived neurotrophic factor; Ca^{2+}, calcium; cAMP, 8(–4 chlorophenylthio cyclic adenosine 3'5' monophosphate); CO^2, carbon dioxide; CNTF, ciliary neurotrophic factor; DIV, days in vitro; DNA, deoxyribose nucleic acid; DSHB, Developmental Studies Hybridoma Bank; EDTA, ethylene diamine tetra acetic acid; GDNF, glial-derived neurotrophic factor; HIB-PM, hibernate processing medium; O^2, oxygen; PBS, phosphate buffered solution; PDL, poly-D-lysine; PET, polyethylene terephthalate; Neurobasal CM, neurobasal based conditioned medium; Mg^{2+}, magnesium.

* Corresponding author.
E-mail address: malcolm.brinn@adelaide.edu.au (M. Brinn).

http://dx.doi.org/10.1016/j.jneumeth.2016.08.012
0165-0270/

1. Introduction

In the absence of cell division, adult primary neurons are difficult to maintain in culture for extended periods. As a consequence, it is not uncommon for neuroscientists to use either embryonic neurons, immortalized neural cell lines or in more recent time's stem cells for in vitro experiments. However, these cells can differ in important aspects from the adult primary neuron (Bar, 2000; Cameron and Núñez-Abades, 2000; Carrascal et al., 2005; Gingras

Table 1
Stage 1 density gradient – prepare in 4 separate 15 mL conical tubes.

Conical Tubes	Optiprep 1.32 g/mLv/v%	OptiPrep1.32 (μL)	Hib-PM (μL)	Total (μL)
Conical 1	17.50%	525	2475	3000
Conical 2	12.50%	375	2625	3000
Conical 3	10.00%	300	2700	3000
Conical 4	7.50%	225	2775	3000

et al., 2007; Jacobson, 1985). Therefore, the use of these cells or cell lines for the investigation of spinal cord injury or degenerative diseases such as Amyotrophic Lateral Sclerosis, Parkinson's disease, and Multiple Sclerosis can be problematic in clinical translation. Neuroscientists are thus, always interested in a well-defined adult primary neuronal cell culture for comparative purposes.

Brewer (1997) succinctly described the sequence of steps required in which to successfully bring adult primary neurons into in-vitro culture, that of; (1) Harvesting, (2) Separation of cells from the extracellular matrix, (3) Removal of growth inhibitory factors, (4) Targeted specificity of cell type, and (5) Provision of an adequate substrate and nutrients to ensure viability. When considered in their entirety, these steps can come together to build a robust protocol. However, in isolation, each step has benefits and consequences that have to be carefully balanced. One such example is between media selection, temperature and time.

Here we describe a protocol to harvest adult rat spinal cords and isolate and process neurons to in-vitro culture. The choice of hydraulic extraction of the spinal cord (De Sousa and Horrocks, 1979; Meikle and Martin, 1981) demonstrates how the risk of ischemia can be balanced to negate the requirement for intracardiac perfusion. We also reiterate the benefits of using Hibernate during processing in ambient air (Brewer and Price, 1996; Brewer and Cotman, 1989). To demonstrate the robust processing methods, the neurons were cultured more than 21 days using the combination C2C12 conditioned media first described by (Montoya-Gacharna et al., 2009). Montoya-Gacharna and associates also used cyclic adenosine-3′,5′-monophosphate (cAMP), which has been previously shown to substantially reduce the need for high quantities of growth factors (Hanson et al., 1998; Meyer-Franke et al., 1998).

2. Materials and methods

A detailed description of all steps in this protocol follows in a format that can be directly applied in the laboratory for the extraction of rat spinal cord motor neurons and their long-term culture.

2.1. Pre-surgical preparation

Prepare the C2C12 muscle conditioned medium in advance (>14 days) from the C2C12 myoblast cell line as previously described by (Montoya-Gacharna et al., 2009, 2012). Briefly, myoblasts are cultured in Dulbecco's modified Eagle medium (DMEM) containing L-Glutamine 20 mM (Sigma), Gentamicin 10 μg/mL and 10% fetal bovine serum (Sigma) reaching 30% confluence. Cells are differentiated into myocytes by replacing the current culture medium with new culture medium containing 10% horse serum (Sigma). After differentiation (i.e. in 3 days), wash the cells in warm phosphate buffered saline (PBS). Then, culture in a serum-free medium containing Neurobasal-A™ (Gibco), 2% B27™ supplement 50x (Gibco), Glutamax 0.5 mM (Invitrogen) and Gentamicin (Invitrogen) 10 μg/mL for 2 days. The supernatant (the conditioned medium) is then collected, filtered through a 0.22 syringe filter and stored at −20 °C until required.

At least 24 h before spinal cord harvesting, sterilize glass 12 mm coverslips. Then, within a laminar flow hood insert them into 24-well culture plates (Corning). Apply to the surface of individual coverslips 100 μL sterile poly-D-lysine (PDL) (50 μg/mL) (Sigma). Note: There is variation in methods of this procedure http://protocolsonline.com/recipes/stock-solutions/polylysine-coated-tissue-culture-surfaces/ (Accessed 4/10/2015). In this protocol apply PDL, and then transfer the culture plates to a culture oven at 37 °C for 1 h. Excess PDL solution is aspirated, and the surface of the coverslip rinsed twice with sterile water. Leave these culture plates within the laminar flow hood under Ultraviolet light overnight to dry off.

Prepare 24 h prior to use, 150 mL of Hibernate™ based processing medium (Hib-PM) containing Hibernate-A (Gibco), 2% B27 supplement 50x (Gibco), Glutamax 0.05 mM (Sigma) and Gentamicin 10 μg/mL (Invitrogen) (Brewer and Torricelli, 2007):

1. Transfer 50 mL of Hib-PM into a 50 mL conical tube mark, "Hib-PM" processing
2. Transfer 7 mL of Hib-PM to each of 3 × 15 mL conical tubes, mark as "Hib-PM" processing
3. Leave in the laminar flow hood 15 mL of Hib-PM in a 15 mL conical tube, mark as "G1."

Store the remaining Hib-PM with the four conical tubes marked Hib-PM processing (1 × 50 mL, 3 × 15 mL) at 4 °C wrapped in foil. Mark ×4 15 mL conical tubes D1 through to D4. Then, prepare stage 1 of the Brewer and Torricelli Optiprep™ 1:32 (Sigma) density

Table 2
Neurobasal conditioned medium (NEUROBASAL CM) (Maintain at 4 °C).

Product	Concentration Required	Qty Per 100mLs	From
Neurobasal A	65%	68 mL	Gibco
C2C12 Conditioned Media	33%	30 mL	Sigma
B27 (50×)Supplement	2%	2 mL	Gibco
Glutamax 100 mL stock = 200 mM	0.5 mM	250 μL	Sigma
BDNF Stock aliquot 100 ng/200 μL (Refer Reagents)	1 ng/mL	200 μL	Sigma
GDNF Stock aliquot 100 ng/200 μL (Refer Reagents)	1 ng/mL	200 μL	Sigma
[a]CNTF Stock aliquot 1000 ng/200 μL (Refer Reagents)	10 ng/mL	200 μL	Sigma
[a]bFGF Stock aliquot 200 ng/200 μL (Refer Reagents)	2 ng/mL	200 μL	Sigma
Gentamicin 10 mg/mL	10 μg/mL	100 μL	Invitrogen
8(-4 Chlorophenylthio cyclic adenosine 3′5′ monophosphate) cAMP 100 mg = MW 493.7	125 μM	618 μL	Sigma

[a] CNTF and bFGF added to the medium to support the survival of nerve cells post-axotomy (Grothe et al., 1991; Sendtner et al., 1991). Note: bFGF at a higher dosage >20ng/mL has the potential to isolate progenitors found in the adult mammalian spinal cord (Shihabuddin et al., 1997).

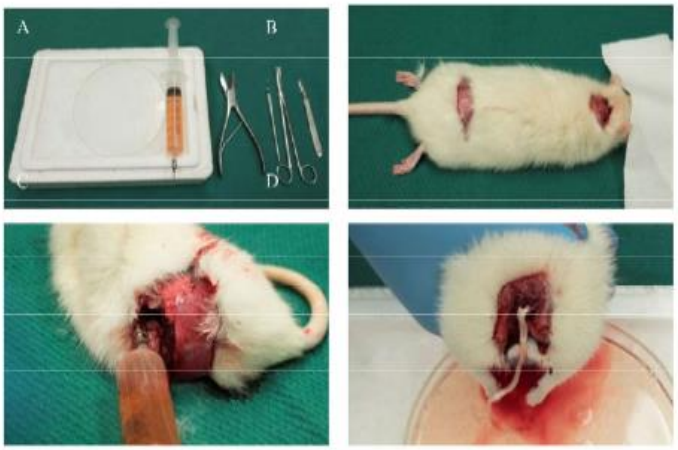

Fig. 1. Spinal Cord Harvesting Technique(De Sousa and Horrocks, 1979; Meikle and Martin, 1981) Standard equipment used to extract the spinal cord. (A) The modified trocar attached to the syringe. (B) Under anesthesia, horizontal skin incisions were made at the atlantooccipital joint and the lumbosacral junction. (C) The spinal column was severed at the lumbosacral junction using bone cutters; the spinal canal was located using a probe then the trocar attached to the syringe was introduced into the canal. (D) The rat is decapitated using the bone cutters and scissors, and the spinal cord was hydrostatically forced into the petri-dish using pressure from the syringe. This procedure took approximately 40–45 seconds.

gradient using the Hib-PM from the tube marked G1 (Table 1) (Brewer and Torricelli, 2007). On completion of preparation of the stage 1 density gradients, vortex each tube, wrap in foil and store at 4 °C. Prepare 24hr before use (with modifications indicated by asterisks – Table 2 Neurobasal™ based conditioned medium (Neurobasal-CM) as described by (Montoya-Gacharna et al., 2009, 2012). Transfer 5 mL of Neurobasal-CM to a 15 mL conical tube and mark "Plating Neurobasal-CM". Transfer 150 mL of Neurobasal-CM to 3 × 50 mL conical tubes marked "Neurobasal-CM feed".

Store the remaining Neurobasal-CM and the plating and feed marked Neurobasal-CM at 4 °C wrapped in foil. The conical tubes are working solutions reducing the risk of contamination of the main feed supply.

Sterile instruments required for surgical extraction of the rat spinal cord:

- Bone cutters
- Large scissors
- Locating probe
- Curved thumb serrated forceps
- Tooth thumb forceps
- Scalpel with size 10 blade
- 16 gauge trocar cannula shortened to 20 mm in length
- 30 mL syringe
- Petri-dish (catchment tray)

On the day of surgery, set up the surgical field containing all instruments suitably arranged for use. Place on ice to the side of the established surgical field, the pre-prepared 50 mL conical tube containing 50 mL Hib-PM, the three 15 mL conical tubes containing 7 mL of Hib-PM each and the cord catchment tray. Attach the 16 gauge trocar to the 30 mL syringe and draw up 25 mL of Hib-PM from the pre-prepared 50 mL conical tube, then lay the syringe adjacent to the instruments.

2.2. Animal ethics and harvesting of the spinal cord

This study was approved by The University of Adelaide Animal Ethics Committee in accordance with the Australian Code of Practice for the care and use of animals for scientific purposes (7th edition 2004) Permit M-2012-205. Adult Sprague-Dawley rats, male or female, aged between 8 and12 weeks and weighing between 230 and 560 g were anaesthetised by a single intraperitoneal injection of Ketamine (80 mg/kg) and Xylazine (12 mg/kg) (The University of Sydney PGC, 1988). A state of deep anesthesia is confirmed by toe pinch method using thumb toothed forceps.

Following confirmation of deep anesthesia, using the bone cutter and large scissors, the vertebral column was severed at the lumbosacral junction; thus dissociating the hind limbs from the body. The field of interest is bloody, as several main arteries are severed, and the heart remains rhythmically beating. However, it is relatively easy when using a thumb probe to locate the caudal end of the spinal canal and insert the trocar. Decapitate the rat and place the rostral end of the spinal canal over the catchment tray. Extrude the spinal cord by pressurized hydraulic ejection (De Sousa and Horrocks, 1979; Meikle and Martin, 1981). Top up the catchment tray containing the spinal cord, using the remaining 25 mL of cold (4 °C) Hib-PM from the 50 mL conical tube. Transfer the catchment tray back onto the ice bed for further processing. For those new to the technique, we suggest practice on previously culled animals(Fig. 1)

2.3. Isolation of cells and proteolytic separation from the extracellular matrix

On a suitably lighted surface and while the spinal cord remains immersed in the cold (on ice) Hib-PM solution, use the scalpel and curved thumb forceps to remove the meninges and cauda equina. Then, without differentiation of ventral and dorsal regions, rapidly cut the cord into 1 mm segments, increasing the overall surface area and penetration of the Hib-PM into the tissue. Transfer the cut segments to one of the three pre-prepared 15 mL conical tubes containing 7 mL of fresh Hib-PM, and keep the cord segments suspended. Allow the two remaining 15 mL conical tubes containing 7 mL Hib-PM and the 15 mL conical tube now containing the cord segments to transition normally to room temperature (i.e., 18–22 °C). Activities are now transitioning to the sterile laminar flow hood.

Table 3
Using Stage 1 density gradient tubes marked D1 through to D4 (Containing Optiprep 1:32 in Hib-PM).

In tubes marked "DG 1" and "DG2" slowly add to the side of the tube 1000 μL of each prepared solution from the tubes marked D1 through to D4 in the following order.	Total (μL)
D1 Conical-Bottom	1000
D2 Conical 2	1000
D3 Conical 3	1000
D4 Conical 4 Top	1000
Step D1 into tube marked DG(x) D2 onto D1, D3 onto D2 and D4 onto D3	

At this point when working within the laminar flow hood, appropriate Level 2 techniques are employed. Transfer all ×3 15 mL conical tubes and the remaining supply of stored Hib-PM to the laminar flow hood and allow all tubes to reach room temperature. On reaching near room temperature, centrifuge the 15 mL conical tube containing the cord segments and one of the two 15 mL conical tubes containing Hib-PM (acting as a centrifuge balance) at 200 g for 2 min. Centrifugation forms a loose pellet of the cord segments.

During centrifugation, weigh out 18 mg of Papain (Sigma) and under the laminar flow hood, add this to the remaining 15 mL conical tube containing 7 mL of room temperature Hib-PM. Vortex and filter the Papain/Hib-PM solution through a 0.22 μm syringe filter (achieving approximately 36 Units/mL) (Brewer and Torricelli, 2007). Note Trypsin has been shown to be inferior to Papain for this purpose (Kaiser et al., 2013).

On completion of centrifugation transfer the two 15 mL conical tubes to the laminar flow hood. Discard the supernatant from the conical tube containing the cut spinal cord segments as a loose pellet, and resuspend the cord segments at room temperature with fresh Papain/Hib-PM solution. Place into a rotating incubator the last remaining 15 mL conical tube containing 7mLs of Hib-PM (previously used as a balance during centrifugation) together with the 15 mL conical tube containing both the Papain/Hib-PM solution and the cut cord segments. Rotate the suspensions for 40 min at 30 °C. Note: At this temperature, Papain is activated, thus breaking the links between the cells and extracellular matrix. The rotating incubator keeps the tissue suspended (Brewer, 1997).

While the rotating incubator processing is in progress, retrieve and place in the laminar flow hood the four labeled (D1 through to D4) pre-prepared stage 1 density gradients from 4 °C storage and gently rotate the tubes ensuring the Optiprep/Hib-PM solution is mixed. Mark two empty tubes "DG1" and "DG2" and prepare "Stage 2" of the Brewer and Torricelli (Brewer and Torricelli, 2007) stepped density gradients (Table 3). Allow these two gradients to reach room temperature. Note: Although only two stepped gradients are prepared, there is sufficient solution in the tubes labeled D1 through to D4 to prepare three stepped density gradients.

2.4. Removal of inhibitory myelin and cell isolation

On completion of the Papain/Hib-PM rotation incubation cycle, centrifuge at 400 g for 2 min the 15 mL conical tube containing the Papain/Hib-PM suspension and the 15 mL conical tube containing fresh 7 mL Hib-PM. Centrifugation achieves a firm pellet in the Papain/Hib-PM tube. After centrifugation and within the laminar flow hood, discard the supernatant from the tube containing the pellet and resuspend the pellet in 2 mL of the fresh Hib-PM obtained from the conical tube that acted as the centrifuge balance. Both solutions are then allowed to return to room temperature.

Upon the solutions returning to room temperature, cell isolation and separation of the extracellular matrix occurs through gentle trituration, using a series of "fire polished", pre-prepared silicone coated (Sigma) Pasteur pipettes with a reduced nozzle size (1.0 mm to 0.5 mm) (Brewer, 1997). After each trituration, the suspension is allowed to settle, and the supernatant (cell suspension) is collected and filtered through a 70 μm cell strainer (Corning). The process is repeated until all of the remaining fresh Hib-PM from the conical tube previously used as the centrifuge balance is used. Of the 7 mL of Hib-PM used for this processing step, approximately 6 mL of cell suspension is recovered for further processing.

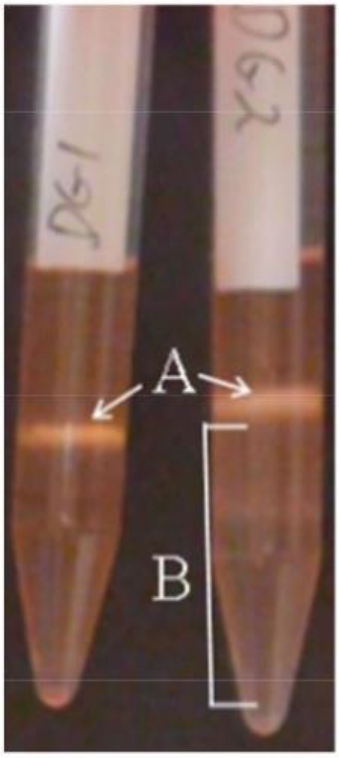

Fig. 2. Post centrifugation image of 4 layered Optiprep density gradient. Note the white band fraction (A) contains debris (myelin) and neurons of high density. Below the white band, but not including the pellet fraction, (B) contains predominantly motor neurons but at a lower density.

2.5. Application of the four step density gradient – cell selection

From the approximate 6 mL of cell suspension recovered, equal amounts are slowly added to the side of the two stepped density gradient tubes marked DG1 and DG2 (Brewer and Torricelli, 2007). These stepped gradients are then centrifuged at room temperature at 800g for 15 min (Brewer and Torricelli, 2007). During centrifugation retrieve the stored 15 mL conical tube marked plating Neurobasal-CM (5 mL) and warm to 30 °C. Also, retrieve ×1 50 mL conical tube marked Neurobasal-CM feed (50 mL) and warm this to 37 °C.

On completion of centrifugation, collect Fractions A and B (Brewer and Torricelli, 2007) (Fig. 2), and dilute from stock with 5 mL of room temperature Hib-PM. Re-centrifuge at 200 g for 2 min forming a loose pellet thus removing the Optiprep. Discard the supernatant and resuspend again with 2 mL of fresh room temperature stock Hib-PM. Either conduct a cell count and plate at a

Table 4
Antibodies.

Primary Antibody	Dilution	Company
2H3 monoclonal antibody isotype IgG1 raised against rat brain membranes, 165 kDa molecule and localizes on neurofilaments of nerve cells (Dodd et al., 1988).	Supernatant 1:200 (Conc not stated)	Developmental Studies Hybridoma Bank
Anti-Choline Acetyltransferase antibody IgG1 ab35948 50 µL, specific for cholinergic neurons in the central nervous system	1:250 (0.004 mg/mL)	abcam
Secondary Antibody		
Alexa Fluor 488 goat anti-mouse IgG(H + L) 2 mg/mL, highly cross-absorbed	1:500 (0.004 mg/mL)	Molecular Probes

high density up to 300 mm^2 (Brewer and Torricelli, 2007) or add 600 µL of Neurobasal-CM and plate using 20 µL per coverslip. On completion of the cell count calculation, re-centrifuge the 15 mL conical tube containing the 2 mL of Hib-PM and cell suspension at 200 g for 2 min forming the last loose pellet (removing Hibernate). Discard the supernatant and add to the cell pellet the calculated dilution of previously warmed (30 °C) Neurobasal-CM using the 5 mL of plating Neurobasal-CM. Note: Neurobasal-CM does not provide buffering against ambient $C0_2$. Therefore, the lid must remain on the conical tube when not in use.

2.6. Plating of the neurons after completion of the cell count

Apply 20 µL of the Neurobasal-CM cell suspension onto each previously coated sterile poly-D-lysine (50 µg/mL) 12 mm glass coverslip, and within 3 min transfer the culture well to a standard culture oven set at 37 °C and 5% CO_2. Note: between 45 min and 1 h, cells attach to the substrates. During this period, it is important to monitor the culture plates to ensure they do not dry out. Once cells are attached, additional Neurobasal – CM delivered at 37 °C is slowly added against the side wall of each culture well. Care must be taken not to dislodge the attached cells.

2.7. Optional debris removal

At 24 h post plating, separate debris from attached cells by angling the wells, and gently aspirating off excess fluid. Then, rinse the coverslips twice with small amounts of fresh (37 °C) Hib-PM, gently aspirating off the excess. On completion replace the Hib-PM again with fresh Neurobasal-CM and maintain in the culture oven at 37 °C with 5% CO_2. Care must be taken not to dislodge the attached cells.

2.8. Ongoing medium replacement

Replace approximately $^2/_3$ of the Neurobasal–CM culture medium every 3–4 days according to medium color change. In our laboratory, these cell cultures are routinely maintained for 28 days. However, longer periods are achievable.

2.9. Immunohistochemistry

Immunohistochemistry was performed to identify motor neurons amongst other cells growing in the cell culture. All primary and secondary antibodies are listed in Table 4, all solutions used in Table 5. Standard procedures as per Damon and associates protocol were used (Damon et al., 2008). Briefly, coverslips containing cells were soaked three times in washing buffer for 5 min, and then cells fixed for 10 min at room temperature. The fixative was removed by soaking the cells three times in washing buffer for 10 min. Following removal of the washing buffer, cells were soaked in Glycine solution for 20 min at room temperature then the Glycine was removed and replaced with 150 µL blocking solution for 30 min. The blocking solution was removed, and 150 µL of primary antibodies were then applied to specifically determined coverslips or 150 µL of blocking solution to specific controls. Cells were then incubated at room temperature for 1 hr and refrigerated at 4 °C for 24 h. After 24 h, solutions were carefully aspirated, and the cells washed three times in blocking solution for 5 min. In the dark, blocking solution was then aspirated, and the secondary antibody applied and cells incubated for 1 hr at room temperature. Following the aspiration of the secondary antibody, cells were soaked three times in 150 µL of blocking solution for 5 min. At conclusion, the blocking solution was removed, and the Glycerol solution used during reverse mounting of coverslips onto slides. Slides were placed in the fridge before microscopic evaluation.

2.10. Post plating cell count (day 7,14,28)

Following Immunohistochemistry using the primary antibody Anti-Choline Acetyltransferase (ab35948) and the secondary antibody Alexa Fluor 488 (Table 4), five random fields of view were selected and imaged from 5 coverslips using Nikon (NIS) Element software version 3.22.4, calibrated to a digital sight DS-5Mc camera attached to an Olympus BHB phase contrast and fluorescent inverted microscope using 20 x objectives. Fluorescent cells were counted, and the mean per mm^2 was determined.

3. Results and discussion

Media, temperature, ischemia, pH fluctuation, and debris are the main factors that influence primary neuron viability during harvesting or processing to culture. In this study, we refine the protocol to harvest spinal cords from rats in less than 60 s without the need to perform intracardiac perfusion, or to deviate significantly from using ambient solution temperatures. The overall protocol has previously been shown to be robust (Montoya-Gacharna et al., 2009, 2012). These modifications reduce complexity and save approximately 2 h of processing time.

3.1. Intracardiac perfusion with artificial cerebrospinal fluid can be omitted when hydraulic extrusion of the spinal cord is used

To minimise the effects of hypoxia and to reduce the presence of red blood cells (RBC's), during harvesting of the spinal cord, cold (4 °C) artificial cerebrospinal fluid (ACSF) saturated with 95% Oxygen (O_2) and 5% Carbon dioxide (CO_2) has been previously intracardially perfused (Montoya-Gacharna et al., 2009, 2012). The rapid cooling is considered to reduce the metabolic rate (Bektas and Ozturk, 2013) and the perfusion will saturate the nerve cells with O_2 during extraction, as well as remove RBC's from the tissue. In this study, the spinal cord was extruded/harvested in less than 45 s minimizing the risk of hypoxia. Similarly, the spinal cord has been extruded using a similar technique in 60 s without the perfusion step (De Sousa and Horrocks, 1979). The omission of the perfusion step has the disadvantage of retention of whole blood in the spinal cord. Red blood cells and other debris in tissue culture may affect the attachment of nerve cells to the substrate during plating.

The effects of omission of perfusion on the retention of RBC's was assessed by staining smears prepared from the four layers of the centrifuged stepped density gradient. The RBC counts of each

Table 5
Immunohistochemistry solutions.

Description	Amount	Store
0.1M Phosphate Buffer Solution (PBS)		
$Na_2HPO_{4\ (anhydrous)}$	1.290g	
KH_2PO_4	0.272g	
NaCl	8.70g	4°C
DD H_20	1Ltr	
Glycine Solution (Made on day of use)		
0.02M Glycine	0.150g	
0.1M PBS	100mLs	4°C
Washing Buffer (Made day prior to use) per 24 wells		
0.1M PBS	150mLs	
8% Sucrose	12g	4°C
Fixing Solution (Made day prior to use)		
Para-formaldehyde* 4%	4g	
Sucrose	8g	4°C
0.1M PBS	100mLs	
*Paraformaldehyde does not dissolve readily in water or buffer.		
Dissolve Sucrose into 60mLs 0.1M PBS (at room temperature)		
Dissolve Paraformaldehyde initially into this PBS/Sucrose solution at 60°C, with frequent mixing.		
To minimise polymerization, add 1–2 drops of 1N NaOH then allow to cool.		
Monitor pH and add as required more 1N NaOH or 1N HCL to achieve a pH 7.4.		
Bring final volume to 100mL with 0.1M PBS.		
Blocking Solution (As required) 20mls req for 12 of 24 wells		
0.01M PBS* (7.4)		
*Dilute 1mL of 0.1M PBS into 9mLs of DD H_20	10 mLs	
1.1% Bovine Serum Albumin (BSA)	0.11g	
2% Goat or Horse Serum	200µL	
0.1% Triton X-100	10µL	
0.05% Tween 20	5µL	
Notes:		
Vortex BSA		
Following vortex and after adding proteins don't shake as it causes frothing & loss of proteins in solution.		

Table 6
Smear test to detect the presence of red blood cells in the Brewer and Torricelli (2007) density gradient without a perfusion step.

		n = Countper mm2	St.Dev	Debris
Top	Fraction 1	0	0	Minimal
	Fraction 2	25	2	High
	Fraction 3	10	2	Low
Bottom	Fraction 4	67	4	Minimal

Result: Fraction 4 contained the bulk of RBC's, therefore as the cell suspension was layered on the top of fraction 1 and during centrifugation; the bulk of the RBC's passed through to Fraction 4. Fraction 2 of the gradient had the next highest number of RBC's. This fraction had a high content of debris, suggesting that RBC's were trapped in this fraction, thus could not pass through to fraction 3. Fraction 3 contained a lower number of RBC's than fraction 2.
Stains used: Leishman followed by a Hematoxylin and Eosin (H&E), RBC's stained bright red and were counted in 4 random fields of view at 200x magnification using Image J program.

Table 7
Post-plating motor neurons identified with anti-choline acetyltransferase (cHat) antibody In this study, the culture medium used is as described by (Montoya-Gacharna et al., 2009, 2012). Thus the viability of the nerve cells should be similar to those of the above authors. However, investigation of cell viability according to the current protocol was maintained at 91% and 63% on day 14 and day 28 respectively.

	CountedSites	Neuronsper mm^2	StDev	% SurvivalFrom day 7
Day 7	n = 25	32	3	
Day 14	n = 25	29	3	91%
Day 28	n = 25	20	3	63%

layer of the gradient are presented in Table 6. Fractions 2 and 3 were the gradient density layers used for cell culture plating and these fractions had the minimum number of RBC's. The amount of debris in the culture will remain the same with or without perfusion extraction of the spinal cord. The cell debris (including any RBC's) could be removed from the culture after nerve cell attachment by introducing the optional debris removal step as described in methods Section 2.7. Therefore, perfusion with the cold ACSF was omitted from this protocol.

Spinal cords that were extruded using cold 4 °C Hib-PM have remained viable up to 2 days at room temperature in normal atmosphere (Brewer and Price, 1996). Therefore, cold Hib-PM was used to extrude the spinal cord, which will lower the metabolic rate of the nerve cells allowing adequate time for the diffusion of HIB-PM into the tissue the following extraction.

3.2. *Papain proteolytic separation is superior for primary neurons*

Papain and Trypsin proteolytic enzymes are widely used for tissue digestion. Kaiser and Associates evaluated Papain (20 U/mL) and Trypsin (0.125%) dissociation kits (in supplemented MACS® Neuro Medium) using inferior colliculi samples with or without a DNase 1 trituration phase (Kaiser et al., 2013). They found that although seeding confluences were comparable, using a 30 min incubation period, the yield of neurons in combination with cellular arborization was superior in the Papain-only method of digestion without the use of DNase 1 for trituration. Moreover, a marked reduction in cell debris was observed. Fitzgerald and Associates (Fitzgerald et al., 1992) also compared Papain (20 U/mL) in a modified Huett and Baughman solution (Huettner and Baughman, 1986) and Trypsin (0.125%) to digest tissue obtained from the upper medulla. Their results were similar to Kaiser and Associates (Kaiser et al., 2013). However, Fitzgerald and Associates used DNase 1 in the

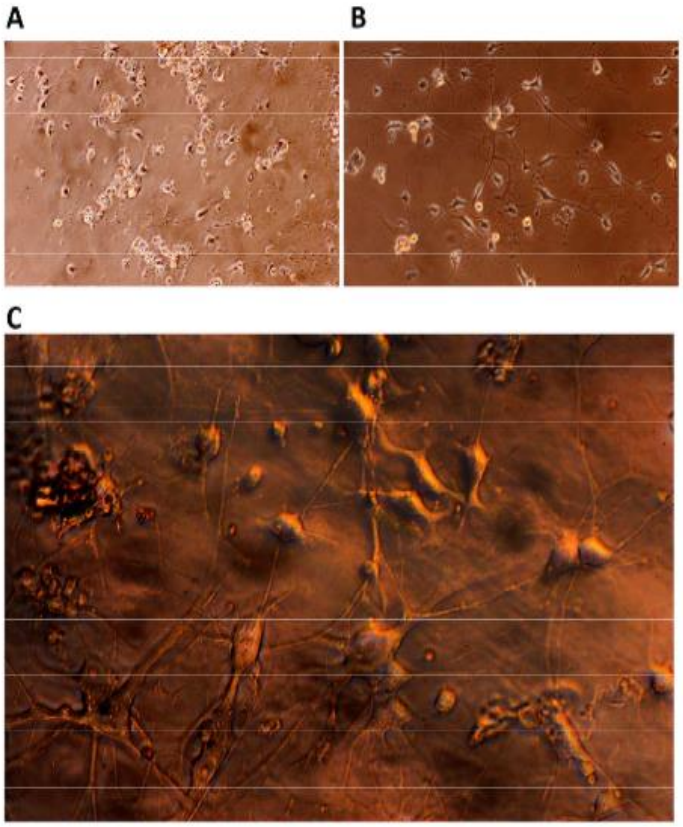

Fig. 3. Images of live nerve cells in NFM culture (Day 7).
Live cell images A and B (×200mag) Image C (×400mag). Images were taken using a Nikon camera attached to a Nikon inverted microscope through the front camera port of the microscope (Scales not shown).

Papain solution and also noted that dissociation time with Papain was almost twice as long as that of Trypsin.

Brewer and Torricelli (Brewer and Torricelli, 2007) commented that there might be differences in quality of Papain obtained from different suppliers. They preferred to use Papain obtained from Worthington rather than Sigma. In this study, we used Sigma Papain at the same higher concentration (36 U/mL) in Hib-PM medium for 30 min as described by (Brewer and Torricelli, 2007; Milligan and Gifondorwa, 2011) and (Montoya-Gacharna et al., 2009, 2012). This was followed by trituration using Hib-PM only (no DNase 1). We also found adequate proteolytic digestion, but initially a higher level of debris than expected. The Sigma papain worked well in our experiments.

In this study, the tissue suspension prepared from the spinal cord was transitioned from 4 °C to room temperature 22 °C before transferring into Papain/Hib-PM solution which initially is at room temperature. Papain enzyme activity was initiated by increasing the temperature to 30 °C and incubated at that temperature for 40 min (Shuaib et al., 1993). As cell survival at 22 °C has been demonstrated in Hibernate/B27 for at least two days, beyond enzymatic digestion, processing was continued at 22 °C (Brewer and Price, 1996).

3.3. Use of a 70 μM cell strainer before use of the stepped density gradient reduces debris

In humans, the neuronal cell bodies vary in size from 5 μM to 135 μM (Kiernan and Barr, 2009). In adult rats, the cell bodies of large motor neurons have been 40–55 μM (Barber et al., 1984). The Montoya-Gacharna group used a 70 μm filter to remove myelin and larger cell debris between the use of two separate stepped gradients. Here we did not use the first 6% Optiprep gradient used by Montoya-Gacharna et al. (2012) but strained the cell suspension using a 70 μm filter before the Brewer and Torricelli 4 step density gradient. The straining of the cell suspension after trituration of the tissue reduced the presence of myelin within the density gradient.

3.4. Optiprep step density gradient processing

In this current protocol, layers 2 and 3 (i.e. top to bottom) of the 4 step density gradient were collected for cell culturing. The same layers were used by Brewer and Torricelli (2007), Montoya-Gacharna et al. (2012) for culturing of nerve cells. However, in the Montoya-Gacharna et al. (2012) protocol, the use of a 6% Optiprep step, before the 4 step Optiprep gradient may have reduced the

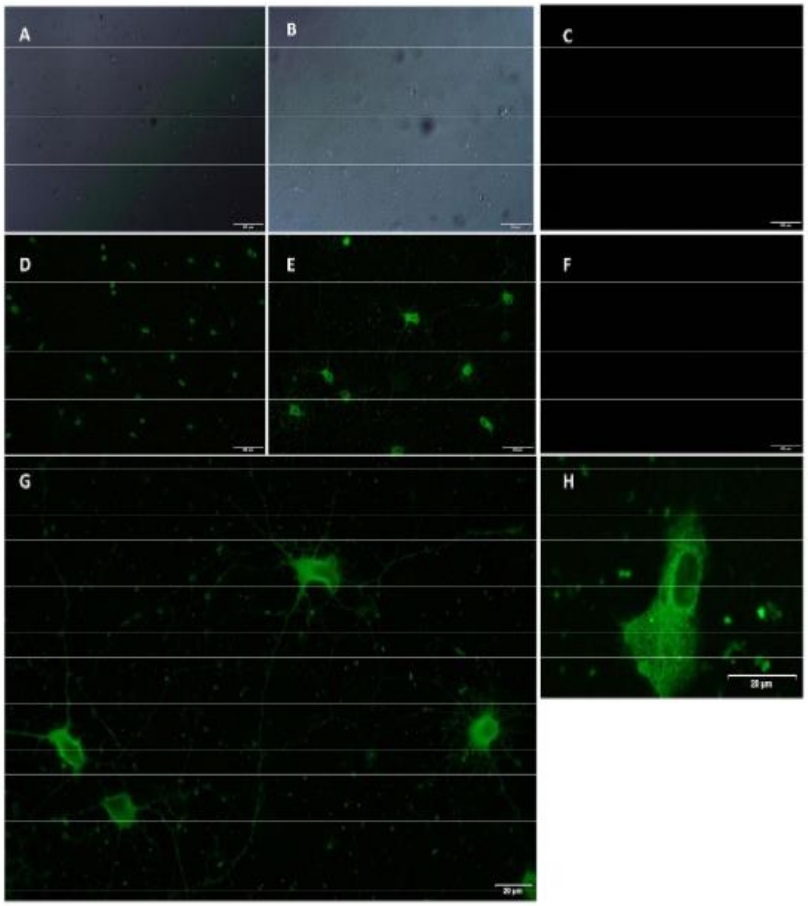

Fig. 4. Simultaneous post-fixation (day 7) diffusion contrast and fluorescence images.
Fluorescence: Anti-Choline Acetyltransferase antibody IgG1 (Abcam ab35948).
A & D: 200 x Magnification, B & E: 400 x Magnification, C: Primary no Secondary, F: Secondary no Primary, G: 1000 x Magnification (oil), H: Enlarged single cell.
Note: Choline Acetyltransferase (ChAT) is expressed in motor neurons and preganglionic autonomic neurons of the spinal cord. At Day 7, although the complete spinal cord is processed, Image B and E highlight that when using C2C12 culture medium it preferences survival of motor neurons over sensory neurons.

amount of debris including RBC and myelin more than in the current method. However, the composition of the layer 3 in the current protocol and that of Montoya-Gacharna et al. (2012) protocol may not have been much different (Fig. 2).

3.5. Post-plating cell counts – viability

Cells were stained per protocol using the primary antibody Anti-Choline Acetyltransferase (ab35948) and the secondary antibody Alexa Fluor 488. Cells obtained from the complete spinal cord which settled in the stepped density gradients two and three were seeded into 600 μL of NFM. At day 1, to reduce the debris field, the cell substrates were gently rinsed using Hibernate-A per protocol and Neurobasal A- Feed medium (NFM) replenished. Higher content of myelin and RBC in layer 2 (top to bottom) compared to that of Montoya-Gacharna et al. (2012) protocol, did not appear to affect the cell attachment to the substrate (Table 7).

3.6. Cell morphology of spinal cord neurons can be observed well by day 7 of culture

It is problematic to determine cell morphology until after day three in-vitro (DIV3) at which time neurites are evident, but axons are difficult to distinguish (Fig. 3A). By DIV7 networks and axons are present and cell body shape is more discernable (Fig. 3B). At DIV28, the projections have matured, axons are clearly evident, and networks are extensive (Fig. 3C). Dendritic arborization and axon projections differ between neurons suggestive of a functional difference (Kiernan and Barr, 2009). Therefore, the broad classification of spinal cord neuronal populations, in particular, differentiation between a motor neuron and sensory neuron, can be achieved

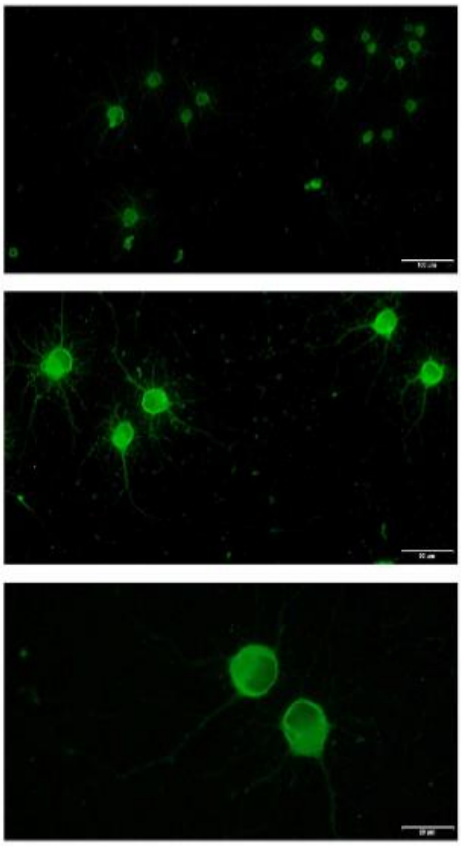

Fig. 5. Immunofluorescence Day 21, Anti-Choline Acetyltransferase antibody (ab35948).

through a microscope and later confirmed by immunohistochemistry (Figs. 4–6).

4. Conclusions

The method described here produces desired results to the same extent as methods used by other authors while it is more parsimonious than previously described methods. It shortens the time of processing and is less expensive.

Contributions

Mr. Malcolm Brinn contributed to defining the concept of this paper, completed the literature review, all experiments, imaging, immunohistochemistry and contributed to the manuscript content as the primary author.

Ms. Katie O'Neill provided level 2 training in the use of laminar flow and culture techniques. Carried out and assisted in calculating various solution concentrations and contributed to manuscript content as the second author.

Dr. Ian Musgrave supervised level 2 training, edited the procedural content of the manuscript, provided consultation during culture issues.

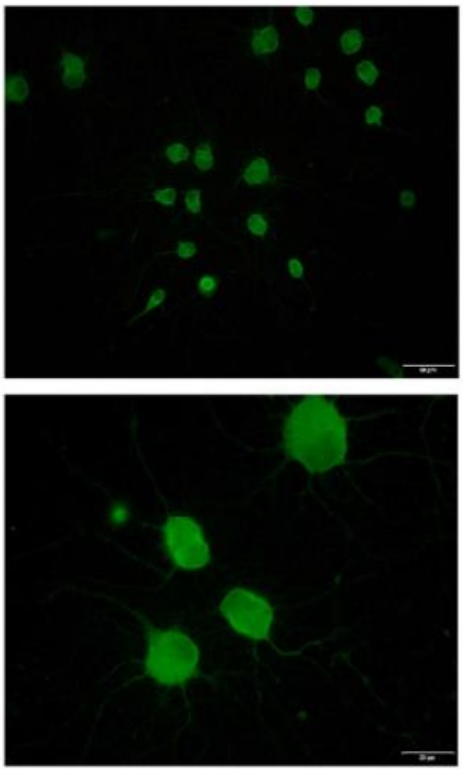

Fig. 6. Immunofluorescence Day 21, Neurofilament 165 kDa antibody (DSHB: 2H3).

Prof. Brian Freeman contributed to defining the concept of this paper, provided consultative advice as well as editing of the final manuscript.

Prof. Maciej Henneberg provided mentoring, assistance with protocol design, primary editing of the manuscript and provided consultative advice on manuscript layout

Dr. Jaylia Kumaratilake participated in the design of the protocol provided technical assistance with immunohistochemistry, supervision of Laboratory work, editing and layout of the manuscript and consultative advice on general laboratory techniques.

Disclosures

Funding for consumables for this investigation was provided from private lecturing funds obtained by Dr. Jaliya Kumaratilake.

Acknowledgments

We would like to thank Mr. Tavik Morgenstern for his assistance with photography and Mr. Chris Leigh for overall technical support. We also thank Adelaide Microscopy for the use of the Olympus BX51 Fluorescence imaging microscope, the use of facilities and support of Dr. Agatha Labrinidis. We would also like to thank Dr. J.V. Montoya-Gacharna for his encouragement and assisting email correspondence and Dr. J. Kumaratilake for providing funding for this study out of private lecturing funds. Finally, we thank the reviewers for their constructive comments and suggestions.

References

Bar, P.R., 2000. Motor neuron disease in vitro: the use of cultured motor neurons to study amyotrophic lateral sclerosis. Eur. J. Pharmacol., 285–295.

Barber, R.P., Phelps, P.E., Houser, C.R., Crawford, G.D., Salvaterra, P.M., Vaughn, J.E., 1984. The morphology and distribution of neurons containing choline acetyltransferase in the adult rat spinal cord: an immunocytochemical study. J. Comp. Neurol. 229, 329–346.

Bektas, S., Ozturk, G., 2013. Enhancement of cultured adult motor neuron survival with cold pre-incubation. Neurosci. Lett. 533, 23–27.

Brewer, G.J., Cotman, C.W., 1989. Survival and growth of hippocampal neurons at low density in defined medium: advantages of a sandwich culture technique or low oxygen. Brain Res. 494, 65–74.

Brewer, D.J., Price, P.J., 1996. Viable cultured neurons in ambient carbon dioxide and hibernation storage for a montNeuroreport. Neuroreport 7, 1509–1512.

Brewer, G.J., Torricelli, J.R., 2007. Isolation and culture of adult neurons and neurospheres. Nat. Protoc. 2, 1490–1498.

Brewer, G.J., 1997. Isolation and culture of adult rat hippocampal neurons. J. Neurosci. Methods 71, 143–155.

Cameron, W.E., Núñez-Abades, P.A., 2000. Physiological changes accompanying anatomical remodeling of mammalian motoneurons during postnatal development. Brain Res. Bull. 53, 523–527.

Carrascal, L., Nieto-Gonzalez, J.L., Cameron, W.E., Torres, B., Nunez-Abades, P.A., 2005. Changes during the postnatal development in physiological and anatomical characteristics of rat motoneurons studied in vitro. Brain Res. Brain Res. Rev. 49, 377–387.

Damon, B.J., Mezentseva, N.V., Kumaratilake, J.S., Forgacs, G., Newman, S.A., 2008. Limb bud and flank mesoderm have distinct physical phenotypes that may contribute to limb budding. Dev. Biol. 321, 319–330.

De Sousa, B.N., Horrocks, L.A., 1979. Development of rat spinal cord. Dev. Neurosci. 2, 115–121.

Dodd, J., Morton, S.B., Karagogeos, D., Yamamoto, M., Jessell, T.M., 1988. Spatial regulation of axonal glycoprotein expression on subsets of embryonic spinal neurons. Neuron 1, 105–116.

Fitzgerald, S.C., Willis, M.A., Yu, C., Rigatto, H., 1992. In search of the central respiratory neurons: I. dissociated cell cultures of respiratory areas from the upper medulla. J. Neurosci. Res. 33, 579–589.

Gingras, M., Gagnon, V., Minotti, S., Durham, H.D., Berthod, F., 2007. Optimized protocols for isolation of primary motor neurons, astrocytes and microglia from embryonic mouse spinal cord. J. Neurosci. Methods 163, 111–118.

Grothe, C., Wewetzer, K., Lagrange, A., Unsicker, K., 1991. Effects of basic fibroblast growth factor on survival and choline acetyltransferase development of spinal cord neurons. Dev. Brain Res. 62, 257–261.

Hanson, M.G., Shen, S., Wiemelt, A.P., McMorris, F.A., Barres, B.A., 1998. Cyclic AMP elevation is sufficient to promote the survival of spinal motor neurons in vitro. J. Neurosci. 18, 7361–7371.

Huettner, J., Baughman, R., 1986. Primary culture of identified neurons from the visual cortex of postnatal rats. J. Neurosci. 6, 3044–3060.

Jacobson, M., 1985. Clonal analysis and cell lineages of the vertebrate central nervous system. Annu. Rev. Neurosci. 8, 71–102.

Kaiser, O., Aliuos, P., Wissel, K., Lenarz, T., Werner, D., Reuter, G., Kral, A., Warnecke, A., 2013. Dissociated neurons and glial cells derived from rat inferior colliculi after digestion with papain. PLoS One 8, e80490.

Kiernan, J.A., Barr, M.L., 2009. Barr Is the Human Nervous System: An Anatomical Viewpoint, Wolters Kluwer Health/Lippincott, 9th ed. Williams & Wilkins.

Meikle, A.D., Martin, A.H., 1981. A rapid method for removal of the spinal cord. Biotech. Histochem. 56, 235–237.

Meyer-Franke, A., Wilkinson, G.A., Kruttgen, A., Hu, M., Munro, E., Hanson Jr., M.G., Reichardt, L.F., Barres, B.A., 1998. Depolarization and cAMP elevation rapidly recruit TrkB to the plasma membrane of CNS neurons. Neuron 21, 681–693.

Milligan, C., Gifondorwa, D., 2011. Isolation and culture of postnatal spinal motoneurons. In: Manfredi, G., Kawamata, H. (Eds.), Neurodegeneration. Humana Press, pp. 77–85.

Montoya-Gacharna, J., Sutachan, J.J., Chan, W.S., Sideris, A., Blanck, T.J., Recio-Pinto, E., 2009. Muscle-conditioned media and cAMP promote survival and neurite outgrowth of adult spinal cord motor neurons. Exp. Neurol. 220, 303–315.

Montoya-Gacharna, J.V., Sutachan, J.J., Chan, W.S., Sideris, A., Blanck, T.J., Recio-Pinto, E., 2012. Preparation of adult spinal cord motor neuron cultures under serum-free conditions. Methods Mol. Biol. 846, 103–116.

Sendtner, M., Arakawa, Y., Stöckli, K.A., Kreutzberg, G.W., Thoenen, H., 1991. Effect of ciliary neurotrophic factor (CNTF) on motoneuron survival. J. Cell Sci. 1991, 103–109.

Shihabuddin, L.S., Ray, J., Gage, F.H., 1997. FGF-2 is sufficient to isolate progenitors found in the adult mammalian spinal cord. Exp. Neurol. 148, 577–586.

Shuaib, A., Sochocka, E., Ishaqzay, R., Hertz, L., Code, W.E., 1993. Protective effect of hypothermia during ischemia in neural cell cultures. Neurochem. Res. 18, 663–665.

The University of Sydney PGC, 1988. Australian Wildlife: The John Keep Refresher Course for Veterinarians: 15–19 February. The Committee, 1988.

bioengineering

MDPI

Appendix 4: Paper 2: Journal of bioengineering

Article

A portable live cell culture and imaging system with optional umbilical bioreactor using a modified infant incubator

Malcolm Brinn[1], Said F. Al-Sarawi[2], Tien-Fu Lu[3], Brian J C Freeman[4&5], Jaliya Kumaratilake[1] and Maciej Henneberg[1]

[1] School of Medicine, Discipline of Anatomy and Pathology, University of Adelaide, SA 5000 Australia
[2] School of Electrical and Electronics Engineering, University of Adelaide, SA 5000 Australia.
[3] School of Mechanical Engineering, University of Adelaide, SA 5000 Australia
[4] Discipline of Orthopaedics and Trauma, School of Medicine University of Adelaide, SA 5000 Australia
[5] Department of Spinal Surgery, Royal Adelaide Hospital, North Terrace, Adelaide, SA 5000 Australia
Corresponding Author: Malcolm Brinn; malcolm.brinn@adelaide.edu.au

Abstract: Here, we present a staged approach for an innovative repurposing of a portable infant humidicrib into a live cell growth, observation, and imaging system. Furthmore, humidicrib can support different variations of "umbilical" bioreactors, and can be used to conduct electrophysiology experiments and *in situ* immunohistochemistry. Modifications incorporate a closed loop carbon dioxide (CO_2) concentration control system with umbilical CO_2 and heating support for tailored bioreactors. The repurposing cost is inexpensive and allows for the continued observation and imaging of cells. This prototype unit has been used to continuously observe and image live primary neurons for up to 21 days. This demonstrates the repurposed units' suitability for use in tissue culture based research, particularly where modifications to microscopes are required or where sensitive manipulation outside of a standard incubator is needed.

Keywords: Cell Culture; Bioreactor; Live Cell Imaging; Tissue Engineering,

1. Introduction

Cell culture ovens and microscopes can typically be found in all cell culture laboratories. For many researchers, cells may only need observation at the time of passaging or during short term experiments and for this purpose quick transfer or stage top incubation systems may be employed. However, in some instances, it is necessary to observe and image cells over extended periods or to use tailored equipment. Commercial live cell imaging systems can be useful but for some, the cost of the equipment may be prohibitive for occasional use, or warranty conditions may limit options. Repurposing of assets is one potential way in which this can be resolved, by reducing expenditure as well as outbalancing the accrued cost of asset decommissioning (Loomba 2014; Opperman 2015).

Infant humidicribs are essential devices used to support neonates who would otherwise have difficulty regulating and maintaining their own homeostasis (Burgess 1978). Advances in the design of many of these devices have enabled them to regulate oxygen and humidity whilst isolating the infant in an aseptic environment. In a hospital setting, failure of this type of equipment can lead to catastrophic outcomes, therefore, these devices are often pragmatically decommissioned early in their working life cycle. However, being complex devices we believe they retain significant inherent value for alternate use. Here we present the novel repurposing of a decommissioned infant humidicrib into a tailored portable imaging culture system that can support different variations of "umbilical" bioreactors in a non-critical setting.

A decommissioned humidicrib as manufactured by Drager (Drager Air-Shields Isolette® C100) was obtained exgratia from a local government hospital. Device dimensions (mm) were 1340 H x 560 D x 1160 W comprising a plexiglass enclosure with a raised bed. The bottom section contained a control module, heating element, a port of oxygen supply, and an internal humidification system (Figure 1). This particular model also has an optional height adjustable strut under the trolley frame allowing user variation to suit standing or sitting.

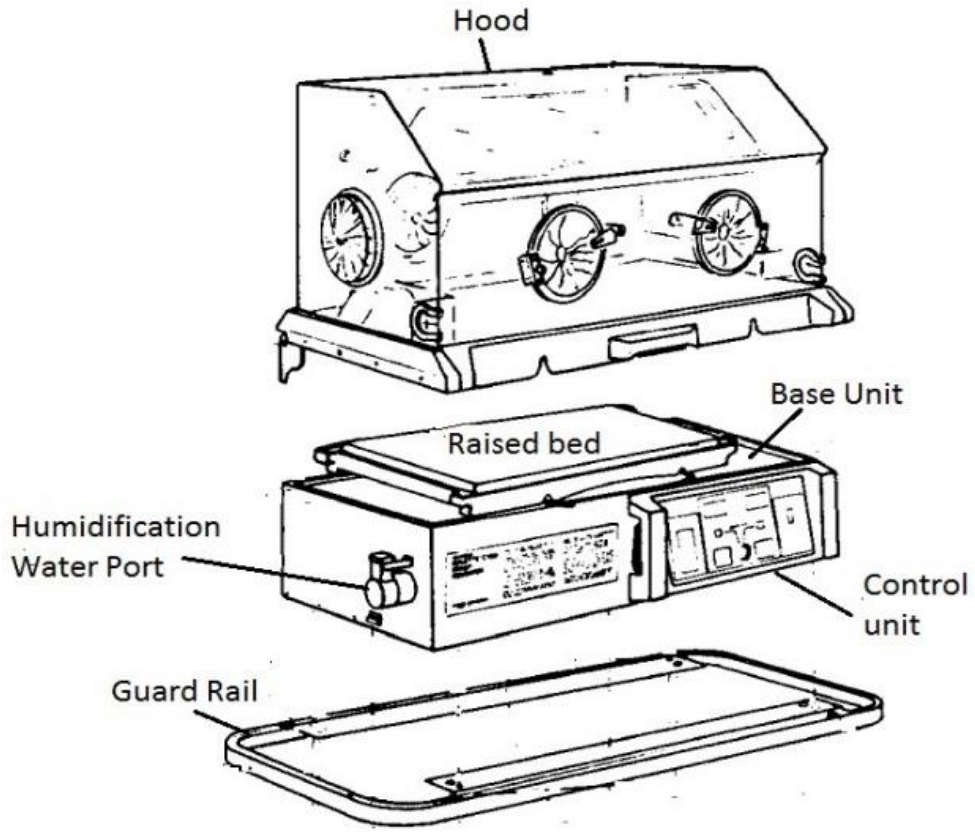

Figure 1. Adapted drawing (service manual) of the Drager Air-Shields Isolette®. C100

Air is actively circulated across a heating element within the base and over an internal humidification tank and then passes into the interior. The plexiglass interior (shroud) of the infant incubator is isolated from the surrounding air by rubber seals. The control panel, has built-in skin or air temperature control devices, with digital displays (range 0 to 38.5^{o}C ± 0.5^{o}C) and visual and audible alarms. Access to the interior of the humidicrib is provided by air tight doors or iris entry ports. The raised infant bed can also be accessed by lowering the complete front panel. Gas can be introduced into the humidicrib through an external port (rear of unit – not shown) to which a gas bottle can be connected.

2.1. Modifications to humidicrib

An Olympus IMT2 inverted research microscope was mounted centrally between the front access ports of the humidicrib shroud, so that coaxial stage controls, revolving objective turret, field brightness, coarse and fine image adjustment controls, as well as a power switch could be accessed either by the right or left hand. Detachable access panels were cut into the centre rear and at the top/front of the humidicribs plexiglass shroud to allow the binocular shaft of the microscope to project neatly through the angled top of the plexiglass. A 3-Dimensional (3D) printer was used to construct tailored trim for the binocular shaft and silicone rubber matting was used to maintain internal seals.

Although the humidicrib had independent heating and humidity systems, it did not have an independent CO_2 monitoring and control system. This was developed using a suitable regulator; gas approved 2W025-08 electric solenoid and an in-house established Arduino controller. When stationary, the gas supply could be either co-located onto the infant incubator making it portable or kept as a larger supply next to the unit. CO_2 sensing was achieved through a fast acting (20 Hz) real time CO_2 sensor (SprintIR GC-0017 0-20%).

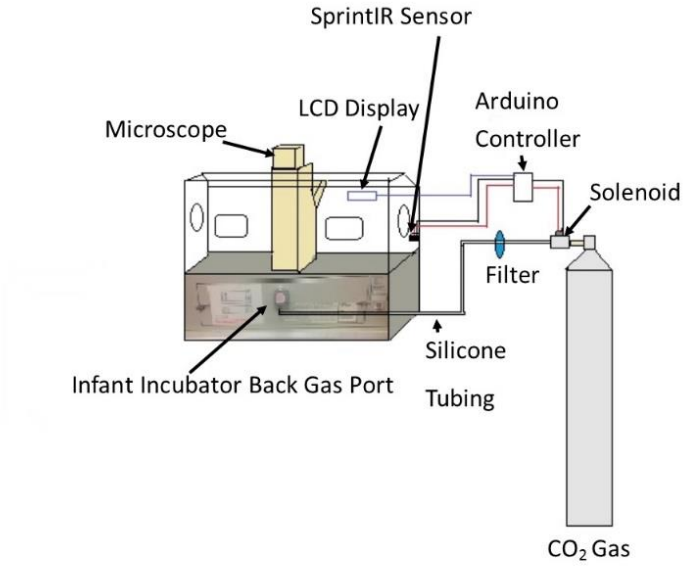

Figure 2 Diagram representing the CO_2 gas connection direct to the incubator

CO_2 gas enters the port and passes over an internal humidification and heating system. A fan circulates the gas up into the shroud where the SprintIR picks up the internal concentration. The closed Arduino circuit displays the CO_2 concentration and activates the solenoid (default off).

Heating: The inner shroud temperature and humidity is maintained by the humidicribs existing infrastructure.

The CO_2 controller comprised a closed loop relay circuit that was routed through a standard Arduino UNO circuit board controlling both the CO_2 display powered via a standard printer USB cable and solenoid powered through a 12-volt adaptor (Figure 3). Arduino technology is an open source electronics platform intended for developing inexpensive interactive systems. Therefore, access to basic forms of Arduino circuit diagrams and source code was freely available from the internet under open access arrangements.

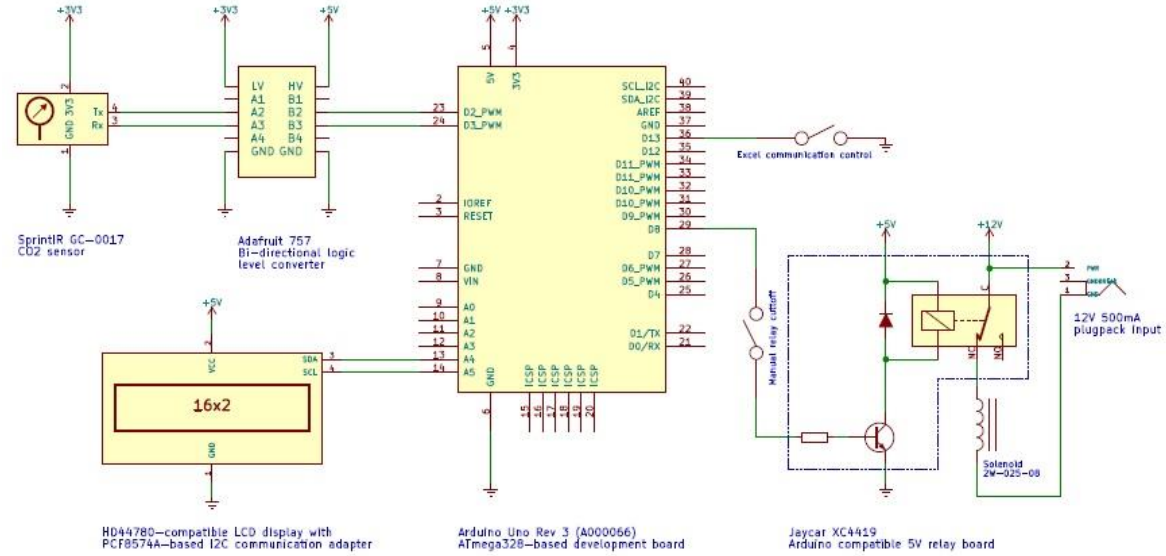

Figure 3. Arduino based circuit diagram for CO_2 control

CO_2 concentration is determined and controlled via a closed loop system. Air concentration is determined using a SprintIR 0-20% CO_2 sensor routed through a bi-directional logic level converter. Gas output is controlled through a 2W-025-08 gas solenoid (Default closed). The Arduino board controls the 5V relay, switching the solenoid on and off. A Liquid Crystal Display (LCD) shows % CO_2 levels. Data logging in CVS format is facilitated through an Excel spreadsheet which can be used to monitor flow over extended periods.

Adapted from www.pellinglab.com. Schematic modifications (incorporating the logic converter, independent 5V relay board, LCD) and final fabrication.

2.2. Bioreactor development – Umbilical support (heating and gas)

Pilot investigations highlighted that removal of cultures from the humidicrib for periods more than a few minutes caused a rapid loss of temperature and in the absence of CO_2, pH variation. This was problematic for the use of equipment that could not be incorporated into the shroud and where cell/tissue homoeostasis was necessary. Provisioning the infant incubator to provide umbilical support to bioreactors rather than acting primarily as a portable culture oven, thus extends versatility and operational flexibility. The length of the umbilicus can be varied to suit requirements (Figure 4).

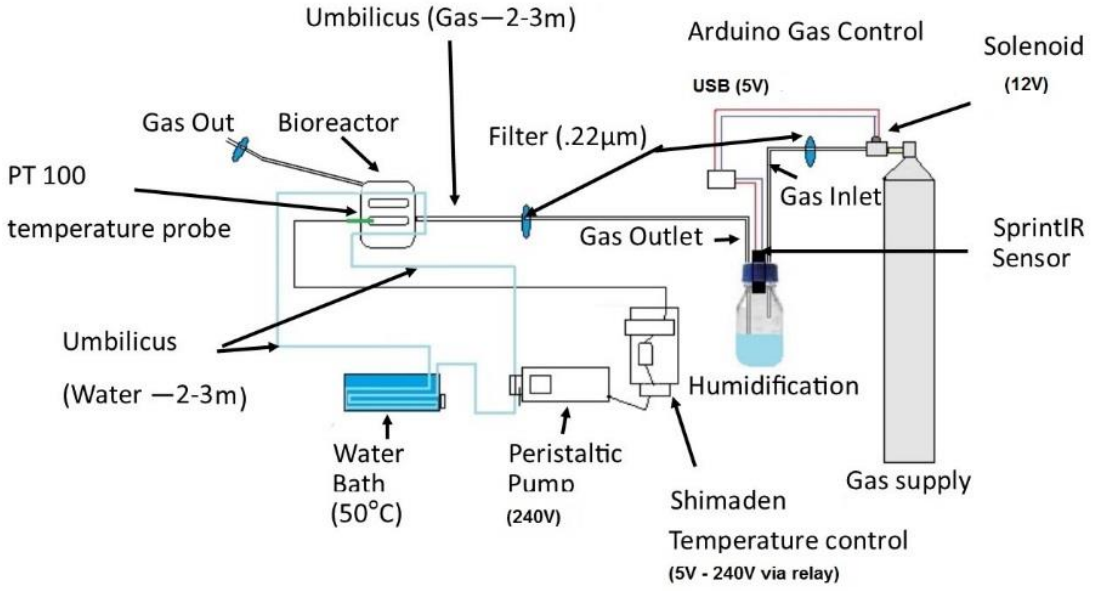

Figure 4: Diagram of heating and gas infrastructure for bioreactor use.

Heating: The PT100 temperature probe picks up the temperature and passes it to the Shimaden controller. At set points, the controller triggers a relay to open power to the peristaltic pump which circulates pre-heated water through the bioreactor.

Gas: The same Arduino control is used. However, gas from the solenoid is passed through a filter into a humidification container. Then the gas is filtered before entering the bioreactor. The operation of the controller remains the same.

Umbilical heating was provided through a water filled silicone tube (6mm) which was weaved longitudinally through channels provided in each bioreactor and passed through a small sealed bath (50^{o}C). A PT100 temperature control probe in contact with the media provided feedback on temperature to a Shimaden Controller (±0.1^{0}C), Schematic details are given Figure 5.

Carbon dioxide was provision to the bioreactor was achieved by fitting 6mm inlet and silicone outlet tubes and the existing CO_2 SprintIR sensor into the lid of a standard glass 500mL laboratory bottle. Before use, the assembly (excluding the sensor) was steam sterilized and then partially filled with sterile water under a laminar flow hood. Filtered (0.22 µm) CO_2 gas was then routed from the gas supply solenoid into the inlet tube. The outlet tube was tailored to appropriate length into the bioreactor CO_2 port. A filter was used on the outlet tube, but care was taken to place this close to the bioreactor as humidity over time could cause the filter to block.

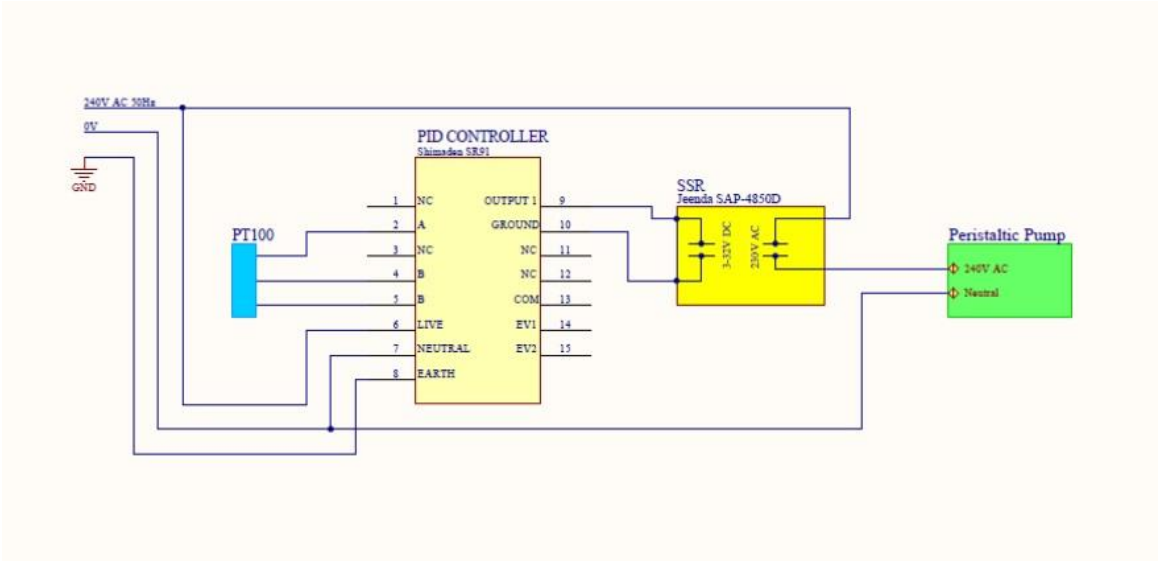

Figure 5: Schematic wiring diagram of the closed loop heating system.

Culture medium temperature is determined using a PT100 temperature sensor that is wired to a Shimaden SR91 proportional integral derivative (PID) controller. The PID triggers the solid state relay (SSR) to provide on/off power to a peristaltic pump that circulates the heated water. The Shimaden controller can be programmed with user-defined minimum and maximum set points and has built-in fuzzy logic. Therefore, over time the controller determines the optimum turn on/off ranges to mitigate overshoot of temperature.

2.3. Bioreactor Design, Manufacture, and Assembly

Here three bioreactors are presented (Figures 6 and 7), which were developed in series for the following experiments. The first example, a basic 3D printed version with the base plate was developed for culturing, monitoring and imaging of motor neurons. The second example, a modification separated the bioreactor component into two parts, with the lower section being machined and used with multiple different top sections. This modification achieved standardisation of the umbilical heating system, improved *in situ* immunostaining capability and facilitated material choice flexibility of the top section for different experiments such as stretching of axons.

All bioreactors were designed using Autodesk® Inventor® Professional software 2017 and were for use with the inverted microscope. All devices were manufactured internally at the University Engineering Prototyping Laboratory. Each bioreactor differed in material selection and method of manufacture. However, all bioreactors used the same supporting infrastructure for both gas and heating. Length and width (mm) were standardized to 130 (L) x 100 (W). Height varied according to requirements. All designs of the bioreactor shared the key basic requirements of being non-toxic, sterilizable, and leak proof. Each featured two tissue culture medium/cell containment wells that accommodated removable standard 60 x 24 mm cover glasses as viewing bases, external culture medium heating channels and provision to use a temperature probe in direct contact with the medium (Figure 6B). A standardised base plate for all versions of the bioreactor was machined from a 3 mm thick stainless steel sheet (Figure 6C).

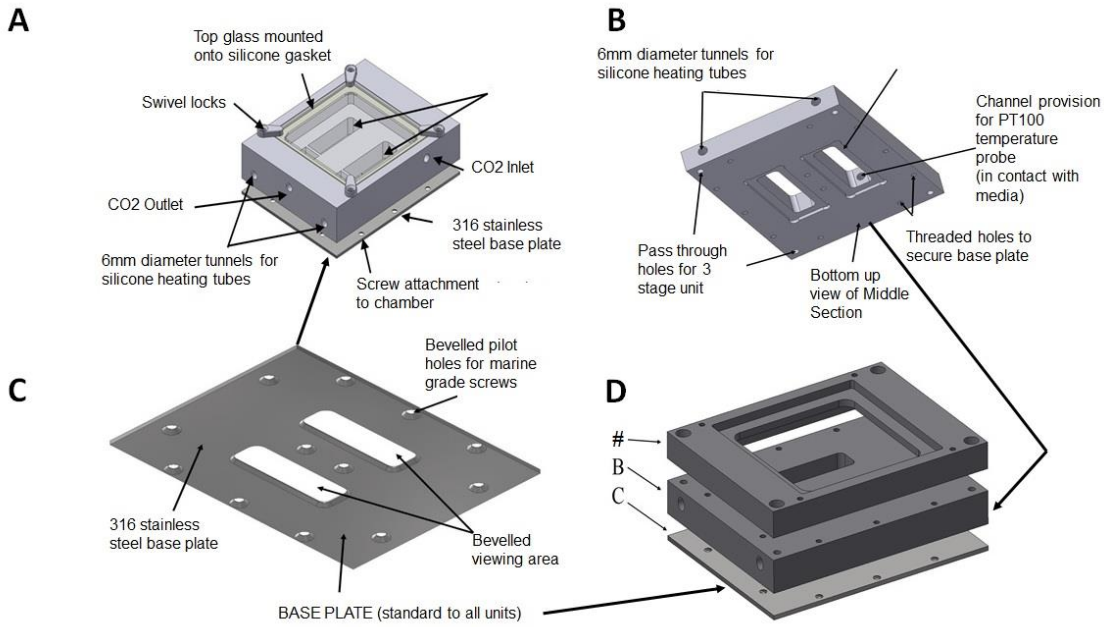

Figure 6: Basic design of bioreactors. **A Top:** Standard 1- piece 3D filament (Acrylonitrile Butadiene Styrene ABS) printed bioreactor with 316 stainless steel base plate **B:** Middle section of a three-piece bioreactor (including the 316-stainless steel base plate) machined from Polytetrafluoroethylene (PTFE). The top section on these units could be varied. **C**: The standard base plate common to all units **D:** Highlighting the 3-piece bioreactor assembly. **#:** The Top and Middle sections of the 3-piece bioreactor are similar to the one-piece design when assembled. However, the middle section was machined from PTFE and the top section 3D filament printed with ABS.

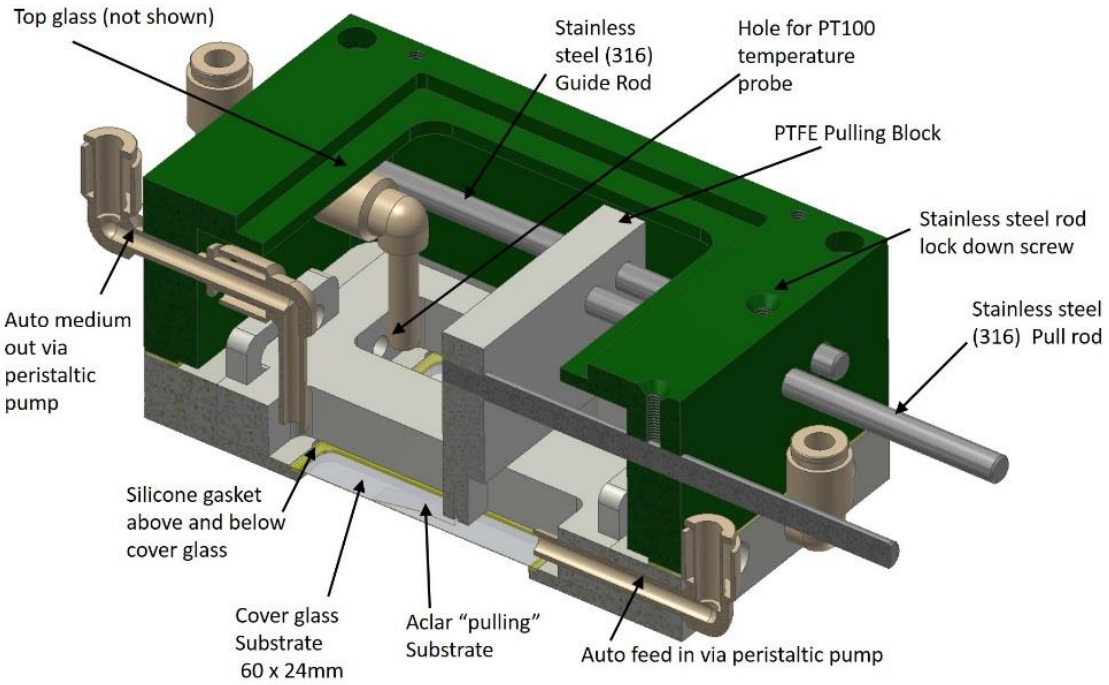

Figure 7: Sagittal view example of a more advanced bioreactor (top aluminium machined (PTFE coated) bottom section machined from solid PTFE). Standard base plate not shown.

This bioreactor incorporates many specialised features. The top section could be removed to conduct electrophysiology experiments and *in situ* immunohistochemistry. It also incorporates axon stretch technology adapted from (Loverde et al. 2011a). The lower (also shown 6B) incorporates a pilot version of an autofeeding system designed to prevent drying of the culture wells. The heating channels are running through the lower chamber on either side and between the medium containing wells (not visible in this view). Cover glasses can be removed for immunohistochemistry processing.

2.4. Basic Live Cell Imaging

Images obtained from this system are dependent both on the quality of the microscope and objectives, as well as on the imaging method. The Olympus IMT2 microscope used for our experiments was ideally suited for this task. We had both the option to use a commercial camera attached to the front port of the microscope or to use an ocular camera (Dino eyepiece camera AnMo Electronics Corporation). Attaching a camera to the front port of the microscope required the correct Olympus fitting for the camera but no calibration was readily achievable. However, the Dino eyepiece could be inserted direct into one of the two ocular viewing ports and taped into orientation. The image could then be projected to screen and captured via the DinoCapture sofware. Captured images can be calibrated and enhanced through the sofware (Figure 8B).

3. Results

3.1. Humidicrib conversion results

The humidicrib's internal heating system was sufficient to maintain cells in standard culture flasks. The internal shroud temperature of the infant incubator remained stable within specification. However, as with fixed culture incubators, it was essential to ensure the temperature of solutions was pre-set to operational requirements before placing cells into the hood. The large space within the humidicrib together with the mounting of an inverted research microscope and a digital camera enhanced functionality. The cutting of the front of the plexiglass shroud and fixing of custom made trim made it possible for the operation of the microscope via the front ports of the shroud without disruption to the cells.

Modifications to incorporate CO_2 control direct into the shroud provided stand-alone capability. A reasonably large gas cylinder could be mounted onto the trolley making the unit fully portable. Alternatively, the unit could be plugged into a gas source or to a larger cylinder at the location when in use. The SprintIR sensor operated within specifications, and the Arduino controller triggered the solenoid to open (default closed) as required to maintain CO_2 levels at the programmed concentration (in our case 5%). The gas supply entered the bottom section of the incubator through a built in filter and humidification system; there was a slight delay in sensor receipt of the gas concentration. Following door opening, this does cause the unit to briefly overshoot gas concentration by as much as 2% for a 10-30 second period.

The above modifications converted the decommissioned humidicrib into a portable culture oven capable of conducting continuous observation and imaging for research, particularly those that require continuous monitoring and sensitive manipulations.

3.1. Bioreactor development- results

Direct supply of CO_2 to the bioreactor (via a humidification tank) reduced the consumption of CO_2. Some problems occurred with the humidification system blocking filters, which were resolved through extending the CO_2 line length and by placement of the post humidification filter closer to the bioreactor.

The internal heating system of the humidicrib was sufficient to maintain internal plexiglass shroud temperature but it a longer time to bring the inner temperature of the bioreactor to 37°C. Supplemental heating of the bioreactor worked exceptionally well and maintained the temperature of the culture medium at 37°C ± 0.1°C. When both heating systems were in operation, the temperature of the culture medium remained very stable.

3.2. Repurposing Costs

The total cost of repurposing the humidicrib is hard to estimate beyond the cost of supplies and materials (Table 1). The cost of labour will depend on specific skills of the staff involved and their commitment to the project. The cost of bioreactors will vary considerably based on production methods. 3D printing bioreactors once designed can be typically produced for under AU$50.00. Costs for imaging will vary according to method used. A Dino eyepiece camera can be purchased for AU$390.00.

Table 1: Equipment requirements for CO_2/Air sensor and control automation

Description	Qty	Estimated Cost AU$
Plastic Reinforced Shelf Humidicrib	1	40.00
Closed loop gas supply		
COZIR CO2 sensor (SprintIR 0-20%) (Internet)	1	140.00
Clear Box (Electronics)	1	15.00
Arduino Uno Controller (Internet)	1	25.00
AdaFruit 757 Bi-Directional logic converter (Internet)	1	6.00
HD44780 Compatible LCD (Jaycar)	1	15.00
XC4419 5V Relay (Jaycar)	1	5.00
Gas Solenoid 2W-025-08	1	16.00
Cables various	1	15.00
Closed loop heating controller		
Shimaden SR1 PID Temperature Controller	1	127.00
PT100 stainless steel probe	1	50.00
Solid State Relay SSR SAP4850D	1	20.00
Electronics Box	1	15.00
Power Socket	1	7.00
Silicone Tubing 6mm	1	50.00
Hot water bath	1	In use
Total cost all		546.00

3.3. Culture Use/Experience

To date, fifty-four neuron cell cultures have been incubated in these bioreactors with experiment duration varying from 3 days to 21 days. The overall picture of the working unit is provided (Figure 8). Recent publication of some images obtained from live cells have been published elsewhere (Brinn et al. 2016)

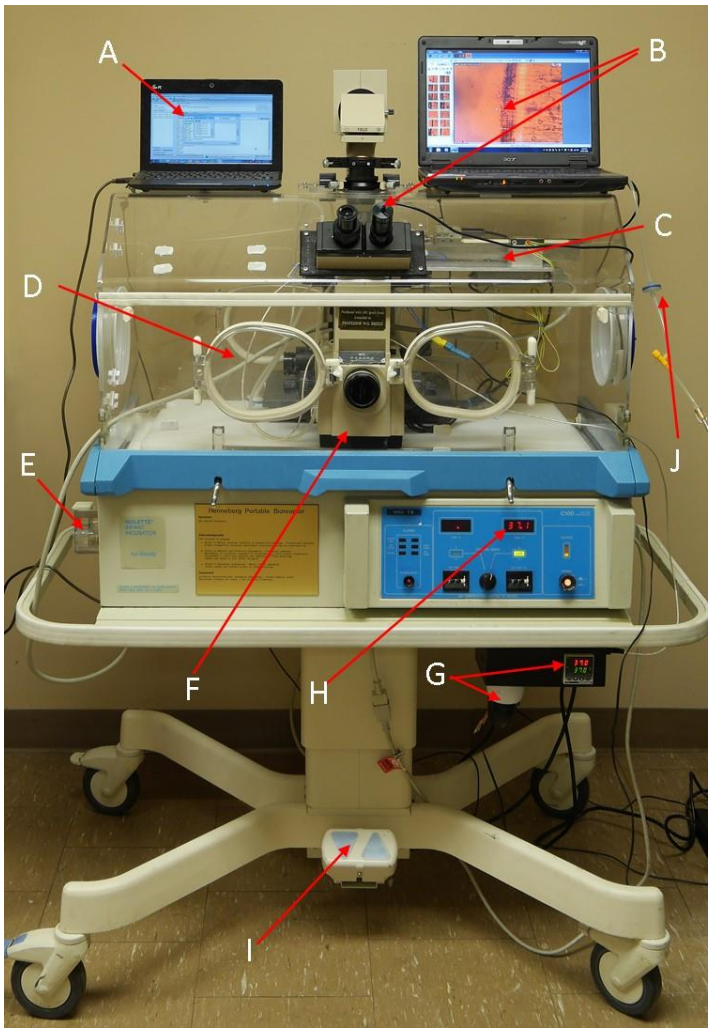

Figure 8. The complete system with assembled and functioning bioreactor in its controlled and protected housing (infant incubator)

The paediatric humidicrib provides a secondary barrier to minimise contamination, vibrations, and external movements during operation. The bioreactor was mounted onto the sample stage (C) of an Olympus IMT2 inverted microscope (F) with 4x, 10x, 20x and 40x objectives. Pre-warmed humidified 5% CO_2 filtered air (0.22μm) was delivered through the small humidification system and piped through sterile tubing directly to the bioreactor gas inlet port (J). Temperature control was maintained using a combination of the humidicrib temperature control system (to prevent fogging) (H), and an internal PT100 sensor attached to an external proportional-integral-derivative (PID) controller (l) activating power to the peristaltic pump to circulate heated water (not shown). Time lapsed imaging was captured using a Microscope Dino-Eye (USB) camera AM7023 connected to Dino-Lite v2 software (B). Laptop system monitoring software (A). A total of 6 intervention ports could be accessed to make adjustments (D).

4. Discussion

Live cell observation and imaging systems suitable for continuous use over several weeks are commercially available but expensive, and due to warranty issues modification can be problematic. Here, we have resolved this problem by repurposing an infant humidicrib and by developing an independent multipurpose bioreactor.

relatively simple exercise to lift off the shroud and install a variety of different microscopes. The advantage of this approach was that it allowed us to use our specifically tailored microscope with a number of onboard instruments. A situation that would not have been possible using a commercial system.

There were also several advantages in using our own internal microscopes. Perhaps the most important was the enhanced functionality, but familiarity was also beneficial when working with instruments. Microscopes of course are delicate instruments and the risk of damage to the optics is heightened during movement. However, this must be balanced against the alternative options available. In our case, removing the shroud and electrically adjusting the height of the stand made this a simple process and limited the risk. Another key benefit was the humidicribs portability. Once the microscope was removed, it could be easily transferred to storage or to another laboratory allowing its reuse with another microscope.

The incorporation of an independent 3D printable bioreactor has been another useful feature. In our case, we now have several different versions for variation in experiments. However, we continue to experiment with designs and materials. Currently, we are printing in standard plastics overnight. However, PEEK is now available for use, and it would be our intention to use this in future bioreactor development as it is autoclavable.

The independent heating system presented in this paper works well with the water filled silicone tubing passing through a standard heated water bath via basic peristaltic pump. The controller uses a standard relay and these can be assembled into a black box and wired by an electrician in less than an hour. The gas controller is built using Arduino technology and a standard gas solenoid, both of which are robust. Although assembly of the Arduino controller is not difficult, most electronics stores can provide this assembly service for a small fee. Source code to run the gas controller was originally written by Andrew Pelling and is available for download (www.pellinglab.net.au). We have subsequently added to the functionality and enclosed the full source code to allow operation of the device.

Equipment failure is of course always an issue. However, the dependency on the humidicrib is limited and heating elements within the unit can always be replaced with alternatives by a qualified electrician.

Although the unit can work as a standard incubator using standard cultureware, it does not have the insulation or advanced decontamination features available in purpose built units. However, the repurposing cost is inexpensive, and these units are frequently decommissioned.

Lastly, prior to use, it is recommended that appropriate electrical safety checks are made to the humidicrib. A CO_2 warning sensor should also be present where culture ovens or this device is in use.

5. Conclusion

Infant incubators have inbuilt features that can be adapted for the growth of tissue cultures. Therefore, they could be modified into live cell imaging systems. Also, this apparatus can accommodate advanced technology. The cost in adopting these modifications may be inexpensive in comparison to new equipment purchase.

Acknowledgement: We gratefully acknowledge the donation of the decommissioned infant incubator provided by Flinders Medical Centre, South Australia, the technical assistance of Mr Chris Leigh, School of Medicine, University of Adelaide and Mr Ian Linke, Mr Brandon Pullen, Mr Aubrey Slater, Mr Alban O'Brien, Mr Hayden Westell and Mr Danny Di Giacomo School of Electrical and Electronic Engineering, University of Adelaide.

References

Brinn, MP, O'Neill, K, Musgrave, I, Freeman, BJC, Henneberg, M & Kumaratilake, J 2016, 'An optimized method for obtaining adult rat spinal cord motor neurons to be used for tissue culture', *J Neurosci Methods*, vol. 273, pp. 128-137.

Burgess, M, (President), 1978, 'Abstracts of Papers Presented at The 11th Annual Meeting', *Journal of Paediatrics and Child Health*, vol. 14, no. 2, pp. 109-127.

Loomba, APS 2014, 'Repurposing medical devices for LRCs; Sustainability considerations', *Engineering, Technology and Innovation (ICE), 2014 International ICE Conference on*, 23-25 June 2014, pp. 1-6.

Loverde, JR, Ozoka, VC, Aquino, R, Lin, LS & Pfister, BJ 2011a, 'Live imaging of axon stretch growth in embryonic and adult neurons', *J Neurotrauma*, vol. 28, no. 11, Nov, pp. 2389-2403.

Opperman, LA 2015, 'Anatomist executive talks device development', *Biomedical Instrumentation and Technology*, vol. 49, no. 2, pp. 125-127.

Supplementary Material

CO2_PID_Controller_Arduino Source Code (Open access source code)

```
// Arduino IDE version used for development/compatibility reasons: 1.0.6
// https://www.arduino.cc/en/Main/OldSoftwareReleases#previous

//Acknowledgement to Andrew Pelling @ www.pellinglab.net for original version
//Modifications:  Danny Di Giacomo and Malcolm Brinn – University of Adelaide www.adelaide.edu.au

/*
 Humidifier and CO2 gas control via 12V normally closed solenoid and CO2 Sensor.
 CO2 Meter (SprintIR 0-20% GC-0017):
 http://www.co2meter.com/collections/co2-sensors/products/sprintir-100-percent-co2-sensor
 also need the latest COZIR library, download from this thread (Using Cozir 0-1-01.zip in this code):
 http://forum.arduino.cc/index.php?topic=91467.0
 CO2 supplied by BOC Gas
 Arduino UNO Pin Connections:
 Pin 2,3: Tx/Rx from CO2  //Pin 2 arduino goes to Tx on Sensor Pin 4
 Pin #5:
```

```
 Pin #6:
 Pin #7:
 Pin #8: Solenoid Relay
 Pin #9:
 SCL/SDA Pins: 12C Display
 */

/* CO2 CONTROL /////////
 Control works by reading the sensor (CO2) 3 times and averaging (to flatten out noise).
 The measurement is compared to a user-defined SETPOINT. If the CO2 is below the setpoint, the solenoid
 opens allowing the flow of CO2 into the incubator. Once the CO2 content comes within a user-defined
 THRESHOLD of the setpoint, a stepping cycle begins. The solenoid opens for a user defined DURATION and
 then closes. The open/closed cycle repeats until the setpoint is reached.

 The cycles allow the system to step up to the setpoints.
 Setpoints, thresholds and durations MUST be set according to your own system by TRIAL AND ERROR.
 May need to increase/decrease depending on size/shape of incubator, CO2 flow rate, etc.
 */

float CO2Setpoint = 1.0;   // Setpoint CO2 level in % 5
float CO2Threshold = 0.85; // Threshold to switch to stepping control in %/100
int SolenoidOnTime = 5000; // Duration time in milliseconds

// CO2 Sensors
#include "SoftwareSerial.h"
#include "cozir.h"
// Cozir library info/download: http://forum.arduino.cc/index.php?topic=91467.0

// Excel logging configuration
// http://www.robertovalgolio.com/sistemi-programmi/arduino-excel
#include <rExcel.h>
long idx = 0; // index
int outputTiming = 1000;   // packet sending timing in ms, determines the output timing
rExcel myExcel;            // class for Excel data exchanging
int save_loop_timer = 1;
/*
char worksheet[16];        // worksheet name
 char range[16];           // range set
 unsigned int row;         // row
 unsigned int column;      // column
 char value[16];           // written or read value
 */
```

```
// I2C LCD interface configuration
// http://forum.arduino.cc/index.php?topic=128635.0
// https://bitbucket.org/fmalpartida/new-liquidcrystal/downloads
// LiquidCrystal_V1.2.1.zip library used
#include <Wire.h>
#include <LCD.h>
#include <LiquidCrystal_I2C.h>
#define I2C_ADDR 0x3F
#define BACKLIGHT_PIN 3
#define En_pin 2
#define Rw_pin 1
#define Rs_pin 0
#define D4_pin 4
#define D5_pin 5
#define D6_pin 6
#define D7_pin 7
LiquidCrystal_I2C lcd(I2C_ADDR,En_pin,Rw_pin,Rs_pin,D4_pin,D5_pin,D6_pin,D7_pin);

////////* RELAY *////////
int Solenoid = 8;          // Relay for controlling 12V solenoid valve

////////* SPRINTIR COZIR CO2 SENSOR  *////////
SoftwareSerial nss(2, 3);  // Rx,Tx - Pin 3,4 on sensor
COZIR czr(nss);
float SingleCO2, CO2 = 0;
float multiplier = 0.001;  // 10/10000 (Hardware multiplier/ppm conversion).
float reading = 0;

void setup()
{
 Serial.begin(9600);               // Start serial port
 czr.SetOperatingMode(CZR_POLLING);  // Start the CO2 sensor and put into POLLING mode
 pinMode(Solenoid, OUTPUT);          // Sets pin for controlling solenoid relay
 digitalWrite(Solenoid, LOW);        // Set LOW (solenoid closed off)
 lcd.begin(16,2);
 lcd.setBacklightPin(BACKLIGHT_PIN,POSITIVE);
 lcd.clear();
 lcd.setBacklight(HIGH);
 lcd.home();
 pinMode(13, INPUT_PULLUP);
 // delay(500);                     // Wait
}
```

```
void loop()
{
 // Read CO2 sensor 3 times and determine the average.
 for (int i = 0; i < 3; i++) {
  SingleCO2 += czr.CO2() * multiplier;
 }
 CO2 = SingleCO2 / 3;
 SingleCO2 = 0;

 // Write CO2 % to LCD
 lcd.setCursor (0, 0);
 lcd.print("CO2 level: ");
 lcd.setCursor (10, 1);
 lcd.print(CO2, 2);
 lcd.print(" %");


 // If switch on GPIO 13 low, enable Excel logging
 if (digitalRead(13) == LOW) {

  static unsigned long  loopTime = 0;
  static unsigned long  time1 = 0;

  loopTime = millis();

  // Output Task
  // Arduino acts as client making requests to Excel
  // instructions performed each outputTiming ms
  if ((loopTime - time1) >= outputTiming) {
   time1 = loopTime;

   myExcel.write("Template", "A5", "%time%");           // write time to sheet "Template" cell A5
   myExcel.write("Template", "B5", CO2, 2);             // write CO2 %
   myExcel.writeIndexed("Template", idx+11, 1,"%date%");  // idx is zero initially, write date to row idx+11,
column 1
   myExcel.writeIndexed("Template", idx+11, 2,"%time%");
   myExcel.writeIndexed("Template", idx+11, 3, idx);
   myExcel.writeIndexed("Template", idx+11, 4, CO2, 2);
   idx++;

   // Save spreadsheet every 60 seconds
   save_loop_timer++;
   if (save_loop_timer == 60) {
```

```
        myExcel.save();
        myExcel.write("Template", "E1", "Autosaved: ");
        myExcel.write("Template", "F1", "%time%");
        save_loop_timer = 1;
      }
    }
  }

  // Open/close the solenoid valve based on the current CO2 reading
  // Solenoid  opens for a duration of 'SolenoidOnTime' and then closes
  if (CO2 < CO2Setpoint && CO2 < CO2Threshold * CO2Setpoint) {
    digitalWrite(Solenoid, HIGH);
  }
  else if (CO2 < CO2Setpoint && CO2 >= CO2Threshold * CO2Setpoint) {
    digitalWrite(Solenoid, HIGH);
    delay(SolenoidOnTime);
    digitalWrite(Solenoid, LOW);
  }
  else if (CO2 > CO2Setpoint) {
    digitalWrite(Solenoid, LOW);
  }
  delay(10);
}
```

bioengineering

MDPI